P O L I T E C N I C O D I M I L A N O

Facoltà di Ingegneria

Dipartimento di Ingegneria Idraulica, Ambientale, Infrastrutture viarie, Rilevamento.

Sezione Ambientale

TREATMENT OF INDUSTRIAL WASTEWATERS BY ANOXIC-AEROBIC AND ANAEROBIC MEMBRANE BIOREACTORS

Dottorando: ing. Aronne TELI
Matricola: 724096

Tutore e relatore : prof. Francesca MALPEI

Co-relatore: dott. Manuela ANTONELLI

Coordinatore del Dottorato: prof. Roberto CANZIANI

Dottorato di Ricerca in Ingegneria Sanitaria-Ambientale
XXIII ciclo (2008-2010)

CONTENTS

1 Introduction

1.1 General background

A membrane bioreactor (MBR) combines an activated sludge process with a direct solid–liquid separation by membrane filtration (micro or ultrafiltration) in replacement of the usual sedimentation step. As a result, MBRs have many advantages, including small footprint and reactor requirements, good disinfection capability, higher volumetric loading and less sludge production. Moreover, the membrane acts as a barrier retaining colloids and particles larger than the membrane cut-off and consequently giving extra contact time for biodegradation compared to conventional activated sludge processes (CASPs). Better growing conditions for bacteria are met as well. In fact, in a secondary clarifier only the fraction of the activated sludge that settles as flocs can be retained, whereas the membrane allows the complete physical retention of bacterial biomass as flocs and free cells. In addition to the high sludge retention time (SRT) applied in MBRs, this fact leads to the formation of a specialised bacterial community with effective degradation features with respect to the organic substrate in the effluent. As a result, higher COD removal rates and a better effluent quality are achieved compared to CASPs. The MBR technology is therefore considered as a reliable and effective treatment for domestic and industrial wastewaters, also containing refractory and very slowly biodegradable COD. On the other hand, main drawbacks of MBRs are related to membrane fouling and its consequences in terms of maintenance and operating costs resulting in the major obstacles for a wider application of MBRs (Le-Clech et al., 2006; Meng et al., 2009). Fouling control and reduction is therefore a key issue for MBR processes and several design and operational strategies can be implemented to achieve this scope such as membrane scouring, relaxation, backwashing, optimization of aeration, sustainable flux operation (Le-Clech et al., 2006; Drews, 2010). At the same time, flux enhancers such as metal salts, cationic polymers or powder activated carbon can be used and dosed into MBRs to control fouling and sludge filterability.

On a whole, the scope of this thesis is to investigate effects and benefits of flux enhancers dosing in an anoxic-aerobic MBR treating a textile wastewater (topic A, Table 1.1) and to investigate treatability and anaerobic biodegradability of a highly problematic industrial wastewater (metal working fluids, MWFs), by an anaerobic MBR (topic B).

With regards to topic A, textile wastewater treatment by means of MBRs has been studied by several authors (*inter alia*: Malpei et al., 2003; Brik et al., 2006; Gori et al., 2010) showing better removal efficiencies of COD, dyes and surfactants with respect to CASPs.

However, further amelioration of permeate quality can be achieved by flux enhancers dosage improving performances of the MBR technology. In fact, even though flux enhancers are primarily dosed in MBRs to control and reduce the fouling rate, at the same time they can improve effluent quality because of coagulation and/or adsorption of pollutants. For this reason, the general aim of topic A was to investigate the effectiveness of flux enhancers addition into a pilot scale MBR fed with a mixed domestic-textile wastewater (70% of COD loading) in terms of permeate quality enhancement, with particular reference to the specific textile macro-pollutants (i.e., dyes and surfactants), and fouling control. In particular, low dosages were considered in this study to limit any detrimental effect to the biological process, resulting in a loss of bacterial activity as reported by several authors (*inter alia*: Zhang et al., 2004; Iversen et al., 2009) and to guarantee economic sustainability for a possible implementation of the flux enhancer addition in full scale MBRs. The pilot scale MBR was designed on purpose according to the Modified Ludzack-Ettinger configuration with an anoxic and an aerobic stage. It was located in a WWTP near Como (Italy) and operated for 7.5 months without any flux enhancers and 2.5 months with a selected chemical.

With regards to topic B, metal working fluids (MWFs) are products widely used in the metalworking industry for cooling and lubricating during the machining process to increase productivity, prolong tool life, prevent corrosion, etc. Used MWFs cause high levels of contamination due to the presence of the complex chemicals, so that their treatment and final disposal must be handled carefully. In the early 1990s, the main disposal methods were electrochemical, chemical and physical processes, such as ultrafiltration, evaporation or high temperature incineration (Cheng et al., 2006; Muszyński and Łebkowska, 2005). Almost all mentioned techniques (except for the incineration) do not solve ultimately the problem, whereas biological treatments offer an alternative solution, although the complexity of MWF compositions can bring significant difficulties in operating bioreactors (Lonon et al., 1999; van der Gast et al., 2001; van der Gast et al., 2003). In this thesis, first results of a project carried out at Imperial College of London (United Kingdom) under the supervision of prof. David Stuckey are reported. The study focused on the treatment of metalworking fluids using submerged anaerobic MBRs (SAMBRs), that are an appropriate configuration to select bacteria consortia and reach high biomass concentration in order to degrade and convert into methane complex organics such as MWFs. In particular, the start-up of a two phases SAMBR treating a synthetic metal working effluent was carried out.

Without distinction between the two topics, the general methodology adopted in this thesis included a literature review, the execution of batch lab scale and continuously fed pilot scale experiments, the selection and then the detection of relevant chemical-physical parameters as well as the assessment of biological activity. In particular, such methodology was

considered and applied to respond to the main goals of the thesis, as discussed in the next section.

Table 1.1. Aim of topic A and topic B.

	Topic	Aim
A	**Treatment of textile wastewaters and fouling control in an anoxic-aerobic MBR** (study carried out at Politecnico di Milano, Milano, IT)	Investigate effects and benefits of flux enhancers dosing in an anoxic-aerobic MBR treating a textile wastewater
B	**Start-up of a submerged anaerobic MBR (SAMBR) treating a synthetic metal working effluent** (study carried out at Imperial College of Science, London, UK)	Investigate treatability and anaerobic biodegradability of metal working effluents by a submerged anaerobic MBR (SAMBR)

1.2 Main goals and outline of the thesis

Main goals of the thesis were defined differently for the two topics because characterized by different specific aims, as stated above (see Table 1.1). In particular, as for topic A, the treatment of textile wastewaters and fouling control in an anoxic-aerobic MBR was investigated and 4 main goals were introduced (Table 1.2), as follows:

- goal 1: assessment of the MBR process along the 7.5 months experimental period (without any flux enhancers), in terms of removal efficiency and process performances. Comparison of MBR permeate quality and the quality of the effluent of the full scale wastewater treatment plant (WWTP) where the pilot MBR was set were also performed along some of the experimental periods;
- goal 2: screening of 3 flux enhancers by lab-scale tests to select the best chemical and define the optimal dosage on continuous operation of the pilot MBR. Screening was done on the basis of different parameters relevant for effluent quality enhancement (COD, TOC, colour) and fouling control (soluble EPS and sludge filterability parameters such as capillary suction time, CST, specific resistance to filtration, SRF, and modified fouling index, MFI);
- goal 3: continuous dosage of the selected flux enhancers for 2.5 months and evaluation of its efficacy in terms of permeate quality enhancement (COD, nutrients and textile macro-parameters, i.e., colour and surfactants) and fouling control (TMP, membrane permeability and resistances to filtration due to fouling);
- goal 4: development of a new methodology for the evaluation of sludge fouling propensity and its implementation to monitor the effects of the flux enhancer.

With regards to goal 1, it was introduced to confirm that textile wastewaters treatment by means of MBRs shows better performances compared to CASPs, as reported in literature. Differently, goal 2, goal 3 and goal 4 are more relevant for the study since related to the flux enhancer addition into the pilot. In particular, after the screening of 3 flux enhancers by lab-scale tests and the selection of the best chemical (goal 2), its dosage into the pilot was planned considering a specific dosing strategy to avoid any risks of process failure since flux enhancer can affect bacteria activity, as reported above. Moreover, such possible negative effects on heterotrophic and autotrophic metabolism were assessed by respirometric techniques. As for goal 3, in order to better understand the complex fouling phenomenon and how flux enhancers act, also factors affecting its occurrence were taken into account in this study, including extracellular biopolymers, sludge filterability and flocs strength. In particular, for the latter, two original indexes were introduced based on the cations content in sludge flocs. Whit the same aim, also the definition of a new method for the evaluation of the fouling propensity of an MBR sludge was investigated and implemented to evaluate the effects of flux enhancers on a weekly basis (goal 4).

With regards to topic B, the start-up of a submerged anaerobic MBR treating a synthetic metal working effluent was investigated. In particular, since MWFs can be poorly biodegradable by anaerobic digestion because of a complex chemical composition and the presence of inhibitors, the main goals were:

- goal 1: evaluation of biodegradability (BMP and VFAs production assays) and the inherent toxicity (anaerobic toxicity assays, ATAs) of MWFs using not acclimatized anaerobic biomass;
- goal 2: the start-up of an anaerobic MBR pilot plant.

In particular, with regards to goal 2, the long-term scope was to achieve a biomass acclimatized to MWFs, with effective biodegradation features and methane conversion capability. In fact, MBRs provide better growing conditions for bacteria compared to other reactor configurations as the membrane allows the complete physical retention of bacterial biomass as flocs and free cells. As a result, in MBRs the selection of biomass occurs according to the biodegradation capability and not to other features like cell aggregation, etc.

This thesis is outlined in 9 chapters, as follows. Chapter 1 is an introduction to the themes and goals considered in the research, whereas Chapter 2 and Chapter 3 provide a literature review summarizing all the relevant information on MBR processes and on the treatment of textile and MWFs effluents, respectively. In particular, fundamentals of MBR processes are presented in Chapter 2 paying attention to biological aspects, reactors configurations,

membrane filtration mechanisms, general equations of filtration, membrane fouling and control with special regard to flux enhancers dosage.

Table 1.2. Topics and main goals of the thesis.

	Topic	Main goals
A	**Treatment of textile wastewaters and fouling control in an anoxic-aerobic MBR**	1. assessment of the MBR process performances and comparison with the full scale WWTP where the pilot MBR was set; 2. screening of 3 flux enhancers by lab-scale tests to select the best chemical and define the optimal dosage; 3. continuous dosage of the selected flux enhancers and evaluation of its effects on fouling control and permeate quality enhancement. 4. development of a new methodology for the evaluation of sludge fouling propensity to monitor the effects of flux enhancer.
B	**Start-up of a submerged anaerobic MBR treating a synthetic metal working effluent**	1. evaluation of biodegradability and the inherent toxicity of MWFs using not acclimatized anaerobic biomass. 2. start-up of a two phases SAMBR.

Chapter 4 and Chapter 5 refer to materials and methods considered in the studies offering information about the design of the research (Chapter 4) and all the procedures, the analytical techniques and data processing applied (Chapter 5). Results and discussions are presented in Chapter 6 and 7 referring to topic A (treatment of textile wastewaters and fouling control in an anoxic-aerobic MBR) and topic B (start-up of an anaerobic MBR treating a synthetic metal working effluent), respectively. In particular, considering topic A (Chapter 6), section 6.2 presents the wastewater characteristics and their variability along the experimental period as well as information on operating parameters of the pilot MBR. Then, the selection of the best flux enhancer is shown in section 6.3, whereas monitoring and the effects of the selected flux enhancer on the effluent quality, on the sludge characteristics (measurement of extracellular biopolymers, sludge filterability and flocs strength, and assessment of the bacteria activity) and on fouling occurrence are presented in section 6.4, 6.5, and 6.6, respectively. The investigation on fouling propensity of the MBR sludge is then showed in section 6.7 and, finally, in section 6.8 all the effects of the flux enhancer addition are summarized and discussed jointly. As for Chapter 7, preliminary assays to characterize the biodegradability and the inherent toxicity in MWFs are presented in section 7.2, whereas the start-up of the two phase SAMBR is discussed in section 7.3.

Finally, main conclusions of the studies, including a brief summary of all the results and recommendations for further research, are drawn in Chapter 8, whereas the list of references is presented in Chapter 9.

2 Fundamentals of MBR processes

2.1 Introduction

In this chapter fundamentals of MBR processes are presented. In particular, the chapter focuses on biological processes, membrane bioreactors configurations, membrane type and materials, equations of membrane filtration and fouling.

2.2 Biological wastewater treatment using membrane bioreactors

2.2.1 Potentials and drawbacks of the MBR technology

The MBR technology combines an activated sludge process with a direct solid–liquid separation by membrane filtration (micro or ultrafiltration) in replacement of the usual sedimentation step to retain the biomass and separate the treated water (Figure 2.1). As a result, MBRs can operate with long solids retention times (SRT) (from 25 to 3,500 d according to Ng and Hermanowicz, 2005) to maintain high biomass concentrations, not compatible with the secondary clarification in CASPs, and therefore reduce sludge production and minimize reactor volumes. However, an excessively high biomass concentration could cause a rise in sludge viscosity affecting the energy requirements for pumping and for oxygen supply of the microorganisms (Drews et al., 2005). Consequently full scale MBRs operate in a MLSS range of 5÷20 g L^{-1} (Metcalf and Eddy, 2003) with an optimum value related to the specific installations, such as pumps, piping, aeration devices and also to biomass characteristics.

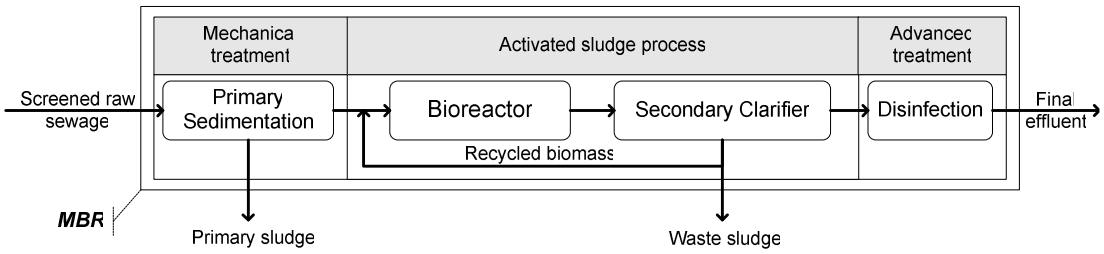

Figure 2.1. Flow sheet of a conventional activated sludge process and an MBR process.

With regards to reduced sludge production, some authors (inter alia: Wagner and Rosenwinkel, 2000, Witzig et al., 2002) found that, compared to conventional activated sludge processes, the majority of the cells in MBRs at high SRT were found to be in a non-growing state, participating in the degradation process just to satisfy their maintenance

energy requirements without further cell division and therefore producing low amounts of excess biomass.

MBRs have also other advantages, such as a tolerance to filamentous bacteria, scum and foam to a certain degree, a small footprint (primarily due to the replacement of the secondary charier by membrane), a particle free effluent and good disinfection capability (Drews et al., 2005; Judd, 2010; Le-Clech et al., 2006; Judd, 2007). In addition, higher COD removal rates and a better effluent quality are achieved compared to CASPs (Drews et al., 2005). In fact, the membrane acts as a barrier retaining colloids and particles larger than the membrane cut-off and consequently giving extra contact time for biodegradation. Better growing conditions for bacteria are met as well. In fact, in a secondary clarifier only the fraction of the activated sludge that settles as flocs can be retained, whereas the membrane allows the complete physical retention of bacterial biomass as flocs and free cells. In addition to the high sludge retention time (SRT) applied in MBRs, this fact leads to the formation of a specialised bacterial community with effective degradation features in relation to the organic substrate in the effluent (Drews et al., 2005). As a result, the MBR technology is recognised to be a reliable and effective treatment for domestic and industrial wastewaters as well, also containing refractory and very slowly biodegradable COD. Moreover, the MBR is now considered as "Best Available Technology" by many industries, and the market is highly competitive over the entire range of plant capacity and wastewater types (Lesjean and Huisjes, 2008).

In contrast, MBRs are to some extent constrained, primarily by a greater process complexity (membrane separation demands additional operational protocols relating to the maintenance of membrane cleanliness), a higher capital equipment and operating costs. In addition, there are some operational issues, including a less dewaterable sludge product and generally greater sensitivity to shock loads (Judd, 2007). Also, mechanical pre-treatment must be designed with care, particularly considering additional sieving stages to avoid operation problems caused by hairs and fibrous substances (Freche et al., 2006).

2.2.2 MBRs configurations

According to the configuration, MBRs can be classified as side-stream and submerged (or immersed) as shown in Figure 2.2 (Judd, 2010). Side-stream MBRs were the first membrane bioreactors developed commercially in the late 1960s (Bemberis et al., 1971), with application to ship-board sewage treatment (Bailey et al., 1971). This configuration consists of a separated membrane module where the sludge from the main bioreactor is pumped into. A permeate stream is then generated by cross-flow filtration (see section 2.3.1) and a concentrated sludge stream (re-circulated stream) is retained by the membrane and

returned into the bioreactor. Both the transmembrane pressure (TMP) and cross-flow velocity (CFV) are generated by the recirculation pump resulting in a high energy demand due to the high pressures and volumetric flows imposed (Judd, 2010). To make the most use of this latent energy, the flow path must be as long as possible, often in excess of 20 m, demanding a large number of membrane modules in series and incurring in a significant pressure drop along the retentate flow channels (Judd, 2010). Aiming to reduce energy consumption associated with the recirculation pump, submerged MBRs were first introduced by Yamamoto et al., (1989). The submerged configuration consists of a membrane module directly immersed in the bioreactor avoiding the high energy demand recycle and using a suction pump to create dead-end filtration (see section 2.3.1) and relying on aeration to promote mass transfer of liquid across the membrane (i.e. enhancing flux) by generating significant transient shear at the membrane/solution interface. Shear can also be promoted by directly moving the membrane, such as in the Huber VRM (Vacuum Rotating Membrane) system.

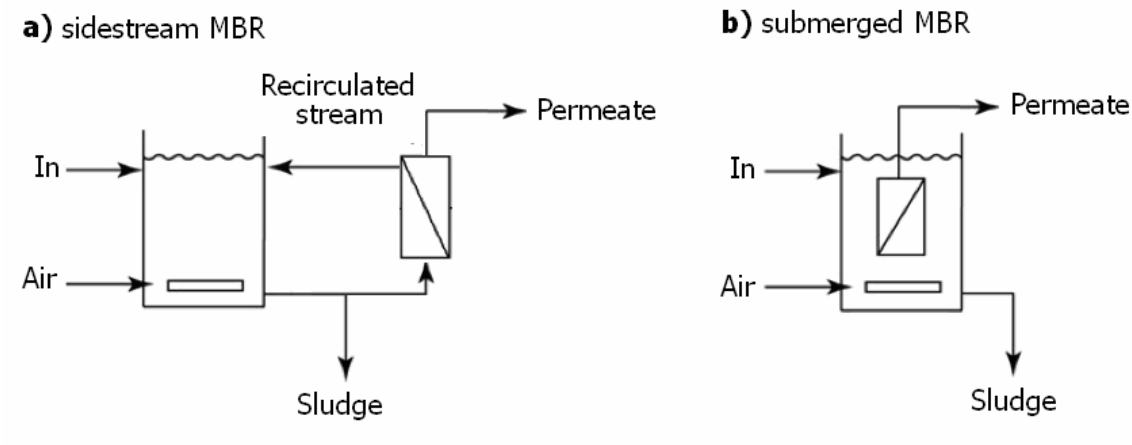

Figure 2.2. Side-stream and submerged MBRs.

Although a few modification were made in side-stream MBRs to reduce the energy consumption such as the addition of a suction pump on the permeate side and the introduction of air in the membrane module (Schimizu et al, 1996; Vant Oever, 2005; Jiang, 2007; Vant Oever et al., 2009), submerged MBRs are more commercially significant (section 2.2.4). In many applications there is a separate membrane compartment, with its own aeration and a circulation flow (Van der Roest et al., 2002; Meraviglia et al, 2003). Advantages and drawbacks of the two configuration are summarised in Table 2.1.

Table 2.1. Advantages and drawbacks of side-stream and submerged MBRs.

	Side-stream	**Submerged**
Complexity	complicate	simple
Flexibility	flexible	less flexible
Robustness	robust	less robust
Flux	high (40÷100 LMH)	low (10÷30 LMH)
Fouling reducing method	- cross-flow - air lift - backwashing - chemical cleaning	- air bubble agitation - backwashing (not always possible) - chemical cleaning
Membrane packing density	low	high
Module replacement	rapid	slow
Energy consumption	High (2÷10 kWh m^{-3})	Low (0.2÷0.4 kWh m^{-3})

As stated above, the biggest advantage of the submerged over side-stream configuration is the energy saving by using suction pumps, coarse bubble aeration and lower fluxes (10-30 LMH), instead of high rate recirculation pump and high fluxes (40-100 LMH) in side-stream MBRs. Gander et al. (2000) reviewed 4 side-stream and 4 submerged MBR systems and concluded that the side-stream MBRs have a higher total energy cost, mainly due to the high recycle flow velocity (1-3 m/s) and head loss within the membrane module.

Moreover, the membranes modules used in many submerged MBRs have very high packing density and low cost, which make it feasible to use more membranes. By comparison, membranes used in side-stream MBRs have low packing density and they are very expensive. However, the side-stream MBRs have the advantage of having more robust physical strength, more flexible cross-flow velocity control resulting in a more readily management of the precipitation of sparingly soluble inorganic solids and organic matter (see section 2.4 and section 2.5.1). Moreover, side-stream MBRs allow easier chemical "in situ" cleaning without any chemical risk to the biomass and rapid module replacement (Judd, 2010). They are now mostly used in industrial wastewater treatment and small scale WWTPs, where influent flow rate and composition has larger variation (Evenblij, 2006).

2.2.3 Anoxic-aerobic and anaerobic MBRs

Since the biological function remains unaltered by the membrane, MBRs may be designed with anoxic and anaerobic tanks to provide biological nutrient removal (BNR) like in conventional activated sludge processes. In particular, an anoxic zone preceding (pre-denitrification) an aerobic zone (nitrification) or a separate post-denitrification reactor can be consider for the removal of nitrogen. In a less common scenario, a single tank can be used for both anoxic and aerobic biological degradation considering the use of extended

intermittent aeration (Nagaoka and Nemoto, 2005; Yeom et al., 1999). Filtration is carried out only in the aerobic phase to take advantage of the anti-fouling properties of the air scouring, since severe fouling has been reported when aeration ceases (Jiang et al., 2005; Psoch and Schiewer, 2005). Moreover, the biological nutrient removal can be design according to a configuration with a preliminary anaerobic zone to remove phosphorus biologically as shown in Figure 2.3 (Drews et al., 2005; Ramphao et al., 2004).

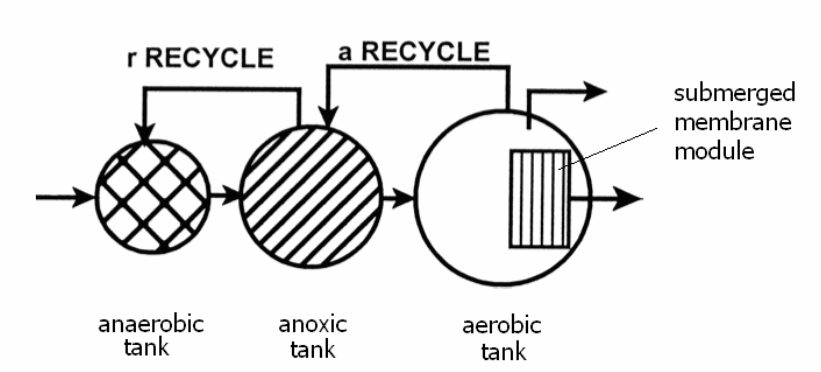

Figure 2.3. The University of Cape Town (UCT) system configuration with membrane solid–liquid separation (submerged membrane module) including a recycle ratio (r) from the anoxic to the anaerobic zone and a recycle ratio (a) from the aerobic to the anoxic zone (Ramphao et al., 2004).

The anaerobic treatment for COD removal is also achievable and enhanced in MBRs. The anaerobic degradation consists of a complex pathway resulting in a combination of series and parallel reactions. Such reactions include hydrolysis, acidogenesis, acetogenesis, and methanogenesis. Pavlostathis and Giraldo-Gomez (1991) proposed that anaerobic digestion metabolising complex substrates can be subdivided into six processes (Figure 2.4):

1. hydrolysis of complex, particulate organic matter;
2. fermentation of amino acids and sugars;
3. anaerobic oxidation of long-chain fatty acids and alcohols;
4. anaerobic oxidation of intermediate short-chain fatty acids (except acetate);
5. homoacetogenesis that involves the production of acetate from hydrogen and carbon dioxide;
6. acetoclastic methanogenesis where acetate is converted to methane and reductive methanogenesis where methane is produced by the reduction of carbon dioxide and hydrogen.

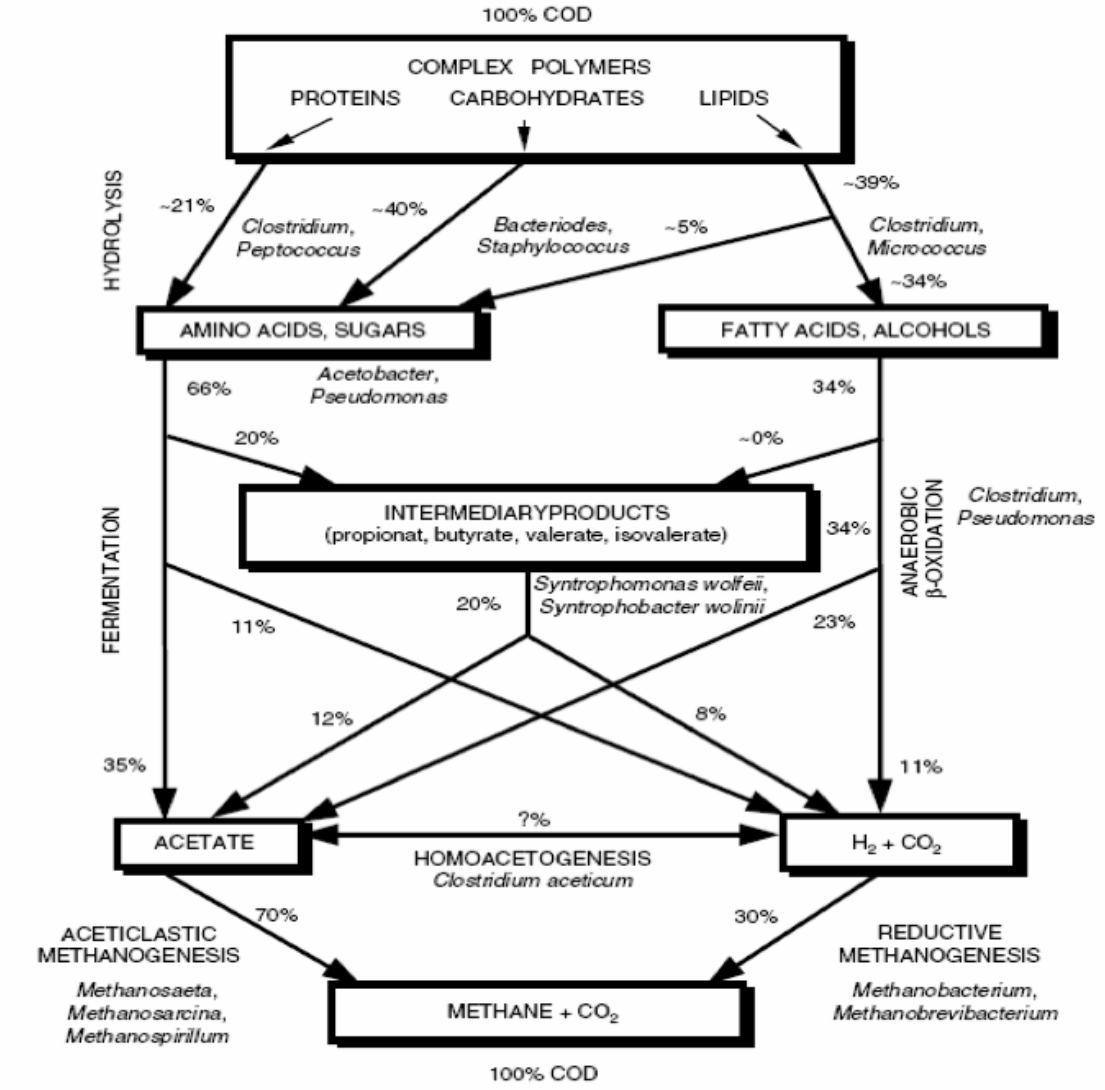

Figure 2.4. Anaerobic degradation pathway (reproduced from Pavlostathis and Giraldo-Gomez, 1991)

Compared with aerobic processes, anaerobic biological treatment is characterised by (Stephenson et al., 2000):

- a lower COD removal (generally 60–90%);
- greater potential for odour generation;
- higher alkalinity necessity;
- a lower energy demand due to the absence of aeration;
- biogas (methane) generation with the possibility of energy production;
- slower microbial growth implying lower sludge production and, on the other hand, longer start up (months vs weeks).

Anaerobic treatment is generally considered for high-strength wastes and where low feed temperatures are less likely to be encountered. Low feed temperatures and strength imply

low biomass growth yield and growth rate so that a high biomass concentration in the reactor is more difficult to maintain, in particular when biomass wash-out from the reactor occur. MBRs circumvent this problem to a large extent, such that the range of anaerobic process operation can be extended to lower limits. This is achieved by the retention of the biomass in the reactor by the membrane independently of the HRT in the same way as for aerobic systems; significant quantities of residual organic matter are hydrolysed and biodegraded as a result (Judd, 2010). With regards to membrane scouring usually achieved by aeration, gas sparging as used in submerged aerobic systems, is more problematic in anaerobic MBRs since air cannot be used routinely. Sparging with head space gas has been shown to be effective for immersed polymeric (Fawehinmi et al., 2004; Stuckey and Hu, 2003) and sidestream ceramic (Kayawake et al., 1991) membranes.

2.2.4 Worldwide research and commercial applications

Membrane bioreactor technology is advancing rapidly both in research and commercial applications. With regards to scientific research, Yang et al. (2006) collected and analyzed a total of 339 scientific papers published in peer-reviewed international journals from 1991 to 2004 exploring four online databases including Web of Science, ScienceDirect, PubMed and EI village. As shown in Figure 2.5, from 1996 to 2001, the numbers of articles published in journals were in the range of 20÷40 a year, whereas they reached 60÷80 a year in the last 3 years of the reference period (2001÷2004).

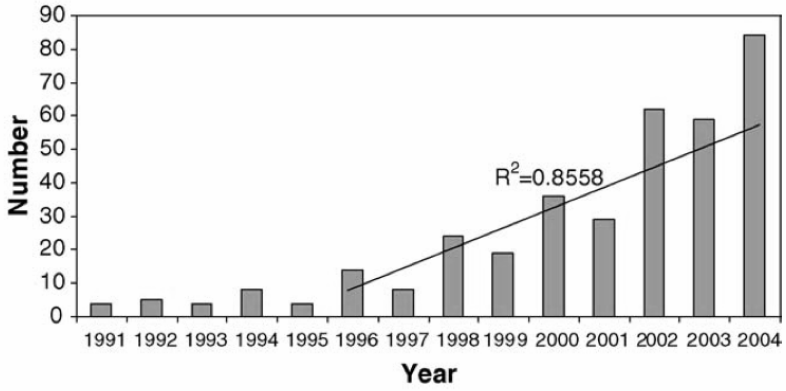

Figure 2.5. Chronological distribution of worldwide, peer-reviewed journal articles involving studies on MBRs (Yang et al., 2006).

Authors from 30 different countries or regions had contributed research articles. However, over 75% of all studies on MBRs were conducted at the following eight countries: UK, USA, Japan, France, China, South Korea, Germany and Canada. Early development efforts on MBR technology were concentrated in UK, France, Japan and South Korea, whereas extensive

research in China and Germany began after 2000. With regards to research topics, the 339 total publications were grouped into six main research areas (Figure 2.6):

- literature and critical reviews (R);
- fundamental aspect including fouling, operation and design parameters, sludge parameters, bacteria characteristics, cost, modelling (FA);
- municipal and domestic wastewater treatment (MWW);
- industrial wastewater and landfill leachate treatment (IWW);
- drinking water treatment (DW);
- others, which includes gas removal, sludge treatment, hydrogen production and gas diffusion (others).

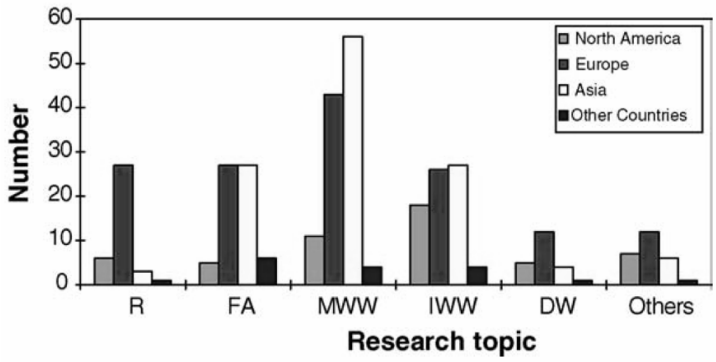

Figure 2.6. Number of papers vs. research topic: R, literature and critical review; FA, fundamental aspects; MWW, municipal/domestic wastewater; IWW, industrial wastewater/landfill leachate; DW, drinking/ground water; others (Yang et al., 2006).

While in Europe and Asia, a larger number of research studies were conducted in the area of municipal wastewater treatment than for industrial wastewater treatment, the situation was reversed in North America. This could be attributed to the high energy, restricted land conditions in Europe and Asia which enabled MBR research and applications to flourish for large flow, low organic strength sources such as municipal wastewater. In contrast, according to the survey of the European MBR market (1990÷2005) performed by Lesjean and Huisjes (2008), a quarter of 409 MBRs considered in the study were related to municipal references (111 plants) and three quarters to industrial applications (298 units). In fact, industrial applications, particularly for high strength, difficult to treat waste streams, however, allowed for the considerations for alternative technologies such as MBRs (Lesjean et al., 2004). In particular, the survey was performed considering MBR units constructed and commissioned up to 2005, with a design capacity greater than 500 p.e. for the municipal applications (i.e. approx. >100 $m^3 d^{-1}$ as nominal flow), or greater than 20 $m^3 d^{-1}$ for the industrial units.

As expected, in Europe the industrial market was the pioneer market in the early 1990s, whereas the municipal market only took off in 1999 (Figure 2.7).

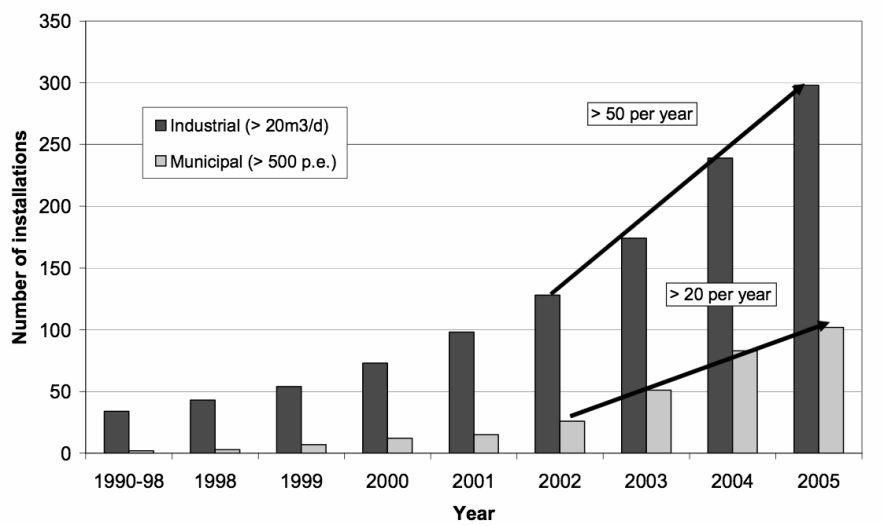

Figure 2.7. Development of industrial and municipal MBR markets in Europe (Lesjean and Huisjes, 2008).

Today, the MBR technology is used for a very broad range of industrial applications presenting carbonaceous wastewater pollution, usually in the range 1,000÷20,000 mg COD L^{-1} (Lesjean and Huisjes, 2008). Apart from landfill leachate treatment, the main applications concern the treatment of wastewaters from origins as diverse as food and beverage processing, chemical plant, automotive plant, fibreglass manufacturing, metal processing plant, dairy plant, computer firm, pharmaceutical plant, cleaning processes, textile industry and laundry (Yang et al., 2006; Lesjean and Huisjes, 2008). Table 2.2 shows the number of MBR plants and the capacity in $m^3 d^{-1}$ related to the industrial applications in North America.

According to Yang et al. (2006) in North America there are four main manufacturers providing membrane bioreactor systems (Table 2.3): Zenon Environmental Inc. (Canada)[1], USFilter (USA)[2], Kubota (Japan) and Mitsubishi-Rayon (Japan). In contrast, only two are relevant in Europe, that is Kubota (Japan) and Zenon Environmental Inc. (Canada) as shown in Figure 2.8 (Lesjean and Huisjes, 2008).

[1] Purchased by General Electric (US).

[2] Purchased by SIEMENS Water Technologies (US).

Table 2.2. MBR installation for industrial wastewater treatment in North America (Yang et al., 2006).

Wastewater resource	Number of plants	Capacity range (m3/d)
Food and beverage processing	10	170-18,925
Chemical plant	7	19-500
Automotive plant	5	114-8,706
Fibreglass manufacturing	2	80-871
Metal processing plant	1	227
Dairy plant	1	908
landfill leachate	1	114
Computer firm	1	1
Pharmaceutical plant	1	72
Not specified	10	19-3,785
Total	39	-

Table 2.3. Number of installation of the four MBR provider in North America (Yang et al., 2006).

Manufacturers	Worldwide	USA	Canada	Mexico
Zenon	331 (204+127)[a]	155 (132+23)	31 (23+8)	6 (1+5)
USFilter	16 (15+1)	13 (13+0)	0	0
Kubota	1538 (1138+400)	51 (48+3)	0	0
Mitsubishi-Rayon	374 (170+204)	2 (2+0)	0	0
Total	2259 (1527+732)	221 (195+26)	31 (23+8)	6 (1+5)

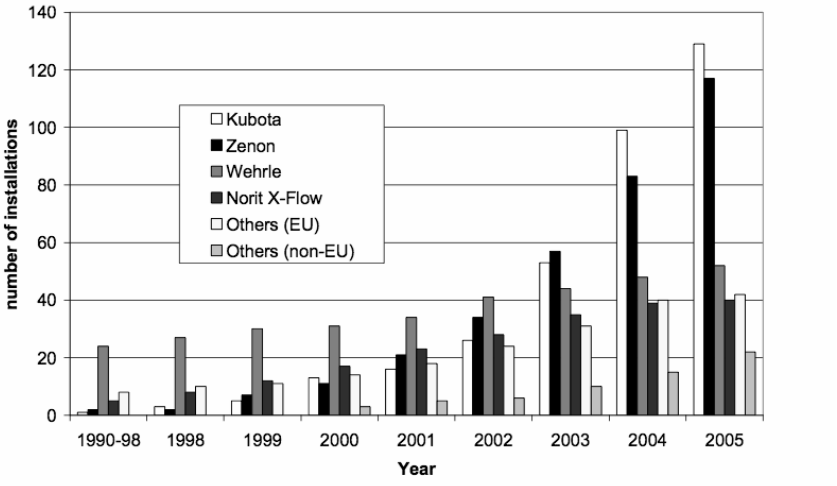

Figure 2.8. Market distribution per supplier in Europe (Lesjean and Huisjes, 2008).

2.3 The membrane filtration process

2.3.1 Membrane processes

Membrane filtration denotes the separation process in which a membrane acts as barrier allowing some physical or chemical components to pass more readily through it than others (perm-selective). The degree of selectivity depends on the membrane pore size (Figure 2.9). The coarsest membrane, associated with microfiltration (MF), can reject particulate matter. The most selective membrane, associated with reverse osmosis (RO), can reject singly charged (i.e. monovalent) ions, such as sodium (Na^{2+}) and chloride (Cl^{-}). On the whole, the four membrane separation processes in which water forms the permeate product are RO, nanofiltration (NF), ultrafiltration (UF) and MF (Judd, 2010). In MF and UF the chemistry of membranes does not play a major role in the separation process (Lonsdale, 1982). However, the chemistry plays an important role in the process performances because of interaction between pollutants/activate sludge components and the membrane (see section 2.4).

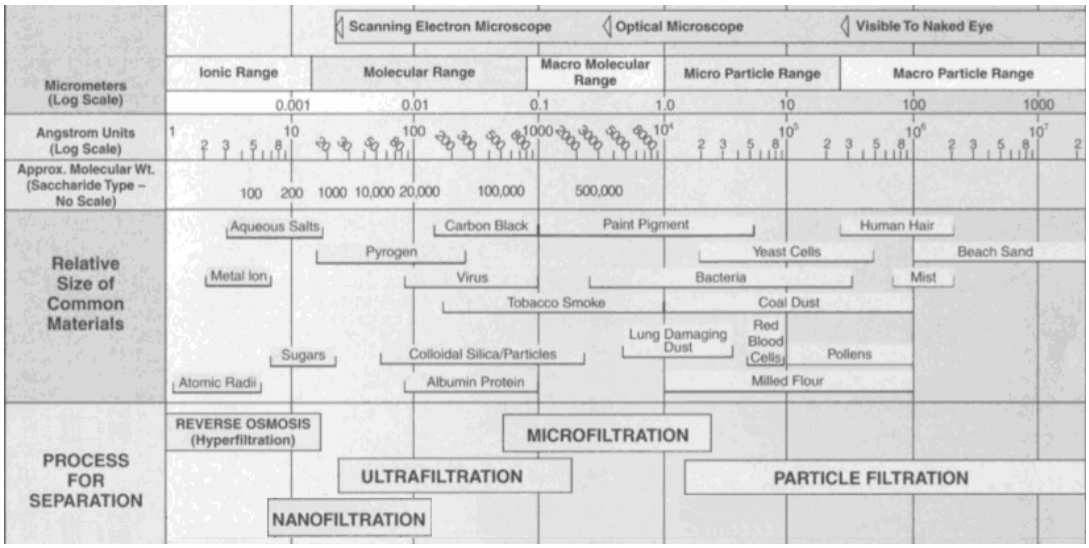

Figure 2.9. The spectrum of particle size (adapted from Svarosky, 2000).

The pore size can be defined either in terms of the effective equivalent pore diameter, normally in μm, or the equivalent mass of the smallest molecule in Daltons (Da) the membrane is capable of rejecting: the molecular weight cut-off (MWCO). Whilst microfiltration membranes are assigned a characteristic pore size in μm, the exact value of which is dependent on the method of measurement; for UF membranes specifically the selectivity is defined by MWCO. As the precise relationship between MWCO and pore size is dependent on the physical and chemical nature of the solute molecule, precise cross-

referencing is impossible (Judd and Jefferson, 2003). Moreover, for a given UF membrane with a distribution of pore sizes there is a relationship between MWCO and the solute rejection coefficient RC (Figure 2.10), defined by:

$$RC = 1 - \frac{C_p}{C_f} \qquad 2.1)$$

where C_f is the concentration of the reference solute in the feed stream and C_p is the concentration in the permeate. The nominal MWCO is normally defined as the molecular weight of a solute for which RC is equal to 0.95. Values of MWCO typically lie in the range 2,000–100,000 Da with values of the order of 10,000 being most common (Richardson, 2002).

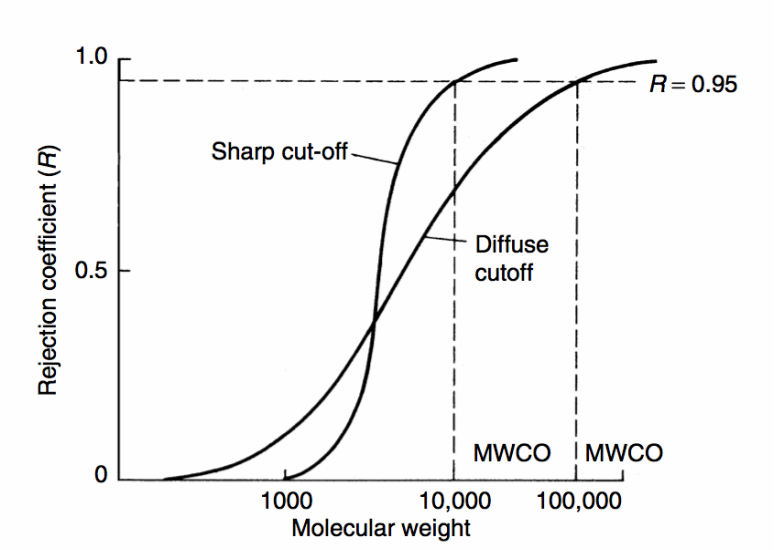

Figure 2.10. Dependence of rejection coefficient on molecular weight for ultrafiltration membranes (Richardson, 2002).

The actual pore size of nanofiltration and reverse osmosis membranes is of little practical consequence, since there are other mechanisms more dominant than simple sieving that determine membrane performance (Judd and Jefferson, 2003). The purification performance of these membranes can only be rated according to their actual demonstrated permselectivity, i.e. the extent of the rejection of key contaminants by the membrane, under some defined set of conditions. NF membranes, which have a charge rejection component, are generally designed to be selective for multivalent rather than univalent ions, whereas RO membranes are designed to reject all species other than water (Judd and Jefferson, 2003).

For the membrane processes identified above, pressure is applied to force water through the membrane operating in one of two modes. If there is no retentate stream then operation is termed "dead-end"; if retentate continuously flows from the module outlet then the

operation is termed cross-flow (Figure 2.11). Cross-flow implies that, for a single passage of feedwater across the membrane, only a fraction is converted to permeate product. This parameter is termed the "conversion" or "recovery". In the case of a dead-end filtration process, the resistance to filtration increases according to particle deposition/adsorption on the membrane (see section 2.4). Air bubbling is used to promote turbulence in order to limit the deposition. For cross-flow processes, this deposition continues until the adhesive forces binding it to the membrane are balanced by the scouring forces of the fluid (either liquid or a combination of air and liquid) passing over the membrane (Judd, 2010).

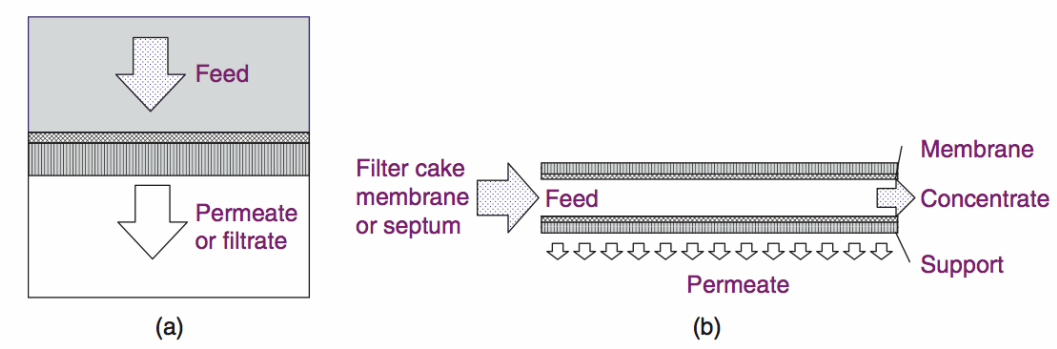

Figure 2.11. Dead-end (a) and Cross-flow (b) filtration (Judd, 2010).

2.3.2 Membrane materials and configurations

There are mainly two different types of membrane according to the material used, even thought metallic membrane filters exist but they are no relevant having very specific applications not related to MBRs:

- polymeric membrane;
- ceramic membrane.

Although featuring superior chemical, thermal and hydraulic resistances, ceramic membranes are not the preferred option for MBR applications due to their high cost (Le-Clech et al., 2006). With regards to polymeric membranes, initially most such membranes were cellulosic in nature. These are now being replaced by polyamide, polysulphone, polycarbonate and most often polyvinylidene fluoride for many MBR membranes. These synthetic polymers have improved chemical stability and better resistance to microbial degradation.

Most MF membranes have a symmetric pore structure, and they can have a porosity as high as 80 per cent. UF membranes have an asymmetric structure comprising a 1–2 μm thick top layer of finest pore size supported by a ~100 μm thick more openly porous matrix, as shown

in Figure 2.12. Such an asymmetric structure is essential if reasonable membrane permeation rates are to be obtained.

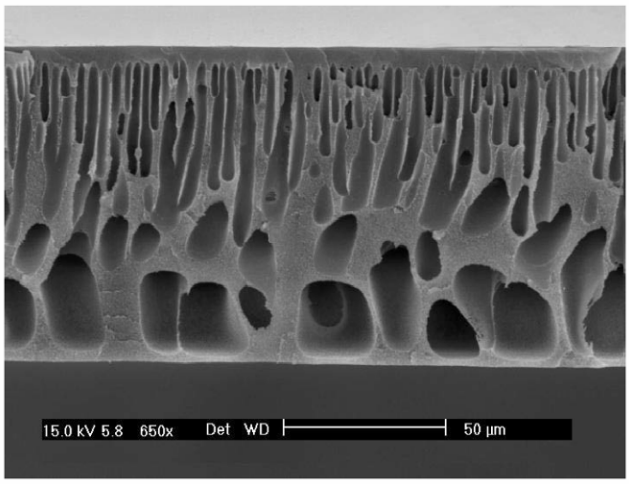

Figure 2.12. Electron micrograph of a section of an asymmetric ultrafiltration membrane showing finely porous "skin" layer on more openly porous supporting matrix (Richardson, 2002).

Polymeric membranes are usually fabricated both to have a high surface porosity and narrow pore size distribution to provide a selective degree of rejection as possible. Moreover, the material would normally have some resistance to thermal and chemical attack, that is, extremes of temperature, pH and/or oxidant concentrations that normally arise when the membrane is chemically cleaned (see section 2.4.1). All the above polymers can be generated by specific manufacturing techniques. However, they are also hydrophobic, which makes the susceptible to fouling by hydrophobic matter in the bioreactor liquors. This normally necessitates surface modification of the base material to produce a hydrophilic surface using specific techniques such as chemical oxidation, organic chemical reaction, plasma treatment or grafting. This modification process and the method for assembling membrane modules (i.e. the configuration of the membrane) from the membrane are proprietary information of the suppliers.

The configuration of the membrane, i.e. the geometry and the way it is mounted and oriented in relation to the flow of water, is crucial in determining the overall process performance. Other practical considerations concern the way in which the membrane elements, that is the individual discrete membrane units themselves, are housed in "shells" to produce modules, the complete vessels through which the water flows.

There are three principal configurations permitting turbulence promotion and an efficient cleaning strategy with regards to MBR processes (Figure 2.13):

1. plate-and-frame/flat sheet (FS)
2. hollow fibre (HF)
3. multitubular (MT)

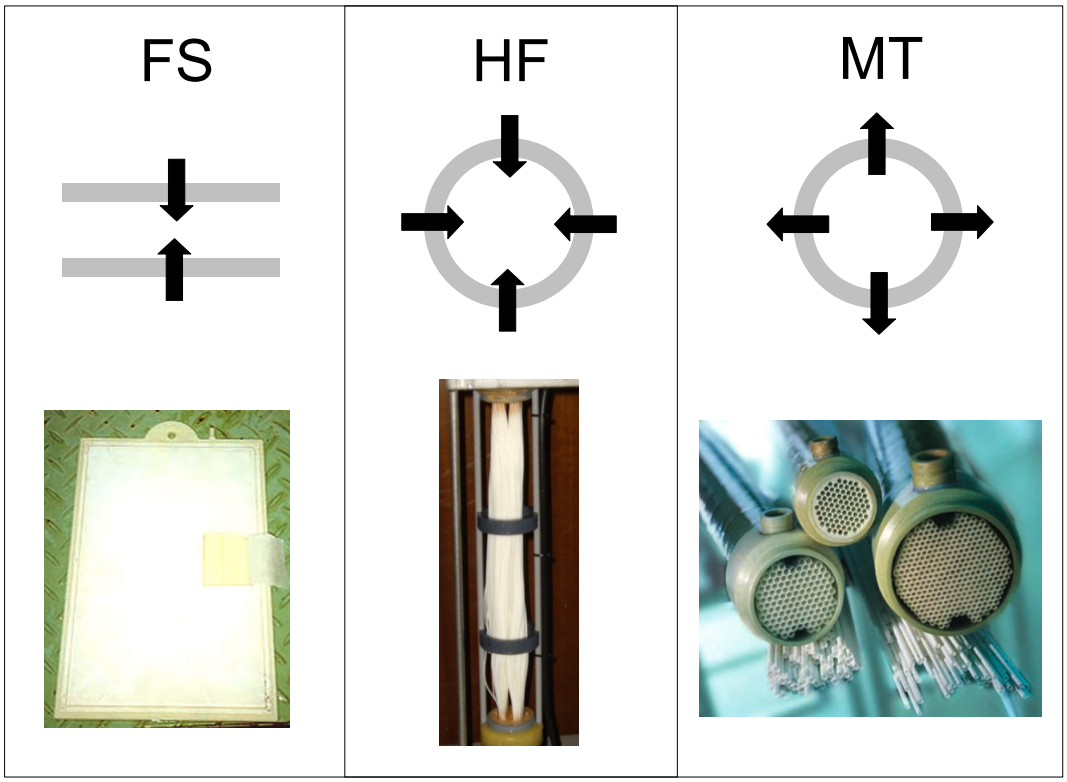

Figure 2.13. Schematic showing flow through membrane and FS (Kubota), HF (SIEMENS Water Technologies), MT modules (Wehrle).

With regards to filtration mode, FS and HF configurations carry out a dead-end outside to in filtration, whereas MT a cross-flow inside to out filtration. Moreover, according to Judd (2007), FS and HF membranes are placed inside the bioreactor in submerged MBRs, whereas MT membranes are placed outside in side-stream MBRs.

An important parameter in MBRs is the interstitial distance, that is defined by:

- the tube diameter for a MT;
- the distance between the filaments for an HF;
- the channel width for an FS.

The membrane packing density of the HF thus becomes critical, since too high a packing density will reduce the interstitial gap to the point where there is a danger of clogging. On the other hand HFs are strong enough not to break or buckle in the case of reversed flow

typically used in physical cleaning procedure performed reversing the flow (i.e. backflushing), at a rate 2–3 times higher than the forward flow, back through the membrane to remove some of the fouling layer on the retentate side (see section 2.4.1). In Table 2.4 advantages and drawbacks of membrane configurations are presented.

Table 2.4. Advantages and drawbacks of FS, HF, MT membrane modules in MBRs (Lesjean et al., 2004; Stephenson et al., 2000).

		FS modules	**HF modules**	**MT modules**
Flux	LMH	15÷25	20÷30	70÷100
Recommended MLSS	g L^{-1}	10÷15	10÷15	15÷30
Fraction of bioreactor occupied by membranes	%	30÷100	10÷40	external set-up (side-stream MBR)
Energy consumption (membrane system only)	KWh m^{-3}	0.3÷0.6	0.3÷0.6	2÷10
Cost	-	high	medium	very high
pH range	-	1÷12	2÷11	1÷13
Temperature range	°C	<60	<40	<100

The cost of hollow-fibre modules are more competitive than flat-sheet modules, but more equipment is required (for example, a backwash system, and fine pre-screen of 1 mm). A broader range of materials is available for flat-sheet and tubular membranes. They can have greater resistance to chemicals and heat, which is sometimes required in difficult industrial applications. As both flat-sheet and hollow-fibre modules are submerged in the aerated biological reactor, and operate with similar MLSS, both systems are expected to fit into the volume of aerated biological tank. However the membrane volume occupied is much greater for flat-sheet systems and therefore it is expected that a larger biological tank is needed, particularly for very large plants.

2.3.3 The general equation of membrane filtration

It is not possible at present to provide an equation, or set of equations, that allows the prediction from first principles of the membrane permeation rate and substances rejection for a given real separation (Richardson, 2002). The general membrane equation is an attempt to state the factors which may be important in determining the membrane permeation rate for pressure driven processes, taking the form of eq. 2.2 (Richardson, 2002).

$$J = \frac{TMP - \Delta\Pi}{\mu_T \cdot R} \qquad 2.2)$$

where J is the flux, i.e. the quantity of liquid phase passing through a unit area of membrane per unit time; TMP is the transmembrane pressure, i.e. is the pressure difference applied across the membrane (it is the driving force for the process); μ_T is the dynamic viscosity of the permeate at temperature T and R is the total hydraulic resistance offered by the membrane and the interfacial region adjacent to it. In SI, J takes the units of $m^3\ m^{-2}\ s^{-1}$, or simply $m\ s^{-1}$, and is occasionally referred to as the permeate or filtration velocity. Other non-SI units used are litres per m^2 per hour (or LMH), which tend to give more accessible numbers (Judd, 2010). TMP takes the units of Pa or bar in non-SI units, viscosity of $Pa\ s^{-1}$ and R of m^{-1}. With regards to $\Delta\Pi$, it represents the difference in osmotic pressure across the membrane and it is relevant only for RO. As a result, considering UF and MF, the general equation takes the form of the Darcy equation for membrane processes:

$$J = \frac{TMP}{\mu_T \cdot R} \qquad 2.3)$$

Since the flux and TMP are interrelated (eq 2.3), membrane filtration processes can be executed in constant flux or in constant pressure operation. However, for conventional pressure-driven water filtration, it is usual to fix the value of the flux and then determine the appropriate value for the TMP (Judd, 2010).

In order to take into account the temperature effect on viscosity eq. 2.4 and 2.5 (Rosenberger et al., 2006) are considered:

$$\mu_T = \mu_{20} \cdot f_T \qquad 2.4)$$

$$f_T = e^{-0.0239 \cdot (T-20)} \qquad 2.5)$$

Moreover the permeability P is introduced with regards to membrane processes as it is an important parameter to measure the effect of fouling during filtration. It is normally quoted as the ratio of flux to TMP (LMH bar^{-1} in non-SI units), hence:

$$P = \frac{J}{TMP} \qquad 2.6)$$

Also, the permeability can be expressed as follows:

$$P = \frac{1}{\mu_{20} \cdot f_T \cdot R} = \frac{1}{\mu_{20} \cdot e^{-0.0239 \cdot (T-20)} \cdot R} \qquad 2.7)$$

As stated in eq. 2.7, the permeability P is correlated to the total hydraulic resistance R. Since fouling implies an increase in R (see section 2.4.1), P is an indicator of the effect of fouling on the filtration process. Unfortunately, P is correlated to the permeate temperature T as well. Consequently, the common approach for comparing hydraulic performances obtained at different temperatures is to normalize the operating flux at a reference temperature. The permeability at a temperature of 20°C (P_{20}) is therefore introduced and calculated as the product of P and the f_t factor (eq. 2.5), hence:

$$P_{20} = P \cdot f_T \qquad 2.8)$$

Also, considering eq. 2.7, P_{20} can be expressed as follows:

$$P_{20} = \frac{1}{\mu_{20} \cdot R} \qquad 2.9)$$

In conclusion, equation 2.9 states that P_{20} is function of R and μ_{20} (permeate viscosity) only. The latter parameter it is considered as a constant value, usually equivalent to the water viscosity at 20°C, that is 0.001 Pa s^{-1}, and consequently P_{20} is an excellent parameter to measure fouling effects over time as its variations depends on R increase.

2.4 Membrane fouling

2.4.1 Fouling mechanisms and cleaning strategies

Membrane fouling refers to various phenomena related to the rejection of solids and their accumulation (deposition and/or adsorption) at the membrane surface (Judd, 2010). As a result, all these phenomena lead to a reduction in the membrane permeability, i.e. a reduction of permeate flux or an increase of transmembrane pressure depending on the operation mode. Such a loss results in larger required membrane surfaces, higher applied pressures or cross-flow velocities/shear rates which both result in higher energy expenditure, or frequent cleanings of the fouled membranes (Drews, 2010).

Fouling can take place through a number of physicochemical and biological mechanisms. Grace (1956) in his early filtration studies found out the link between filtration mechanisms and rejection of contaminants causing fouling, comprising (Figure 2.14):

- complete blocking, i.e. the occlusion of pores by particles with no particle superimposition;
- standard blocking, i.e. the deposit of particles smaller than the membrane pore size onto the pore walls, reducing the pore size, and onto the membrane surface;

- intermediate blocking, i.e. the occlusion of pores by particles with particle superimposition;
- cake filtration, i.e. the deposit of particles larger than the membrane pore size onto the membrane surface.

In MBRs, sludge flocs, colloids and soluble macromolecular species affect these fouling mechanisms. In particular, with regards to foulants comparable with the membrane pores (i.e., colloids), or smaller than the membrane pores (i.e., soluble macromolecular species) adsorption onto the membrane surface (gel layer formation) and within the membrane structure (pore restriction or pore plugging/occlusion) may occur (Judd, 2010; Wang et al., 2008). On the other hand, foulants much larger than the membrane pores (i.e., sludge flocs and colloids) tend to form a cake layer, a porous media with a complex system of interconnected inter-particle voids, on the membrane surface (Meng et al., 2009).

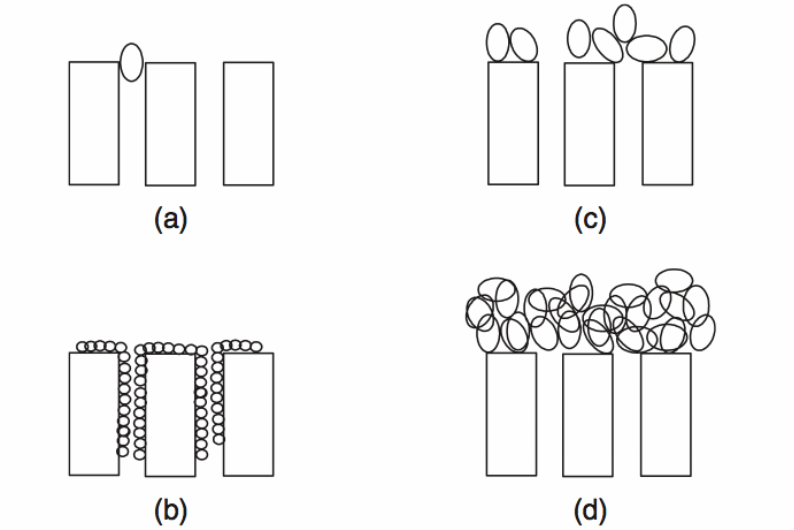

Figure 2.14. Fouling mechanisms: (a) complete blocking, (b) standard blocking, (c) intermediate blocking, (d) cake filtration (Judd, 2010).

For complex fluids such as activated sludge, the interactions between small macromolecules and the cake structure occur by adsorption. As a result macromolecules are entrapped binding the particulates together (Figure 2.15). Moreover, the cake layer acts as a prefilter (Le-Clech et al., 2006).

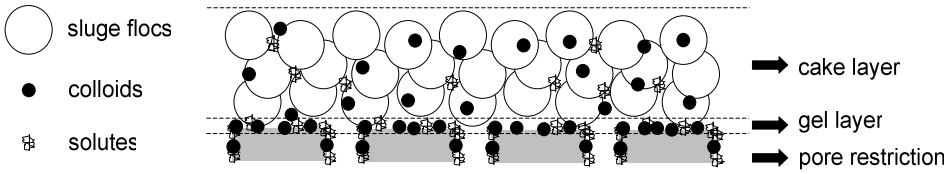

Figure 2.15. Fouling mechanisms in MBRs.

The membrane resistance is fixed, unless its overall permeability is reduced by mixed liquor components accumulated (deposition and/or adsorption) at the membrane surface (Judd, 2010) inducing an increased resistance, usually described through the resistance in series model (Lim and Bai, 2003; Bae and Tak, 2005):

$$R = R_m + R_c + R_f + R_{cp} \qquad 2.10)$$

According to the model the resistance to filtration R (m^{-1}) includes a number of components, namely:

- the membrane resistance R_m (m^{-1});
- the cake layer resistance R_c (m^{-1});
- the fouling resistance caused by pore restriction and adsorption of foulants onto the membrane pore wall or surface (gel layer) R_f (m^{-1});
- the resistance at the membrane/solution interfacial region associated with concentration polarisation R_{cp} (m^{-1}).

The membrane resistance is governed by the membrane material itself, and mainly the pore size, the surface porosity (percentage of the surface area covered by the pores) and the membrane thickness. The cake and fouling resistances are associated with the filtration mechanism, which are then dependent on the membrane and filtered solids characteristics. Moreover, the velocity orthogonal to the surface due to the permeate flux implies the rate of fouling as deposits are brought to the membrane mainly by convective transport. If the correlation between flux and fouling rate was known, an optimisation could be performed (Drews, 2010). Unfortunately, the rate of fouling depends on numerous other and inter-related parameters (see section 2.5). However, fouling resistances can be reduced by promoting turbulence and reducing flux. In particular, as stated above, for side-stream MBRs turbulence can be promoted simply by increasing the cross-flow velocity, whereas for a submerged system this can only reasonably be achieved by increasing the membrane aeration (Judd, 2010).

With regards to concentration polarisation (CP), it is a concept originated from reverse osmosis (RO) describing the tendency of the solute to accumulate at membrane-solution interface within a boundary layer (Evenblij, 2006). Rejected materials nonetheless build up in the region adjacent to membrane, increasing their concentration over the bulk value. The thickness of the boundary layer, on the other hand, is determined entirely by the system hydrodynamics, decreasing in thickness when turbulence is promoted (Judd, 2010). However, for microfiltration and ultrafiltration the resistance by concentration polarization may be negligible because of the membrane high molecular weight cut off (Lim and Bai,

2003, Evenblij, 2006) even though the adsorption followed by retention of macromolecules during filtration could result in CP (Le-Clech et al., 2006).

In general, the membrane resistance R_m only dominates when fouling is either absent or is suppressed by cleaning strategy of membrane, which may be by either physical or chemical means. According to the cleaning strategy, practical definitions of fouling can be defined as follows. Traditionally, the term reversible fouling (or temporary fouling) refers to fouling that can be removed by physical means such as backflushing, that is, reversing the flow, or relaxation, which is simply ceasing permeation whilst continuing to scour the membrane with air bubbles (Judd, 2007). These two techniques may be used in combination, and backflushing may be enhanced by combination with air. On the other hand irreversible fouling (or permanent fouling) refers to fouling which can only be removed by chemical cleaning that is carried out with mineral or organic acids, caustic soda or, more usually in MBRs, sodium hypochlorite, and can be performed either in situ ("cleaning in place") or ex situ. Furthermore, a low concentration of chemical cleaning agent can be added to the backflush water to produce a "chemically enhanced backflush" (Judd, 2007).

Physical cleaning is less onerous than chemical cleaning. It is generally a rapid process lasting no more than 2 min. It demands no chemicals and produces no chemical waste, and also is less likely to incur membrane degradation. On the other hand, it is also less effective than chemical cleaning. In fact, physical cleaning removes gross solids forming sludge cake due to external deposition of flocs (reversible fouling). Chu and Li (2005) reported that the cake layer was not uniformly distributed on the entire surface of all of the membrane fibers. According to the them, the membrane is covered partially by a static sludge cake that could not be removed by the shear force due to aeration. Jeison and van Lier (2007) in a lab-scale study observed that cake formation was removable on a short-term basis, however, cake consolidation was observed when a long-term operation was performed at a flux close to the critical flux. The consolidated cake could not be removed by the backflush cycles, and required an external physical cleaning procedure.

Differently, chemical cleaning removes more tenacious material related mainly to the gel layer formation and the pore restriction phenomenon (irreversible fouling, Drews, 2010). However, the original virgin membrane permeability is never recovered once a membrane is fouled through normal operation. Therefore, there remains a residual resistance which can be defined as irrecoverable fouling (Judd, 2010). It is this fouling which builds up over a number of years and ultimately determines membrane life. According to Drews (2010), one more practical definition, the residual fouling, must be defined since weak chemical cleans (maintenance cleans) are usually performed in full-scale MBRs between two consecutive more intensive chemical cleans (main cleans).

In Table 2.5 all the fouling definitions mentioned above are summarized and related to the cleaning procedure, typical fouling rate and cleaning frequency, whereas Figure 2.16 provides a schematic representation of the effects of cleaning strategies and fouling rates during long-term operation of full-scale MBRs in constant flux and dead-end filtration. In particular, it shows that reversible fouling occurring due to external deposition of material (cake filtration) is mostly removed during filtration breaks (relaxation) or backflush cycles. Nevertheless, physical cleaning does not eliminate a residual fouling that can be removed by maintenance cleans leaving an irreversible fouling base line to be treated by main cleans. Finally, Figure 2.16 shows the irrecoverable fouling base line, occurring over long periods (Drews, 2010).

Table 2.5. Practical fouling definitions and ranges of the different fouling rates occurring at full scale (Kraume et al., 2009; Drews, 2010).

Category	Cleaning type	Fouling rate mbar/min	Time frame
Reversible fouling	physical cleaning	0.1-1	10 min
Residual fouling	weak chemical cleaning (maintenance cleaning)	0.01-0.1	1-2 weeks
Irreversible fouling	strong chemical cleaning (main cleaning)	0.001-0.01	6-12 months
Irrecoverable fouling	-	0.0001-0.001	Years

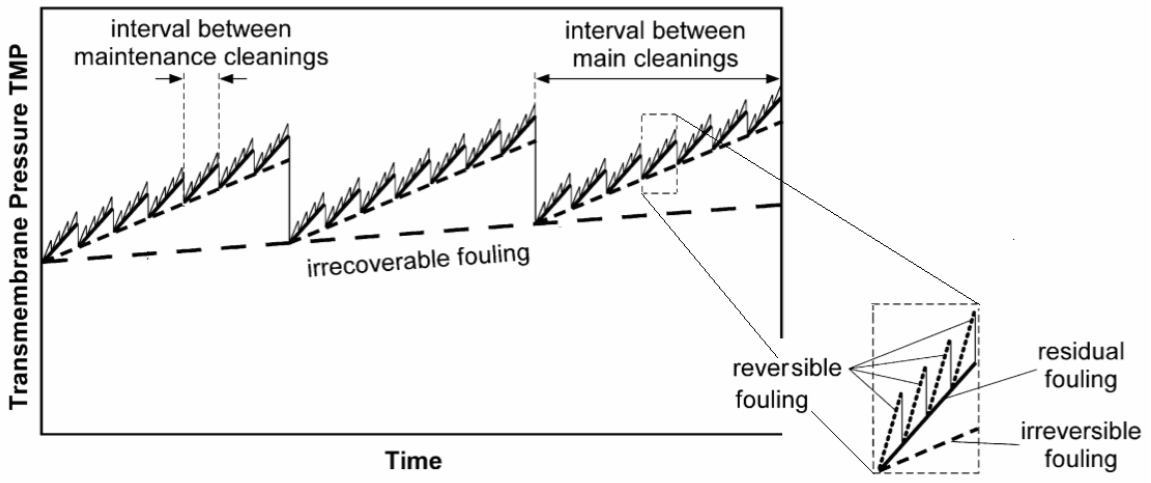

Figure 2.16. Schematic representation of the effects of cleaning strategies and fouling rates during long-term operation of full-scale MBRs in constant flux and dead-end filtration (Kraume et al., 2009; Drews, 2010).

From the viewpoint of components, fouling in MBRs can be classified into three major categories:

- biofouling;
- organic fouling;
- inorganic fouling.

Biofouling refers to the deposition, growth and metabolism of bacteria cells on the membranes (Pang et al., 2005; Wang et al., 2005). Biofouling may start with the deposition of individual cell or cell cluster on the membrane surface, after which the cells multiply in the gel layer. The deposition of bacteria cells can be visualised by techniques such as scanning electron microscopy (SEM), CLSM, atomic force microscopy (AFM), and direct observation through the membrane (DOTM) (Meng et al., 2009). The high shear stress induced by aeration can select the deposition of cells. Some cells can be detached easily by the shear stress, but other ones still adhere to membrane surface tightly. Organic fouling in MBRs refers to the deposition of extracellular biopolymers, proteins and polysaccharides mainly, on the membranes (see section 2.5.1). Due to the small size, the biopolymers can be deposited onto the membranes more readily due to the permeate flow, but they have lower back transport velocity due to lift forces in comparison to large particles (sludge flocs) and they represent the irremovable fouling fraction (see section 2.5.1). In general, membrane fouling in MBRs is mainly governed by biofouling and organic fouling rather than by inorganic fouling, although all of them take place simultaneously during membrane filtration of activated sludge. More recently, Wang et al. (2008) observed that the gel layer was formed by organic substances and inorganic elements such as Mg, Al, Fe, Ca, Si, etc. As a result, the organic foulants coupled with the inorganic precipitation enhance the formation of the gel layer. In particular, the inorganic fouling can act in two ways: chemical precipitation and biological precipitation. Chemical precipitation occurs when the concentration of chemical species exceeds the saturation concentrations due to the concentration polarisation. In contrast, biological precipitation describes the phenomena in which metal ions can be captured by acidic functional groups (R–COOH) forming complexes and building a compact gel layer. The formation of inorganic fouling on MF membranes was also investigated by Kim and Yoon (2010). Authors found that scaling (i.e. inorganic fouling) occurred on the membrane surface significantly in an MBR treating calcium-rich industrial wastewater. Results showed that the coverage of the membrane surface by the inorganic fouling consisted mostly of calcium while the internal fouling within membrane pores due to the scale formation was almost negligible. Most of calcium was rejected on the MF membrane surface as scale formation of calcium carbonate (>90% as rejection).

As inorganic fouling can result in severe irremovable fouling, chemical cleaning using acid solutions is usually performed (Meng et al., 2009). However, according to Kim and Yoon (2010) the sequence sodium hypochlorite-citric acid was more effective than the sequence citric acid-sodium hypochlorite cleaning. In fact, it appeared that the structure of organic compounds combined with calcium became loose by the addition of the sodium hypochlorite, thereby releasing calcium more easily from the membrane by applying the acid cleaning agent.

Finally, struvite (a magnesium ammonium phosphate salt) precipitation can also occur in anaerobic MBRs. However, this seems to play a key role in ceramic membranes rather than in organic membranes where fouling appears to be governed by biological/organic interactions with the membrane rather than by struvite formation (Judd, 2010).

2.4.2 The concepts of critical and sustainable flux

The cake and fouling resistances (R_c and R_f) are related to the convective and back transport provided by turbulence generated as well as the specific particle–membrane interactions. With regards to the convective transport, it is related to the imposed flux and it is obvious that reducing the flux reduces fouling but clearly then impacts directly on capital cost through membrane area demand. According to the idea that reducing fluxes less intense fouling occurs, the critical flux concept was introduced for microfiltration by Field et al. (1995). In particular, the original hypothesis stated that a critical flux exists below which a decline of permeability with time does not occur, and above which fouling is observed. Two distinct forms of the original concept have been defined, with, respectively, no fouling and little fouling occurring at sub-critical operation for the strong and weak forms. In practice, the flux obtained during sub-critical flux (strong form) equates to the clean water flux obtained under the same TMP conditions. In the alternative weak form, the sub-critical flux is the flux rapidly established on start-up and maintained, but does not necessarily equate to the clean water flux (Le-Clech et al., 2006). According to Bacchin et al. (2006) by plotting flux against the TMP (Figure 2.17) it is possible to observe a transition between the linearly pressure-dependent flux and the onset of fouling, where deviation from linearity commences. In particular, the authors stated that the flux at this transition is the critical flux.

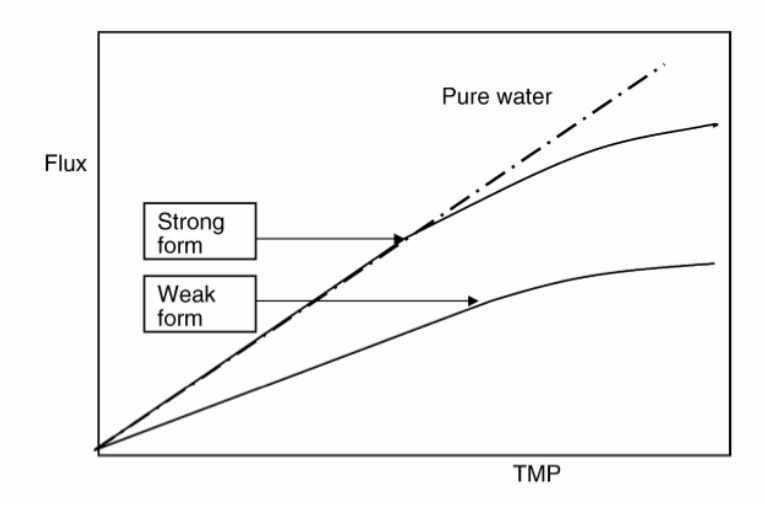

Figure 2.17. Critical flux determination according to the weak and strong definition (Bacchin et al., 2006).

In fluids with both macromolecules and particulates, membrane fouling takes place even at low flux rates, but changes rapidly when the so-called critical flux (in its weak form) is reached (Le-Clech et al., 2006) depending on the back transport provided by the turbulence generated and the specific particles–membrane interactions, which are affected by charge and hydrophobicity.

In theory, critical flux can be mathematically derived by force balances, i.e., as long as drag forces do not exceed dispersive (diffusive, shear induced lift, etc.) forces, a particle does not deposit on the membrane. In MBRs with their complex fluids, other processes like adsorption or aggregation of particles also occur. Therefore, the governing forces are difficult to quantify and also subject to changes over time which makes a comprehensive mechanistic mathematical model of critical flux in MBRs impossible (Drews, 2010).

Given this limitations of applying particle hydrodynamics to the identification of the critical flux in complex systems, recourse generally has to be made to experimental determination (Judd, 2010). The most common practice for the experimental critical flux determination is to incrementally increase the flux for a fixed duration for each increment, giving a stable TMP at low flux but an ever-increasing rate of TMP increase at higher fluxes.

This flux-step method (Figure 2.18a) defines the highest flux for which TMP remains stable as the critical flux. This method is preferred over the corresponding TMP-step method since the former provides a better control of the flow of material deposition on the membrane surface, as the convective flow of solute towards the membrane is constant during the run (Defrance and Jaffrin, 1999). No single protocol has been agreed for critical flux measurement (Judd, 2010) and therefore the precise identification of the critical flux value from flux-stepping experiments strongly depends upon the conditions used (step duration,

step height, initial state of the membrane; Le-Clech et al., 2003a). Moreover, since zero rate of TMP increase is generally not attained in filtration of complex fluids (Figure 2.19), such as sludge in MBRs, the critical flux can be evaluated taken the highest flux at which dTMP/dt (or dP/dt as it appears in Figure 2.19) is smaller than an arbitrary value such as 0.1 mbar min^{-1} (Le-Clech et al., 2003a). Apart from the variable experimental set-ups and criteria, different flux-stepping procedures have been introduced. In an attempt to obtain filtration mechanisms closer to real plant operation, relaxation breaks have been introduced (Figure 2.18b). Moreover, to study the reversibility of fouling some steps have been introduced returning to a previous, smaller flux (Figure 2.18c, Figure 2.18d, Figure 2.18e).

In stepping experiments without breaks, Wu et al. (2008) found that an increase of step length or height lowers the critical flux. On the one hand, steps should be small to enable an accurate determination of Jc (inherent measurement accuracy: ±step height). On the other hand, using many small steps extends the duration of the experiment so that fouling propensity might change as a result of continuous pumping, or lack of oxygen and substrate. Also, the effects of ionic strength and pH on adsorptive or cohesive forces and polymer folding also need to be considered (Bacchin et al., 2006).

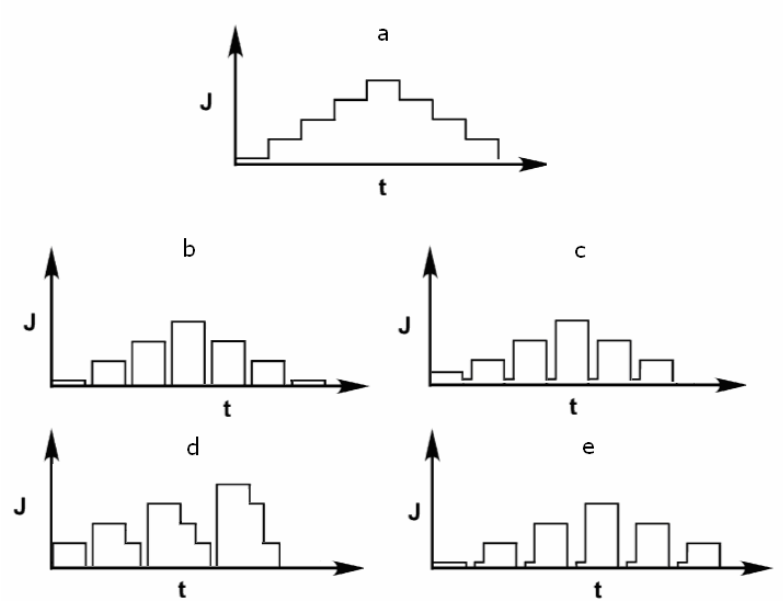

Figure 2.18. Flux step method procedures: a) standard procedure (Le-Clech et al., 2003a), b) modification by De la Torre et al., 2008, c) modification by Van der Marel et al. (2009), d) modification by Koseoglu et al. (2008), e) modification by De la Torre et al., 2008.

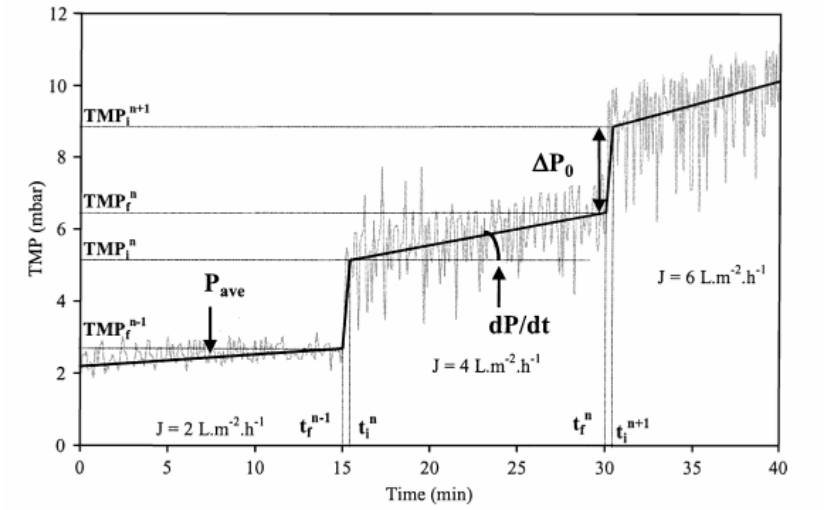

Figure 2.19. TMP evolution over time during the first steps of the standard procedure for critical flux evaluation (2 LMH, 4 LMH and 6 LMH) and relevant pressure parameters according to Le-Clech et al. (2003a).

It is now generally accepted that the short-term determination methods for the critical flux (especially the flux-stepping approach) does not yield predictive absolute permeability data for extended operation of complex fluids (Le-Clech et al., 2006). In particular, since the value of Jc is determined during short-term experiments, it is expected that Jc indicates the deposition of suspended solids rather than colloidal and soluble materials (Le-Clech et al., 2006). Within the last few years, it has become apparent from bench and pilot-scale studies that irreversible fouling of MBR membranes can take place at operation well below the critical flux (Pollice et al., 2005). Sub-critical flux fouling appears to be characterised by a sudden discontinuity of the TMP, known as TMP jump (Cho and Fane, 2002), also at low flux operation after some extended time period (Brookes et al., 2004; Ognier et al., 2001; Wen et al., 2004).

As a consequence, critical flux has become simply a term for a certain flux at which changes in the system behaviour can be observed in flux-stepping experiments (Drews, 2010). In spite of the arbitrary aspect of this method, critical flux determination by this short-term experiment remains an efficient approach to assess the fouling behaviour of a given filtration system and to compare different operating conditions. Interestingly, this method was recently used as a standard test to assess the fouling propensity of an MBR on a daily basis (Fan et al., 2006). This approach allows the plotting of fouling intensity against an MBR parameter such as biomass characteristics. The challenge remains to use short-term experimental data to project long-term fouling characteristics. Thus, the focus may be shifted to considering a "sustainable flux" instead of critical flux where reversibility of the

foulant deposition and global operational constraints for productivity and costs are taken into account (Le-Clech et al., 2006). In particular, the sustainable flux is defined as the flux for which the TMP increases gradually at an acceptable rate, to limit rapid and severe membrane fouling, such that chemical cleaning is not necessary (Ng et al., 2005).

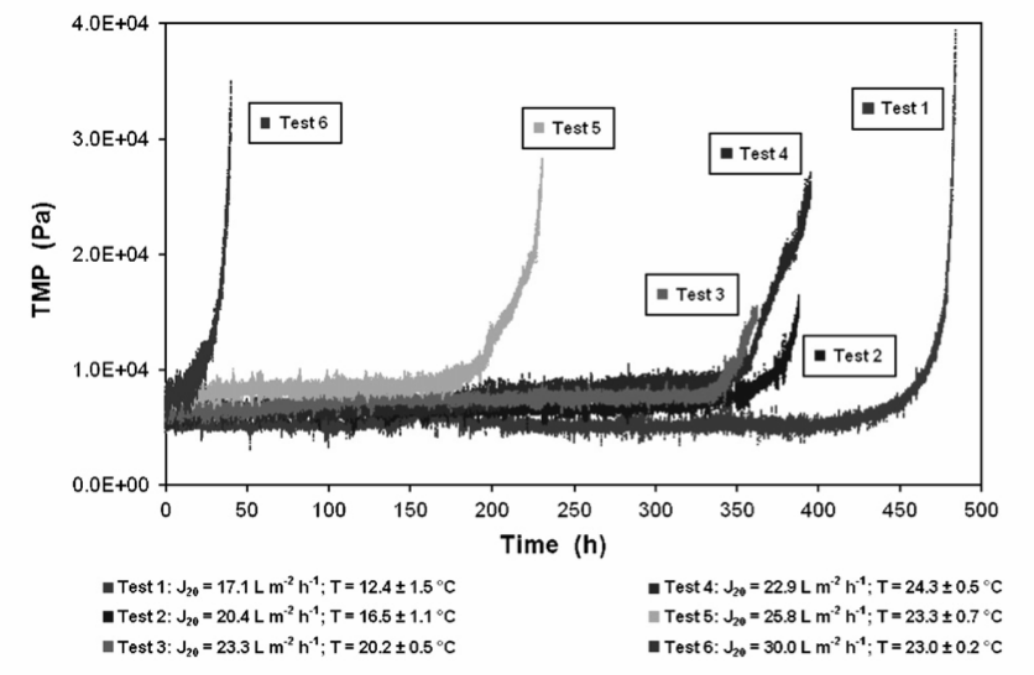

Figure 2.20. TMP profiles for the long-term trials (Guglielmi et al., 2007).

The rate of TMP increase and the period of filtration before chemical cleaning is required are left to the operators discretion, and therefore a more detailed definition of sustainable flux cannot be possible (Le-Clech et al., 2006). While critical flux was mainly determined during short-term experiments, sustainable flux can only be assessed through longer filtration periods. However, sustainable flux can also be defined as sub-critical flux by default. In such a system, not only the flux value is of importance but also the strategies used to maintain this given flux (Le-Clech et al., 2006). Therefore, it might be more accurate to speak of an "apparent sustainable flux" when values are obtained from short-term lab trials. For instance, Guglielmi et al. (2007) were able to verify the reliability of short-term flux-stepping trials over a longer period by estimating the sustainability time (i.e., the time before TMP jump occurs) by mathematical modelling and verifying it experimentally.

2.4.3 Sub-critical fouling

As described above, fouling occurs in MBRs also at fluxes lower than the critical flux. In particular, a three stage fouling evolution over time has been proposed as shown in Figure

2.21 (Cho and Fane, 2002; Zhang et al., 2006). In a first step (stage 1) an initial rapid rise in TMP can be observed due to adsorption of solutes/particles onto the new membranes. In fact, a monolayer of particles and solutes can grow even in the absence of permeation flux leading to an additional hydraulic resistance (Bacchin et al., 2006). In a second stage (stage 2) a long-term weak rise in TMP occurs, mainly due to the accumulation of organic macromolecules into pores and/or onto the membrane surface leading to progressive increase of resistance to filtration (Pollice et al., 2005). Differently, in stage 3 a sharp increase in TMP takes place (i.e., the TMP jump). The TMP jump is believed to be the consequence of severe membrane fouling. Cho and Fane (2002) attributed the TMP jump to the changes in the local flux due to fouling eventually causing local fluxes to be higher than the critical flux. According to this concept, a number of models have been proposed to assess the critical time (or sustainability time) above which the development of the TMP jump comes out (Ognier et al., 2004; Ye et al., 2005; Ye et al., 2006).

In addition, Zhang et al. (2006) reported that the sudden jump was possibly not only due to the local flux effect, but also caused by sudden changes in the gel layer or cake layer structure. Moreover, according to the authors, due to oxygen transfer limitation, the bacteria causing biofouling tend to die and release extracellular biopolymers. This fact was also confirmed by Hwang et al. (2008).

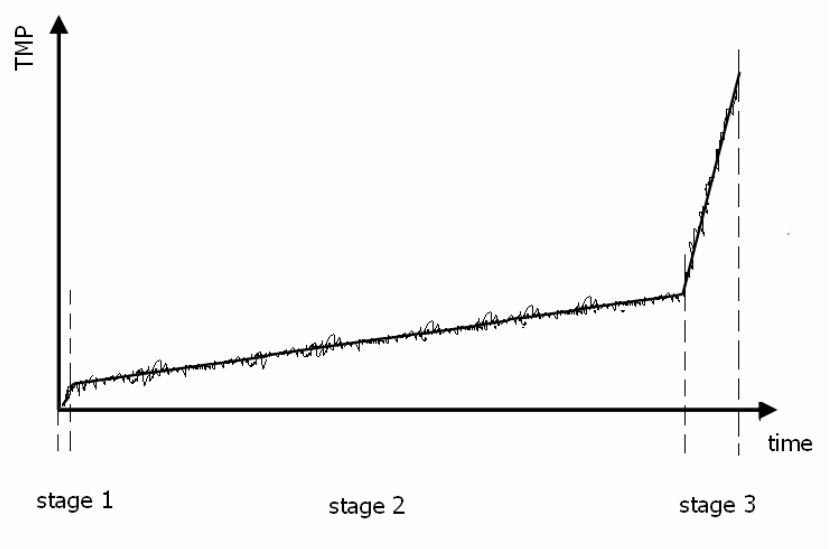

Figure 2.21. Stages of TMP profiles for the long-term trials (Meng et al., 2009).

Even thought the TMP jump is more frequently observed in small-scale experiments (Pollice et al., 2005) when TMP reaches a threshold value the execution of a main chemical cleaning in necessary to recover the membrane permeability. But, chemical cleaning for the elimination of irremovable fouling should be limited to a minimum frequency because they

may shorten the membrane lifetime and disposal of spent chemical agents causes environmental problem (Yamamura et al., 2007; Drews, 2010). In order to reach this goal, factors affecting membrane fouling must be well understood and control strategies must be implemented as well. In particular, the major factors affecting membrane fouling and control strategies to reduce chemical cleanings frequency are described in section 2.5 and 2.6, respectively.

2.5 Factors affecting membrane fouling

Factors affecting membrane fouling can be classified in five groups (Le-Clech et al., 2006; Meng et al., 2009; Drews, 2010):

1. membrane characteristics;
2. feedwater characteristics;
3. biomass characteristics;
4. hydrodynamic conditions;
5. operating conditions.

With regards to membrane characteristics, pore size, roughness, hydrophobicity and membrane materials are the most relevant aspects. However, these parameters are expected to play only a minor role during extended filtration periods. Once initially fouled, the membrane characteristics would become secondary to those of the sludge materials covering the membrane surface (Le-Clech et al., 2006). The complex interactions between all the other aspects (aspect 2 to aspect 5) complicate the perception of membrane fouling (Meng et al., 2009). Moreover, while some of these parameters have a direct influence on MBR fouling, others result in subsequent effects on the phenomena. In particular, for a given MBR process, the fouling behaviour is directly determined by sludge characteristics and hydrodynamic conditions. But, operating conditions (i.e., SRT, process temperature, dissolved oxygen, etc.) and feedwater have indirect actions on membrane fouling by modifying biomass characteristics (Meng et al., 2009). In paragraph 2.5.1 the major fouling factors including extracellular polymeric substances, biomass physical characteristics (concentration, floc size, viscosity), and hydrodynamic conditions are discussed. Moreover, the influence of operating conditions and feed water characteristics on fouling are discussed in paragraph 2.5.2. Nevertheless, due to the complexity of the biological system results presented are often inconsistent and contradictory.

2.5.1 Factors directly affecting membrane fouling: biomass characteristics and hydrodynamics conditions

Direct effects on fouling provided by extracellular polymeric substances, biomass physical characteristics and hydrodynamic conditions are discussed in this section.

Extracellular biopolymers. Extracellular biopolymers can be classified in extracellular polymeric substances (EPS) when they are bound to the flocs or soluble microbial products (SMP) when freely suspended/dissolved in the supernatant as soluble and colloidal compounds (Drews, 2010). In particular, EPS consist of proteins, polysaccharides, nucleic acids, lipids, humic acids, etc. which are located at or outside the cell surface. SMP can be defined as the pool of organic compounds that are released into solution from substrate metabolism (usually with biomass growth) and biomass decay (Barker and Stuckey, 1999). Thus, SMP can be subdivided into two categories (Laspidou and Rittmann, 2002): substrate-utilisation-associated products (UAP), which are produced directly during substrate metabolism, and biomass-associated products (BAP), which are formed from biomass, presumably as part of decay. The interrelations between bound EPS and SMP are very complex. A unified theory for EPS and SMP was proposed by Laspidou and Rittmann (2002), who pointed out that cells use electrons from the electron-donor substrate to build active biomass and EPS and UAP in the process and part of the EPS can be hydrolysed to BAP. Moreover, some SMP can be utilised by active biomass as recycled electron donors; and some can be adsorbed by the biomass flocs and then, become EPS. In addition, the generation of EPS and UAP is in proportion to substrate utilisation.

It has been now widely accepted that the terms "extracellular polymeric substances" can be referred to both bound to the flocs compounds and freely suspended/dissolved substances in the supernatant (Le-Clech et al., 2006). Therefore, terms such as "bound-EPS" and "soluble-EPS" (term utilized instead of SMP) have been introduce (Meng et al., 2009) and therefore the acronym "EPS" is used as a general and comprehensive concept of biopolymers including different classes of macromolecules such as polysaccharides, proteins, nucleic acids, (phosphor-)lipids and other polymeric compounds which have been found in the intercellular space of microbial aggregates and in the supernatant (Flemming and Wingender, 2001). By definition, all these groups of compounds are produced and excreted by microorganisms. However, what is analysed as bound-EPS and soluble-EPS by commonly agreed methods is not necessarily of microbial origin but can also be terrestrial or man made (Judd, 2007). Therefore, the exact definitions of bound-EPS and soluble-EPS are directly dependant of the methods used to obtain and characterize chemically these solutions. With

regards to bound-EPS, so far, no standard method of extraction exists, making comparison between research groups difficult. Methods of extraction include centrifugation with formaldehyde (Judd, 2007), cation exchange resin (Frolund et al., 1996; Gorner et al., 2003; Jang et al., 2005) and heating methods (Morgan et al., 1990), that are sometimes preferred because of their simplicity and cheapness. As for soluble-EPS, several methods of separating the water phase (i.e., the supernatant) from the biomass have been proposed including centrifugation followed by filtration and simple filtration. Le-Clech et al. (2006) suggested to filter the solution with, at least, a 1.2 μm filter in order to remove colloids. Typically, the solutions containing bound-EPS and soluble-EPS are then characterized by the relative content of protein and carbohydrate, measured by photometric methods (Lowry et al., 1951 and Dubois et al., 1956 methods, respectively) since protein and carbohydrate are assumed to be the major fractions that contribute to fouling (Drews, 2010). Table 2.6 shows typical concentration of proteins, that have generally a hydrophobic tendency, and carbohydrates, more hydrophilic, in bound and soluble extracellular polymeric substances (Liu and Fang, 2003).

Table 2.6. Concentration of the bound-EPS and soluble-EPS components in different MBR systems (Le-Clech et al., 2006).

bound-EPS (mg gSS^{-1})		**soluble-EPS** (mg L^{-1})		**Details**	**References**
P	C	P	C		
25÷30	7÷8	8	25	Real ww, SRT=10d	Cabassud et al. (2004)
29	36	n.d.	n.d.	Syntethic ww	Ahn et al. (2005)
120	40	n.d.	n.d.	Syntethic ww, SRT=∞	Gao et al. (2004)
31÷116	6÷15	0.5÷9*	n.d. ÷10*	Four pilot-scale plants, municipal	Brookes et al. (2003)
11÷46	12÷40	0.5÷1*	n.d.	Three full-scale plants, municipal	
25	9	0.5*	n.d.	Full-scale plants, industrial	
30÷36	33÷28	n.d.	n.d.	SRT=20÷60d	Lee et al. (2003)
73	30	n.d.	n.d.	Syntethic ww, SRT=∞	Le-Clech et al. (2003b)
60	17	n.d.	n.d.	Real ww, SRT=∞	
116÷101	22÷24	4.5÷6	4.5÷3.7	Syntethic ww, SRT=20d	Ji and Zhou (2006)
n.d.	n.d.	n.d.	3÷14	Real ww, SRT=8d	Rosenberger et al. (2006)
n.d.	n.d.	n.d.	2÷6.5	Real ww, SRT=15d	
n.d.	n.d.	23	7	Real ww	Evenblij and van der Graaf (2004)
n.d.	n.d.	10÷34	5÷33	Real ww, SRT=40-8d	Grelier et al. (2005)

n.d. = non-detected, P=proteins, C=carbohydrates, * = data in mg g $MLSS^{-1}$

Moreover, the EPS solutions can also be characterized by 2D-fluorescence or in terms of TOC or COD level and, less frequently, aromaticity or hydrophobicity (Le-Clech et al., 2006; EC, 2007; Jiang et al., 2008). Also, several chromatographic methods have been applied to give "fingerprint" information on foulants such as size exclusion chromatography (SEC) and gel filtration/permeation chromatography. Moreover, in order to identify specific proteins and thus to track down their origin, gel electrophoresis has recently been adapted to activated sludge samples (Kuhn et al., 2007) and Fourier transform infrared (FTIR) spectroscopy has been applied to identify functional groups of organic molecules adsorbed on membrane surfaces (Nataraj et al., 2008; Loh et al., 2009; Wang et al., 2009).

Bound-EPS have been reported not only as major sludge floc components keeping bacteria in a three-dimensional matrix, but also as important key factor in MBRs fouling. Cho et al. (2005) found a close relationship between the bound-EPS and the specific cake resistance and established a functional equation in which the specific cake resistance was proportional to the bound-EPS concentration. Ahmed et al. (2007) also observed that as bound-EPS concentration rose, the specific cake resistance increased, and this consequently resulted in the rise of TMP. On the contrary, since the EPS matrix plays a major role in the hydrophobic interactions among microbial cells and thus in the floc formation, it was proposed that a decrease in EPS levels may cause floc deterioration (Liu and Fang, 2004) and consequently the repercussion of low EPS level, and correlated floc deterioration, on cake resistance may be detrimental for the MBR performances. A confirmation of this theory can be found in experimental results obtained by Jang et al. (2005). Furthermore, bound-EPS was found to have no effect on the specific resistance below 20 and above 80 mg g $MLVSS^{-1}$, but played a significant role on MBR fouling between these two limits (Le-Clech et al., 2006). This was confirmed by another study reporting no clear relation between bound-EPS and membrane fouling for concentrations lower than 10 mg EPS g $MLSS^{-1}$ (Meng et al. 2006). Moreover, Ramesh et al. (2006) fractionated bound EPS into loosely bound EPS and tightly bound EPS, and proved that the fouling cake resistance was primarily caused by the loosely bound EPS, but not by the tightly bound EPS. The loosely bound EPS correlates with the performance of flocculation and sedimentation processes (Li and Yang, 2007). An important study by Ji and Zhou (2006) indicated that both composition and quantity of attached extracellular polymeric substances on the membrane surface influenced membrane fouling, and the total biopolymers in sludge suspension played a more important role than bound-EPS in reflecting the extent of membrane fouling. Despite the fact that the research results on bound-EPS are different from each other, bound-EPS are closely connected to sludge characteristics such as sludge volume index, flocculation ability, hydrophobicity, surface charge, sludge viscosity (Meng et al., 2009).

With regards to soluble-EPS in MBRs, they impact on membrane fouling significantly, and concentration and composition would determine their fouling propensity (Meng et al., 2009). In particular, during filtration, they adsorb onto the membrane surface, block membrane pores and form a gel structure where they provide a hydraulic resistance to permeate flow and also a possible nutrient source for biofilm formation (Chang et al., 2002). Although the influence of dissolved matter has been studied for a decade, the concept of soluble-EPS fouling in MBRs is relatively new as no report on soluble-EPS levels existed for MBRs prior to 2001 (Chang et al., 2002). Now, soluble-EPS are maybe the fraction now most often mentioned in relation with fouling. Rosenberger et al. (2006) reported that soluble-EPS were found to impact on fouling and to cause the difference in membrane performance between two identical MBRs. Iritani et al. (2007) reported that they were the controlling factor in microfiltration of an anaerobic activated sludge. Wang and Li (2008), making comparison between permeate and supernatant, introduced the new concept of biopolymer clusters (BPCs). BPCs are defined as organic compounds forming cluster, ranging from 2.5 to 60 μm in size (Sun et al., 2008), on membrane surface. BPCs, evaluated as the difference in TOC concentration between permeate and supernatant, were found weakly correlated to TMP in trials with a lab-scale MBR fed on synthetic wastewater. Lesjean et al. (2005) conducted a different comparison between permeate and supernatant solutions. Assuming that the materials observed in the biological supernatant and not in the permeate solution were responsible for MBR fouling, this group clearly revealed the higher concentration of carbohydrates, proteins and organic colloids in the MBR supernatant compared to those in the permeate. Since, direct relationships between the carbohydrate level in soluble-EPS solution with fouling rate (Lesjean et al., 2005), filtration index and CST (Evenblij et al., 2005a; Grelier et al., 2005; Tarnacki et al., 2005), critical flux tests (Le-Clech et al., 2005b), and specific flux (Rosenberger et al., 2005) have been clearly described, this reveals the carbohydrates in soluble-EPS as the major foulant indicator in MBR systems.

According to Jarusutthirak et al. (2002) and Rosenberger et al. (2005) mainly colloidal polysaccharides have been considered to cause fouling, but sometimes also soluble polysaccharides were found to cause more fouling than colloidal ones (Wu and Huang, 2009). So far, the effect of the protein fraction contained in the soluble-EPS solution on MBR fouling has been more rarely reported. Since a significant amount of proteins is retained by the membrane (from 15%, Evenblij and van der Graaf, 2004, to 90%, Drews et al., 2006, it is expected that this plays a role in MBR fouling. This was recently confirmed by the value of specific resistance increasing by a factor of 10 as the proteins in soluble-EPS increased from 30 to 100 mg L^{-1} (Hernandez Rojas et al., 2005). However, in two separate studies, analyses of the fouling layer have revealed a higher concentration of carbohydrate and lower

concentration of proteins compared to their levels in the activated sludge (Zhang et al., 2006).

With a smaller MW, humic substances contained in the liquid phase are not retained by the membrane, and therefore Drews et al. (2006) supposed that humic substances were not significantly participate to MBR fouling. On the other hand, Lyko et al. (2007) found an important influence of these compounds on membrane fouling.

With regards to the fouling property of soluble-EPS some contradictions are present in the literature. For example, while a linear relationship between fouling rate and soluble/colloidal polysaccharides concentration was reported for a hollow fibre MBR operated at SRT = 8 d (Lesjean et al., 2005; Rosenberger et al., 2006), the fouling rate cannot always be correlated with the SMP concentration (Drews et al., 2006, 2008). Moreover, data collected from several MBRs across Europe confirm that soluble-EPS concentration does not correlate with fouling propensity of the sludge (Moreau et al., 2009).

Biomass physical characteristics. As stated above, biomass characteristics are related to bound-EPS rather than soluble-EPS content. In fact, although some authors found the soluble-EPS have great impact on some characteristics of sludge, such as filterability (Rosenberger and Kraume, 2003), other studies observed that a decreasing filterability did not necessarily correspond with an increase of soluble-EPS concentrations (Geilvoet et al., 2007).

Biomass characteristics relevant in MBR fouling could be MLSS concentration, sludge viscosity, flocs hydrophobicity and floc size.

According to the conventional cake filtration theory, MLSS concentration would impact directly fouling increasing the cake layer resistance R_c (m^{-1}), as follows (Shimizu et al., 1993; Chang et al., 2001):

$$R_c = \alpha \cdot \frac{V \cdot C_b}{S} \qquad 2.11)$$

where α is the specific cake resistance (m kg^{-1}), V the permeate volume (m^3), S the membrane surface area (m^2), whereas C_b represents bulk MLSS concentration (kg m^{-3}). However, equation 2.11 does not consider the effect of bubbling adopted in MBRs contrasting the cake layer formation as mathematically described and modelled elsewhere (Di Bella et al., 2008).

Experimentally, controversial findings about the effect of MLSS concentration on membrane filtration have been reported so far. In fact, the increase in MLSS concentration seems to have a mostly negative impact (higher TMP or lower flux) (Cicek et al., 1999; Chang et al.,

2005), but some authors have reported positive impact (Defrance et al., 1999; Brookes et al., 2006), and some observed insignificant impact (Hong et al., 2002; Le-Clech et al., 2003b; Lesjean et al., 2005). Moreover, according to Bin et al. (2004), at high concentration the creation of a rapid fouling cake layer potentially protecting the membrane occurs, whereas progressive pore restriction created by colloids and macromolecules was thought to take place at lower MLSS concentration.

All these controversial findings about MLSS concentration can be due to the fact that the majority of parameters cannot be changed independent of each other, particularly with regards to sludge rheology (Drew, 2010). For instance, sludge viscosity is closely related to MLSS and a critical MLSS concentration exists under which the viscosity remains low and rises only slowly with the concentration. Above this critical value, suspension viscosity tends to increase exponentially with the solids concentration (Itonaga et al., 2004). The importance of viscosity is that it modifies bubble size and can dampen the movement of hollow fibers in submerged bundles (Wicaksana et al,. 2006). The net result of this phenomenon would be a greater rate of fouling. On the whole, a threshold concentration above which membrane filtration occurs with difficulties exists. For instance, a MLSS concentration of 30 g L^{-1} was reported threshold value with negative influence on membrane hydraulics (Lubbecke et al., 1995).

With regards to flocs characteristics, the relative hydrophobicity of flocs can be directly measured by bacterial adhesion to hydrocarbons (hexane), or estimated by contact angle determination (Yu et al., 2005; Le-clech et al., 2006). Hydrophobic flocs lead to high flocculation propensity and low interaction with the (generally) hydrophilic membrane. Low hydrophobicity of flocs or bound-EPS is typically assumed to cause higher fouling because of floc deterioration and consequent increase of the resistance to filtration due to cake layer formation (Jang et al., 2005) and stronger interactions with the typically hydrophilic membrane. The latter becomes less important as the surface chemistry is quickly masked during the process by adsorption and cake formation (Judd, 2007). As a results, reports of highly hydrophobic flocs fouling MBR membranes can be found in the literature (Le-clech et al., 2006).

Moreover, the filamentous index (parameter related to the relative presence of filamentous bacteria in sludge) have a direct influence on the relative hydrophobicity of the biomass floc. The excess growth of filamentous bacteria, known to be responsible for severe MBR fouling, also resulted in higher EPS levels, lower zeta potential, more irregular floc shape (Meng et al., 2006). In addition, the filamentous bacteria can enhance and fix the foulants on the membrane surface. Sun et al. (2007) observed that with increasing sludge volume index

(SVI), which results from filamentous bulking, the average increasing rate of TMP increased and the stable filtration period was shortened.

With regards to flocs size, biomass suspensions in MBRs present a wide distribution, which ranges significantly from one study to another. In general, the particle size of an activated sludge floc ranges from 1.2 to 600 μm (Jorand et al., 1995). On the whole, Tam et al. (2006) claimed that the floc size distribution obtained with the MBR sludge are lower than the results generally obtained from CASP because of high turbulence generation. Moreover, a bimodal distribution can be observed for MBR sludge because of the high concentration of small colloids, particles and free bacteria caused by their complete retention by the membrane. In particular, Cabassud et al. (2004) found a bimodal distribution: 5÷20 and 240 μm. Given the large size of the floc particles, compared to the pore size of the membrane generally used in MBRs, it is expected that floc cannot directly block pore entrances and they play a major role in the formation of the fouling cake on the membrane surface. According to the well-known Carmen–Kozeny equation applied to conventional filtration, specific resistance of the cake layer (α) is a function of particle diameter(d_p), porosity of cake layer (ε), and particle density (ρ), as follows (Baker et al., 1985):

$$\alpha = 180 \cdot \frac{(1-\varepsilon)}{\rho \cdot d_p^2 \cdot \varepsilon^3} \qquad 2.12)$$

Rc is thus strongly dependent on cake particle size: the smaller floc size, the greater cake resistance.

According to Drews (2010) high concentrations of bound-EPS increase floc size and thereby sludge dewaterability decreasing cake layer resistance. Finally, Geng and Hall (2007) observed that the floc size distribution and the amount of soluble-EPS in the mixed liquor were the most important properties that significantly influenced the fouling propensity of sludge, and the content of bound-EPS was not found to be directly associated with membrane fouling.

Hydrodynamic conditions. The current trend in scientific research and real applications tends to favour submerged over side-stream configurations. As a consequence, most of the recent studies on hydrodynamic conditions are focused on the reduction of aeration demand by enhancement of aeration efficiency.

With regards to side-stream MBRs, the membrane fouling can be limited promoting turbulence by increasing cross-flow velocity. It is thought that an excessive cross-flow velocity implying higher shear can imparts such a shear stress on the flocs to cause them to break-up (Tardieu et al., 1999; Wisniewski and Grasmick, 1998). As a results, the reduction

of flocs particle size and the release of bound-EPS can occur and consequently side-stream MBRs are considered to have an inherently higher fouling propensity (Judd, 2010). However, in a small crossflow cell, fouling was found to decrease linearly with increasing CFV (up to 4.5 m/s), and no CFV optimum was observed (Choi et al., 2005).

With regards to submerged systems, the aeration is used to generate a shear stress on the membrane surface without requiring a recirculation pump. Basically, the bubbles flowing near to the membrane surface induce local shear transients and liquid flow fluctuations, increasing back transport phenomenon. The effect of tangential shear at the membrane surface is a function of particle diameter. In particular, it prevents large particle deposition on the membrane surface (Choo et al., 1998). Aeration also affects MBR performance by causing fiber lateral movement (or sway) in hollow fiber configurations (Wicaksana et al., 2006) also helping to overcome issues related to their high packing density. Hong et al. (2002) examined the effect of aeration on cake removal and suction pressure using a pilot scale submerged MBR and concluded that aeration was a significant factor governing the filtration conditions. Another investigation (Han et al., 2005) showed that the cake removing efficiency of aeration did not increase proportionally with the increase in the airflow rate and that the airflow rate had an optimum value from the cake-removing point of view. In fact, aeration is an important parameter determining sludge flocs characteristics. For instance, a high aeration rate certainly can reduce sludge attachment to the membranes, but a too high aeration intensity will lead to breakage of sludge flocs and relate of soluble-EPS. Moreover, under high aeration intensity, the colloids and solutes would become the major membrane foulants (Fan and Zhou, 2007). In fact, according to authors the resistance of colloids and solutes cannot be reduced effectively by increasing shear stress because the back transport of the colloids and solutes from the membrane surface is determined by Brownian diffusion, especially for solutes.

Applied aeration flow rates are based on previous experiences and manufactures' recommendations and defined in term of specific aeration demand: air flow rate per membrane surface area (SADm in m^3 $(m^2\ h)^{-1}$) or air flow rate per permeate flow produced (SADp in $m^3\ m^{-3}$). To characterise the hydrodynamics of the system, however, the superficial air velocity (air flow rate per channel cross-section area) is the more appropriate parameter (Drews 2010). In full-scale MBRs, SADm values range from 0.18 to 1.28 N $m^3\ m^{-2}\ h^{-1}$ and SADp from 10 to 65 (Judd, 2010). Typically, flatsheet membranes have higher SADm but lower SADp values since they are commonly operated at higher flux (Drews, 2010). Based on pilot and full-scale data, Judd (2010) proposed that SADm was a roughly linear function of net flux, albeit at a very flat slope and large scatter.

In a low pressure membrane process, such as MBRs, the bubble size and bubble flow rate play significant roles in hydrodynamic conditions and energy demand. Fane et al. (2005) compared the effect of two nozzle sizes, 0.5 and 1.0 mm diameter, on bubble size and membrane fouling. The larger nozzle could produce higher bubble sizes than the smaller nozzle. However, the fouling control, characterised by dTMP/dt, was noticeably improved using the smaller nozzle with the smaller bubbles. A more recent study by Prieske et al. (2008), however, suggests that the smaller bubble size (1 mm) could induce a slower circulation velocity than large bubbles (2 and 3 mm) and concluded that larger bubbles seem to be more efficient for air scour of the membrane surface because the resulting drag and lift forces on the membranes are much higher due to higher circulation velocities.

In addition to aeration intensity, the rheological properties of sludge suspension have a strong influence on transport phenomena near the membrane surface. For a given aeration intensity, the increase of sludge viscosity weakens the hydrodynamic conditions close to the membranes. An example is the sharp decrease of the shear stress at the membrane surface with increasing sludge viscosity (Meng et al., 2007b). According to the rheological properties of activated sludge, Van Kaam et al. (2008) proposed an intermittent aeration mode, which allows activated sludge to restructure and can effectively prevent MBR fouling and provide energy saving.

2.5.2 Factors indirectly affecting membrane fouling: feed water characteristics and operating parameters

Indirect effects on fouling offered by feed water characteristics and operating parameters (i.e., SRT, temperature and dissolved oxygen concentration) are discussed in this section. Moreover, the implications of their rapid variations over time are considered.

Feed water characteristics. Whilst membrane fouling in physical wastewater filtration depends directly on the water quality (Fuchs et al., 2005; Judd and Jefferson, 2003; Schrader et al., 2005), MBR membrane fouling is mostly affected by the interactions between the membrane and biological suspension rather than feed water (Choi et al., 2005). Feed water is supposed to be more important in the case of recalcitrant substances that may undergo more limited biochemical transformation and unmodified feed interacts directly with membranes. However, pre-treatment of the effluent such as pre-coagulation/sedimentation before its introduction in the bioreactor revealed a less intense fouling (Le-Clech et al., 2006). Moreover, carbon source type can affect the formation and elimination of soluble-EPS. For instance, McAdam et al. (2007) observed that carbon substrate had a great influence on floc stability. Acetic acid resulted in the production of high concentrations of

small particles (i.e., colloids and solutes) due to the weakly formed flocs. Ethanol, on the other hand, encouraged the growth of strong flocs that were capable of withstanding shear.

With regards to inorganic feed water material, divalent and trivalent cations can affect the fouling propensity of a certain system. According to the divalent cation bridging (DCB) theory (Sobeck and Higgins, 2002) and the polymer bridging model (PBM) theory (Wilén at al., 2003) divalent, such as calcium and magnesium, and trivalent cations play a major role in bioflocculation and bridging negatively charged functional groups within the EPS, thus helping bioflocculation and improving sludge filterability. Also trivalent cations can improve bioflocculation. Addition of an optimum calcium concentration could induce lower soluble-EPS concentration, lower hydrophobicity, lower concentration of filamentous bacteria, which resulted in the reduction in cake layer resistance and pore blocking resistance (Kim and Jang, 2006). Furthermore, calcium ion in the form of Ca^{2+} interacts with alkalinity and forms $CaCO_3$ which is known to increase the density of sludge. Kim and Jang (2006) found that higher concentration of calcium is beneficial to membrane fouling. According to their study higher calcium concentration in the feed (2.86 mM compared to 0.026 mM) resulted in 11 times lower fouling rate. However, it should be noted that the aforementioned study was conducted at mixed liquor suspended solid concentration of 2 g/L, atypically low for MBRs.

On the contrary, high concentration of divalent cations inducing $CaCO_3$ formation may lead to sludge displacement and scaling (inorganic fouling) by chemical and biological precipitation (see section 2.4.1). According to Arabi and Nakhla (2008) the effect sludge displacement and scaling play a major role at high concentration of calcium in feed water. On the other hand, lower concentrations can improve bioflocculation as stated above. In particular, authors studied fouling at different calcium levels adopting two MBRs operating on a synthetic municipal wastewater at a solids retention time of 15 days: a control MBR at an influent calcium level of around 35 mg L^{-1} and a test reactor at two influent calcium concentrations of 280 and 830 mg L^{-1}. The test reactor at 280 mg L^{-1} of calcium showed 35% higher permeability than the control. However, at 830 mg L^{-1}, the permeability was approximately 50% lower than the control. According to authors, the low level of calcium was beneficial in controlling biofouling due to binding and bridging soluble-EPS and enhancing bioflocculation. In fact, the introduction of 280 mg L^{-1} to the system resulted in the formation of larger flocs as confirmed with the results of the particle size distribution (Figure 2.22). The cake formed by larger flocs was more permeable having a lower resistance to filtration. Despite the reduction in soluble-EPS (60% ad 30% for carbohydrate and protein, respectively) at 830 mg L^{-1}, substantial inorganic fouling of the membrane occurred resulting in the decline in the membrane permeability.

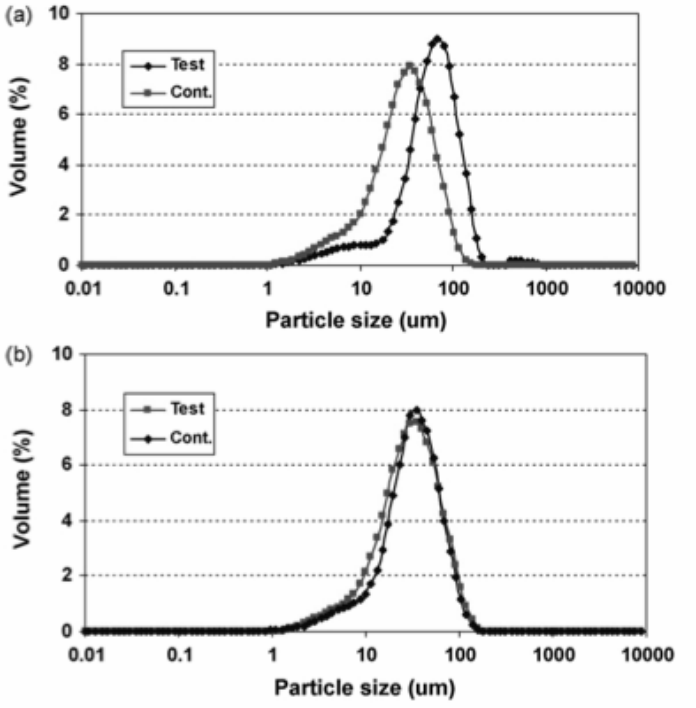

Figure 2.22. Mixed liquor particle size distribution of test samples (a=MBR at 280 mg L^{-1}; b=MBR at 830 mg L^{-1}) and control (Arabi and Nakhla, 2008).

Operating condition. Sludge retention time, and consequently the F/M ratio, is probably the most important operating parameter impacting on fouling propensity in MBRs since it ultimately controls biomass characteristics (Le-Clech et al., 2006). In particular, SRT has been identified as the main parameter influencing EPS concentration (Jiang et al., 2008). An investigation by Ng et al. (2006) showed that longer SRTs improved membrane permeation (10 day and 20 day SRTs were better than 3 day and 5 day SRTs). They also observed that membrane fouling rate increased with rising soluble and bound-EPS concentrations, both of which increased with decreasing SRT. Lee et al. (2003) found a decreasing contribution of the soluble-EPS to overall membrane fouling with increasing SRT (20÷60d). Liang et al. (2007) tested SRTs of 10, 20, and 40 d and observed that accumulation of soluble-EPS in the Pilot MBR became more pronounced at short SRTs. Zhang et al. (2006b) operated a submerged MBR a short SRT of 10 d and a moderate SRT of 30 d. During steady operation the total amount of EPS extracted from the flocs and the supernatant was approximately the same for the two SRTs under the same organic loading rate. However, the soluble polysaccharide concentration in the sludge suspension was about 100% higher for the SRT of 10 d than that for 30 d. Similarly, Rosenberger et al. (2006) found that at an SRT of 8 d, the soluble-EPS polysaccharide concentration varied in the range of 3÷15 mg L^{-1}, while at an

SRT of 15 d, it varied in the range of 3÷8 mg L-1; whereas Lee et al. (Lee et al., 2003) observed stable polysaccharide levels and an increase in protein concentration when SRT was increased. Al-Halbouni et al. (2008) could confirm the decreasing relevance of polymers at higher SRT by analysing the amount of polymers attached to membranes that had been in operation in two parallel pilot MBRs. At SRT=40 d, 40 times less proteins and 5 times less polysaccharide were present on the membrane than at 23 d. With regards to bound-EPS Masse et al. (2006) found that their content decreased from 45÷70 to 20÷40 mg gMLVSS^{-1} when SRT increased from 10 to 53 d. Furthermore, Ahmed et al. (2007) showed that the specific cake resistance decreased with SRT. This fact can be justified considering that Liu and Fang (Liu et al., 2003) observed a positive effect of long SRT on hydrophobicity and flocculation for CASP. Operating an MBR at higher SRT also leads inevitably to an increase in MLSS concentration, but this in itself may not necessary lead to greater fouling (see section 2.5.1). However MLSS concentration affects viscosity attenuating therefore the effect of bubbling. On the other hand, Meng et al. (2007b) reported that there were high bound-EPS concentrations and high sludge viscosity as F/M ratio increased (decrease of SRT). Overall, it is likely that an optimal SRT exists, between the high fouling tendency of low SRT operation and the high viscosity suspension prevalent or very long SRT. In particular, according to recent findings shown in Figure 2.23, the optimum SRT of MBRs should be controlled at 20÷50 d (Meng et al., 2009). Moreover, Pollice et al. (2008) observed that the capillary suction time (CST) and sludge resistance to filtration (SRF) values, which are used to characterise the sludge filterability, were minimized for SRT in the range of 40÷80d.

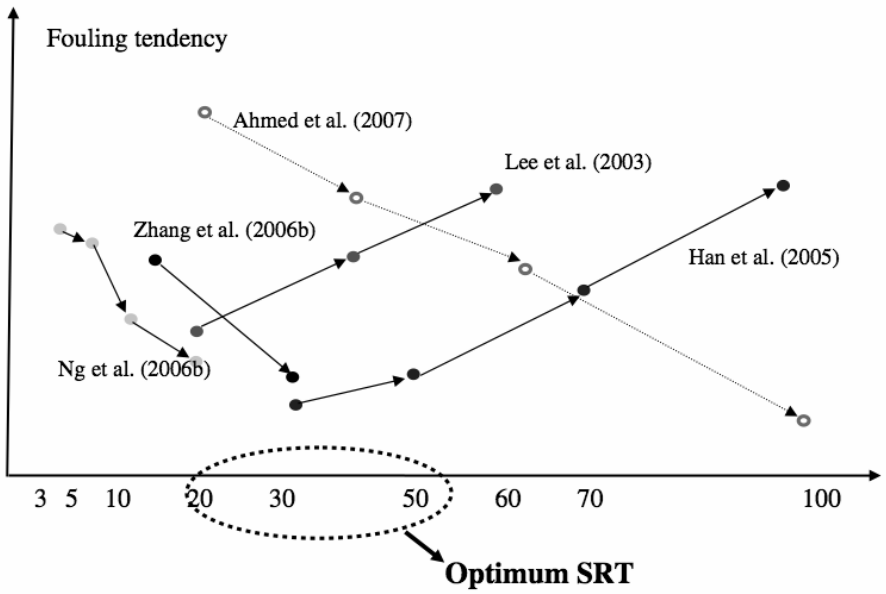

Figure 2.23. Comparison of recent literature about the effects of SRT on fouling rate (Meng et al., 2009).

Finally, other two aspects related to operating at high SRT must be considered. Firstly, the accumulation of inert material occurs in MBRs particularly at high SRT. In fact, the progressive accumulation of non-biodegradable materials (like hair and lint), which are not completely removed by the pre-treatment processes, can lead to clogging of the membrane module (Le-Clech et al., 2005a). Afterwards, SRT is also a key factor for nitrification. In fact, high SRT usually applied in MBRs permits the growth of nitrite oxidisers that play a significant role in determining the properties of soluble-EPS. Larsen et al. (2008) observed that typical representatives of ammonia and nitrite oxidisers formed strong microcolonies, with *Nitrospira spp*. being even stronger than *Nitrosomonas oligotropha* colonies. Even under high shear, only the largest *N. oligotropha* colonies fragmented, and deflocculated fractions of both species were much lower than those of biomass in general. The authors hypothesised that the reason for these higher adhesion forces could be a stronger entanglement of the species EPS, but quite possibly their properties are also different.

Temperature affects permeate viscosity so it is commonly corrected in order to compare permeability obtained at different temperatures (see section 2.3.3). Moreover, temperature affects membrane filtration and fouling through other several phenomena, as follows (Le-Clech et al., 2006; Van der Marel et al., 2009; Drews, 2010):

- the viscosity of the sludge increases at a lower temperature reducing the shear stress created by the air bubbles; for instance, Jiang et al. (2005) found that sludge viscosity increased by 10% varying temperature from 18°C to 14°C;
- generally, intensified deflocculation occurs both at low temperature and at high temperature; for instance, Morgan-Sagastume and Grant Allen (2005) found that deflocculation of sludge flocs occurred under a temperature shift from 30 to 45°C;
- back transport velocity of solutes from the membrane decreases at a lower temperature since Brownian diffusion decreases linearly with decreasing temperature;
- biodegradation of COD is reduced at decreased temperature, resulting in a higher concentration of solute and particle COD in the reactor;
- material adsorption is reduced at increased temperature.

All of these factors are directly linked to membrane fouling. On the whole, it is expected to observe greater deposition of materials on the membrane surface at lower temperatures (Rosenberger et al., 2006). But, in an MBR with short SRT (13 d), Miyoshi et al. (2009) observed that only reversible fouling (cake layer formation) was more significant in the low temperature period, while irreversible fouling (gel layer formation and pore restriction phenomenon) developed more rapidly in the high temperature period. In contrast, in an MBR with long SRT (50 d), the authors did not observe any significant seasonal variations in either type of membrane fouling.

With regards to dissolved oxygen (DO), as a general trend, higher average levels of DO tend to lead to better filterability, and lower fouling rate (Kang et al., 2003; Le-Clech et al., 2006). For instance, Yun et al. (2006) and Yoon et al. (2006) found a rate of fouling was 5 times higher in low DO conditions. In particular, the effect of oxygen limitation causes a lowering of the cell surface hydrophobicity, and consecutive floc deterioration with EPS release in supernatant (Le-Clech et al., 2006; Drews, 2010). In addition, Min et al. (2007) observed that under DO limited conditions the sludge suspension contained a larger amount of high molecular weight compounds which led to higher cake resistance. With regards to biofilm formation on membrane surface (biofouling), because of the poor oxygen transfer within the biofilm structure, the fouling sub-layers may become anaerobic, and therefore affect membrane fouling differently (Le-Clech et al., 2006). Endogenous decay, similar to that expected within the fouling layer, was simulated and revealed the level of carbohydrate in bound-EPS to significantly increase (Le-Clech et al., 2006). Since the transition between aerobic to anaerobic conditions seems to produce a large amount of EPS, this phenomenon could also be responsible for MBR fouling (Zhang et al., 2006).

Changes in feed water characteristics and in operating condition. Variations in operating conditions, in feed water characteristics and shifts in oxygen supply seem to be important factors leading to changes in MBR fouling propensity. For instance, sudden temperature changes have been observed to yield spontaneous changes in soluble-EPS concentration (Drews et al., 2007). Furthermore, the addition of a spike of acetate in the feed water significantly decreased the filterability of the biomass in an MBR; this was due to the rise in soluble-EPS levels resulting from the feed spike (Evenblij et al., 2005b). Moreover, by changing the ratio of monovalent over polyvalent cations in the influent, deflocculation–reflocculation events were induced by Van den Broeck et al. (2010). A high ratio resulted in severe sludge deflocculation and worsened filtration characteristics. A low ratio influent was subsequently fed, and within 3 weeks, the sludge reflocculated and filtration characteristics improved significantly. What is more, the effects of starvation conditions on the biological suspension have been assessed by incorporating different substrate impulses in batch tests (Lobos et al., 2005). Exogenous phases were followed by starvation periods, both characterized by precise F/M ratios. For high F/M, multiplication of bacteria cells was observed, while compound storage, absence of soluble-EPS proteins production and bacteria lysis, were obtained at low F/M ratio, comparable to conditions generally applied in MBRs.
According to Drews (2010), the rate of change might be even more important than the new condition itself, because it imposes a shock on the biomass which takes time to get accustomed to by floc restructuring, metabolic or population changes. Especially the latter is

a process with relatively high time constants. Finally, in full-scale applications, such unsteady state conditions could occur regularly and therefore further research on the exact impact of these unsteady states is required.

2.6 Fouling control

As discussed in section 2.4.3, operating at sustainable fluxes is not sufficient to avoid membrane fouling that can occurs rapidly and severely according to the previously stated TMP-jump concept. In a given system, apart from chemical and physical cleanings adopted for the removal of fouling (see section 2.4.1), it is possible to prevent and control fouling before its occurrence by (Le-Clech et al., 2006; Judd, 2010; Drews, 2010):

- providing favourable hydrodynamic conditions;
- operating specific non or little fouling conditions;
- pre-treating the biomass suspension to limit its fouling propensity.

According to Meng et al. (2009) the enhancement of hydrodynamic conditions (see section 2.5.1) can be an effective approach to mitigate membrane fouling in MBRs. But, they have close relation with aeration intensity, bubble size, MLSS concentration and sludge viscosity, membrane module configuration, etc. Therefore, the hydrodynamic conditions in MBRs are very complex and a systematic optimisation of all geometrical and operational parameters (tank size, liquid level, riser/downcomer cross-section area, membrane spacing, module height, bottom clearance, aerator dimensions and location, bubble size, aeration rate) from which engineering design rules could be derived is as yet pending (Drews, 2010). Moreover, the back transport mechanisms due to the aeration intensity can be excellent for suspended material (i.e., biomass flocs) but they are not so effective for colloids and solutes such as soluble-EPS causing irreversible fouling. Therefore, the control of soluble-EPS concentration in MBRs is crucial. In general, it can be achieved by two approaches: adjusting the operation parameters (see section 2.5.2) and pre-treating the biomass suspension with the addition of adsorbents or coagulants/flocculants, also refereed as "flux" or "membrane performances enhancers", to reduce soluble-EPS concentration.

Finally, another relevant topic in MBRs research regards the development of new membrane material since chemical modifications of the membrane surface have been shown to efficiently improve anti-fouling properties (Le-Clech et al., 2006). However, this section will mainly focus on biomass suspension pre-treatment using flux enhancers since new material development is not a key issue with relation to thesis topics.

2.6.1 Mechanisms of action and main effects of flux enhancers

The fouling control by flux enhancers consist of pre-treating the biomass suspension mainly to reduce concentration of colloids and solutes such as soluble-EPS causing irreversible fouling. Flux enhancers can be classified according to functionality in coagulants/flocculants, adsorbents and other substances (see Table 2.7) and can act through a number of different phenomena such as adsorption of soluble-EPS, charge neutralisation, coagulation, flocculation, bridging flocs and/or soluble-EPS also enhancing the flocculation ability (Figure 2.24).

In particular, coagulants/flocculants can remove soluble-EPS by charge neutralisation and bridging (Wu et al., 2006). For instance, an MBR-based example reported that small biological colloids (from 0.1 to 2 μm) coagulated and formed larger aggregate when alum was added (Llee et al., 2001). Moreover, bridging cause particular aggregation creating larger macroscopic flocs and therefore leading to the flocculation of activated sludge (EC, 2009) and therefore improving the sludge filterability with benefits on cake layer resistance. In addition, because of back transport and shear induce fouling control mechanisms, large microbial flocs are expected to have a lower impact on membrane filtration (Le-Clech et al., 2006). According to Hwang et al. (2007) soluble-EPS are also entrapped by microbial flocs during the course of the flocculation, leading to an increase in the concentration of bound-EPS. Furthermore, according to Le-Clech et al. (2006), metal salts form hydroxide precipitates which adsorb materials such as colloids soluble organics.

Table 2.7. Main flux enhancer categories and substances.

Category	Subcategories and substances	
A) coagulants/flocculants	A1) metal salts	A11) monomeric coagulants/flocculants: - alum, - aluminium sulphate, - ferric chloride, A12) polymeric coagulants/flocculants: - poly aluminium chloride (PACl), - polymeric ferric sulphate (PFS).
	A2) organic polymers	A21) cationic polymers: - general use polymers, - developed on purpose polymers. A22) green biopolymers: - chitosan, - starch.
B) adsorbents	- powdered activated carbon (PAC)	
C) others	- zeolite (a mineral) - diatomite (a sedimentary fossil of ancient diatom)	

Since Yoon et al. (2005) presented the effects of adding a cationic polymer to the MBR mixed liquor to improve filterability, the interest in flux enhancers has greatly increased. In particular, attempts have been made to use monomeric metal salts (category A11 in Table 2.7) such as alum, aluminium sulphate and ferric chloride (Wu et al., 2006; Iversen et al., 2008; Ji et al., 2008; Koseoglu et al., 2008; Song et al., 2008; Tian et al., 2008; Zhang et al., 2008). Zhang et al. (2008) reported that the addition of ferric chloride at the optimal concentration reduced both soluble-EPS with MW major than 10 kDa in the supernatant and the fraction of small particles (sludge flocs) in the range of 1–10 μm. In MBR-based trials, Holbrook et al. (2004) found that the addition of alum led to a significant decrease of the carbohydrates soluble-EPS, along with an improvement in membrane hydraulic performances. Ferric hydroxide flocs have also been used in the MBR process as a membrane pre-coating agent as investigated by Zhang et al. (2004). They concluded that this technique has a great potential to reduce fouling, at the same time they found a strong decrease in pH and a reduction of microbiological activity with increased dosing (see section 2.6.3). Similar results were presented by Song et al. (2008), who investigated the effect of alum and ferric chloride as coagulants in MBR. Although both additives were able to improve phosphorus removal and filtration resistance, the authors excluded ferric chloride from further tests as it strongly decreased the pH.

It has been reported that polymeric coagulants (category A12 in Table 2.7) could supply more positive charges and longer chain molecules, so that they had a better effect on flocculation than monomeric coagulants (Wu et al. , 2006). Based on the increase rate of the zeta potential with varying doses, the coagulants ability to supply positive charges was in the order of PFS>PACl> $Al_2(SO_4)_3$>$FeCl_3$ (Wu et al., 2006). According to Ji et al. (2008) the membrane fouling rate was higher for an $Al_2(SO_4)_3$ MBR than a polymeric ferric sulfate (PFS) added MBR. As result, PFS was identified as the most effective in controlling membrane fouling between metal salts, also comparing to polyaluminium chloride (PACl) (Wu et al., 2006; Wu et al., 2008). However, results obtained by (Wu et al., 2006) showed the decrease in pH is lower for PACl than PFS for doses greater than 1 mM.

Organic cationic polymers (category A21 in Table 2.7) were found to be favourable due to their steady and successful performance in fouling control (Koseoglu et al., 2008). Using a cationic polymer, Lee et al. (2007) observed that soluble foulants in the bulk phase were entrapped in sludge flocs within the flocculation process. Moreover, by analysing the porosity and the biovolume of the biofilm formed on the membrane surface, they were also able to prove that the addition of a cationic polymer led to a more porous biofilm and subsequently to an enhanced filtration performance. Moreover, with the addition of modified cationic polymers, the cost of aeration can decrease of 40–55% to achieve the same flux

(Yoon et al., 2007). A novel membrane performance enhancer (MPE50) has been recently developed on purpose by Nalco and applied to MBRs (Le-Clech et al., 2006). When 1 g L^{-1} of cationic polymer-based compound was added directly to the bioreactor, carbohydrates soluble-EPS was found to decrease from 41 to 21 mg L^{-1} (Yoon et al., 2005). The interaction between the polymer and the soluble organics in general, and carbohydrates soluble-EPS in particular, was named as the main mechanism responsible for the performance enhancement when MPE50 was used (Le-Clech et al., 2006). Several studies have already validated the effectiveness of MPE50 even at full-scale (Yoon et al., 2005; Yoon and Collins, 2006; Lee et al., 2007; Wozniak, 2009ì). With regards to green biopolymers (category A22 in Table 2.7), the biodegradable nature of chitosan and its relatively high costs are significant limits for widespread use of this chemical even thought providing interesting effects in fouling control (Koseoglu et al., 2008; Iversen et al., 2009b). On the other hand, starch, a cheap a common biopolymer was tested (Iversen et al., 2009a). Ngo and Guo (2009) utilized a natural starch-based cationic flocculant offering inherent advantages over inorganic and synthetic polymers such as being derived from a renewable source of raw materials and easily degradable in the environment after use. Its ability to significantly reduce membrane fouling and energy consumption (less backwash frequency) was proved. Moreover, its addition also at with low doses led to a reduction of the total phosphorus of approximately 99.5%.

With regards adsorbents, powered activated carbon (PAC) is usually utilized (category B in Table 2.7). In particular, during long-term runs, PAC gradually incorporates to the biofloc to form biologically activated carbon (BAC, Ng et al., 2006). In addition, because of adsorption of soluble-EPS on PAC lower fouling propensity is expected in MBR processes when biomass is mixed with adsorbents (Le-Clech et al., 2006). In particular, (Liu et al., 2005) found the optimum PAC concentration of 1.2 g L^{-1} for filtration of activated sludge. In this study, floc size distribution and apparent viscosity of the biomass were the main factors responsible for the lower cake resistance observed after PAC addition. However, no significant improvement of filtration was obtained with the addition of 5 g L^{-1} of PAC and no sludge wastage (Ng et al., 2005). Consequently it was postulated that the originally introduced-PAC was quickly saturated with organic pollutants and only the regular addition of PAC into the bioreactor showed good fouling limitation, as the system was operated at lower SRT. Results reported by Fang et al. (2006) confirmed this hypothesis as virgin PAC was responsible for 22% reduction of the filtration resistance, while presorbed PAC only reduced the resistance by 14%. The addition of PAC to MBRs provides a solid support for biomass growth, and hence reduces floc breakage (Hu and Stuckey, 2007). Moreover, the BAC flocs in MBRs are very strong and dense, which can help to prevent particle accumulation onto the membranes.

Park et al. (1999) assumed that the solid and sharp-edged PAC works as a scouring agent that removes deposited foulants from the membrane surface when applied at 5 g L^{-1} in anaerobic MBRs. Akram and Stuckey (2008) studied the impacts of PAC addition on the performance of a submerged anaerobic MBR, and found that in the presence of 1.67 g L^{-1} a significant flux improvement from 2 to 9 LMH was obtained. However, the addition of 3.4 g L^{-1} reduced the flux to 5 LMH. As discussed by the authors, this evidence might be due to the increased sludge viscosity at high PAC addition. It suggests that PAC addition can improve membrane flux significantly; but, if the addition of PAC is beyond the optimal value, it will do harm to membrane permeation.

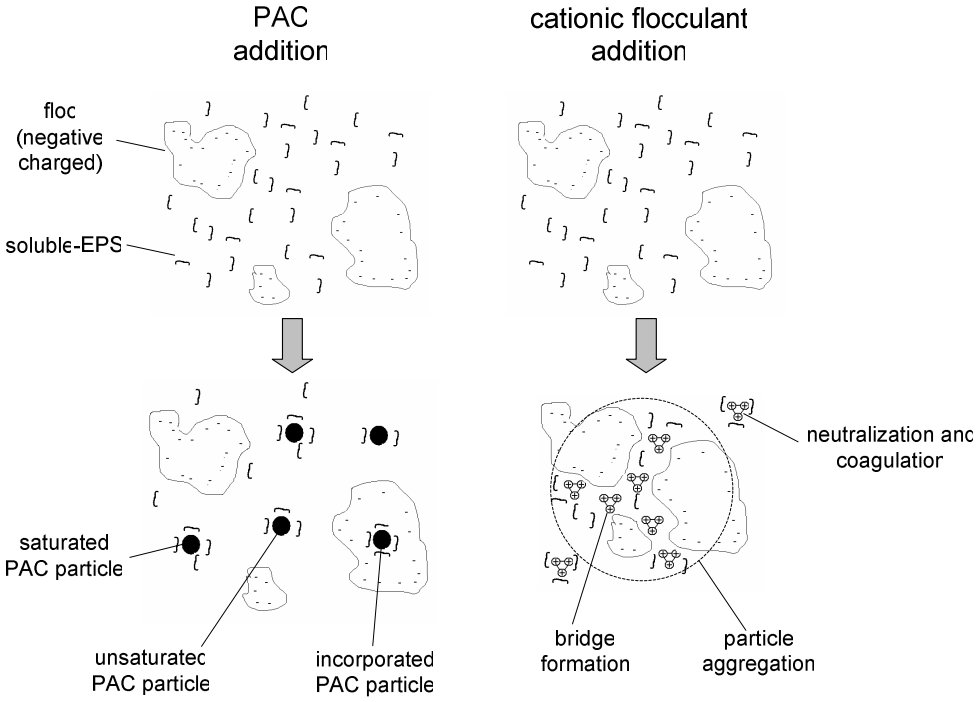

Figure 2.24. Major mechanisms of flux enhancers, particularly, for PAC and cationic flocculants, i,e. metal salts and cationic polymers.

Remy et al., (2009; 2010) investigated the effect of low dose powdered activated carbon addition in membrane fouling reduction. In particular, the authors showed that a PAC dosage of only 0.5 g L^{-1} (or approximately 50 mg g $MLSS^{-1}$), combined with a long sludge retention time (SRT=50 d), effectively reduced fouling in a pilot-scale MBR, while the increase of operational costs associated with PAC addition kept as low as 0.008 € m^{-3} treated wastewater. Interestingly, the authors found out an improved flocculation ability of colloidal foulants in presence of PAC and of not-activated powered carbon (PC) as shown in Table 2.8. Apparently, the removal of the "colloidal" COD fraction does not rely on adsorption and therefore is independent from the pore size distribution of the carbon particles.

Table 2.8. Concentration of COD, proteins and polysaccharides in supernatant and removal with PAC and PC after 72 hrs of contact time (Remy et al., 2010).

		supernatant mg L^{-1}	**removed with PAC** %	**removed with PC** %
Colloidal	COD	199	56	53
	Proteins	28.3	29	24
	Polysaccharides	37.8	46	44
Soluble	COD	64	60	<0
	Proteins	8	53	11
	Polysaccharides	14.3	33	<0

This can also be seen from the microscopic images in Figure 2.25, comparing individual PAC particles in demineralised water with PAC particles surrounded by flocculated material in the supernatant after 72 h of contact time. In particular, PAC particles are dispersed in demineralised water (Figure 2.25a) while they aggregate when suspended in supernatant (Figure 2.25b). However, according to the authors, the formation of stronger sludge flocs with a higher shear resistance was the major effect of PAC instead of adsorption of soluble foulants or the flocculation of colloidal foulants, as stated above. As a result, according to idea that particles inclusion creates strong and dense flocs, they concluded that not-activated powered carbon (PC), or even PAC previously used for post-treatment may be used as a cheaper alternative for PAC to reduce membrane fouling in MBRs.

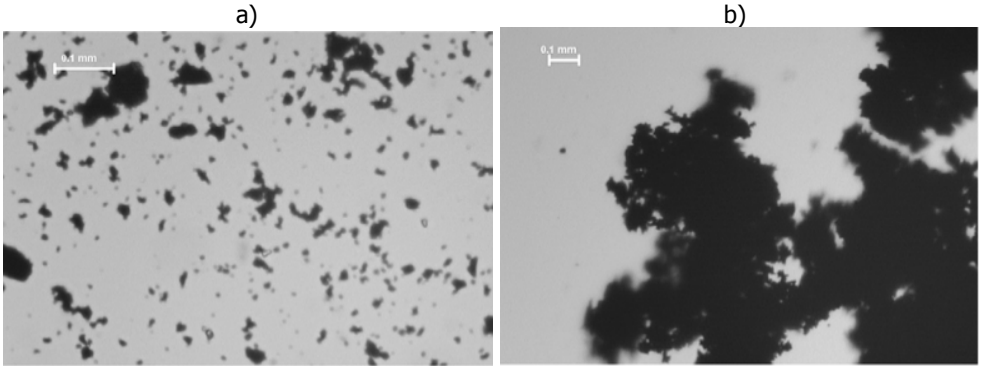

Figure 2.25. Microscopic observation of PAC particles: a) PAC in demi. water; b) PAC in supernatant (Remy et al., 2010).

Finally other substances (category C in Table 2.7) such as zeolite and diatomite were used as flux enhancers. Zeolite dosed in MBRs allowed the creation of rigid flocs that had lower specific fouling resistance (Le-Clech et al., 2006), whereas diatomite resulted as a reliable and effective approach in terms of both membrane fouling mitigation and pollutants removal improvement (Yang et al., 2010). The MBR system with diatomite addition of 50 mg L^{-1} enhanced the removal of COD, nitrogen and phosphorus by 0.9%, 6.9% and 31.2%,

respectively, as compared to the control MBR, without diatomite addition (Yang et al., 2010). Due to the hybrid effect of adsorption and co-precipitation on fine colloids and dissolved organic matter from the addition of diatomite, a reduction in foulants amount, an increase in microbial floc size and an improvement in sludge settleability have been achieved simultaneously. As a result, the membrane fouling rate was mitigated successfully (Yang et al., 2010).

2.6.2 Comparison of flux enhancers effectiveness in short-term and long-term experiments

Although a wide range of studies on different additives in MBR has been performed, these often investigate only one or two additives. Therefore the critical interpretation of data and their comparison is very difficult because results from different studies refer to specific feed waters, operating conditions, etc. and also use different equipment. Moreover, the comparison of the effects and results obtained by flux enhancers adopted in literature should be treated with extreme care (Drews, 2010). However, impartial studies were carried out to evaluate a broad range of different chemicals on the base of short-term (lab-scale trials) and long-term (pilot trials) experiments by the research group on membrane fouling from Technical University of Berlin (Iversen et al., 2006; Koseoglu et al., 2008; Iversen et al., 2009b; Iversen et al., 2009c). Firstly, a total number of 30 substances were screened previously in shaking flask tests with activated sludge (Iversen et al., 2006). Then, the research group focuses on approximately half the original number of chemicals as shown in Table 2.9 and Table 2.10. In particular, a first study (Iversen et al., 2009b) aimed at a better understanding of impact of selected 12 flux enhancers (see study 1 in Table 2.9) on particle size distribution in activated sludge was carried out. Of further interest was also the shear stability and dewaterability of sludge (capillary suction time, CST detection). For most additives, a significant effect on CST was observed. Most additives formed aggregates that were stable in the tested shear range (0÷4,000 s^{-1}). Nevertheless, only the tested chitosans and polymers were able to significantly increase the volume based particle size (up to 127%). In order to examine the long term effect of shearing on particle size three of the tested additives (see Table 2.9) were surveyed in pilot plant experiments. Here the increase in particle size was only 17÷18% for the tested polymers. In lab scale tests these polymers had caused an increase of approx. 50%.

Another important study was performed (Koseoglu et al., 2008), where authors aimed to determine the effectiveness of various 7 selected (3 cationic polymers, a biopolymer (Chit), a starch (Sta), and 2 metal salts, see study 2 in Table 2.9) on filterability and fouling reduction in MBR mixed liquors. Initially, batch shaker tests were carried out for each additive to

determine the optimum dosages in terms of soluble-EPS (or SMP) removal. Then, short-term filtration trials and critical flux tests were performed. The specific removal of different organic fractions from sludge supernatant (humic substances, organic acids, biopolymers and soluble EPS) were also performed and the impact on filtration performance was investigated using capillary suction time (CST) in lab-scale for 5 chemicals (2 cationic polymers, 2 powdered activated carbons and a starch, see study 3 in Table 2.9) in a third study (Iversen et al., 2009c).

Table 2.9. Relevant studies carried out by the research group on membrane fouling from Technical University of Berlin (1 = Iversen et al., 2009b; 2 = Koseoglu et al., 2008; 3 = Iversen et al., 2009c).

	Additive tested	**sludge lab-scale charact.**	**supernatant lab-scale charact.**	**pilot-scale trials**
Metal salt	Merck - ferric chloride (symbol = $FeCl_3$)	2	2	
	Ciba – polyaluminium chloride Magnasol 5108 (symbol = PACl)	1, 2	2	
cationic polymers	Nalco - MPE-50	1, 2, 3	2, 3	1, 3
	Kurita - MPH30	1		
	Kurita - MPL30	1, 2, 3	2	
	Adipap - Adifloc KD 451	1		
	Adipap - Adifloc KD 452	1, 2, 3	2, 3	1, 3
green biopolymers	France Chitine - Chitosan 221 (symbol = chit)	1, 2	2	
	France Chitine - Chitosan 652	1		
	Tate&Lyle - starch Mylbond 168 (symbol =sta)	1, 2, 3	2, 3	1, 3
	Rhodia - starch Jaguar C162	1		
PACs	Norit - SA Super	1, 3	3	
	PICA - Picahydro LP27	1, 3	3	

Table 2.10. Relevant parameters considered in: 1 = Iversen et al., 2009b; 2 = Koseoglu et al., 2008; 3 = Iversen et al., 2009c.

	Sludge lab-scale characterization	**Supernatant lab-scale characterization**
1	- capillary suction time (CST) - shear stability - particle size analysis	-
2	- filterability (short-term filtration tests) - critical flux	- soluble-EPS (proteins and polysaccharides)
3	- capillary suction time (CST)	- humic substances, organic acids and biopolymers (detected by SEC) - soluble-EPS (proteins and polysaccharides) - turbidity

Figure 2.26 shows the impacts of selected additives on soluble-EPS removals in study 2. As shown in the graph, all tested additives were able to remove soluble-EPS, but at different extent. At their respective optimum dosages, the removals were of 33, 45, 51, 36, 38, 54, and 56% for MPL30, MPE50, KD452, $FeCl_3$, PACl, chitosan, and starch, respectively. The cationic polymer KD452 exhibited the best performance in terms of the extent of soluble-EPS removal and the required dosage.

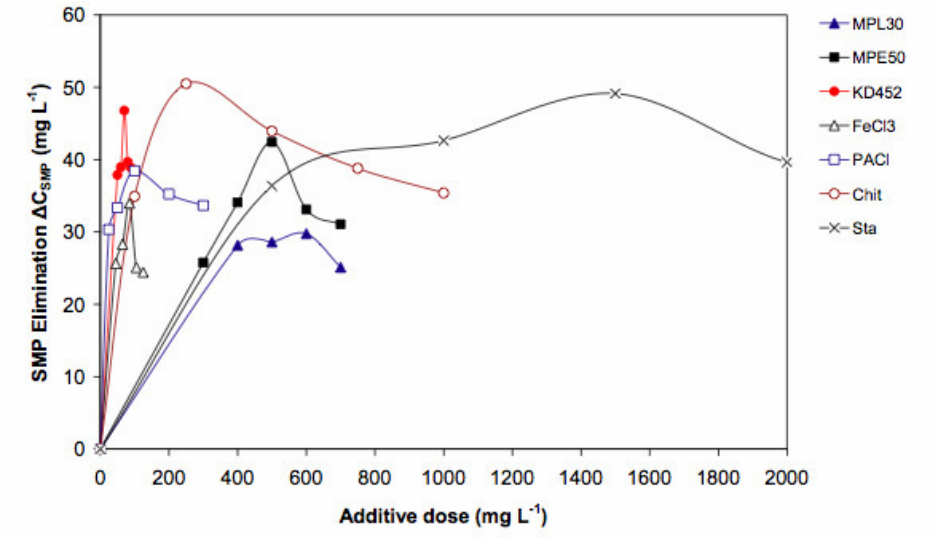

Figure 2.26. Impacts of additives on soluble-EPS (or SMP) removals (Koseoglu et al., 2008). SMP reported are averages of duplicate measurements as the sum of the protein and polysaccharide fractions.

With regards to short-term filtration tests, all tested cationic polymers, starch and chitosan significantly reduced fouling rates and increased permeability values. At their optimum dosages, the cationic polymers MPE50, MPL30 and KD452 provided 96, 80 and 74% reductions in fouling rates, respectively. PACl and FeCl3 exhibited the least improvement in fouling rates and average TMP values among tested additives. Overall, based on the lab-scale tests conducted, cationic polymeric additives were found to be favourable over the other additives due to their steady and successful performance in fouling control. The performance of cationic polymers was independent of small variations in dosing, while for other additives, particularly $FeCl_3$ and chitosan, over- or under-dosing showed detrimental effects on filterability. The critical flux values found for MPL30, MPE50, KD452, FeCl3, PACl, Chit, and Sta were 51, 54, 51, 42, 42, 36, 45 LMH, respectively. Such values correspond to critical flux enhancements of 38, 46, 38, 14, 14, 0, and 22% with respect to raw mixed liquor. Interestingly, cationic polymers increased critical flux values to levels above 50 LMH.

Figure 2.27 and Figure 2.28 shows the impacts of selected additives on removal rates related to soluble-EPS (proteins and polysaccharides, PS), organics detected by size exclusion chromatography (SEC), turbidity and CST in study 3.

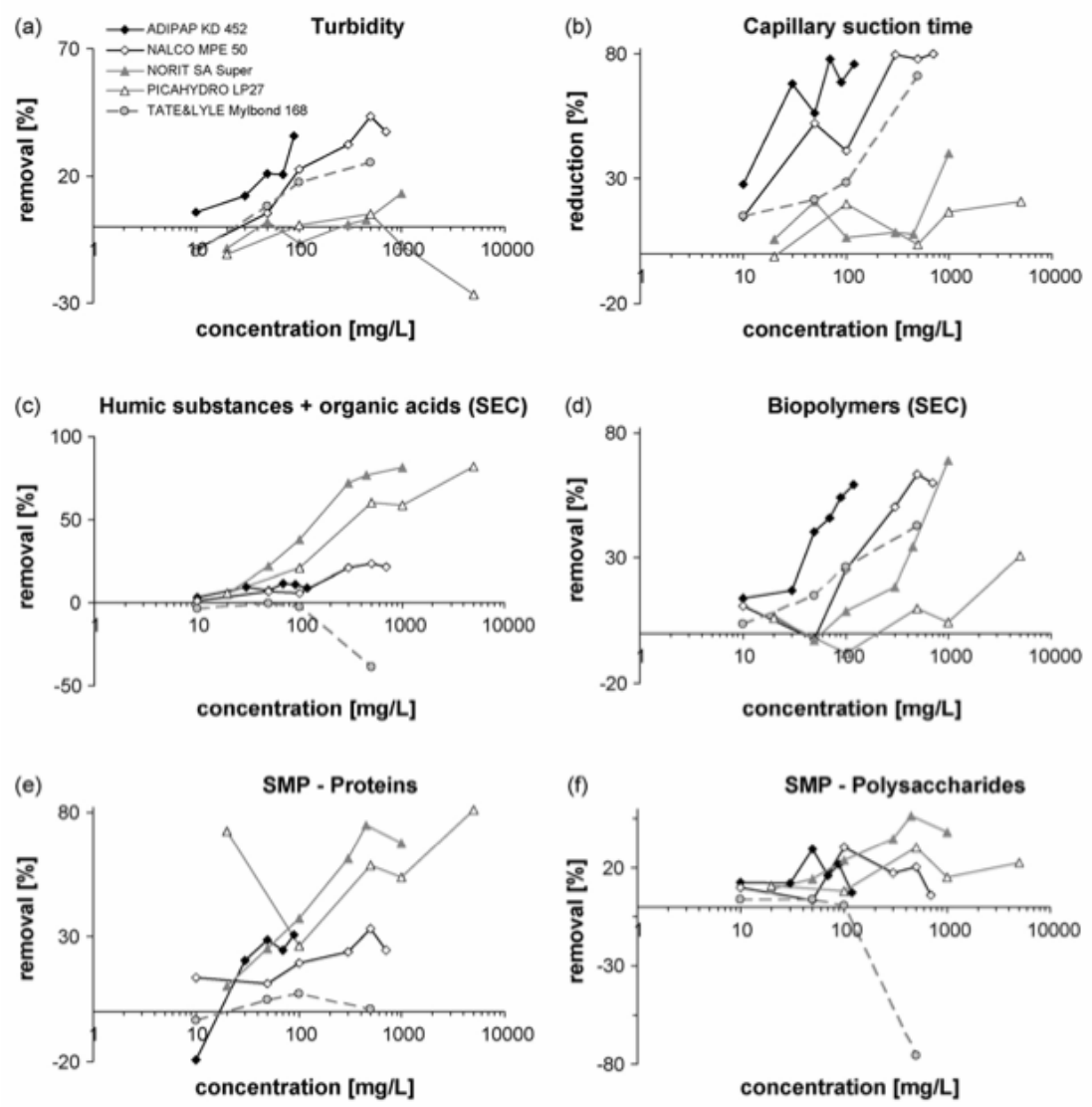

Figure 2.27. Removal of different fractions of sludge supernatant (a, c–f) and improvement of CST (b) by selected flocculants (Iversen et al., 2009c).

The cationic polymers showed positive impacts on almost all of the tested parameters. They removed efficiently biopolymers (up to 60%), polysaccharides (by 55% at optimum dosing) and proteins (around 30%) and reduced CST by 80%. The flocculants seem to be recommendable for application in MBR, since they removed specifically larger molecules that are presumably the fouling causing substances.

PAC showed no distinct selectivity for the removal of macromolecules, and removed organics detected by size exclusion chromatography (SEC) throughout the whole range of macromolecular weight. Also, soluble-EPS was removed quite effectively. By this, sludge dewaterability (CST) could be improved by 20÷40%. However, at high concentrations PAC particles remained in the supernatant what may amplify the particulate fouling during the filtration performance and cause abrasion of the membrane. Since the described experiments are only short time experiments, aspects like adsorption capacity of PAC during time and possible enhanced microbiological degradation of specific wastewater compounds could not be examined and have to be taken into account for by long-time filtration tests. The tests with starch revealed that this additive had positive and negative impacts on the supernatant. It eliminated efficiently the biopolymers (up to 40%) and reduced CST by 70%; however, the concentration of polysaccharides increased to 76% at the highest tested dosage due to residues in the supernatant..

	Adipap KD 451	*Nalco MPE50*	*Norit SA Super*	*Picahydro LP27*	*Tate&Lyle Mylbond168*
Turbidity	+	++	o / --	--	+ / o
DOC	+	+	++	++	o / --
Biopolymers	++	++	++ / +	o / +	++
Humics+Acids	o	+	++	++	--
Proteins	+	+	++	++	o
Carbohydrates	+	+	++	+	--
CST	++	++	+ / o	+	++

++	very good effect (removal > 40%)
+	good effect (removal 15-40%)
o	small / no effect (removal 0-15%)
--	negative effect (removal < 0)

Figure 2.28. Effects of selected flocculants with reference to removal of different fractions of sludge supernatant CST (Iversen et al., 2009c; EC, 2009).

The three additives that showed the most promising results, i.e., KD452, MPE50 and starch, were then tested in pilot-scale trials (Figure 2.29). In particular, two identical pre-denitrification MBRs (1.6 m^3 working volume each) equipped with 22 m^2 flatsheet modules (PVDF, 0.2 μm, A3 Water Solutions, Germany) and fed with municipal wastewater were operated in parallel. One plant served as a reference while the other received flux enhancers. Each additive was dosed for 3 months, and between flux enhancer addition

cycles, a non-dosing period of 3 SRT ensured the removal of residual additive. Chemical membrane cleanings were carried out in both plants prior to the next dosing cycle.

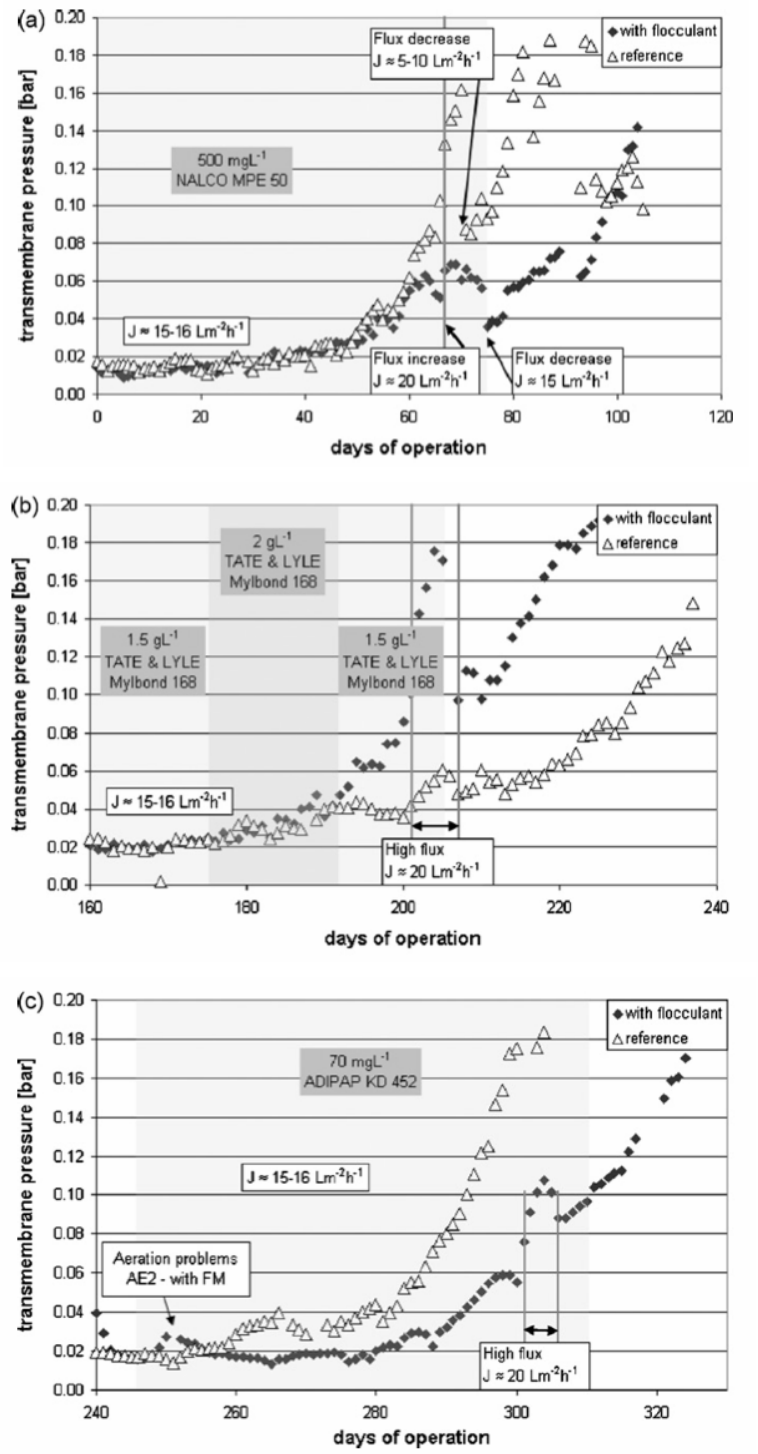

Figure 2.29. TMP evolution for plant with (a) NALCO MPE 50, (b) TATE & LYLE Mylbond 168 and (c) ADIPAP KD 452 dosing and for respective reference plant operation (Iversen et al., 2009c).

The cationic polymers (KD452 or MPE50) were found to lower the rate of fouling in comparison with the untreated reference. Especially KD452 delayed the "TMP jump" significantly. Moreover, both polymers increased the particle size by 17–19%, whereas the positive effects of starch could not be confirmed in pilot trials because fouling phenomena were much stronger than in the reference pilot. However, gel permeation chromatography showed that more high molecular weight compounds were present in the reference plant than in the one that was treated with starch. With regards to supernatant polysaccharides and proteins concentrations were not as strongly affected by the addition of flux enhancers as expected from short-term experiments, possibly because of the different mixing behaviour of the plant.

2.6.3 Side effects of flux enhancers

The potential impacts of coagulants/flocculants or adsorbents on biomass community or biomass metabolism need to be taken into account. For example, flux enhancers can imply negative effects on biology because of pH variation. In particular, it has been proven that metal salts imply a decrease in pH (Wu et al., 2006). According to Zhang et al. (2004) ferric chloride had a great potential to reduce fouling, but at the same time it decreased pH involving a reduction of microbiological activity with increased dosage. Similar results were presented by Song et al. (2008), who investigated the effect of alum and ferric chloride as coagulants in MBR. Nevertheless, they excluded ferric chloride from further bench scale tests as it decreased the pH strongly. Iversen et al., (2009a) testing chemicals showed in Table 2.9 found that only one of the dosed PAC (PICA - Picahydro LP27) strongly decreased the pH of the suspension (pH: 5.7 in comparison to 7.1 for the reference). It should be noted that for this additive a very high dosage (5 g L^{-1}) was used. On the other hand, this was not observed for metal salts probably due to the high buffer capacity of feed water. The pH variation due to PAC addition strongly impacted on the endogenous oxygen uptake rate (-28%), exogenous oxygen uptake rate (-25%), nitrification (-90%) and denitrification rate (-43%). In particular, as both nitrification and denitrification processes optimally take place at a neutral to slightly alkaline pH (a pH of 7.5÷9 is ideal for nitrifying bacteria). Moreover, the tested PACl (100 mg L^{-1}, 10÷20 mg g $MLSS^{-1}$) impacted on nitrification (-16%) and denitrification rate (-43%). Wolborska et al. (2006) also found a reduction in the activity of nitrifying microorganisms when alum was added. On the other hand, Song et al. (202 DREWS) did not observe an influence of alum on nitrogen removal (2.2÷50 mg L^{-1} of Al^{3+}).
According to results obtained by Iversen et al., (2009)a the changes in k_{La} values were mostly not significant (<±10%) except for PACL (decrease of 13%) probably due to the highly viscous nature of this additive. While the supernatant viscosity was not changed when

PACl was added, the viscosity of the mixed liquor increased slightly. Also other important parameters for oxygen transfer (surface tension, bubble diameter, viscosity, diffusion coefficient, and rise velocity) might change if PACl is added (Iversen et al., 2009a). These change of sludge characteristics, particularly different diffusion coefficient affecting the transport phenomena through the liquid and the floc, could result in a negative impact on nutrient removal (EC, 2009).

3 Treatment of textile wastewaters and metal working effluents

3.1 Introduction

The aim of this chapter is to review the information present in literature on textile and metal working effluents focusing on the characteristics of the wastewaters, their treatment, particularly by biological processes, and the applicability of the MBR technology. Moreover, section 3.2 refers to textile wastewater, whereas section 3.3 to metal working effluents.

3.2 Treatment of textile wastewaters

3.2.1 Characteristics of textile wastewaters

Textile industry comprise processes which convert natural origin (e.g. cotton, wool, silk, flax, jute, etc.), natural polymer (e.g. viscose, acetate), and synthetic polymer (e.g. polyester, acrylic) fibres into fabrics and other products, such as home furnishings, and industrial goods (IPPC, 2003). In particular, four key activities can be identified within this industrial sector (Mattioli et al., 2002):

- the treatment of raw materials, i.e. the preparation or production of various textile fibres, and/or the manufacture of yarns;
- the production of knitted and woven fabrics;
- the finishing activities, aimed at giving fabrics the visual, physical and aesthetic properties demanded by consumers;
- the transformation of those fabrics into products such as: garments (knitted or woven), carpets and other textile floor coverings, home textiles and technical textiles.

A number of textile manufacturing processes are chemical wet processing operations, also called "wet processes", necessary to properly prepare, purify, colour or finish the product. As a result, huge amount of wastewater is produced and the pollution load arises not only from the removal of impurities from the raw materials but also from the residual chemical reagents used for processing. The freshwater demand is specific to the type of textile processing operation, the type of material or final product and the specific machine or technique used (Table 3.1). However, the average demand is approximately 160 L per kg of finished product (EPA, 1997).

Table 3.1. Average, minimum and maximum water supply for different textile operations (EPA, 1997).

	Subcategory	Min water usage L kg^{-1}	Average water usage L kg^{-1}	Max water usage L kg^{-1}
1	Wool scouring	4.2	11.7	77.6
2	Wool finishing	110.9	283.6	657.2
3	Low water use processing	0.8	9.2	140.1
4	Woven fabric finishing			
	a. Simple processing	12.5	78.4	275.2
	b. Complex processing	10.8	86.7	276.9
	c. Complex processing plus desizing	5.0	113.4	507.9
5	Knit fabric finishing			
	a. Simple processing	8.3	135.9	392.8
	b. Complex processing	20.0	83.4	377.8
	c. Hosiery processing	5.6	69.2	289.4
6	Carpet finishing	8.3	46.7	162.6
7	Stock and yarn finishing	3.3	100.1	557.1
8	Non-woven finishing	2.5	40.0	82.6
9	Felted fabric finishing	33.4	212.7	930.7

The "wet processes" are mainly implemented by the textile finishing industry, where woven and knitted fabrics pass several water-intensive finishing operations to enhance the appearance, durability, and serviceability so that fabrics can be processed into finished goods. Finishing processes include four main stages (EPA, 1997; IPPC, 2003), as follows:

- Fabric preparation (or pre-treatment). Preparation is made up of several treatment and rinsing steps. Natural impurities or processing chemicals, potentially able to interfere with the down-stream processes, need to be removed. Typical preparation treatments include desizing (to remove the sizes applied to the yarn during the sizing operations), scouring (to remove different substances both naturally present and artificially applied), and bleaching (to remove the natural yellowish colour of cotton and other fibres). Moreover, preparation steps can include processes such as singeing and mercerising, aimed to chemically or physically alter the fabric.
- Dyeing. Dyeing operations are used to add colour to textiles by applying a wide range of dyestuffs, typically derived from coal tar and petroleum-based intermediates, and by using different techniques and equipment. In particular, dyeing can be performed by using continuous or batch processes. In batch dyeing (e.g., beam, beck, jet and jig processing), a certain amount of textile substrate is loaded into a dyeing machine and brought to equilibrium with a solution containing the dye. Auxiliary chemicals and controlled dyebath conditions accelerate and optimise the process. Then, the dye is fixed on the fibre using heat and/or chemicals, and the tinted textile substrate is washed to

remove unfixed dyes and chemicals. By comparison, in continuous dyeing processes, textiles are fed continuously into a dye bath and the process consists of dye application, dye fixation with chemicals or heat, and washing. Continuous operation yields smaller volumes of more concentrated dye waste than batch operation, equating to typically a 4-fold factorial difference with respect to dye concentration and a 2.5-fold difference in volume (Glover and Hill, 1993).

- Printing. Fabrics are often printed using a variety of techniques and machine types. The printing techniques are numerous: rotary screen, direct, discharge, resist, flat screen, and roller printing. Pigments cover about 75 to 85 percent of all colouring matter. Compared to dyes, they are typically insoluble and have no affinity for the fibres. Resin binders are typically used to attach pigments to substrates, while solvents are used as vehicles for transporting the pigment and resin mixture to the substrate.
- Finishing: Finishing encompasses chemical or mechanical treatments performed on fibre, yarn, or fabric to improve appearance, texture, or performance. Mechanical finishes can involve brushing, ironing or other physical treatments used to increase the lustre and feel of textiles. Application of chemical finishes to textiles can impart a variety of properties ranging from decreasing static cling to increasing flame resistance. Chemical finishes are usually followed by drying, curing, and cooling steps.

Desizing and scouring contribute to a relevant part of the total organic pollution in wastewater (Snowden-Swan, 1995). In particular, the organic load due to desizing can be roughly calculated on the basis of the amount of size applied in the previous phases considering a specific polluting load of sizing agents of 1÷2 grams of COD per gram of size. Natural sizes, such as those based on starch or proteins, are also characterised by a high BOD and a BOD/COD ratio of 0.6 – 0.7. On the contrary, synthetic size agents such as polyvinyl alcohol or carboxymethyl cellulose have an almost null BOD. With regards to the pollutants content in scouring effluents, it depends on the nature and quantity of the impurities present on the fibres and on the intensity of the process itself. High TSS and high organic loads are common in effluents from natural fibres scouring, due to the removal of dirt, waxes, suint, vegetable matter, etc. Soaps, detergents, alkali, solvents, as well as pesticides may also be present (Mattioli et al., 2002). Bleaching is an operation generally required when the finished fabric is to be white or dyed a light colour. It is usually carried out by chemical oxidation with sodium hypochlorite or hydrogen peroxide (Judd and Jefferson, 2003). Auxiliary chemicals such as sulphuric acid, hydrochloric acid, caustic soda, sodium bisulphite, surfactants and chelating agents are generally used during bleaching or in the final rinses, contributing to the pollution load (Cooper, 1978; Nolan, 1972).

With regards dyeing, in the past, concerns related to highly coloured waste streams were due to aesthetic reasons. More recently, attention has been paid to the recalcitrance and potential toxicity of xenobiotic compounds (Tan, 2001) even though some potentially toxic dyes were withdrawn from the market and new, more biodegradable molecules have recently been developed. According to Delée et al. (1998) another problem originated in the dyehouse is related to the nutrient load due to the need for dyebath additives. Moreover, according to Judd and Jefferson (2003) coloured wastewaters demand special consideration since they are one of the most problematic of all textile wastewaters, for a number of reasons, particularly:

- they are produced in large volumes (approximately 100÷150 L kg^{-1} textile product);
- they are not readily biodegradable (e.g., conventional municipal wastewater treatment plant generally remove only 20÷30% of colour associated with synthetic dyes);
- they require removal to very low levels prior to discharge.

Dyes are generally small molecules comprising two key components: the chromophores, the aromatic groups absorbing visible light to impart colour, and the auxochromes, which can not only supplement the chromophore but also render the molecule soluble in water and give enhanced affinity toward the fibres. A large number of dyes are reported in specialised literature (Colour Index, 1987). They can be classified according to the nature of the chromophore or to the mode of application. With regards to the former criterium, twelve dye classes are usually defined among which the most important group are azo dyes, including one or more azo groups (–N=N–), because of the great extent in number and tonnage of their application on natural fibres (cotton, silk, wool) and synthetic fibres such as polyesters, polyacrylic, rayon, etc. (Carliell et al., 1998). The latter classification includes seven classes: acid, basic, direct, disperse, reactive, sulphur and vat. Overlaps of the two classifications are possible e.g. azo dyes may belong to the acid, direct, disperse, basic, reactive and vat dye classes. Significant differences in the degree of fixation are reported for the various dye classes. Reactive dyes, which correspond to 20÷30% of the total dyes market (Vandevivere et al., 1998), are characterised by a low fixation rate and consequently by a high residual colour and COD discharged in dyeing and rinsing operations. Moreover, a large range of substances other than dyes can be found in a dye effluent. In fact, dyes are always used in combination with other chemicals (acids, alkali, salts, fixing agents, carriers, dispersing agents, surfactants, etc.) to control the adsorptive strength, levelling and retention (Judd and Jefferson, 2003).

On the whole, the major pollutant types in textile wastewater and the related process of origin are summarized in Table 3.2.

In particularly, five basic topics can be underlined (Delée et al., 1998), these being:

1. organic load;
2. colour;
3. nutrients;
4. pH and salt effects.
5. toxicants and refractory organics;

With regards to topic 4, several authors have identified as a potential problem the presence of salts in textile dyeing wastewater (EPA, 1997). Many salts are either used as raw materials or produced as by-products of neutralisation or other reactions in textile wet processes. Salt concentrations in effluent from cotton dyeing may reach 2,000 to 3,000 ppm and quantities of salts added in dyeing operations range from 20 to 80 % of the weight of the good.

With regards to topic 5, the concentration of heavy metals in textile mills has decreased in the last decade, mainly because of the reduction of metals contents in the dyes. In particular, sources of metals in the effluents may be fibres, supply water, dyes and chemical impurities. For example, dyes may contain metals such as zinc, nickel, chromium and cobalt, as functional part of the dye molecule or as impurities (EPA, 1997). Heavy metals concentrations in dyebath effluents, typically in the range of 1 to 10 mg l^{-1}, were reviewed by Correia et al., (1994).

The biodegradability of textile wastewater has been increasing during recent years, thanks to substitutions of the chemicals used in the process. In addition to the dye molecules, mostly non biodegradable in aerobic conditions, the persistent organics include: surfactants or their by-products, dyeing auxiliaries such as polyacrylates, phosphonates, sequestering agents (EDTA), synthetic sizes, anti-static, dispersing or fixing agents, preservatives and a large number of finishing auxiliaries.

Hazardous organic wastes may also result from the use of solvents in some scouring or printing operations (EPA, 1997), while halogenated organic compounds (AOX) may derive from hypochlorite bleaching operations or from spent liquors following shrink-proofing finishing treatment by chlorine.

Table 3.2. Major pollutant types in textile wastewaters, their origin and relevance/impact in biological treatment (Delée et al., 1998).

Pollutants	Major chemical types	Main processes of origin	Major relevance/impact on biological treatment
Organic load	Starches, enzymes, fats, greases, waxes, surfactants	Desizing Scouring Dyeing	High demand on aeration systems Activated sludge bulking problems
Colour	Dyes, scoured wool impurities	Dyeing Scouring	Insufficient removal in bioreactors
Nutrients (N,P)	Ammonium salts, urea, phosphate-based bu†ers and sequestrants	Dyeing	Not removed in anaerobic processes Increased complexity and sensitivity of aerobic processes (biological nutrient removal required)
pH and salt effects	NaOH, mineral/organic acids, sodium chloride, silicate, sulphate, carbonate	Scouring Desizing Bleaching Mercerising Dyeing	Inhibition/collapse of bioreactors
Sulphur	Sulphate, sulphide and hydrosulphite salts, sulphuric acid	Dyeing	Sulphate-reduction in anaerobic reactors
Toxicants	Heavy metals, reducing agents (e.g. sulphide), oxidising agents (e.g. chlorite, peroxide, dichromate, persulphate), biocides, quaternary ammonium salts	Desizing Bleaching Dyeing Finishing	Inhibition of sensitive microbial groups (nitrifiers, methanogens) in bioreactors
Refractory organics	Surfactants, dyes, resins, synthetic sizes (e.g. PVA), chlorinated organic compounds, carrier organic solvents	Scouring Desizing Bleaching Dyeing Finishing	Insufficient removal in bioreactors Possible accumulation in biomass aggregates/films, leading to inhibition

Finally, effluent characteristics related to macro-pollutants are presented in Table 3.3 for seven of the most important textile industry categories (EPA, 1982):

- raw wool scouring;
- yarn and fabric manufacturing;
- wool finishing;
- woven fabric finishing; knitted fabric finishing;
- carpet finishing;
- and stock and yarn dyeing and finishing.

Table 3.3. Textile processing categories and effluent characteristics (EPA 1997).

Category	BOD mg L^{-1}	COD mg L^{-1}	TSS mg L^{-1}	Oil and grease mg L^{-1}	Colour ADMI*	pH	Temp. °C
Raw wool scouring	6,000	30,000	8,000	5,500	2,000	8	28
yarn and fabric manufacturing	300	1,040	130	-	1,000	7	62
wool finishing	350	1,000	200	-	-	10	21
woven fabric finishing	650	1,200	300	14	325	10	37
knitted fabric finishing	350	1,000	300	53	400	8	39
carpet finishing	300	1,000	120	-	600	8	20
stock and yarn dyeing and finishing	250	800	75	-	600	11	38

*) ADMI (American Dye Manufacturers Institute) colour values result from a special procedure for determination of colour in dyeing wastewaters (Allen et al.. 1972; Little,1978).

3.2.2 Treatment of textile wastewaters

According to the Reference Document on Best Available Techniques for the textile industries (IPPC, 2003), the treatment of textile wastewaters can be carried out by different strategies. In particular, well-accepted general principles include the characterization of different wastewater streams arising from textile processes. Then, the segregation of the effluents at source according to their contaminant type and load, before mixing with other streams, has to be taken into account allocating them to the most appropriate treatment. In particular, streams containing a relevant non-biodegradable fraction has to be treated by appropriate techniques before, or instead of, a final biological treatment. However, the Reference Document stated that if such non-biodegradable water streams cannot be treated separately, they can be directed to a biological treatment on site, or off site in a municipal waste water treatment plant including an activated sludge systems with low F/M ratio to enable the degradation of both readily and hardly biodegradable substances. However, this technique is not sufficient for degrading or eliminating non-biodegradable compounds. Therefore, additional physical-chemical treatments would be required to achieve higher performances (IPPC, 2003). In particular, tertiary treatments carried out after the activated sludge are flocculation, precipitation, coagulation, adsorption, precipitation, ozonation (IPPC, 2003). Moreover, treatment such as chemical oxidation (hydrogen peroxide, and Fenton's reagent), electrochemical processes, UV radiation, filtration, membrane filtration, evaporation, ion exchange are also considered (Rott and Minke, 1999; Oller et al., 2010).
An example of a complete system (biological and tertiary treatment) is shown in Figure 3.3, where a WWTP for a medium-size textile finishing factory consisted of a biological aerobic

process supported by the addition of lignite coke (as an adsorbent), a precipitation/flocculation phase with sedimentation and filtration and adsorption is presented.

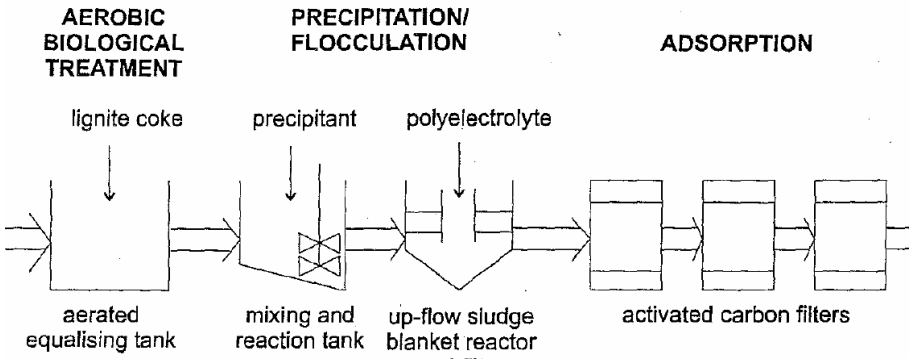

Figure 3.1. Schematic diagram of effluent treatment and recycling for a medium-size textile finishing factory in Tuttlingen, Germany (Rott and Minke, 1999).

According to Rott and Minke (1999) the efficiency of each treatment step became clear by considering the parameter COD (see Figure 3.2 left) and the removal efficiencies computed from the average values (see Figure 3.2 right). The main elimination of COD was achieved in the biological step, while this contributed to the decolourization at 15-18%. The main part of the dye was removed in precipitation/flocculation step, where the COD-elimination was 31%. The subsequent activated carbon filters contributed only insignificantly to the elimination of both the COD and the spectral absorption coefficient (SAC). Their performance was limited to a "police filter" function.

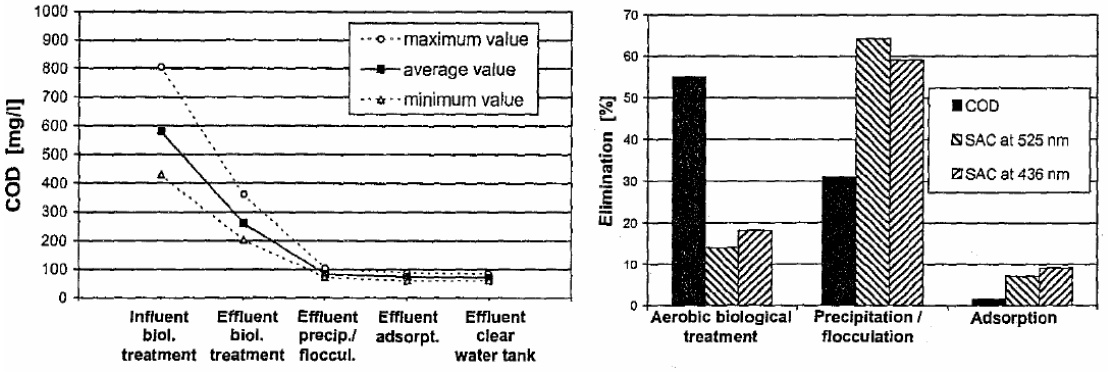

Figure 3.2. COD in the feed and effluent of each treatment step (left) and removal efficiency referring to raw water quality (right; Rott and Minke, 1999).

According to the Reference Document on Best Available Techniques for the textile industries (IPPC, 2003) physical-chemical treatments should preferably be carried out before the final

biological treatment, but in practice this is done only in a few mills. Ozonation, when applied at the end of the treatment process, mainly has the effect of degrading the chemicals into intermediate degradation by-products, whereas other treatments such as flocculation/precipitation, coagulation/adsorption/precipitation just transfer to sludge the substances that escape bioelimination. Moreover, combined biological, physical and chemical treatments with the addition of powdered activated carbon and iron salt to the activated sludge system with reactivation of the excess sludge by "wet oxidation" can be considered (IPPC, 2003). In particular, the process was introduced in the early seventies and industrialised with the commercial name of PACT® systems.

In the PACT system, the excess sludge (a mixture of spent powdered carbon and biomass) from the aerobic aerator is regenerated by means of a hydrothermal treatment (wet oxidation). This is a liquid phase reaction in water using dissolved oxygen (or air) to oxidise soluble and suspended oxidisable contaminants. The oxidation reaction is carried out at moderate temperatures of 150÷315°C and at pressures from 10 to 207 bar. The process destroys the large molecules in waste water, converting them predominantly to carbon dioxide, water and short chain organic acids, which are highly biodegradable and more suitable for biological treatment. This regeneration process provides continual reuse of the activated carbon and ensures high levels of waste treatment. A second improvement (the so-called $PACT^{++}$) could only be achieved by changing and extending the conventional activated sludge process with a nitrification/denitrification step followed by a filtration of the effluent to retain suspended solids. Then, the $PACT^{3+}$ system was also introduced. This concept is a combination of different available techniques, with the aim of improving performance, flexibility and economy of scale of the PACT® system. In the $PACT^{3+}$ system, activated carbon is added to the aerobic tank together with iron, which is used as a coagulant to precipitate phosphate and increase the binding of dyes into the sludge. The reactivation of the spent sludge containing powdered carbon and iron, is carried out at low temperature (below 130°C) using hydrogen peroxide to destroy concentrated or adsorbed substances creating the conditions for the Fenton reaction (H_20_2, Fe^{2+} at pH=3). Then, both the reactivated carbon and the iron are recycled back to the aerobic system.

Considering textile macro-pollutants fate (i.e., colour and surfactants) in conventional activated sludge systems, some consideration follows. With regards to colour, decolourization of dyes can be brought about by either adsorption to microbial cells (bio-sorption) or biodegradation. As for bio-sorption, dead bacteria, yeast, and fungi have been found to biosorb dyes from textile effluents and decolorize them (Robinson et al., 2001). The interaction involves adsorption, deposition, and ion-exchange and depends on factors including, structure of the dye, metal ions (metal ions could neutralize the surface charges

bridging dyes closer and making the bio-sorption process more favourable), surfactants (surfactants could reduce the binding efficiency of the cells), temperature (lower temperatures favoured bio-sorption if the process is physical adsorption), pH (pH affects the solubility of some dyes as well as the bio-sorption capacity), and ionic strength (Doble and Kumar, 2005). As for dyes biodegration, aerobic condition was found to be ineffective in decolorizing textile effluents even in cases where these are mixed and treated together with municipal sewage (Vandevivere et al., 1998). In particular, considering azo dyes, that according to Pearce et al. (2003) make up approximately 30% of the total dye market, such recalcitrant compounds are not readily metabolised under aerobic conditions (Robinson et al., 2001). In fact, azo dyes can be reduced by organisms grown under aerobic conditions (Stolz, 2001), but to be significant in the reductive process the bacteria must be specifically adapted. This adaptation involves long-term aerobic growth in continuous culture in the presence of a very simple azo compound (Pearce et al., 2003). In particular, the bacteria synthesise an azoreductase specific for this compound which, under controlled conditions, can reductively cleave the azo group in the presence of oxygen. In contrast, bacterial reduction under anaerobic conditions is relatively unspecific with regard to the azo compounds involved, and is, therefore, of more use for the removal of colour in azo dye wastewater (Stolz, 2001). In fact, under anaerobic conditions, many bacteria reduce the highly electrophilic azo bond in the dye molecule, reportedly by the activity of low specificity cytoplasmic azoreductases, to produce colourless aromatic amines. These amines are resistant to further anaerobic mineralization and can be toxic or mutagenic to animals. Fortunately, once the xenobiotic azo component of the dye molecule has been removed, the resultant amino compounds are good substrates for aerobic biodegradation (Stolz, 2001). Lourenço et al. (2000) suggested that if a sequential anaerobic–aerobic system is employed for wastewater treatment, the amines can be mineralised under aerobic conditions by a hydroxylation pathway involving a ring opening mechanism. Thus, for the most effective wastewater treatment, a two-stage process is necessary in which oxygen is introduced after the initial anaerobic reduction of the azo bond. The balance between the anaerobic and aerobic stages in this treatment system must be carefully controlled because it is possible for the re-aeration of a reduced dye solution to cause the colour of the solutions to darken. This is to be expected, as aromatic amines, produced when azo dyes are reduced under anaerobic conditions, are spontaneously unstable in the presence of oxygen. This results in the oxidation of the hydroxyl groups and of the amino groups to quinines and quinine imines. Compounds such as these can undergo polymerisation, leading to the development of new, darkly coloured chromophores, which are clearly unwanted by-products (Bromley-

Challenor et al., 2000). However, when the correct operating conditions have been established, many strains of bacteria are capable of achieving (Pearce et al., 2003).
With regards to surfactants, in the textile wastewater, most of non-ionic surfactants are made up of ethoxylate compounds (The Society of Dyers and Colourists, 1990), for which biodegradation possibility exists, according to different authors (*inter alia*: Maki et al., 1994; Tidswell et al., 1996). Consideration about surfactants removal will be made in the next section.

3.2.3 Treatment of textile wastewaters by means of the MBR technology and comparison with conventional activated sludge processes

Textile wastewater treatment by means of MBRs has been studied by several authors. In particular, two distinct approaches can be found in literature. The first one concerns the treatment of textile wastewater focusing on the overall performance of the MBR technology with reference both to the standard macro-parameters for wastewater, such as COD, BOD_5, nutrients and to specific textile macro-pollutants, i.e., dyes and surfactants. Moreover, some authors compared results of pilot plant MBRs with full scale conventional activated sludge processes (CASPs). On the other hand, the second approach focuses on only one specific textile macro-pollutant, such as colour or specific surfactants.
Considering the first approach, Malpei et al. (2003) tested a pilot MBR in parallel with a full-scale activated sludge WWTP fed on the wastewater from a textile factory aiming to investigate the possibility to upgrade the final effluent for internal reuse. The average COD removal efficiency of the existing WWTP during the experimental period was approximately of 90±4.7%, whereas the pilot MBR provided an excellent and quite constant COD removal efficiency close to 94% (93.8%), with a standard deviation of 2.3%. In particular, the MBR responded very well to unexpected and occasional peaks in the influent concentration, as it happened during a first period of operation, maintaining permeate COD values below 100 mg L^{-1} with influent concentrations of 4,000÷5,000 mg L^{-1} and F/M ratio of 0.2÷0.25 kg COD kg SS^{-1} d^{-1}. According to authors, neither the COD removal efficiency nor the effluent COD appreciably depend on the COD load, on the F/M ratio or on other parameters, such as temperature, DO concentration or MLSS. Colour was removed very efficiently by the MBR. The average abatement of absorbance was 96.5% at 426 nm and 98.7% at 660 nm. Non-ionic detergents, the only surfactants used at the factory, were found in the raw wastewater at concentrations ranging from 75÷95 mg L^{-1}; whereas in the permeate, their concentration dropped to 1.5÷5 mg L^{-1}, with removal rates in the range 95÷98%. Differently, Lubello and Gori (2004, 2005) carried out an experimental activity at the Baciacavallo Wastewater Treatment Plant (WWTP) (Prato, Italy) treating municipal

wastewater, in which textile industry wastewater predominates. The studied was aimed to verify the efficiency of a pilot-scale MBR and make a comparison with the Baciacavallo WWTP performances. In particular, the Baciacavallo WWTP biological section was followed by a coagulation–flocculation treatment and ozonation. During the 5 months experimental period, the pilot-scale MBR proved to be very effective for wastewater reclamation. On average, removal efficiency of the pilot plant (93% for COD, 96% for ammonium) was higher than the WWTP ones. Moreover, also the pilot plant constant efficiency was noteworthy: outlet values were substantially independent from inlet loads. Moreover, with respect to the full scale plant, the nitrification process efficiency appeared considerably higher. With regards colour, it was removed as in the WWTP. In fact, measured permeate absorbance values were significantly lower than the effluent values downstream the clariflocculation treatment, and comparable to those of the effluent from the ozone treatment. According to authors, such results can be explained with the increase in the absorption capacity by the biomass because of its destructuration, with respect to conventional sludge. This phenomenon was further stressed by the higher concentration of colorants in the oxidation tank, due to partial retention operated by the membranes. Finally, authors did not exclude a partial biodegradation of colorants (difficult in an aerobic environment) and limited to the chromophore group simple breakage. With regards to surfactants, anionic surfactants removal of pilot plant and WWTP were very similar (92.5 and 93.3% respectively), while the non-ionic surfactants removal was higher in the pilot plant (99.2 vs. 97.1%). In this case, a significant removal increase was noticed, both with respect to the conventional activated sludge treatment and to the ozone treatment; the latter, as everyone knows, shows a lesser efficiency with respect to non-ionic surfactants. Moreover, authors believe such a removal increment had to be ascribed to an actual increase in the biological removal, since the removal operated by the MF membranes can be deemed.

Similar results were achieved by Lubello et al. (2007), that carried out an experimental study to evaluate the possibility of upgrading the conventional activated sludge WWTP of Seano (Prato, Italy) treating municipal and textile wastewaters, by using membrane bioreactor technology. Badani et al. (2005) investigated the operation of an external pilot scale MBR for the treatment of textile wastewaters. The study showed that the average removal rate of the COD was of 97%, the rate of elimination of the ammoniac nitrogen was 70%, whatever was the age of sludge. Wit regards colour, a decrease of 70% was observed. Brik et al. (2006) conducted a laboratory-scale study considering a textile wastewater originating from a polyester finishing factory. On the basis of the experimental data obtained authors concluded that the MBR resembles a highly effective system for treating textile wastewater. They demonstrated that the system was largely resistant to changing loading rates and that

even at high loading rates efficient COD removal occurred, particularly greater than 90%, when influent COD values were at its maximum level (between 5,110 and 6,033 mg L^{-1}). The apparent sludge yield was very low underlining an additional advantage of the MBR system. Despite the deficiency in nutrient composition of the treated wastewater addition of nitrogen and phosphorous did not much contribute to COD removal. With regards to colour, removal efficiencies varied between 30 and 99.5%. Greatest deviations were examined at 436 nm, whereas colour removal at 525 and 620 nm were found to be between 46 and 98.5% and between 57 and 99.8%, respectively. Authors found that sludge growth was of critical importance in colour removal. In fact, they assumed that the main mechanism inducing colour removal was adsorption on biomass, whereas biodegradation seemed to play a minor role in colour removal as the persistent nature of textile dyes in activated sludge as discussed above. As a consequence, low sludge ages should be employed, to generate sufficient new biomass allowing adsorb incoming colour loads.

Baumgarten et al. (2006) found COD removal rates of 90% and 80÷60% treating wool and cotton finishing and yarn finishing wastewater, respectively.

Yigit et al., 2009 investigated the performance of a pilot scale MBR for the treatment of a highly concentrated mixed wastewater from wet processes (dyeing, finishing, and sizing). The system was operated at two different operation stages: (1) no sludge wastage with a typical permeate flux of 20 LMH and (2) a solids retention time of 25 days with the same flux. Results indicated that complex and highly polluted textile wastewaters was treated very effectively by MBR systems. In particular, the performance of the MBR system was not adversely affected by the variations in the influent characteristics, F/M ratio, organic load rate, specific substrate utilization rate, and DO levels. At SRT equal to 25 days, effluent quality was slightly better than at infinite SRT (i.e. no sludge wastage). Although not targeted, a significant degree of denitrification (TN removals as high as 78%) was achieved due to high MLSS concentrations and thus anoxic regions formed among flocs or at the bottom of the reactor. The average values of removal rates were BOD_5, 97%; COD, 97%; total nitrogen, 79%; total phosphorus, 59% and colour, 98%. With regards to membrane fouling, an increase in the TMP up 0.560 bar was observed only once in no sludge wastage conditions (after 35 days of operation). Such fouling was eliminated by applying chemical backwashing and chemical cleaning procedures. In the second stage of operation, no chemical cleaning was required and regular backwashing was sufficient to maintain the operation.

With regards to specific experimentations on colour removal or surfactants in MBRs relevant studies were reported herein. In particular, studies on colour removal were performed by You et al. (2008, 2009). Authors investigated and compared performances of a batch reactor

(SBR), an aerobic membrane bioreactor (AMBR), an anaerobic-oxic membrane bioreactor (AOMBR) and an AOMBR/RO processes treating the synthetic textile dyeing wastewater (Reactive Black 5). After more than 2 year process operation the COD of the effluents were 133, 95, 37, and 38 mg L^{-1}, respectively. The BOD of the effluents were 68, 3, 3, and 0 mg L^{-1}, respectively, and as for colour the above effluents were 548, 513, 196 and 32 ADMI, respectively. Therefore, it was found that the anaerobic tank of AOMBR and AOMBR/RO can lower the COD concentration. This revealed that the processes containing the membrane unit performed excellent efficiencies and BOD removal. Additionally, the anaerobic tank can enhance the COD and true colour removal, while the RO unit can further remove the true colour. This study also isolated higher decolorized performance microorganisms by microbiologic techniques. In particular, 18 isolates cultured from a specific anaerobic medium showed more than 90% Reactive Black 5 removal efficiency, revealing that the anaerobic tank did enhance the growth of the high decolorized microorganisms, especially anaerobic bacteria.

Since aerobic degradation of dyes is difficult in an aerobic environment, and therefore permeate in aerobic MBR presents residual colour not compatible with eventual reuse, Brick et al. (2004) tested the performance of chemical advanced oxidation on the elimination of the colour downstream of an MBR, particularly considering: ozonation, chlorination and hydrogen peroxide oxidation. For chlorination, even with 250 mg L^{-1} (active chlorine) only 80% colour removal was achieved which is considered unsatisfactory by authors. For hydrogen peroxide, the colour removal was even poorer; it was just 10% at a concentration of 250 mg L^{-1}. In contrast, good results were obtained by ozonation. By using only 38 mg L^{-1} within 20 minutes, it was possible to achieve the reuse recommendation with a satisfactory colour removal of 93%.

With regards to surfactants, most of the studies reported no significant differences between MBR and CASP for compounds such us linear alkylbenzene sulfonates, LAS, but showed higher performances for compounds such as nonylphenols, NP, and nonylphenol ethoxylates, NPEO (Li et al., 2000; De Wever et al., 2004; González et al., 2007; González et al., 2008). In particular, González et al. (2007) investigated surfactants removal in a pilot plant MBR working in parallel to a full-scale wastewater treatment plant using conventional activated sludge process (CASP). In the CASP system 87% of parent long ethoxy chain NPEOs were eliminated, but their decomposition yielded persistent acidic and neutral metabolites which were poorly removed. The elimination of short ethoxy chain NPEOs (NP_1EO and NP_2EO) averaged 50%, whereas nonylphenoxy carboxylates (NPECs) showed an increase in concentrations with respect to the ones measured in influent samples. Nonylphenol (NP) was the only nonylphenolic compound efficiently removed (96%) in the

CASP treatment. On the other hand, MBR showed good performance in removing nonylphenolic compounds with an overall elimination of 94% for the total pool of NPEO derived compounds (in comparison of 54%-overall elimination in the CAS). The elimination of individual compounds in the MBR was as follows: 97% for parent, long ethoxy chain NPEOs, 90% for short ethoxy chain NPEOs, 73% for NPECs, and 96% for NP. Gori et al. (2010) investigated the fate of linear LAS, NPEOs, NPECs, and NP operating two membrane bioreactors at high SRT, between 30 and 75 d, in parallel to a conventional activated sludge plant (CASP) conducted at SRT of 10 d. All systems were very efficient in the removal of LAS (around 99%). However, the analysis of variance showed that the difference in the removal efficiency of LAS in the CASP and the MBRs (respectively 99.0±0.43 and 99.8±0.11%) were significant ($p<0.05$), confirming the importance of SRT in the removal of LAS. Comparison between the CASP and the MBRs in the removal efficiency of nonylphenolic compounds were conducted by authors considering long ethoxy chain NPEOs ($NP_{3-15}EO$), short ethoxy chain NPEOs (NP_1EO and NP_2EO), $NP_{1-2}EC$, and NP. In all cases MBRs were more efficient than the CASP. In the case of NP the removal was about 76±7.5% for the CASP and 90±12.1% and 82±8.7% for the MBRs. According to authors, better performance of MBRs in the removal of nonylphenolic compounds was attributed to a better degradation. For example, considering the sum of $NP_{1-15}EO$ and $NP_{1-2}EC$, estimated biodegradation was about 48% for the CASP and 72% for MBRs.

3.3 Treatment of metal working effluents

3.3.1 Characteristics of metal working fluids

Metalworking fluids (MWFs) are widely used in the metalworking industry for cooling and lubricating during the machining process to increase productivity, prolong tool life, prevent corrosion, etc. They are also adopted for carrying away metal chips and swarf in operations, such as grinding, milling, turning, cutting, drilling, etc. (Muszyński et al., 2007), as shown in Figure 3.3 and Figure 3.4. MWFs can be straight machining oils, water soluble oils or oils in water emulsions, semi-synthetic metalworking fluids, synthetic metalworking fluids, strong/mild alkaline cleaners and mineral solvent emulsion cleaners (Burke, 1991; Cheng et al., 2005; Muszyński et al., 2007). The most widely used are emulsifiable oils, which account for approximately 80% of the annual MWFs consumed worldwide (Muszyński et al., 2007).
MWFs are composed of constituents that improve lubrication and cooling performance and complex chemicals such as emulsifiers, corrosion inhibitors, extreme pressure additives, foaming inhibitors. More than 300 different substances are known to be used in MWFs and a single MWF can contain up to 60 different components (Rabenstein et al., 2009). The exact

chemical composition is unknown because it is normally proprietary and varies depending on the specific use (Baker, 1983). Moreover, it cannot be determined because substances of technical purity grade are used, which means a purity of 85–95% (Rabenstein et al., 2009).

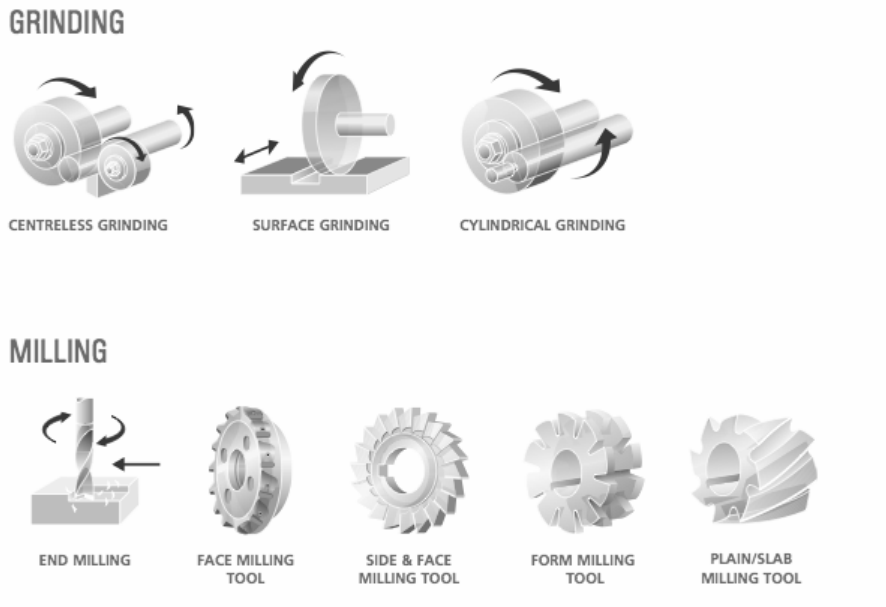

Figure 3.3. Examples of grinding and milling operations (www.castrol.com/industrial)

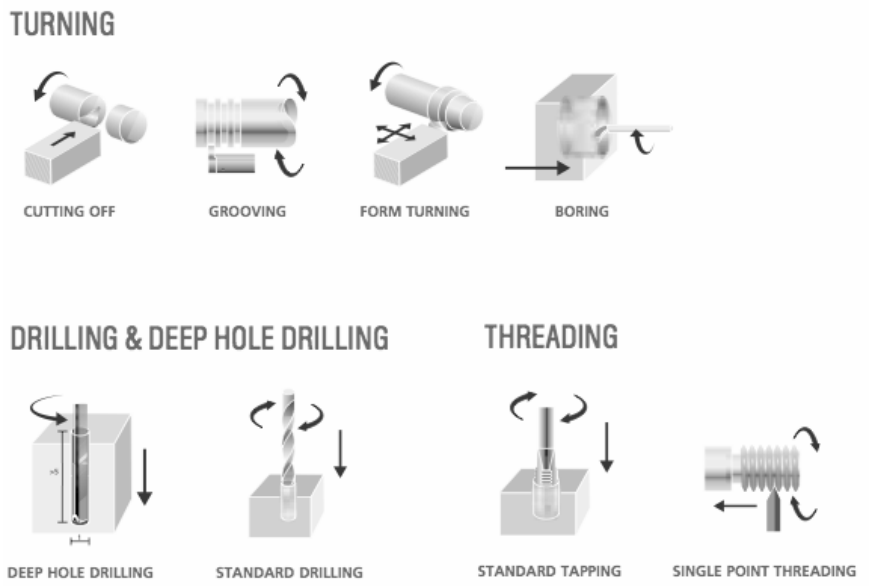

Figure 3.4. Examples of turning, drilling and threading operations (www.castrol.com/industrial)

However, Cheng et al. (2005) listed the main constituents of MWFs (Table 3.4), that can be classified by functionality. For example, chemicals used as lubricating would be from the oil category (mineral oil, petroleum oil, etc.) and in order to eliminate mist forming, ester base oils or ester molecules have been used. Alkanolamines are generally known as corrosion inhibitors but other amines and fatty acids are also used. In addition, boric acid is also widely used as an additive for corrosion protection, pH buffering and hard water compatibility (BLF, 2003). Substances derived from alcohols or alcohols themselves are the main components in emulsifiers. Phosphate esters and sul-phurised esters are mainly used as pressure additives. Biocides are also used since the microbial contamination of water miscible MWFs is a common problem leading to functional and hygienic concerns. In fact, these fluids are prone to contamination by bacteria and fungi, causing problems of discolouration of the emulsion and the loss in quality of the work pieces and tool failure. One source of microbial contamination can be the water used to dilute the concentrate. Residues of used MWF, remaining after cleaning in tubing or dead spaces may lead to a contamination of the new MWFs emulsion as well. In addition, microorganisms can enter MWFs through work pieces or personnel handling the machines and through dust particles on which they attach (Rabenstein et al., 2009). A partial list of bacteria isolated from fresh and spent MWF is provided in Table 3.5. There is a wide range of biocides used in MWFs and typically they are metallic or chlorinated organic compounds designed for use as a preservative, but other compounds are also used (Rossmoore, 1981).

The MWFs worldwide annual usage is estimated to exceed 2 million of m^3 and the waste could be more than ten times the usage, as the MWFs have to be diluted prior to use (Cheng et al., 2005). Used MWFs cause high levels of contamination due to the presence of the complex chemicals, so that their treatment and final disposal must be handled carefully. In terms of influent COD, the concentration can vary from 1 to 1,337 g L^{-1} (Schreyer and Coughlin, 1999; Hilal et al., 2005). Other significant negative aspects related to MWFs include safety and health concerns, including cancer risks associated with MWF exposure (Calvert et al., 1998) due to harmful vapours in the workplace environment and toxic hazardous substances, and occupational allergic contact dermatitis directly linked to alkanolaminebo rates (Sandin et al., 1990; Bruze et al., 1995). Moreover, a correlation between pneumonitis hypersensitivity and *Mycobacterium* contamination (Moore et al., 2000) and even stroke mortality has increased among workers exposed to MWFs (Park, 2001). In addition to the toxicity of chemical substances, there are some pathogenic bacteria found in MWF samples, e.g., *Pseudomonas aeruginosa* and *Klebsiella pneumoniae* (Chazal, 1995). Despite these significant effects from waste MWFs and in-used MWFs, very few studies have been carried out directly related to toxicity in the environment.

Table 3.4. Summary of different metalworking fluid compositions (Cheng et al., 2005).

Type of MWFs	Composition
Synthetic	Ethanolamines, polyglycols, chlorinated or sulphonated paraffins, mineral oil polyglycols, glycol ether, alcohol amine salts, little or no oil, alkanolamine, emulsified oil Sodium O, O-diethyl dithiophosphate, ethyldiethanolamine (MDEA) 2-amino-2-ethyl-1, 3-propanediol (AEPD), 2-(2- aminoethoxy) ethanol Ethanolamine; 2-aminoethanol, N,N0-methylenebismorpholine
Semi-synthetic	Triethanolamine, sodium sulphonate, 2-ethoxyethanol, alcohol ethoxylate phosphate ester, polysulphides, di-tert- dodecyl, alcohol, C11-14-iso, C13-rich, sodium sulphonate, 1-[2-(allyloxy)-2-(2,4-dichlorophenyl)-1H-imidazole, N,N0-methylenebismorpholine
Not stated whether synthetic/semi-synthetic	Petroleum oil, petroleum sulphonates, linoleic acid, oleic acid, fatty acids, alkanolamines, alcohols, polyglycols, amino acids, carboxylic acids, surfactants containing sulphur, chloroalkanes, triazoles, triazines triethanolamine, cyclohexanamine, benzotriazole, indole, heptanoic acid decanoic acid, hexadecanoic acid, 9-octadecenoic acid Mineral oil, sulphonated products, emulsifying agents Alkanolamineborates, ethanolamines Boric acid, nonyl phenol 10 MEO, fatty acids, nonyl phenol 4 MEO, ethoxylated alcohols; benzotriazole, amine propoxylate, propylene, formaldehyde-based biocide, benzotriazole, dodecanedioic acid, lauric acid, sebacic acid, amine propoxylate, glycerin, propylene glycol
Cleaners	Silicic acid, dipotassium salt, ethanolamine; 2- aminoethanol, alcohol, C8-10, ethers with polyethylene- polypropylene, glycol monobenzyl ether, sodium hydroxide, silicic acid, sodium salt, alcohol, C11-14-iso-, C13-rich

Table 3.5. Partial list of bacteria isolated from in-use MWFs and spent MWFs (Cheng et al., 2005).

Organism
Mycobacterium immunogenum, Pseudomonas fluorescens, Alcaligenes xylosoxydans, Bacillus pumilius, B. sphaericus, B. marinus, B. oleronius, B. licheniformis, Brevibacterium brevis, Brevibacterium lyticum, Brevundimonas diminuta, Cellulomonas flavigena, Clavibacter michiganensis, Comamonas acidovorans, Comamonas testosteroni, Curtobacterium flaccumafaciens, Gordona rubropertinctus, Methylobacterium mesophilicum, M. radiotolerans, Nocardia globerula, Enterococcus faecium, P. putida, P. saccharophilia, Ralstonia pickettii, Rhodococcus erythropolis, Stenotrophomonas maltophilia, Proteobacteria and, high G+C Gram + bacteria, Ochrobactrum anthropi, CDC Group B-1/B-3, Alcaligenes faecalis ss faecalis, Tetragenococcus halophilus, P. glathei, Streptococcus pneumoniae, Staphylococcus hominis, Corynebacterium halophilus, Staphlococcus auricularis, P. pseudoalcaligenes Comamonas terrigena, Citrobacter freundii, Serpens flexibilis, Xanthomonas oryzae, Micrococcus sp. P. dimuta, traphylococcus sp. Comamonas testosteroni, P. fragi, Aeromonas, Pseufomonas, Flavobacterium, Bacillus, Salmonella spp., Shigella spp., Vibrio spp., Gram (+) cocci, P. aeruginosa, P. putida, P. fluorescens, Klebsiella pneumoniae, P. pseudoalcaligens, P. stutzeri, Shewanella putrefaciens, Aerococcus viridans, Enterobacter agglomerans, K. pneumoniae, K. oxytoca, Proteus vulgaris, E. coli, Citrobacter diversus, Citrobacter freundii, Serratia spp., A. viridans, Morganella morganii, Corynebacterium spp., Streptococcus spp., fungi, yeast Candida spp., Mould Fusarium spp., Acinetobacter calcoacetucus subsp. Anitratus subsp. Lwoffi, Acinetobacter haemolyticus, P. putida, P. stutzeri, P. alcaligenes, P. putrefaciens, P. cepacia, Alcaligenes denitrificans, Acinetobacter, Aeromonas, Alcaligenes, Caulobacter, Corynebacterium, Hyphomonas, Flavobacterium, Listeria, Microcyclus, Noraxella, Pseudomonas, Seliberia, Sphaerotilus, Spirosoma

3.3.2 Biological treatment of metal working effluents

The main disposal methods for metal working effluents are electrochemical, chemical and physical processes (Muszyński and Łebkowska, 2005; Cheng et al., 2006) including flocculation (inorganic chemicals or cationic/anionic organic compounds), hydrothermal oxidation, high temperature incineration, evaporation, membrane separation (MF, UF, NF and RO), peat adsorption etc. Almost all mentioned classical techniques (except for the incineration) do not solve ultimately the problem of MWFs treatment, since the emulsion is split into water and oil phases. Moreover, because of the adoption of complex synthetic organics (Table 3.4) in MWFs, the aim of the disposal is not only the removal of oily compounds but also the removal of organic matter. Therefore, biological treatment offers an alternative solution considering both suspended growth and attached growth systems. In fact, generally the biological treatment efficiency in terms of COD removal ranges form 60% to 99% (Cheng et al., 2006). Sutton et al. (1985) were the first authors investigating MWFs biological treatment. In particular, they used a fluidised bed reactors and found COD removal rates of 66÷81%. The selection of carriers in fluidised bed reactors directly affects the overall performance of wastewater treatment. For instance, granular activated carbon (GAC) provides not only surface area for biological growth, but also adsorption capacity. Moreover, recent developments in carriers have provided other alternatives, such as polypropylene beads (Harris et al., 2001), polyurethane foam (Peng et al., 1997) and ceramic particles (Peng et al., 1999). Activated sludge systems were considered firstly by Polak (1986), who found COD removal rates of 70÷84%; whereas Kim et al. (1989, 1992a, 1992b) appeared to be the first authors to investigate whether aerobic or anaerobic conditions were better for waste MWFs treatment. All their investigations were carried out with simulated wastewater consisting of eight selected fresh MWFs mainly composed of fatty acids, alkanolamines, alcohols, polyglycols, amino acids, carboxylic acids, sulphur containing surfactants, chloroalkanes, triazoles and triazines. Following their studies, they concluded that aerobic treatment removed more than 88% COD, whereas only 64% was removed anaerobically using an anaerobic, granular activated carbon (GAC), fluidized-bed process. Results indicated that approximately 68% of the COD biodegraded was converted to methane suggesting that biodegradation was the major constituent of COD removal, compared to MWFs adsorption on GAC and biomass. Further investigation indicated that approximately 65% of residual COD from the anaerobic process was aerobically biodegradable. Recently, Perez et al. (2006) studied the anaerobic treatment of spent cutting oils using an anaerobic thermophilic fluidized bed. At the start-up vinasses was considered as the only carbon source and then reduced progressively while increasing the amount of cutting oil wastewater, as follows: 0, 42.4, 66.6 and 100%. When the reactor was

fed with cutting oil wastewater as the only source of carbon removal rates were: 85.8% and 58.1% for COD and TOC, respectively, whereas the volumetric methane produced in the digester was negligible. By comparison, at the beginning of the reactor operation (vinasse only) removal rates were: 87% and 94.6% for COD and TOC, respectively, whereas the specific volumetric methane produced in the digester reached 0.45 m^3 m^{-3} d^{-1}. According to the authors, the cutting oil wastewater tested was toxic and the biological activity in reactor, as indicated by methane and VFA production, which decreased dramatically as soon as it was added. On the other hand, considerable COD removal continued throughout the testing whereas TOC removal also was observed in decreasing amounts. The authors carried out another study (Perez et al.; 2007) without any co-substrate addition and same qualitatively results were observed. These findings show how the complexity of MWFs compositions can affect their biodegradability.

In order to improve MWF biodegradability Muszyński and Łebkowska (2005) proposed a biotechnological method including: multiple reinoculating of biomass by adding active microorganisms into the bioreactor, immobilizing microorganisms on the PVC foam carrier, and carrying out the process in the anoxic/aerobic conditions at phase durations of 0.5 and 5.5 hours, respectively. The above parameters allowed to obtain the following removal rates: 87% of COD, 97% of BOD_5, 98% of petroleum ether extractable organic and more than 96% of total content of hydrocarbons (determined by infrared spectrophotometry). Moreover, the chromatographic analyses showed almost complete reduction of oily hydrocarbons contained in the used MWF.

From the composition of MWFs, it can be seen clearly that there is sufficient carbon, nitrogen, sulphur, etc. As for phosphorous, it seems relatively absent and a supplement would improve the efficiency. According to Schreyer and Coughlin (1999), a phosphorous supplement has improved the growth of microorganisms and the overall treatment performance. Therefore, the level of phosphorous present in the treatment of spent MWF streams should be considered either by adding it as a supplement or by combining other waste streams to enhance the overall efficiency. With regards reactor temperatures, Deepak et al. (1994) found that COD was reduced as temperature increased from 15 to 30°C. Cheng et al. (2004) also increased temperature to 40°C and found the COD removal rate was effectively double that at 30°C; whereas Cheng et al. (2006) studying aerobic biological wastewater treatment over the temperature range of 25÷75°C found the best treatment performance at 50°C (COD removal rate of 97.27%). Cell viability was observed throughout the operation and it was found that higher temperature did not directly correlate to low viability. However, under thermophilic conditions, many physico-chemical parameters, which are affected by higher temperature, need to be taken into account either in the reactor

design or operational conditions. These physico-chemical parameters include viscosity, surface tension, gas–liquid solubility, diffusivity, and solid–liquid solubility. The first three parameters decrease with temperature and conversely, the last two factors increase with temperature (Lapara and Alleman, 1999; Lapara et al., 2001). Moreover, the narrower range of bacterial communities within the thermophilic category could reduce the consistency of the bioreactor (Lapara et al., 2002). In addition to temperature, pH is also an important factor that needs to be considered when operating a bioreactor. As high pH helps biocide activity (Rossmoore, 1981; Sandin et al., 1990), alkaline compound formations in the treatment process have to be limited. Van der Gast and Thompson (2004) found that the optimal pH range for biological treatment is between 6 and 7; whereas Deepak et al. (1994) between a pH range from 6 to 7.5. Van der Gast and colleagues have also carried out a series of waste MWF treatment studies (Van der Gast and Thompson, 2004; Van der Gast et al., 2001, 2002, 2003a, 2003b) comparing the overall performance among activated sludge from municipal sewage works, indigenous communities and bacterial consortia. They proved that introducing specific bacterial consortia was more effective. The technique of bacterial inoculation is named bioaugmentation, which is where additional organisms are added to enhance the treatment level when the existing microorganisms are not degrading the pollutant satisfactorily (Goldstein et al., 1985; Kaplan and Kitts, 2003). According to Hilal 2005, aerobic biological treatment can be applied to nanofiltration permeate and part of the nanofiltration retentate can be re-used when its quality is compatible with machining processing. In particular, the authors investigated a method to develop a bioconsortium from microbes found in the waste metalworking fluid. The method took place in three phases: feasibility, bioconsortium development and optimisation. Flask tests were used to show the feasibility of using the metalworking fluid indigenous microbial community for the degradation of the nanofiltration permeate of the metalworking fluid. A suspended bioreactor allowed the development of a better-adapted consortium. Finally, a fixed bed bioreactor inoculated with the developed bioconsortium was set up and run for 8 months to test the bioconsortium's robustness and to optimise the biological process. A bioconsortium was successfully developed using a simple method and a 90% reduction in the original nanofiltration COD level was achieved by the fixed bed bioreactor.

3.3.3 Treatment of metal working effluents by the MBR technology

With regards to MBR technology applied to MWFs, only aerobic biological treatments have been considered so far and results of the most important studies are discusses herein.

Sutton et al. (1994) and Knoblock et al. (1994) were the first authors to consider and investigate aerobic submerged MBRs applied to oily wastewaters. In particular, the authors

demonstrated the technical and economic advantages of applying the MBR technology to the treatment of automotive manufacturing plant wastewaters by different pilot plant studies. Moreover, the results of pilot studies provided the basis of the design of a full scale demonstration MBR. With regards to pilot scale studies, COD removal rates varied from 82 to 96%, BOD_5 removal rates from 96 to 99.8%, total and hydrocarbon fats, oils and grease removal rates from 96 to 99% and from 97 to 99.9%, respectively. According to the authors, no advantage was gained with respect to treatment performance by operating at longer HRT and SRT conditions. Moreover, the accumulation of non-reactive compounds due to the presence of UF membrane and high SRT employed (>40d) did not affect microbial activity at least to the extent of affecting the degree of ammonium oxidation to nitrate. Considering the full scale demonstration MBR results revealed a number of apparent design discrepancies. Despite a COD volumetric loading during the evaluation period of more than double that anticipated, the performance of the system exceeded design expectations in terms of COD removal (94% vs 91%) and effluent total oils and grease (25 mg L^{-1} vs 18 mg L^{-1}). Later, in 1998, in the course of the Great Britain Biotechnology Means Business Initiative, the Department of Trade and Industry (DPI) published a document about the development of an integrated membrane bioreactor system for the treatment of used cutting fluids and other oily wastes in the engineering industry (DPI 1998). In particular, several wastewaters with spent MWFs, ranging from 48 to 68 g COD L^{-1}, were investigated and treated by MBRs and resulted in COD removal rates of 95÷99%.

With regards to fouling behaviour in MBRs treating industrial oil contaminated wastewaters, studies were carried out by Bienati et al. (2008) using a submerged membrane bioreactor. In particular, the MBR was able to treat the wastewater with high removal efficiency (98% as COD) in different operating conditions, low hydraulic retention times (10 h) and high biomass concentration (from 14 to 27 g/L). The critical flux of three different types of membranes (ultrafiltration PVDF membrane, and microfiltration PP and PE membranes) was assessed using the flux-step method. The PVDF membrane showed the lowest critical flux value (6 LMH) which anyway was not very different from the value of the other two membranes (9 LMH). It was found that the PP microfiltration membrane tested in the long-term experiment was fouled (although very slowly) also when permeating fluxes below the critical flux. The PP and PE microfiltration membranes were more sensitive to the irreversible fouling than the ultrafiltration membrane. In fact, after the cleaning procedure water permeability was not completely recovered, indicating that some material could be entrapped in the membrane structure permanently. According to the authors, although the PVDF membrane showed a lower value of critical flux it should be considered in a possible economic evaluation because of the lower fouling tendency.

4 Design of the research

4.1 Introduction

In this chapter, information on the overall planning of the research is presented, whereas specific details about experimental procedures, data processing and analytical techniques are provided in the following materials and methods sections (Chapter 5).

4.2 Design of the research

4.2.1 Treatment of textile wastewaters and fouling control in an anoxic-aerobic MBR (topic A)

With regards to topic A, the treatment of textile wastewaters and fouling control in an anoxic-aerobic MBR was investigated. In particular, a pilot MBR was designed on purpose according to the modified Ludzack-Ettinger process for the biological nitrogen removal, with a separate membrane compartment equipped with two lab-scale Siemens Water Technologies (Memjet®) membrane modules (surface area of 0.5 m^2 and pore sizes of 0.04 μm; see section 5.2.1). The pilot MBR was located in a full scale WWTP near Como, Italy, fed with a mixed domestic-textile wastewaters (65% of the flow rate and 70% of the COD loading), whose characteristics are presented in Table 4.1. Mixed wastewater, prior to be fed into the pilot MBR, was pre-treated through the full scale WWTP pre-treatments, as shown in Figure 4.1.

Table 4.1. Mixed wastewater characteristics (average value and standard deviation).

Parameter	Average value ± std. dev.	Parameter	Average value ± std. dev.
COD	316.9 ± 134.8 mg L^{-1}	VSS/TSS	80%
TKN	37 ± 14.6 mg L^{-1}	abs. at 426 nm	0.069 ± 0.034 cm^{-1}
N-NO3- + N-NO2-	1.5 ± 1.3 mg L^{-1}	abs. at 558 nm	0.052 ± 0.028 cm^{-1}
TSS	117.2 ± 49.4 mg L^{-1}	abs. at 660 nm	0.025 ± 0.013 cm^{-1}

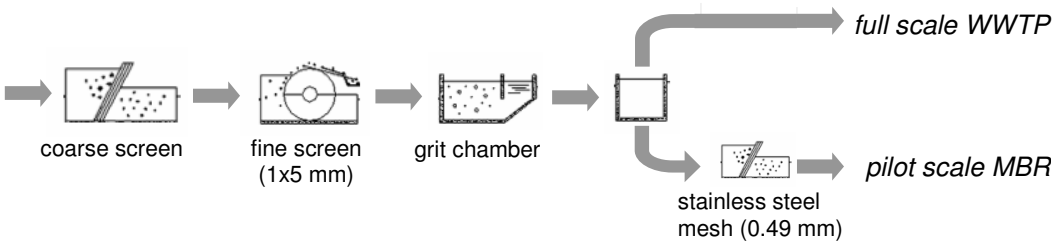

Figure 4.1. Pre-treatments of the full scale WWTP and position of the pilot MBR.

Research activities were planned in three major steps, including (1) the MBR "collaudo", (2) the membrane characterization with clean water, and, (3) the experimental activities with the pilot MBR and batch tests executed in parallel as shown in Figure 4.2. Apart from the MBR start-up (~1.5 months, see over), a first stage of the MBR operation (stage 1, ~7.5 months) was planned as a reference period (no flux enhancer dosage) during which steady MBR operation was achieved. Then, in a second stage of the MBR operation (stage 2, ~2.5 months) the addition of a flux enhancer, previously selected on the basis of a jar test campaign (flux enhancer selection), was employed. As shown in Figure 4.2, membrane main cleanings were planned and performed at the beginning of each stage adopting a procedure designed with the manufacturer (see section 5.3.2). Differently from the real scale, the aim was not to recover membrane permeability because of severe fouling, but 3 cleans were planned to operate with clean membranes (i.e., comparable initial conditions) in each stage. Such experimental activities, were properly designed in order to respond to the main goals of the study, that are briefly recalled herein:

- goal 1: assessment of the MBR process in terms of removal efficiency and comparison with the full scale wastewater treatment plant (WWTP);
- goal 2: screening of 3 flux enhancers by lab-scale tests to select the best chemical and define the optimal dosage on continuous operation of the pilot MBR;
- goal 3: continuous dosage of the selected flux enhancers and evaluation of its efficacy in terms of permeate quality enhancement and fouling control;
- goal 4: development of a new methodology for the evaluation of sludge fouling propensity and its implementation to monitor the effects of the flux enhancer.

With regards to goal 1, the assessment of the MBR process in terms of removal efficiency was performed along the 7.5 months experimental period of stage 1 (without any flux enhancers). In particular, ordinary macro-parameters, i.e., COD, TOC, TSS, VSS, nitrogen compounds (TKN, N-NH_4^+, N-NO_2^-, N-NO_3^-), total phosphorus and textiles macro-pollutants, i.e., colour (absorbance at 426 nm, 558 nm, 660 nm) and surfactants (non-ionic surfactants,

and anionic surfactants) were monitored weekly. Moreover, statistics related to the permeate quality in stage 1 were calculated and then compared with the biological and the final effluent quality of the full scale WWTP (Figure 4.3). Data available for the full scale WWTP were related only to COD, nitrogen compounds and colour.

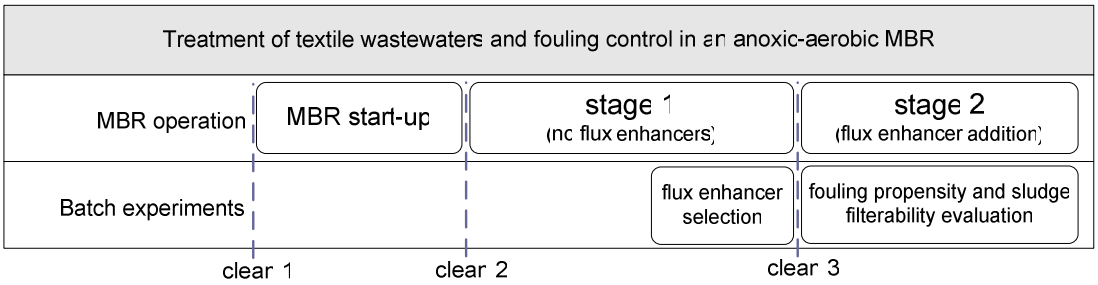

Figure 4.2. Timetable of the research phases (topic A).

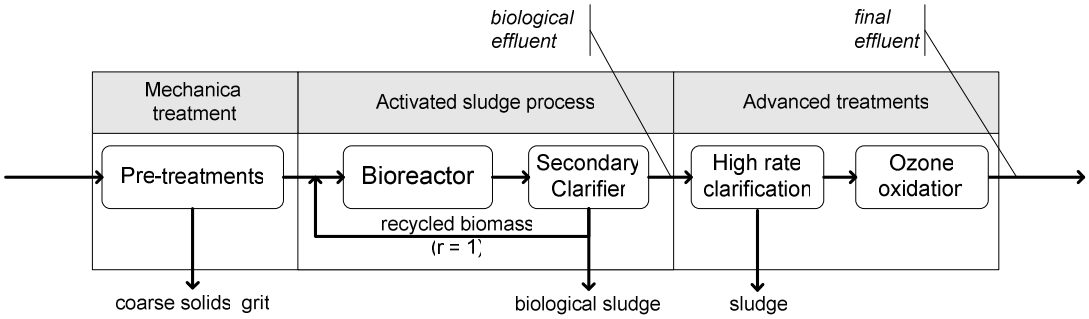

Figure 4.3. Flow diagram of the full scale WWTP.

Considering goal 2, a specific chemical for each type of flux enhancer used in literature was selected (3 flux enhancers overall) and, then, flux enhancers were screened by lab-scale tests considering sludge samples collected at the end of stage 1, when pseudo stationary conditions were achieved. The selection of the best chemical and the optimal dose were executed as described below. Then, a dosing strategy was properly designed to increase the concentration of the flux enhancer in mixed liquor progressively from a lower to the optimal value. In fact, in order to avoid any risk of inhibition on the biological activity, the strategy was planned to consider a first instantaneous dosage (first arrow in Figure 4.4) to reach an initial low concentration (i.e., half the optimal concentration) and then a continuously dosage to reach progressively the optimal concentration as shows in Figure 4.4. The second arrow indicates another instantaneous addition of flux enhancer follows by a continuously dosage to keep the concentration constant at the optimal value.

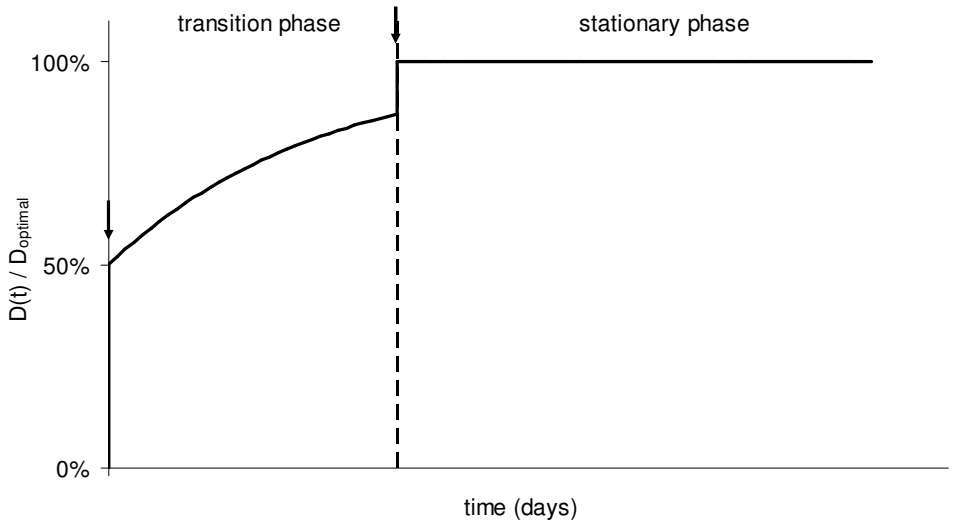

Figure 4.4. Dosing strategy of the selected flux enhancer (black arrows indicate instantaneous additions of the selected flux enhancer).

During the transition phase, attention was paid to the efficiency of MBR since a loss in effluent quality would have meant an inhibition of bacterial biomass. Moreover, with this aim, respirometric techniques were employed to evaluate the heterotrophic and autotrophic activities at the beginning and at the end of stage 2 (see section 5.3.2, method A.8).

As for goal 3, two main topics were investigated: (1) the permeate quality enhancement and (2) fouling control provided by the selected flux enhancer (Table 4.2). With regards to the permeate quality enhancement, both standard quality parameters (COD, TOC, TSS, VSS, nitrogen compounds and phosphorous) and textiles macro-pollutants (colour and surfactants) were considered and removal rates were also calculated. Differently, with regards to fouling control, the following aspects were taken into account:

- relevant characteristics of mixed liquor related to fouling;
- parameters describing the hydraulic performance of UF membranes and fouling monitoring.

As for the relevant characteristics of mixed liquor related to fouling, since biopolymers represent an important cause of fouling and impact on its occurrence (see section 2.5.1) soluble-EPS and bound-EPS were monitored (see section 5.3.2, method A.3) measuring proteins and carbohydrates in bulk liquid and in the extracted solution (see below, Table 4.3). Moreover, the mean oxidation state of organic carbon (see section 5.3.2, method A.4) and organic carbon apportionment between proteins, carbohydrates and other organics (see section 5.3.2, method A.5) were evaluated. In particular, these methods were applied also to influent and effluent to investigate any correlation between the organic composition of

the mentioned media. Moreover, it has been demonstrated that divalent cations influence strength and filterability of sludge and, on the other hand, enhance fouling as well (see section 2.5.2). Therefore, particular attention was paid to cations content in bulk, extracted solution, mixed liquor, and permeate. Also, the evolution of flocs strength was assessed introducing two indexes: "the divalent cation content in biomass flocs" (SI_1) and the "cations extraction efficiency" of the thermal method (SI_2; see section 5.3.2, method A.6). According to the divalent cation bridging (DCB) theory (Sobeck and Higgins, 2002) and the polymer bridging model (PBM) theory (Wilén at al., 2003), divalent cations bridge negatively charged functional groups within the EPS aggregating cells and stabilizing flocs (see section 2.5.2). Therefore, the higher the values of SI_1 , the better the flocs strength is. Differently, index SI_2 indicates the percentage of low bounded divalent cations in flocs, which can be extracted by thermal flocs break-up (see section 5.3.2, method A.3). As a consequence, the higher the fraction of low bounded divalent cations, the slighter the compactness and strength of flocs are.

With regards to sludge filterability, i.e., the propensity of mixed liquor to be filtered, it was investigated considering specific resistance to filtration (SRF) and modified fouling index (MFI; see section 5.3.2, method A.7) evaluating such parameters during filtration with paper filters (SRF) and mixed acetate-celllulose filters (MFI). In particular, SRF gives an indication of sludge filterability related to the resistance to filtration offered by sludge cake (aggregation of biomass flocs mainly) forming during the test. Differently, MFI provides information about the effects of little particles (<8 μm) and colloids forming a sort of gel structure on the filter during the test. In this way, SRF and MFI, overall, provide more complete information about sludge filterability with reference to membrane filtration even though these parameters do not take into account the resistance due to macromolecules (see section 2.4.1). Moreover, since resistances to filtration and fouling are obviously related to the presence of the membrane and to the filtration conditions, SRF and MFI can provide only a partial indication of filterability and fouling propensity of a sludge. Therefore, a modified flux step method for the critical flux determination was introduced and implemented using a batch test unit equipped with UF membranes, as described below, to evaluate the effects of flux enhancer on a weekly basis (goal 4).

As for parameters related to hydraulic performance of UF membranes and fouling monitoring, TMP, permeability at a temperature of 20°C (P_{20}) and total resistance to filtration (R) were evaluated (see section 5.3.2, method A.9) since effective parameters to monitor fouling evolution over time. Moreover, according to the methods A.11 (see section 5.3.2) the determination of the membrane resistance (R_m), the cake layer resistance (R_c), the fouling resistance caused by pore restriction and adsorption of foulants onto the

membrane pore wall or surface (R_f) were evaluated. As a results, it was possible to investigate the mechanisms of fouling and how flux enhancers could limit them. Moreover, the rate (i.e., the rapidity of occurring) of the irreversible fouling, due to R_f, was evaluated in stage 1 and stage 2.

Table 4.2. Major monitored parameters related to goal 3.

Parameter	Reference method
- standard quality parameters (COD, TOC, TSS, VSS, N, P) - textiles macro-pollutants (colour and surfactants)	-
- soluble and extracted bound-EPS (P, C)	method A.3
- organic content characterization of bulk liquid, extracted solution, influent and effluent: - mean oxidation state of organic carbon - organic carbon apportionment	method A.4 and A.5
- flocs strength (Ca^{2+}, Mg^{2+}, SI_1, SI_2)	method A.6
- sludge filterability (SRF, MFI)	method A.7
- filtration performance (TMP, P_{20}, R)	method A.9
- R apportionment (R_m, Rc, R_f)	method A.11
- irreversible fouling rate FR	method A.11

MBR start-up. The start-up phase, during which the pilot plant operated with clean water (potable water), was planned in order to check the functioning of all equipments properly and to evaluate important parameters such as the standard oxygen transfer efficiency (SOTE) and the mean hydraulic retention time (HRT). Both parameters were relevant for the ordinary operating and monitoring of the pilot MBR. In fact, SOTE, characterizing the aeration system for the biological oxygen supply, was important to fix the exact aeration flowrate in order to keep dissolved oxygen (DO) in mixed liquor at proper values. On the other hand, the mean HRT value was utilized in designing the sampling strategy during stages 1 and 2. The SOTE determination was performed according to the ASCE standard method, whereas the residence time distribution was modelled and experimentally determined by the trace elements method for the determination of the mean HRT (see section 5.3.1, method A.1 and method A.2, respectively). In addition, in the start-up phase, the pilot MBR was inoculated using the full scale WWTP sludge (biomass from the recycle) and monitored for approximately 1 months to gain important information on the filtration process. In particular, a stainless steel mesh (0.49 mm) was introduced as pre-treatment (Figure 4.1) in order to remove textile fibres present in wastewaters more efficiently, because of their incompatibility with membrane filtration. Also, after the introduction of the

mesh, optimal RX cycles were found to be 8:1 (i.e., brakes of 1 min every 8 min of filtration).

MBR operation and monitoring. At the beginning of stage 1, the pilot MBR was re-seeded using biomass collected from the full scale WWTP (from the recycle) because of the textile fibres presence in mixed liquor at the end of the MBR start-up. MBR monitoring were planned according to Table 4.3.

Table 4.3. Sampling strategies, point of measurement, parameters and weekly frequency.

Sampling strategy	Point of measurement		Parameter	Weekly frequency
Flow-proportional, 24-hour time-based samples (effluent samples collected after an HRT time from the influent samples collection)	influent and effluent		TSS, VSS	1
			COD	
			Nitrogen compounds	
			Non-ionic surfactants	
			Anionic surfactants	
			Colour	
			Total phosphorus	0.5
			Proteins	
			Carbohydrates	
			Calcium	
			Magnesium	
			TOC	
Instantaneous samples	aerobic tank	mixed liquor	MLSS, MLVSS	2
			Calcium	0.5
			Magnesium	0.5
		bulk liquid and extracted EPS solution*	Proteins	0.5
			Carbohydrates	0.5
			Calcium	0.5
			Magnesium	0.5
			TOC	0.5
			COD	0.5
			Nitrogen compound (TKN, NH4)	0.5
	anoxic tank		MLSS	2
	membrane tank		MLSS	2

* Bulk liquid separation and bound EPS extraction according to the methods explained in section 5.3.2.

What is more, control parameters, such as pH, dissolved oxygen (DO) and temperature were continuously monitored in the aerobic tank, whereas pH and redox potential in the anoxic tank, by using probes installed in the pilot MBR (see section 5.2.1). In addition, absolute pressure in the suction line of the process pump (i.e., the pump used for the filtration

process) was measured using a pressure gauge (see section 5.2.1). Consequently, it was possible to evaluate and monitor TMP (see section 5.3.2, method A.9).

Flux enhancer selection. According to the literature review, major flux enhancers used for the fouling control have been so far: metal salts, organic polymers and powdered activated carbon (see section 2.6). In the study, for each type of enhancer, a specific product was selected (see Table 4.4) on the basis of the criteria that follows. As for metals salts, it has been reported that polymeric coagulants (category A12 in Table 2.7) can supply more positive charges and longer chain molecules, so that they have a better effect on flocculation than monomeric coagulants. Therefore, polyaluminium chloride (PACl), a polymeric coagulant, was considered for the metal salt category. In fact, within this category, even if polymeric ferric sulphate (PFS) showed higher performances than PACl, the latter was preferred because of a lower acidification effect on pH and therefore lower possible side effects on biology (see section 2.6). In particular, TILLMANS TILLPAC 18 was selected as the PACl to test in the study. As for organic polymers, a cationic polyaminic coagulants specifically designed for decolouring was picked (DALTON FLODAL), whereas a powdered activated carbon (PAC) with excellent filtration characteristics and adsorbing capabilities of high molecular weight organics, such as dyes and proteins, was chosen (NORIT CA1, Table 4.5).

Table 4.4. Tested flux enhancers.

Product		Description	Price (€ kg^{-1})
powdered activated carbon (PAC)	NORIT CA1	NORIT CA1 is a powdered activated carbon with an excellent adsorptive capacity (large colour bodies and proteins) and an excellent filtration characteristics. It is produced by chemical activation using the phosphoric acid process.	1.80
polyaluminium chloride (PACl)	TILLMANNS TILLPAC18	TILLMANNS TILLPAC18 is polyaluminium chloride at a concentration of 18%.	0.22
cationic polymeric flocculants	DALTON FLODAL	DALTON FLODAL is cationic polyaminic coagulants with high decolouring power.	0.82

Table 4.5. NORIT CA1 specifications and properties (from manufacturer's data sheet).

Parameter	Value	Parameter	Value
specific area (m^2 g^{-1})	1,400	ash (% m/m)	2
methylene blue ads (g $100g^{-1}$)	>25	calcium (acid extr.; mg kg^{-1})	<200
d10 (µm)	7	iron (acid extr.; mg kg^{-1})	<150
d50 (µm)	30	phosphate (acid extr.; mg kg^{-1})	<3.5
d90 (µm)	75	CAS number	7440-44-0
moisture (% m/m)	<15	Food Chemicals Codex	passed

Since goal 2 was aimed to the evaluation of the effects of flux enhancers on fouling control and permeate quality enhancement, the selection of the best flux enhancer, then dosed into the pilot, was planned considering a jar test campaign (see section 5.3.3) for the evaluation of:

- soluble-EPS (proteins and carbohydrates) removal, sludge filterability enhancement, measuring capillary suction time (CST), specific resistance to filtration (SRF) and the modified fouling index (MFI), as for fouling control;
- TOC, COD and colour removal occurring in mixed liquor bulk liquid, as for quality enhancement.

The optimal dosage of the selected flux enhancer was then fixed at a proper value on the basis of a multi-criteria approach considering effects related to parameters listed above, economic sustainability, negative effects detectable in short period batch tests and any risk of biological activity inhibition (see section 5.3.3, method A.14). However, the risk of biological activity inhibition is related to long period operations of bioreactors (see section 2.6.3) and therefore it is not possible to be detected properly during a jar test campaign (short term batch experiments). As a results, this kind of risk was taken into account in stage 2, particularly planning the specific dosing strategy, as stated above.

Determination of fouling propensity. The determination of critical flux was recently adopted as test to assess the fouling propensity of MBRs on a daily basis (Fan et al., 2006). With this aim, the standard flux step procedure and a modified one (see section 5.3.4) were implemented weekly using a batch filtration unit (see section 5.2.3). The modified procedure, as descried in materials and methods section, takes into account breaks between filtrations at different fluxes. This sort of RX was not aimed to obtain filtration conditions closer to real plant operation, as introduced by De la Torre et al. (2008). In fact, brakes in real RX are about 15÷60 sec every 3÷12 min of filtration (Drews, 2010) in order to not increase too much the membrane surface requirement keeping the real flux (i.e., flux in the active filtration phase of RX) at proper values. Differently, RX in the modified method was

set to 5 min, therefore adopting a security factor of 5 (i.e., adopted RX break = 5 × real RX break), in order to be sure that the cake layer, forming during filtration (reversible fouling), had been removed efficiently during the break so that a new cake formation had been observed at each new filtration phase.

4.2.2 Start-up of a submerged anaerobic MBR (SAMBR) treating a synthetic metal working effluent (topic B)

With regards to topic B, the start-up of a submerged anaerobic MBR treating a synthetic metal working effluent was investigated. In particular, a raw metalworking fluid was selected and utilized as the synthetic effluent to treat because of constant and reproducible characteristics over time compared to real metal working effluents. In particular, a water soluble coolant for aluminium and ferrous alloy machining (Cooledge BI, Castrol) was used and the water emulsion of the coolant represented the synthetic effluent to treat. According to the Material Safety Data Sheets provided by the manufacturer, the coolant was chlorine, nitrite and boron free. The mineral oil content was major than 60%; chemicals such us sodium sulphonate, isotridecanol, fatty amide derivative, amine neutralised carboxylic acids, (ethylenedioxy) dimethanol and alcohol ethoxylate accounted for 1÷5% each. Moreover, traces of 3,3'-methylenebis (5-methyloxazolidine) and 3-Iodo-2-propynyl butylcarbamate were present.

Apart from a preliminary characterization of the synthetic effluent ("effluent characterization and direct filtration test"), research activities were planned according to the timetable in Figure 4.5 in order to respond to the main goals of topic B, briefly recalled herein:

- goal 1: evaluation of biodegradability (BMP and VFAs production assays) and the inherent toxicity (anaerobic toxicity assays, ATAs) of MWFs using not acclimatized anaerobic biomass;
- goal 2: the start-up of an anaerobic MBR pilot plant.

In particular, as for goal 1, the evaluation of the anaerobic biodegradability and the inherent toxicity of the MWF was planned considering three different screening assays using anaerobic biomass not acclimatized to MWFs, from a conventional sewage sludge digester in Mogden, UK, as described below. Then, the start-up of the submerged anaerobic MBR (SAMBR) was planned in order to achieve an MBR biomass acclimatized to MWFs (goal 2) in the long run.

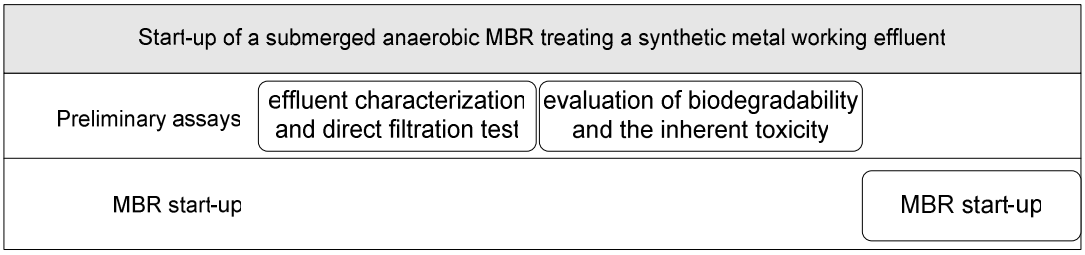

Figure 4.5. Timetable of the research phases (topic B).

Effluent characterization and direct filtration test. A fresh emulsion (0.1% m/m) was characterized considering macro-parameters such as TOC, COD, and pH. Particle size distribution was also analyzed for the fresh coolant emulsion and mixed samples containing the coolant and biomass in order to investigate the propensity of MWFs to adsorb/attach on biomass. Secondly, the direct filtration of the fresh emulsion through a Kubota flat sheet module (surface area of 0.1 m^2 and pore sizes of 0.4 μm), the same used in the SAMBR pilot, was carried out. In particular, scopes of the direct filtration step were the estimation of the amount of the coolant retained by the membrane and its fouling propensity in absence of biomass.

Evaluation of biodegradability and the inherent toxicity. Three different screening assays were employed to give a preliminary estimation of the biodegradability and any toxicity inherent in the selected MWF (Figure 4.6):

1. biochemical methane potential (BMP) assays;
2. volatile fatty acids (VFAs) production assays;
3. anaerobic toxicity assays (ATAs).

In particular, BMP assays were employed to give an estimation of the potential amount of the organic substrate bio-convertible into CH_4, giving therefore a general indication on the complete anaerobic digestion pathway.

Differently, VFAs assays, where the addition of 2-bromoethanesulfonate (BES) was taken into account, were considered in order to evaluate the upper pathway of anaerobic digestion as BES inhibits the acetoclastic methanogenesis (Xu et al., 2010).

With regards to ATAs, the presence of any toxicity inherent in MWFs on the lower pathway (i.e., acetoclastic methanogenesis and methane production from formate) was assessed adding formic acid and acetic acid separately in samples with the coolant at different concentrations (see section 5.4.1).

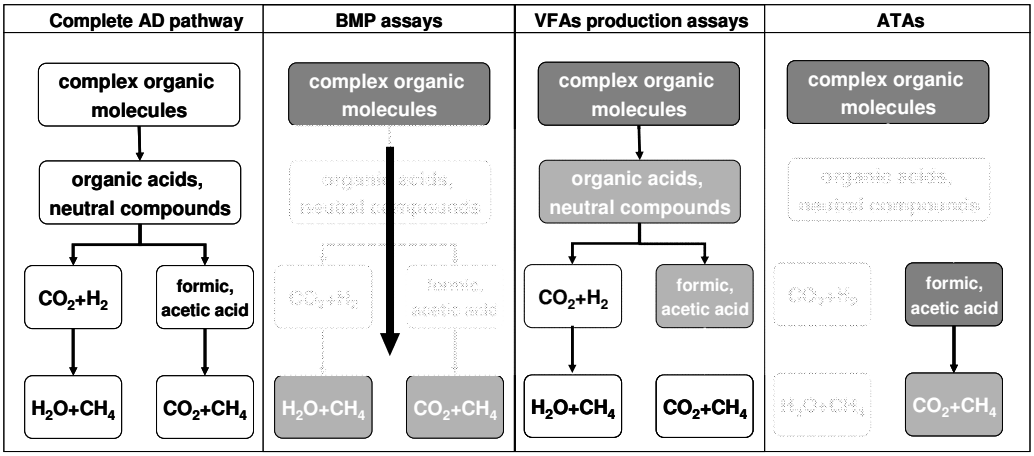

Figure 4.6. Preliminary assays for the biodegradability and inherent toxicity assessment.

Start-up of SAMBR. Differently from topic A, the pilot MBR used in the study was not designed and realized on purpose. In fact, it was used the submerged anaerobic MBR (SAMBR) developed at Imperial College of Science, London by professor David C. Stuckey and his research group (see section 5.2.2). The start-up strategy of SAMBR (duration = 40 days) is reported in the results and discussion section of the thesis (see section 7.3) since it was planned on the basis of the preliminary assays outcomes, performed as described above. With regards to SAMBR monitoring, see the table below (Table 4.6).

Table 4.6. Parameters monitored during the start-up of the SAMBR.

Parameter/Determination	**Point of measurement**
Temperature	Mixed liquor
pH	Mixed liquor
TSS, VSS	Mixed liquor
TOC	effluent, bulk liquid*
VFAs	effluent, bulk liquid*
Particle size distribution	Mixed liquor
Biogas composition	Biogas
Biogas and methane volumetric production	Biogas
Pressure and TMP	suction line of the process pump

* With regards to bulk liquid, all the samples collected were centrifuged at 7,500 rpm and the supernatant was then filtered through a 0.45 μm filter (Millipore Millex-HA filters, 33 mm) to remove suspended material and any residual biomass.

5 Materials and methods

5.1 Introduction

In this chapter, detailed information about materials and methods employed in the study is provided, including:

- a description of pilot scale treatment plants (see section 5.2.1 and section 5.2.2);
- a description of the batch filtration unit, utilized for critical flux determination in topic A (see section 5.2.3);
- experimental procedures and data processing procedures considered for topic A and topic B (see section 5.3 and section 5.4, respectively);
- analytical techniques overall employed (see section 5.5).

5.2 Pilot scale MBRs

5.2.1 MBR pilot plant (topic A)

The pilot MBR was designed on purpose according to the modified Ludzack-Ettinger process for the biological nitrogen removal. It consisted of an anoxic and an aerobic stage (pre-denitrification and nitrification, respectively) and a separate membrane compartment equipped with two lab-scale Siemens Water Technologies (Memjet®) membrane modules (Table 5.1).

Table 5.1. Characteristics of the Siemens Water Technologies (Memjet®) lab scale modules (manufacturer's data sheet).

Membrane type	hollow fiber
Configuration	vertical immersion
Material	polyvinylidene fluoride
Pore size	0.04 μm
Module size	0.5 m^2
Max TMP value	0.65 bar
Max temperature value	50°C

As shown in Figure 5.1, the Memjet® lab scale module had two connection holes, one on the top head (A) and the other one on the bottom head (B). Permeate was drawn from the connection A using a process pump, whereas connection B was for input air, which was then supplied close to the bottom, where four orifices were located.

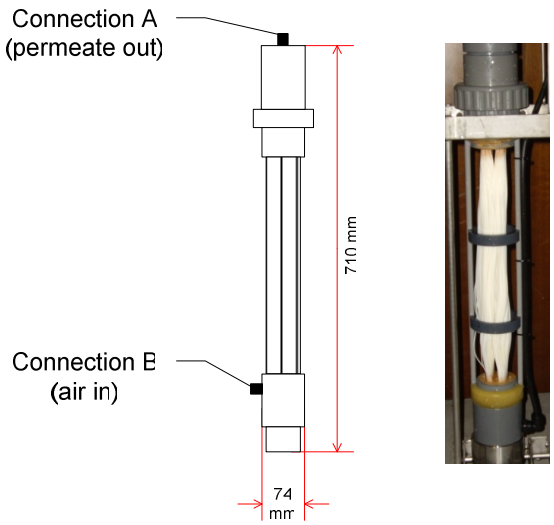

Figure 5.1. Siemens Water Technologies (Memjet®) lab scale module.

Description of the pilot plant. The MRB pilot is shown in Figure 5.2 and Figure 5.3, where a simplified P&ID (piping and instrumentation diagram) and a picture are presented, respectively. A variable-speed Novarotor progressive cavity pump (P1, Model MN 010-2) was used to feed the anoxic tank with the influent wastewater. Then, the anoxic mixed liquor (i.e., the mix of influent and biomass) flowed into the aerobic tank by gravity and two variable-speed Novarotor progressive cavity pumps (P2, P3, Model MN 013-2) were used for the nitrate recycle and to feed the membrane tank with aerobic mixed liquor, respectively. The process pump for filtration was a variable-speed Debem peristaltic pump (P4, Model MP-3086.6) connected to the membrane filtration modules. Since the flow entering the membrane tank was greater than the permeate flow, the excess was recycled back into the aerobic tank by gravity. Two linear membrane Emmecom blowers were used for aeration purpose (B1, model DB120L, aerobic tank) and for fouling control (B2, model DB40A, membrane tank), respectively. The flow rates employed were controlled by gas flow meters (model R-R, la tecnica-fluidi) and valves. Moreover, for aeration purpose, an Emmecom fine bubbles membrane air diffuser (model DMKAD250) was immersed in the aerobic tank. Two ECO-MIX mixers (M1, M2, model MR-018-4-56/100) were installed in the anoxic and aerobic tanks to mix properly in order to avoid sludge settling. In particular, the anoxic tank mixer (M1) was strictly necessary since it was the unique machine inducing turbulence and mixing sludge, whereas in aerobic tank turbulence was also promoted by aeration.

The excess biomass was collected manually (using valve V1) and wasted each day (apart form the portion necessary for physical-chemical determinations) in order to maintain constant SRT at a proper value (section 5.3.2).

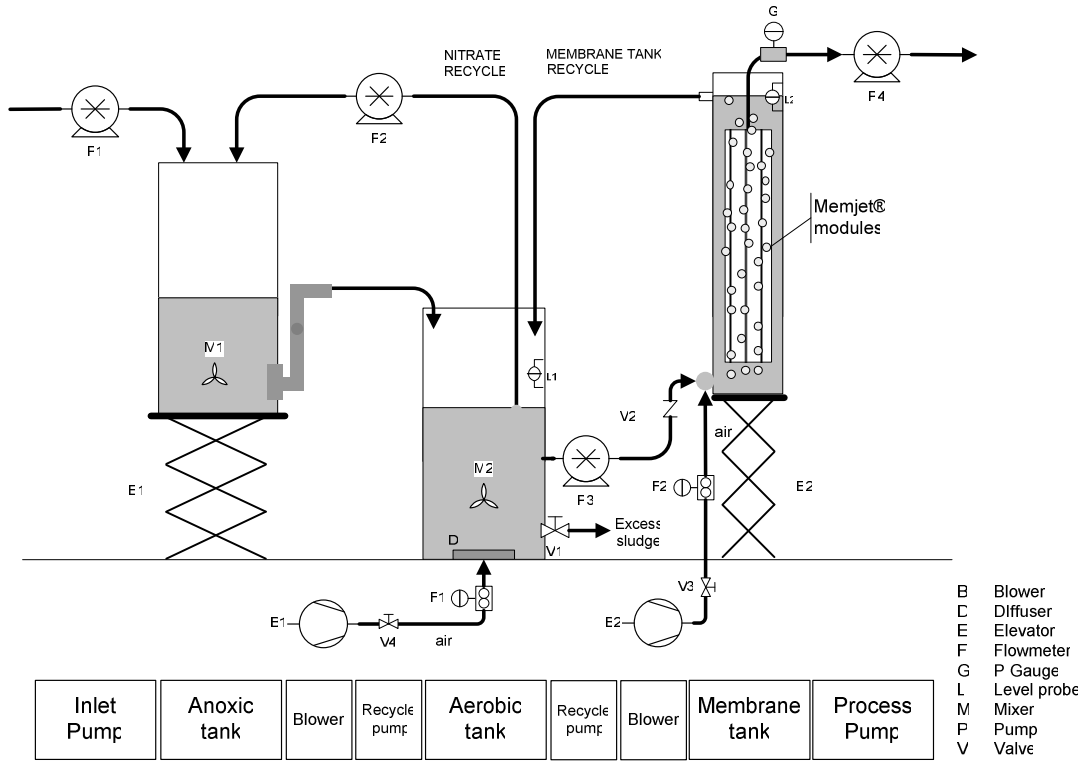

Figure 5.2. P&ID of the MBR.

A controller unit (not shown in Figure 5.2) was design for a proportional–integral–derivative (PID) control, particularly, related to the influent flow control, whereas the permeate flux was fixed at a given value (see over) kept constant over the entire study period. The controller set the P1 flowrate on the basis of pressure data measured by a transmitter installed at the bottom of the aerobic tank (not shown in Figure 5.2), since the measured pressure is linearly related to the liquid level in tank. In particular, a correlation approximately of 1 cm $mbar^{-1}$ was considered. This level controlling system considering pressure data was particularly designed and selected in order to do not be sensible to foam.

Moreover, two alarm systems related to levels in tanks were present. In fact, a max-level probe (L1) in the aerobic tank and a min-level probe (L2) in the membrane tank were installed in order to stop all the engines installed on the pilot plant. In particular, L1 was considered in order to prevent accidentally sludge overflow and L2 in order to make sure that membranes would have been wet in all possible situations.

A Keller digital pressure gauge (G, model LEO record) with recoding functions (record frequency of 30 data per hour) was installed in the suction line of the process pump in order measure the absolute pressure and to be able to evaluate transmembrane pressure, TMP (see section 5.3.2, method A.9). An IFM pressure transmitter (model PN 3029) was also used for security reason. In fact, the IFM pressure transmitter was connected to the

controller unit in order to stop all the engines in the case of excessive TMP values (major than 0.5 bar).

The controller unit was also used to perform RX and to start the in-out sampling using 2 volumetric pumps (not shown in Figure 5.2), one for the influent, and one for the effluent. In addition, two 15 L tanks were used for samples collection and placed in a fridge (at 4°C) till the analysis were performed.

Moreover, pH , DO, T, redox potential probes (Table 5.2) were connected to the unit, where instantaneous data were shown on a digital display and recorded with a frequency of 4 data per hour.

Table 5.2. Probes installed in tanks (provided by B&C Electronics).

Aerobic tank	pH probe
	DO probe
	T probe
Anoxic tank	pH probe
	redox potential probe

Figure 5.3. A picture of the MBR (from right to left: anoxic tank, aerobic tank, membrane tank).

Design parameters. The pilot MBR was designed according to standard procedures for activated sludge processes (Metcalf and Eddy; 2003) in order to achieve the permeate quality shown in Table 5.3. Differently, main biological and filtration parameters resulting from the designing process are shown in Table 5.4.

It can be seen from the table that operating parameters related to flows, reactor volumes, etc. presented a wide range to provide high flexibility during the research period. With regards to SRT and F/M values, see section 5.3.2.

Table 5.3. Permeate quality considered during the design of the MBR.

Parameter	Reference value
COD (biodegradable fraction only)	< 5 mg L^{-1}
TSS	< 1 mg L^{-1}
TKN	< 2 mg L^{-1}
$N\text{-}NO_3^-$	<10 mg L^{-1}

Table 5.4. Main parameters of the MBR bioreactor.

	Parameter	Value	UM
Filtration parameters	Memjet® modules	2	-
	Total membrane surface area	1	m^2
	RX - filtration phase	8 (4÷12)	min
	RX - break phase	1 (0,5÷1)	min
	J (in the filtration phase)	10 (5÷15)	LMH
Biological parameters	Average influent flowrate (q_{P1}) *	213 (100÷350)	L d^{-1}
	Nitrate re-cycle ($r = q_{P2}/q_{P1}$) *	3 (2÷4)	-
	Membrane in-flow ($m = q_{P3}/q_{P1}$) *	5 (3÷6)	-
	aerobic tank DO	2,5 (1÷9)	mg L^{-1}
	aerobic tank volume	60 (40÷120)	L
	anoxic tank volume	40 (10 ÷ 90)	L
	membrane tank volume	37.5	L
	aerobic tank reference TSS	5.5	g L^{-1}
	anoxic tank reference TSS	4.0	g L^{-1}
	membrane tank reference TSS (< 12 g_{TSS} L^{-1})	7.0	g L^{-1}
	air flowrate - aerobic tank	100 (100÷3.000)	NL h^{-1}
	air flowrate - membrane tank	420 (100÷900)	NL h^{-1}

* The symbol "$q_{P\#}$" indicates the flowrate of the pump # in Figure 5.2.

5.2.2 SAMBR pilot plant (topic B)

Two 3.2 L working volume bioreactors equipped with one Kubota flat sheet module each (Table 5.5, Figure 5.4) were used in the study. In particular, the flat sheet module was comprised of a solid acrylonitrile butadiene styrene support plate (5 mm thick) with a spacer layer and a polyethylene flat sheet membrane. The membrane was welded to the side of the spacer layer on both sides of the module.

Table 5.5. Characteristic of the Kubota flat sheet module (from manufacturer's data sheet).

Membrane type	Flat sheet
Configuration	Vertical immersion
Material	Polyethylene
Pore size	0.4 μm
Module size	0.1 m^2

Figure 5.4. Picture of a Kubota flat sheet module.

Since bioreactors (Figure 5.5 and Figure 5.6) worked in anaerobic mode, a biogas recycling system was used to generate coarse bubbles to minimise the fouling on the membrane surface. Moreover, the biogas recycle provided a good mixing since an internal baffle was used to split the moving liquid into two flow regimes, the upcomer and downcomer. The biogas was recycled from the headspace of the reactor using a vacuum pump (B100 SEC, Charles Austin) and then transferred to a stainless steel diffuser. The sparging rates (2÷7.5 LPM) employed were controlled by a gas flowmeter (101 Flo-Sen, Cole Palmer) and a valve. The top of the MBR unit contained a number of openings in order to connect pipes for liquid and gas flows, a relative pressure gauge (not shown in Figure 5.5) to verify and avoid the possible occurrence of vacuum conditions in reactor, a level sensor connected to an electronic system with switching functions for the inlet and outlet pumps, one sampling point for biomass and one for biogas.

In order to control the flow rates based on an appropriate HRT, variable-speed Watson–Marlow peristaltic pumps (Model No. 101U) were used for the influent and effluent and they were connected to the level controller quoted above. The process pump for filtration was a variable-speed Watson-Marlow peristaltic pump (Model No. 520S) connected to the membrane. In order to ensure that the total flux was comparable with data in the literature, the total flow of the process pump was greater than the effluent flow at certain HRTs, and therefore the excess flow was recycled back into the reactor.

A Keller pressure transmitter (LEO record) with recoding functions (recording frequency of 30 data per hour) was placed into the pump suction line in order to be able to evaluate transmembrane pressure, TMP (see section 5.4.2, method B.4). A glass cylinder (100 mL) and a timer were used for the flow and flux evaluation.

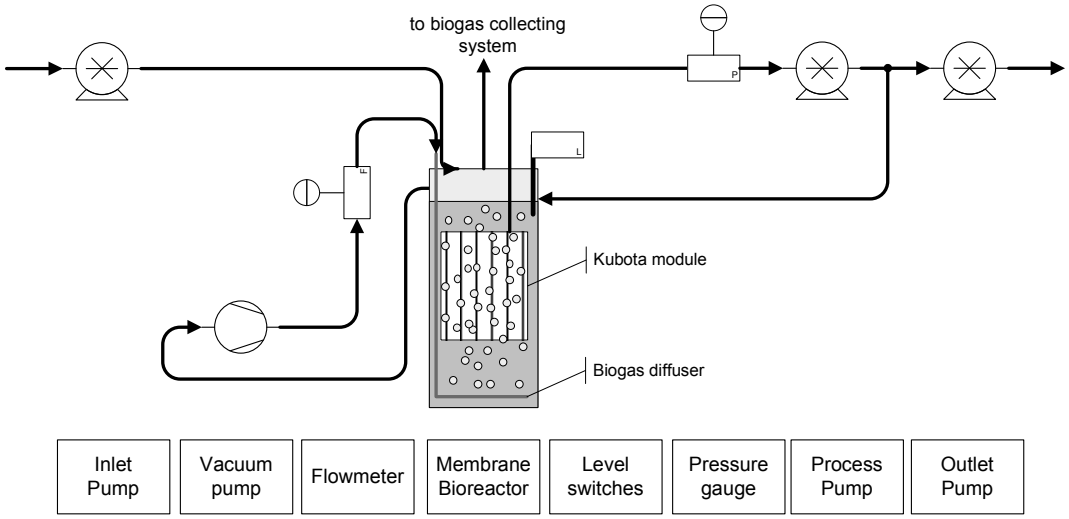

Figure 5.5. P&ID of the SAMBR.

As shown in Figure 5.6, the 2 reactors were placed into a warm water bath equipped with a heater comprising the automatic control of temperature.

With regards to the biogas produced in the reactor, it was determined by a liquid displacement arrangement. In particular, a biogas collecting system consisting of an upside-down graduated cylinder (500 mL) inserted in a beaker (500 mL) filled with deionised water was connected to the reactor.

In particular, the biogas collecting system is shown in Figure 5.7.

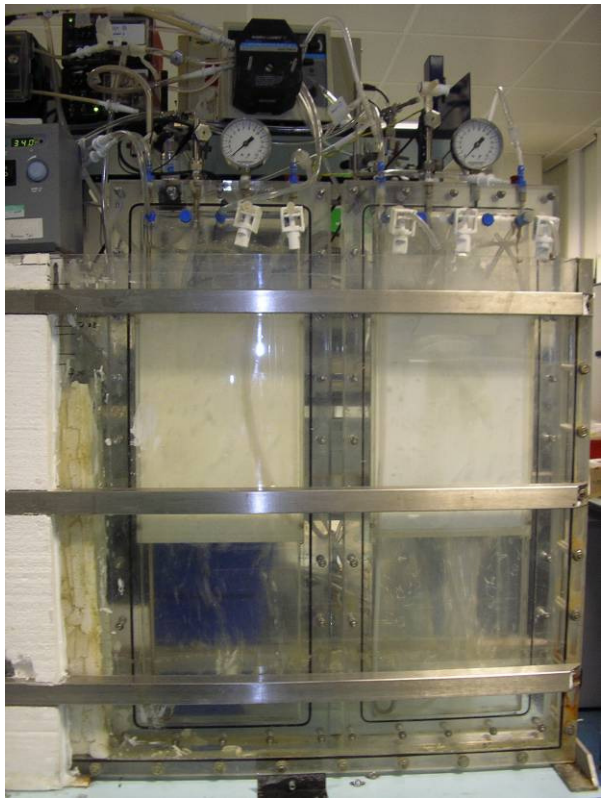

Figure 5.6. Picture of SAMBRs.

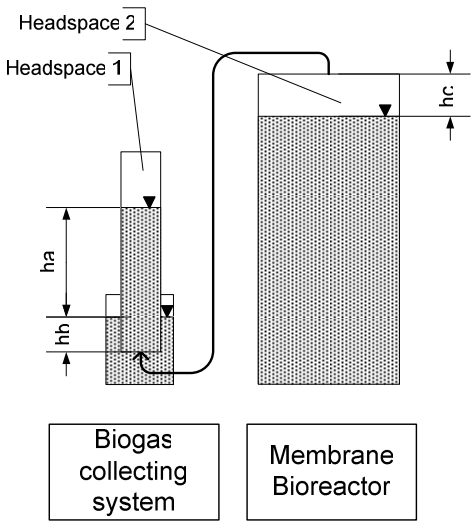

Figure 5.7. Biogas collecting system.

5.2.3 Batch filtration unit (topic A)

A 7 L working volume reactor was used for the implementation of standard and modified flux step methods (topic A). The batch filtration unit was equipped with one GE Water & Process Technologies (ZW-1) lab scale module (Table 5.6), because lab-scale Siemens Water Technologies (Memjet®) membrane modules, used on the pilot MBR, were to large for entering the reactor even if they were the smaller size available in commerce provided by SIEMENS. With regards to the ZW-1 module, as shown in Figure 5.8, fibers are much shorter and tighter compared with larger modules that have substantial slack to permit fibre movement. This fact was taken into account in the choice of air flowrate during the critical flux determination since compared to bigger scale experiments a higher flowrate is necessary. Moreover, the ZW-1 module has two holes on top head, one for the permeate (A) and one for input of air (B), which is then supplied close to the bottom, where orifices are located, through a central aeration tube.

Table 5.6. Characteristics GE Water & Process Technologies (ZW-1) lab scale module (manufacturer's data sheet).

Membrane type	Hollow fiber
Configuration	Vertical immersion
Material	Proprietary
Pore size	0.04 μm
Module size	0.098 m^2
Max TMP value	0.8 bar
Max temperature value	40°C

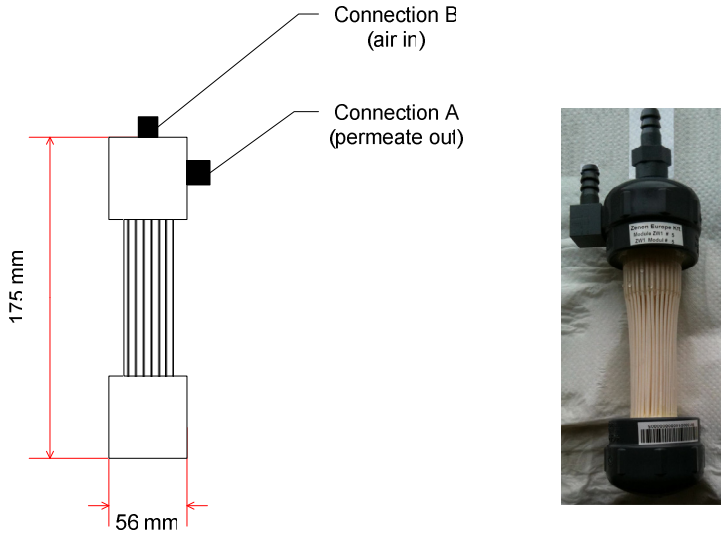

Figure 5.8. GE Water & Process Technologies (ZW-1) lab scale module.

The batch filtration unit was a fermenter originally designed and realized by Diachrom S.A., Switzerland, then modified for the specific purpose. Figure 5.9 and Figure 5.10 shows the P&ID and a picture of the filtration unit, respectively.

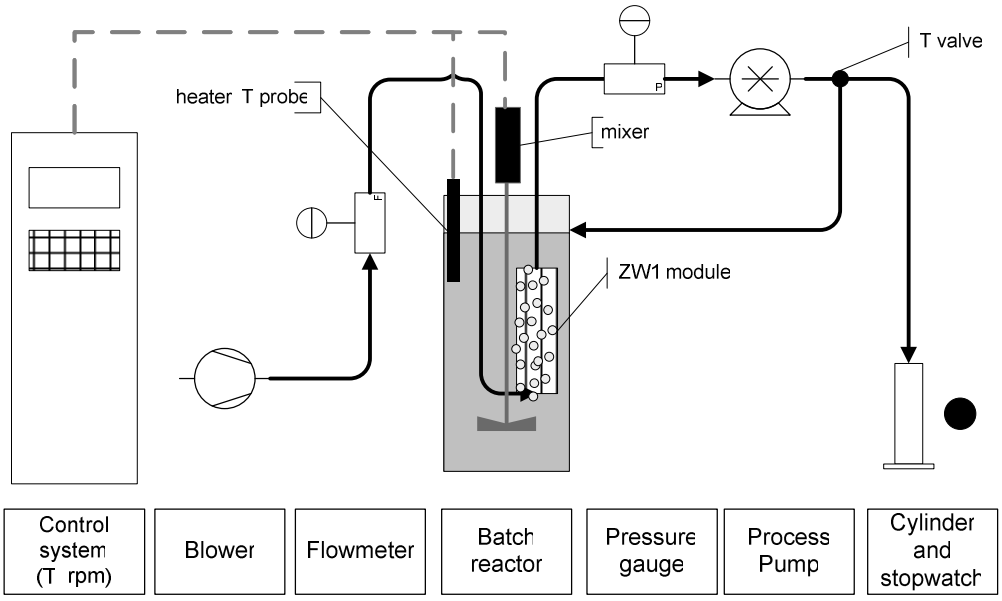

Figure 5.9. P&ID of the batch filtration unit.

The process pump for filtration was a variable-speed Watson-Marlow peristaltic pump (Model No. 323S) connected to the membrane. A Keller pressure transmitter (LEO record) with recording functions (record frequency of 30 data per hour) was placed into the pump suction line in order evaluate transmembrane pressure, TMP, using equation 5.46 (see section 5.3.2).

A glass cylinder (100 mL) and a timer were used for the flow and flux evaluation. When the glass cylinder was not in use, a T valve was switched in order to recycle the permeate into the reactor.

A linear membrane Emmecom blower (B2, model DB40A) was used to create turbulence at the base of the membrane. The flow rates employed were controlled by a gas flow meter (model R-R, la tecnica-fluidi) and a valve.

A mixer connected to the control system was used to mix sludge volume and maintain homogenous conditions inside the reactor.

Moreover, a heater and a temperature probe were installed and connected to the controller unit to keep temperature constant at 20°C.

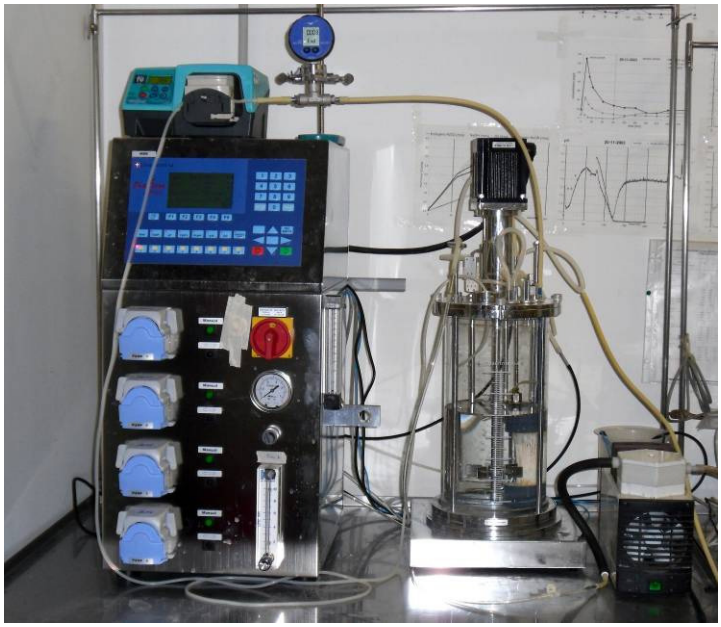

Figure 5.10. A picture of the batch filtration unit.

5.3 Experimental procedures and data processing (topic A)

5.3.1 Methods applied during the start-up of the pilot

The MBR start-up indicates the preliminary phase during which the pilot plant operated with clean water in order to check the functioning of all equipments properly and to evaluate parameters such as the standard oxygen transfer efficiency (SOTE) and the mean hydraulic retention time (HRT). Then, in a second phase of the start-up, the MBR was inoculated using the full scale WWTP sludge (biomass from the re-cycle) and monitored for approximately 1 months to gain important information on the filtration process. The main result of this phase was the introduction of the stainless steal mesh and definition of proper RX cycles.
In this section, methods for SOTE and HRT determination and information related to the stainless steal mesh are provided.

Determination of the standard oxygen transfer efficiency (method A.1). The determination of the standard oxygen transfer efficiency (SOTE) of the aeration system installed in the aerobic tank was performed according to experimental procedures developed by the American Society of Civil Engineers (ASCE, 1993). Before describing the method, some preliminary definitions has to be stated, as follows.

- *Standard and actual conditions*: standard conditions are related to (1) clean water equivalent in quality to a potable public water supply, (2) zero DO concentration at all points in the water volume, (3) water temperature of 20°C, (4) barometric pressure of 1 atm. Differently, actual conditions refers to the real sewage or mixed liquor at the real condition of DO concentration, water temperature and barometric pressure.
- *Oxygen transfer rate* (OTR): OTR is the mass of oxygen per unit of time dissolved in a volume of water by an oxygen transfer system (or aeration system) operating under given conditions of DO, temperature, barometric pressure, and gas flowrate. If standard conditions are met, OTR represents the standard oxygen transfer rate (SOTR), whereas in actual conditions, OTR represents the actual oxygen transfer rate (AOTR).
- *Oxygen transfer efficiency* (OTE): OTE is the fraction of oxygen in an injected gas stream dissolved into the water volume under given conditions, e.g., if standard conditions are met, OTE represents the standard oxygen transfer efficiency (SOTE), whereas in actual condition, OTE represents the actual oxygen transfer efficiency (AOTE).

The method for SOTE determination consisted of 5 operational steps using clean water (potable water), constant water temperature and barometric pressure closer as much as possible to 20°C and 1 atm, respectively. In particular:

1. the aerobic tank was filled with a proper volume of clean water and mixer M1 was switched on at the maximum rpm value (1,000).
2. the cobalt catalyst ($CoCl_2 \cdot 6H_2O$) was added to reach a concentration of 0.3 mg/L in test water and dispersed adopting the mixing condition of step 1 for approximately 30 min;
3. sodium sulfite (Na_2SO_3) was dosed for the deoxygenation, adopting an excess of 100% over the theoretical dosage, i.e., 7.88 mg L^{-1} per 1.0 mg L^{-1} of dissolved oxygen (DO), whose concentration was measured at the end of step 2 by using the probe installed on the pilot (see section 5.2.1); the dosage was fixed in order to reach a zero DO concentration.
4. the rpm value of mixer M1 was reduced to a proper value (100) then considered in stage 1 and stage 2 of the study.
5. blower B2 was switched on at fixed air flow rates and DO concentration was monitored over time till to the saturated concentration was reached.

With regards to data analysis, the basic model used for the parameters estimation follows:

$$\frac{dC}{dt} = K_L a \cdot (C_\infty - C) \qquad 5.1)$$

where C is the DO concentration (mg L^{-1}), C_∞ the determination point value of the steady state DO saturation concentration as time approaches infinity (mg L^{-1}) and K_La the determination point value of the apparent volumetric mass transfer coefficient (h^{-1}). Considering an initial zero DO concentration condition, the solution of equation 5.1 is:

$$C(t) = C_\infty \cdot \left(1 - e^{-K_La \cdot t}\right) \qquad 5.2)$$

Non linear regression was then employed to fit equation 5.2 to the DO profile measured during the re-oxygenation phase. The quality of the interpolation was assessed by measuring the correlation coefficient between data and predicted values by equation 5.2. In this way, estimates of C_∞ and K_La were obtained and then adjusted to standard conditions ($C_{\infty,\,20}$ and $K_La_{\,20}$), as follows:

$$C_{\infty,\,20} = \frac{C_\infty}{\tau \cdot \Omega} \qquad 5.3)$$

$$K_La_{\,20} = \frac{K_La}{1.024^{\,T-20}} \qquad 5.4)$$

where τ and Ω represent the temperature and pressure correction factors for DO saturation concentration, whereas 1.024 represents the empirical temperature correction factor, for K_La. As for τ and Ω, they can be evaluated as follows:

$$\tau = \frac{C_{S\,T}}{C_{S\,20}} \qquad 5.5)$$

$$\Omega = \frac{P_b}{P_s} \qquad 5.6)$$

where $C_{S\,T}$ and $C_{S\,20}$ are the tabular values (Table 5.7) of DO surface saturation concentration (mg L^{-1}) at a pressure of 1 atm, 100% of relative humidity and a test temperature T ($C_{S\,T}$) or 20°C ($C_{S\,20}$); P_b and P_S are the barometric pressure at test site during the test and the standard barometric pressure of 1 atm, respectively. Then, according to the definitions given above, SOTR (g_{O2} h^{-1}) and SOTE (%) can be evaluated as follows:

$$SOTR = K_La_{\,20} \cdot C_{\infty\,20} \cdot V \cdot 10^{-3} \qquad 5.7)$$

$$SOTE = \frac{SOTR}{0.3 \cdot Q_{air}} \qquad 5.8)$$

where V is the water volume (L) and Q_{air} is air flow rate (NL h^{-1}).

Table 5.7. Tabular values of DO surface saturation concentration (mg L^{-1}) at a pressure of 1 atm, 100% of relative humidity and a temperature T (Metcalf and Eddy, 2003).

T °C	**$C_{S\,T}$** mg L^{-1}
0	14.60
5	12.76
10	11.28
15	10.07
20	9.08
25	8.24
30	7.54
35	6.93
40	6.41

In particular, standard oxygen transfer efficiency (SOTE) was evaluated at two different air flowrates (650 and 1,000 NL h^{-1}) and results are presented in Figure 5.11, showing non linear regressions employed to fit equation 5.2 to the DO profiles measured during the re-oxygenation phases. Differently, Figure 5.12 shows DO profiles modelled by equation 5.2 both for 650 and 1,000 NL h^{-1} tests. As shown in the chart, the adoption of the higher values of flowrate implied a sharp profile of DO (K_La_{20} values were 25.4 and 30.0 h^{-1} for 1,000 and 650 NL h^{-1}, respectively) but with almost the same steady state saturation concentration (8.8 and 8.9 mg L^{-1} for 1,000 and 650 NL h^{-1}, respectively).

Temperature was set at 20.0±0.1°C for both tests and therefore temperature correction factors were not considered. On the other hand, atmospheric pressure compensation was applied because pressure conditions during tests were not equivalent to standard conditions.

The evaluation of SOTE resulted in 9.9% and 8.2% for 650 and 1,000 NL h^{-1}, respectively, and therefore, the average value was 9.2±1.2%.

This mean value of SOTE was used to fix at proper values the air flowrate during the operating of the MBR in stage 1 and stage 2, when reactors were in operation. Firstly, the actual oxygen transfer efficiency (AOTE) was evaluated applying correction factors to SOTE using equation 5.9, where α and β represent the oxygen transfer correction factor for mixed liquor (0.3÷1 in relation with the concentration of MLSS and surfactants; in this study it was assumed to be 0.6) and the salinity-surface tension factor for DO surface saturation (0.95÷0.98 in relation with salinity and surfactants concentration; in this study it was assumed to be 0.98), respectively; $\overline{C}$ represents the actual DO concentration in aerated mixed liquor; $C_{S\,20}$ is the tabular value of DO surface saturation concentration (mg L^{-1}) at a pressure of 1 atm, 100% of relative humidity and 20°C; τ and Ω represent the temperature and pressure correction factors for DO surface saturation (see above) .

$$AOTE = \alpha \cdot 1.024^{T-20} \cdot \left(\frac{\beta \cdot \Omega \cdot \tau \cdot C_{S\,20} - \overline{C}}{C_{S\,20}} \right) \cdot SOTE \qquad 5.9)$$

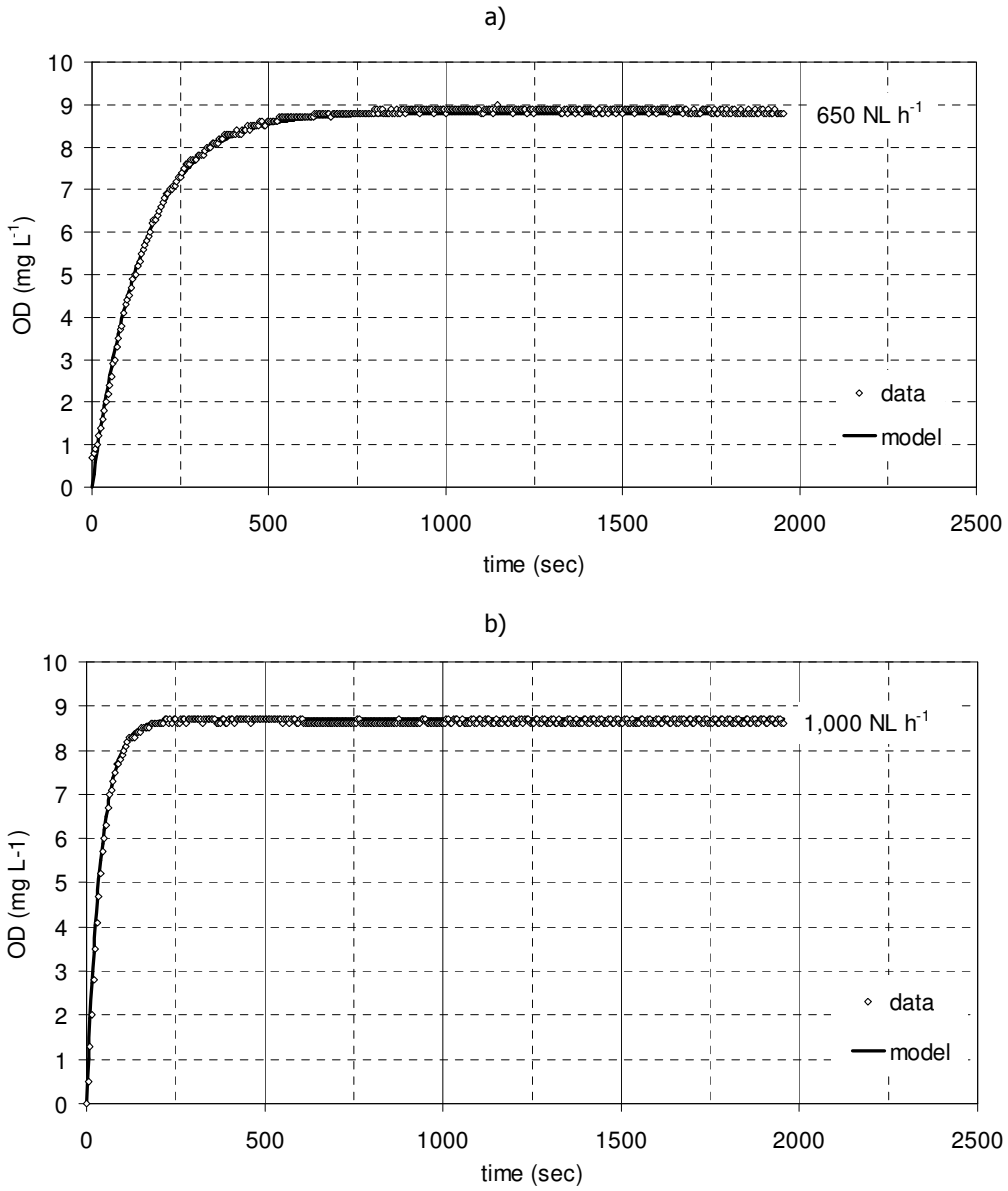

Figure 5.11. Non linear regression employed to fit equation 5.2 (model) to the DO profile (data): a) test at 650 NL h^{-1} (r=0.998); b) test at 1,000 NL h^{-1} (r=0.998).

Then, the air flowrate ($Q_{air\ actual}$) was evaluated applying equation 5.8 modified for actual conditions, as follows:

$$Q_{air\ actual} = \frac{\Delta O_2}{0.3 \cdot AOTE}$$

where ΔO_2 represents the average quantity of oxygen ($g_{O2}\ h^{-1}$) for aerobic biological activity (net consumption due to organics biodegradation, nitrification and denitrification) estimated weekly using ordinary equations of biological wastewater treatments (Metcalf and Eddy, 2003). So, the actual air flowrate ($Q_{air\ actual}$) was set using valve V4 and the flowmeter F1 (see section 5.2.1).

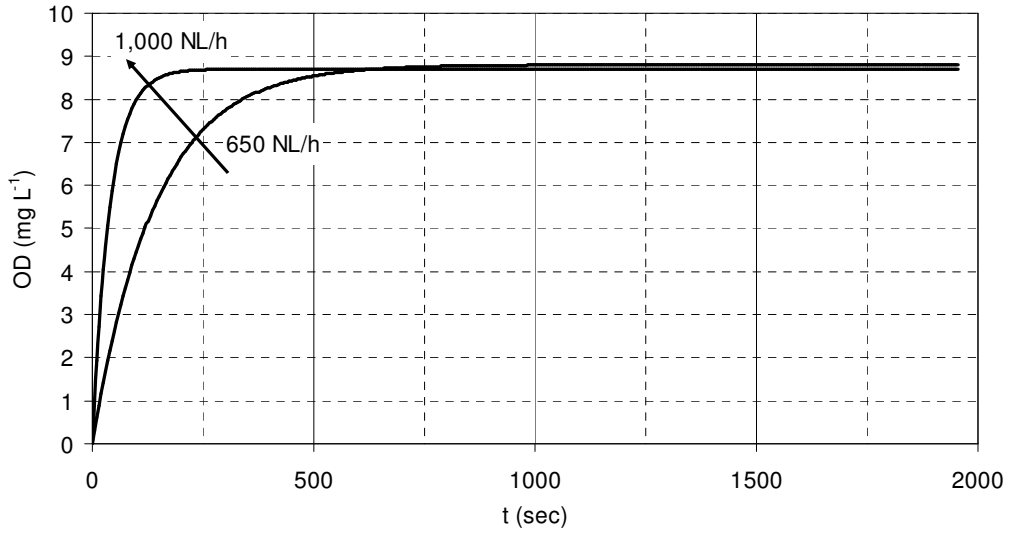

Figure 5.12. DO profile modelled using equation 5.2 during the re-oxygenation phase at flowrates of 650 and 1,000 NL h^{-1}.

Determination of the mean hydraulic retention time (method A.2). The determination of the mean hydraulic retention time (HRT) was employed analyzing the reactor hydraulic performance using tracers and fitting the tracer response profile, i.e., the evolution of the concentration in the effluent over time, using appropriate model equations, developed on purpose. Apart from equations development, the procedures and the methods adopted are reported by Metcalf and Eddy (2003). In particular, in this study, the impulsion tracer method was applied. It consisted of the injection of a quantity of tracer into the pilot plant, filled with potable water, over a short period of time. With regards to the used tracer, a number of substances have been used so far, such as dyes and chemicals including fluorescein, hexafluoride gas, lithium chloride, potassium chloride, rhodamina WT, etc. (Metcalf and Eddy, 2003). Because water conductivity and potassium chloride (KCl) are linearly dependent, the latter can be detected easily using a conductivimeter. For this reason, potassium chloride was considered in the study.

Firstly, a KCl quantity of 45 g was dissolved into 5 L potable water. Afterwards, it was poured into the anoxic tank trough the inlet piping (see Figure 5.2). Then, a conductivimeter and a thermometer with recording functions were used to measure conductivity (mS m^{-1}) and temperature (°C) in the effluent (output from membrane tank). In particular, the record frequency was fixed at 12 data per hour and the total duration of the test was approximately 2 days. During the test, all the pilot parameters related to hydraulic performance, such as tanks volumes, pumps and blowers flow rates, mixers rpm, and RX cycles were fixed to the values then considered in stage 1 and 2 of the study (see section 5.2.1). At the end of the test, each conductivity measurement (K_T) was converted into the corresponding conductivity at 20°C (K_{20}) and then into KCl concentration according to the following equations:

$$K_{20} = \frac{K_T}{[1 + i \cdot (T - 20)]} \qquad 5.10)$$

$$KCl = \frac{(K_{20} - \beta)}{\alpha} \qquad 5.11)$$

where T is temperature (°C), i, α and β are empirical parameters previously estimated through calibration experiments with the same potable water used in the test. In particular, i was estimated to be 1.25%, α 1.85 mS L m^{-1} mg^{-1} and β at 667 mS m^{-1}.

Appropriate model equations were then developed (all symbols employed in equation 5.12, 5.13 and 5.14 are explained in the caption of Figure 5.13) in order to obtain a function fitting the tracer response profile, i.e., the evolution of the measured KCL concentration in the effluent over time. Firstly, the pilot plant was considered as composed by ideal flow complete-mix reactors, also called continuous flow stirred-tank reactors (CFSTR), and mass balance equations were developed following indication of the flow diagram in Figure 5.13.

$$\frac{dC_1}{dt} = -C_1 \frac{(q + q_{r1})}{V_1} + C_2 \frac{q_{r1}}{V_1} \qquad 5.12)$$

$$\frac{dC_2}{dt} = C_1 \frac{(q + q_{r1})}{V_2} - C_2 \frac{q_{r1}}{V_2} - C_2 \frac{(q + q_{r2})}{V_2} + C_3 \frac{q_{r2}}{V_2} \qquad 5.13)$$

$$\frac{dC_3}{dt} = C_2 \frac{(q + q_{r2})}{V_3} - C_3 \frac{q_{r2}}{V_3} - C_3 \frac{q}{V_3} \qquad 5.14)$$

Since equations 5.12, 5.13, 5.14 represent a linear homogenous system, the analytical solution of the model exists and the KCl concentration in the effluent, i.e., $C_3(t)$, is a function of the initial conditions (i.e., the concentration of KCL in the 3 tanks at time zero) flow rates

(q, q_{r1} and q_{r2}), reactors volumes (V_1, V_2 and V_3) and time (t), as follows:

$$C_3(t) = f(C_1^{\,0}; C_2^{\,0}; C_3^{\,0}; q; q_{r1}; q_{r2}; V_1; V_2; V_3; t) \qquad 5.15)$$

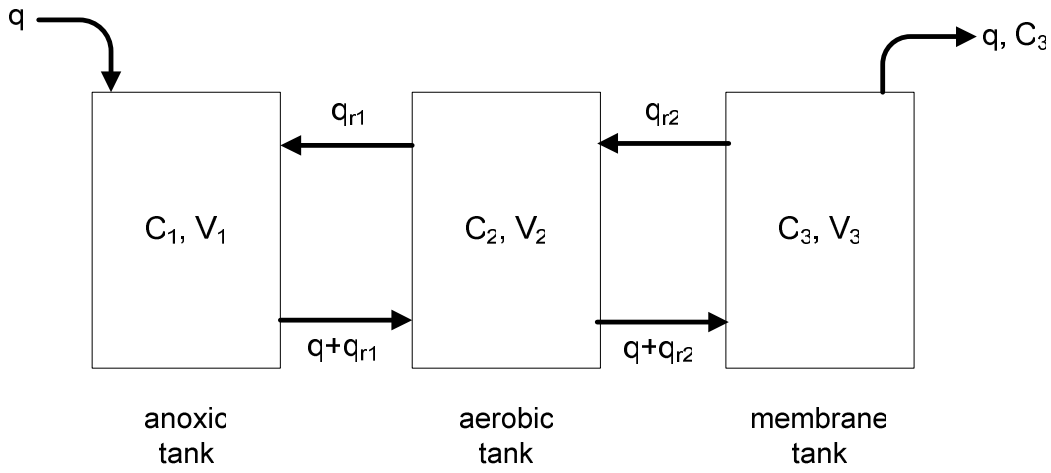

Figure 5.13. Flow diagram of the pilot MBR plant; C_1, C_2 an C_3 represent the KCl concentration in tank (mg L^{-1}), whereas V_1, V_2, and V_3 the water volume in reactors (L) and q, q_{r1} and q_{r2} the influent-effluent, the nitrate recycle and the membrane tank recycle flows respectively (L h^{-1}).

With regards to initial conditions, it was assumed that only the condition of the first reactor was different from zero as the tracer was injected into it so that the resulting instantaneous concentration was:

$$C_1^{\,0} = \frac{M}{V_1} \qquad 5.16)$$

where M represent the KCl mass (mg) introduced into the reactor. Then, some modifications of the ideal model were implemented as the flow in complete-mix reactors is seldom ideal, existing always some deviation from theoretical conditions, as follows:

$$KCl(t) = C_3(t) = f\left(C_1^{\,0}; q; q_{r1}; q_{r2}; V_1; V_2; (\varepsilon \cdot V_3); (t - t^*)\right) \qquad 5.17)$$

In particular, the lag time t^* characterizing the non ideal conditions of the overall pilot plant was introduced because, in real systems, dispersion in water volume does not occur instantaneously, but it happens according to the characteristic time of the mixing process; in particular t^* represents the time period between the injection and the observation of a response of the system. The factor ε, identifying the fraction of the membrane tank volume effective in dispersion, was also introduced (Figure 5.14).

Then, non linear regression was then employed to fit model equations to the measured KCL response data. The quality of the interpolation was assessed by measuring the correlation coefficient between data and predicted values by modelling. In this way, estimates of t* and ε were obtained.

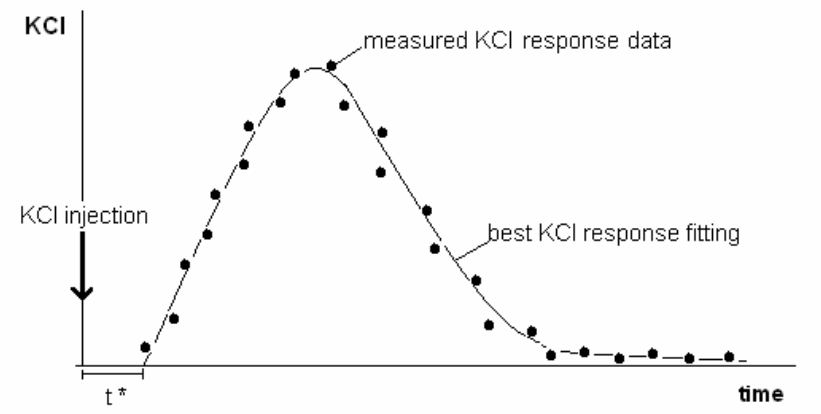

Figure 5.14. Measured KCl response data and best fitting (qualitative information is provided in this graph).

Finally, to standardize the analysis, the KCl response modelled by using equation 5.17, was normalized obtaining the residence time distribution curve, E(t):

$$E(t) = \frac{KCl(t)}{\int_0^{+\infty} KCl(t) \cdot dt} \qquad 5.18)$$

The mean HRT normalized to the theoretical HRT (HRT_{th}) value, θ, was then evaluated, as follows:

$$\theta = \frac{\text{mean HRT}}{HRT_{th}} = \frac{\int_0^{+\infty} t \cdot E(t) \cdot dt}{(V_1 + V_2 + V_3)/q} \qquad 5.19)$$

Results of tracer experiments are shown in Figure 5.15. It can be seen from the chart that experimental data collection lasted 50 h, when the test ended and the recovered tracer mass was the 92% of the mass added originally. It was assumed that such a recover factor was enough for a good estimation of mean HRT by modelling the KCL profile, even if the modelled profile showed a response till to hour 75. In fact, it would have been difficult to keep temperature variations within a small range (in which the correction factor i for temperature was applicable) since atmospheric temperature dropped down severely after

approximately 2 days (50 h). Sensible variations in temperature would have affected strongly conductibility so that any interpretation would have been unattainable.

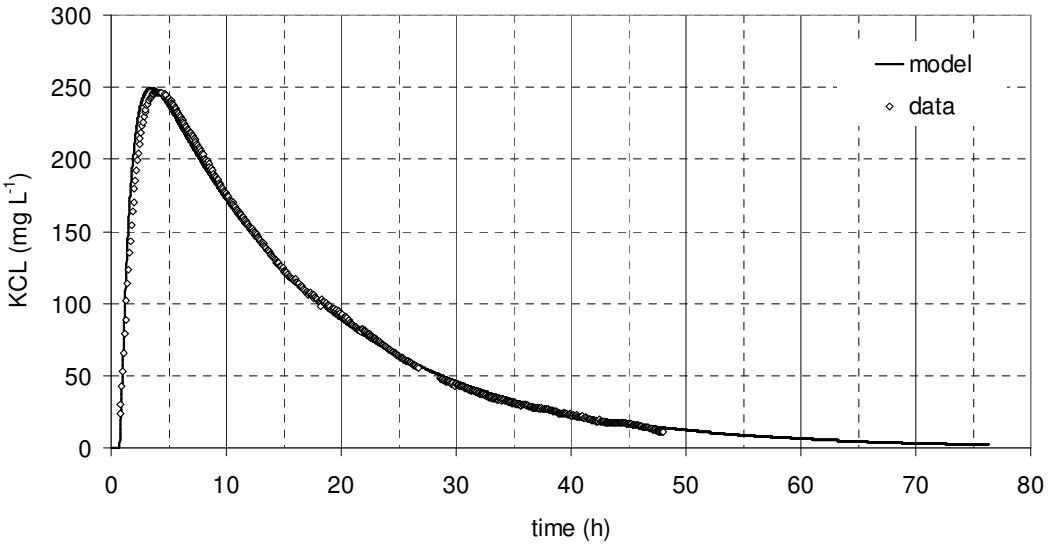

Figure 5.15. Non linear regression employed to fit equation 5.17 (model) to the tracer (KCl) profile (data).

Regression parameters (t^* and ε, Table 5.8) represent two non ideal-flow constant as introduced above. Lag time t* was estimated to be approximately 40 min, that, compared to the entire duration of the tracer test (50 h) resulted to be a not significant value.
Differently, the factor ε identifies the fraction of the membrane tank volume effective in dispersion. In fact, in membrane tank, dead space can be present because of the absence of mixers, the tank geometry, flow hydrodynamic and the presence of membranes. Moreover, the latter implies the occurrence of short circuiting. In fact, piping from aerobic tank was connected to the bottom of membrane tank and membrane recycle piping was connected to the top of the tank (Figure 5.2) providing a sort of down-up movement of water to promote scouring in membrane tank. The presence of vertical hollow fibre modules implied that a portion of the flow that entered the reactor reached the modules (water flowing through membranes at the bottom of the module) before the remaining flow (water flowing through membranes at the top of the module) even if membrane aeration provided an intense turbulence. Results showed that ε was 61.3%, but overall, since the membrane tank volume was only a fraction of the entire pilot plant volume, the real hydraulic reactors performance was close to the ideal one as shown in Figure 5.16, where two tracers profiles are simulated:

- real condition profile (t^*= 40 min; ε = 61.3%);
- ideal condition profile (t^*= 0 min; ε = 100%).

Table 5.8. Results of non linear regression.

Parameter	Value
ε	61.3%
t*	40 min
correlation coefficient (r)	0.998

As a results, the mean HRT normalized to the theoretical (or geometrical) HRT value, θ, was estimated to be 91.6% and therefore the mean HRT was 14.5 h. Such a value was then utilized to design the sampling strategy during stages 1 and 2 for influent and permeate. In fact, flow-proportional, 24-hour time-based samples were considered, and, the sample collection of the effluent was shifted of 14.5 h from the influent sampling in order to make comparable the data and calculate removal rates properly.

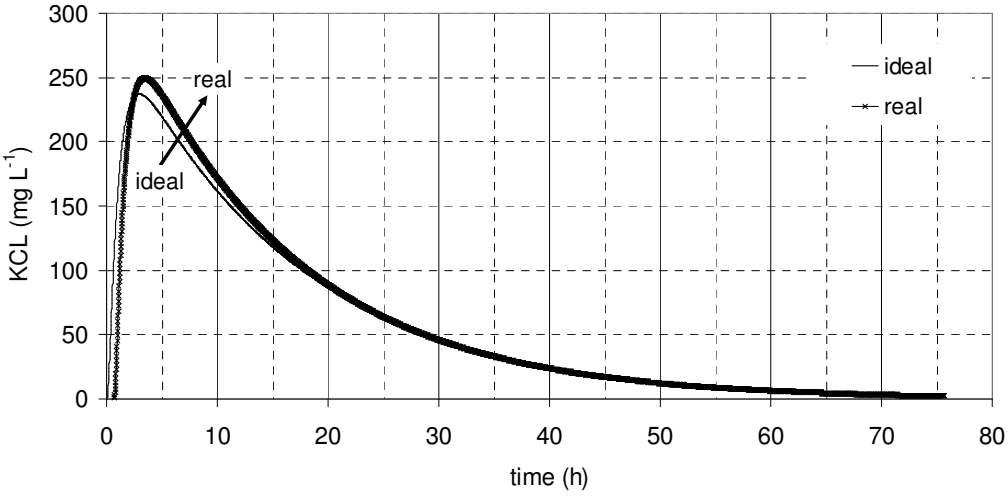

Figure 5.16. Model simulation considering ideal (t^*= 0 min; ε = 100%) and real (t^*= 40 min; ε = 61.3%) conditions.

Introduction of the stainless steal mesh as pre-treatment for the raw effluent. During the start-up phase of the MBR, preliminary filtration tests with biomass and real feed were also performed (results not shown in the thesis). The evolution of severe TMP values came out rapidly because of the presence of textile fibers affecting the filtration performance. It seemed that textile fibres created a sort of cake layer with very poor filtration features, but removable manually. A stainless steal mesh (0.49 mm, AISI 304) was then introduced as pre-treatment to remove such fibers before entering the MBR. On the other hand, a reduction of COD and TSS was caused by the filter and as a result the

production of a biodegradable solid waste was generated. In Table 5.9 average values of COD and TSS reduction rates are shown.

Table 5.9. COD and TSS reduction rate due to the stainless steal mesh.

Parameter	Reduction
COD	19%
TSS	65%

5.3.2 Methods applied during the pilot operation and monitoring

In this section all the methods adopted during the MBR operation and monitoring (stage 1 and stage 2) and introduced in chapter 4 are presented in detail, as follows:

- inoculation of the pilot MBR at the beginning of stage 1;
- methods for the evaluation of characteristics associated to the biomass, i.e., bulk liquid separation and bound-EPS extraction, biopolymers TOC apportionment, evaluation of the flocs strength, sludge filterability and the evaluation of biological activity using respirometric tests;
- methods for the evaluation of parameters related to hydraulic filtration performance and fouling monitoring, i.e., evaluation of TMP, P_{20}, R, description of membrane cleaning procedure, and apportionment of the total resistance to filtration R

Inoculation of MBR. At the beginning of stage 1, the pilot MBR was inoculated using biomass collected from the full scale WWTP (from the biomass re-cycle) because of the textile fibres presence in mixed liquor at the end of the MBR start-up period.

The initial MLSS concentrations were approximately 4.0, 5.5, 7.0 g L^{-1} in anoxic, aerobic and membrane tanks, respectively and the initial food to microorganisms ratio (F/M) was 0.1 kg COD kg SS^{-1} d^{-1}.

All the operating parameters were then fixed at the values previously summarized in Table 5.4 (see section 5.2.1) and monitoring parameters were evaluated according to the design provided in chapter 4 and to the following experimental procedures.

With regards to excess sludge, form day 120 (stage 1) proper volumes of aerobic excess sludge were collected manually (using valve V1, see Figure 5.2) and wasted (apart form the portion necessary for physical-chemical determinations) each day in order to maintain constant the sludge retention time (SRT) at a value of 25±2 days.

Bulk liquid separation and bound-EPS extraction (method A.3). Bulk liquid separation and bound EPS extraction were performed according to procedure shown in Figure 5.17. In particular, a first centrifugation step (ALC4235, 2,600 g, 10 min) of an aerobic mixed liquor sample (80 mL) was carried out in order to separate the supernatant from the biomass flocs. Then, the supernatant was filtered (WATHMAN ME25, 0.45 μm, 47 mm) to remove residual low density suspend material (LDSS, little flocs) and obtain the bulk liquid, mainly containing residual organic substrate and soluble-EPS (proteins and carbohydrates).

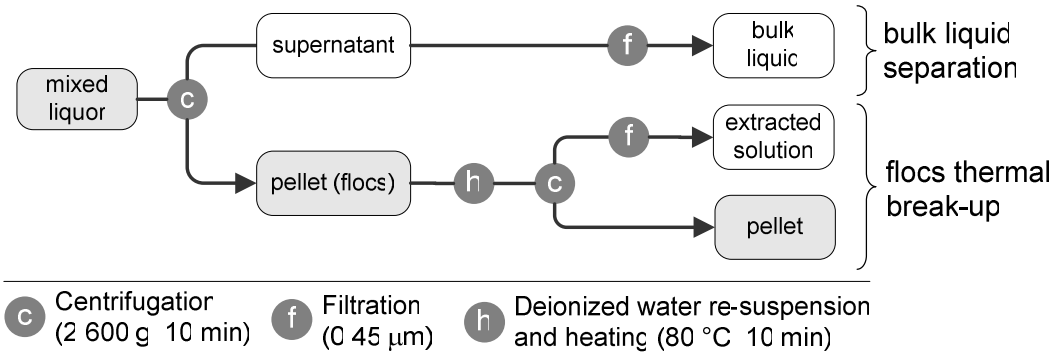

Figure 5.17. Procedure for separation of bulk liquid and extraction of bound EPS.

With regards to bound EPS extraction, the thermal method, originally introduced by Brown and Lester (1980), was considered in this study because of its simplicity and cheapness compared to other physical or chemical methods (Le-Clech et al., 2006). Firstly, the pellet was re-suspended into deionized water (final volume of 80 mL) and heated in a oven at 80°C for 10 min. Then, the sample was cooled to ambient temperature and centrifuged (ALC4235, 2,600 g, 10 min). After the supernatant had been filtered (WATHMAN ME25, 0.45 μm, 47 mm) to remove residual low density suspend material, a solution containing extracted bound-EPS was obtained. For simplicity, extracted bound-EPS are named extracted-EPS (eEPS).

Differently from bulk liquid, parameters characterizing the extracted-EPS were related to MLVSS (C_{eEPS}, mg g $MLVSS^{-1}$), as follows:

$$C_{eEPS} = \frac{C_{extraxted\ solution} \cdot V_{extraxted\ solution}}{MLVSS \cdot V_{mixed\ liquor}} \qquad 5.20)$$

where $C_{extracted\ solution}$ (mg L^{-1}) and $V_{extracted\ solution}$ (mL) are the concentrations detected in extracted solution and its volume, respectively; whereas $V_{mixed\ liquor}$ is the original volume of aerobic mixed liquor sample used for the procedure (80 mL) and MLVSS indicates the concentration of mixed liquor volatile suspended solids (g MLVSS L^{-1}).

Evaluation of the mean oxidation state of carbon (method A.4). The evaluation of the mean oxidation state of carbon was executed adopting equation 5.21 (Stumm and Morgan, 1996), where TOC and COD are the concentration of TOC (mg TOC L^{-1}, or mg TOC g $MLVSS^{-1}$ for eESP) and COD (mg COD L^{-1}, or mg COD g $MLVSS^{-1}$ for eESP) respectively.

$$\text{Oxidation state} = 4 \cdot \frac{\frac{TOC}{12} - \frac{COD}{32}}{\frac{TOC}{12}} \qquad 5.21)$$

The mean oxidation state is an important index of the organic matter composition in aqueous samples, as shown in Figure 5.18. For instance, Wang et al. (2009) considered it as a surrogate parameter to estimate the main EPS components, whereas in this study it was used to assess any variation over time of organic matter composition and to compare different media, i.e., the influent, the bulk liquid and the extracted solution.

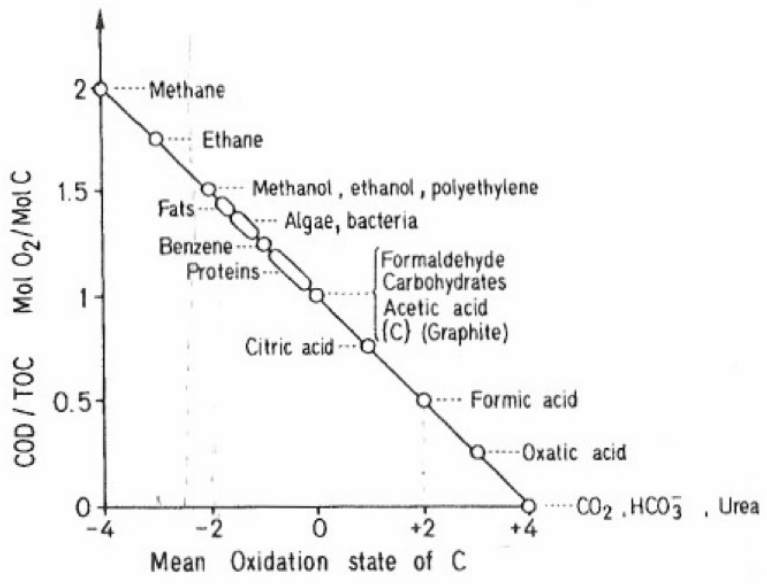

Figure 5.18. COD/TOC and mean oxidation state of C in organic compounds (Stumm and Morgan, 1996).

TOC apportionment (method A.5). The organic carbon of proteins and carbohydrates measured in all the analyzed samples was estimated assuming a reference compound for proteins, BSA, and for carbohydrates, glucose. In particular, these two compounds were used for the calibration of the Lowry and Dubois methods (see section 5.5), respectively. The organic carbon associated to proteins and carbohydrates was evaluated multiplying their concentration by the ratio between the carbon content and the molecular weight of the

reference compounds ($Carbon_{STD}$, mg OC $mmole^{-1}$, MW_{STD}, mg STD $mmole^{-1}$). Consequently the TOC apportioning between proteins ($\%Pr_{TOC}$) and carbohydrates ($\%Cr_{TOC}$) was carried out according to the following equations:

$$\%Pr_{TOC} = \frac{Pr \cdot \frac{Carbon_{BSA}}{MW_{BSA}}}{TOC} \qquad 5.22)$$

$$\%Cr_{TOC} = \frac{Cr \cdot \frac{Carbon_{GLUCOSE}}{MW_{GLUCOSE}}}{TOC} \qquad 5.23)$$

where Pr, Cr and TOC represent the concentration of proteins, carbohydrate and total organic carbon, respectively in the medium considered (i.e., influent or effluent or bulk, or extracted solution). Moreover, the unknown organic carbon was assessed by difference, as follows:

$$\%unknown_{TOC} = 1 - \%Pr_{TOC} - \%Cr_{TOC} \qquad 5.24)$$

In particular, the unknown TOC represent other organics substrates in feed water, low degradable substrates and biopolymers (different form proteins and carbohydrates) in bulk liquid and effluent, whereas only biopolymers (different form proteins and carbohydrates) in the extracted solution. With regards to the this media, the portion of organic carbon related to proteins ($\%P_{TOC}$) was assessed also in a second way, assuming that all the organic nitrogen content in extracted solution (N_{org}, mg N L^{-1}) was related only to proteins, as follows:

$$\%Pr_{TOC} = \frac{N_{org} \cdot \left(\frac{Carbon}{Nitrogen}\right)_{EPS\ proteins}}{TOC} \qquad 5.25)$$

where the term shown in brackets represents the average value of the ratio between the mass of carbon and nitrogen of proteins in eEPS. In particular, this term was estimated according to equation 5.26, adopting the proteins bound-EPS pool detected by Dignac et al. (1998), identified in Table 5.10.

$$\left(\frac{Carbon}{Nitrogen}\right)_{EPS\ proteins} = \frac{12}{14} \cdot \frac{\sum_{i=1}^{16} Carbon_i \cdot \chi_i}{\sum_{i=1}^{16} Nitrogen_i \cdot \chi_i} \qquad 5.26)$$

where $Carbon_i$ and $Nitrogen_i$ represent the carbon and nitrogen moles contained in one mole of the generic component i of the amino acids pool (Table 5.10), whereas χ_I is the mole

fraction of every component i.

Table 5.10. Composition of the eEPS amino acids pool detected by Dignac et al. (1998).

Amminoacid	%i m/m	χ_i
glycine	7,5%	12,2%
alanine	8,8%	12,0%
valine	7,2%	7,5%
leucine	8,1%	7,5%
isoleucine	5,1%	4,7%
methionine	2,2%	1,8%
phenylalanine	4,5%	3,3%
proline	4,9%	5,2%
serine	5,0%	5,8%
threonine	6,6%	6,7%
tyrosine	3,8%	2,6%
aspartic acid	12,8%	11,7%
glutamic acid	12,0%	9,9%
arginine	4,8%	3,4%
histidine	2,4%	1,9%
lysine	4,6%	3,8%

In particular, the following parameters were calculated:

$$\frac{Carbon_{BSA}}{MW_{BSA}} = 0.4 \quad mg_{oc}\, mg_{BSA}^{-1}$$

$$\frac{Carbon_{GLUCOSE}}{MW_{GLUCOSE}} = 0.4 \quad mg_{oc}\, mg_{GLUCOSE}^{-1}$$

$$\left(\frac{Carbon}{Nitrogen}\right)_{EPS\ proteins} = 2.5 \quad mg_{oc}\, mg_{N}^{-1}$$

Evaluation of flocs strength (method A.6). It has been demonstrated that divalent cations (Ca^{2+}, Mg^{2+}) influence strength and filterability of sludge (see section 2.5.2). Therefore, the evaluation of flocs strength was assessed introducing two indexes related to divalent cations content in flocs: "the divalent cation content in biomass flocs" (SI_1) and the "cations extraction efficiency" of the thermal method (SI_2). However, before introducing such indexes, it is necessary to point out some preliminary aspects, as follows.

Firstly, the concentration of divalent cations was detected in aerobic mixed liquor, bulk liquid and extracted solution, in symbols $C_{Ca+Mg,\ ml}$, $C_{Ca+Mg,\ bl}$ and $C_{Ca+Mg,\ es}$ (mg L^{-1}), respectively (see Figure 5.17). Then, the apportionment of the mass of divalent cations (M_{Ca+Mg}, mg) in mixed liquor was executed according to Figure 5.19, equations 5.27 and 5.28, where V

indicates the volume (mL) of the mixed liquor (ml), the bulk liquid (bl) and the extracted solution (es).

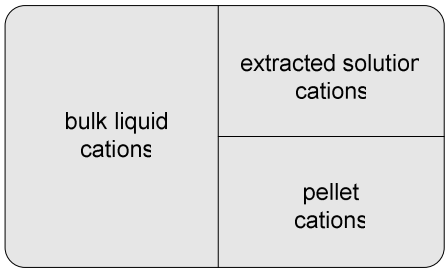

Figure 5.19. Apportionment of divalent cations in mixed liquor.

$$M_{Ca+Mg,\,ml} = M_{Ca+Mg,\,bl} + M_{Ca+Mg,\,es} + M_{Ca+Mg,\,pellet} \qquad 5.27)$$

$$C_{Ca+Mg,\,ml} \cdot \frac{V_{ml}}{1{,}000} = C_{Ca+Mg,\,bl} \cdot \frac{V_{bl}}{1{,}000} + C_{Ca+Mg,\,es} \cdot \frac{V_{es}}{1{,}000} + M_{Ca+Mg,\,pellet} \qquad 5.28)$$

Moreover, since the divalent cations content in flocs ($M_{Ca+Mg,\,flocs}$, mg) can be represented conceptually by the sum of divalent cations in pellet and in the extracted solution, it was assessed by difference, as follows:

$$M_{Ca+Mg,\,flocs} = C_{Ca+Mg,\,ml} \cdot \frac{V_{ml}}{1{,}000} - C_{Ca+Mg,\,bl} \cdot \frac{V_{bl}}{1{,}000} \qquad 5.29)$$

Finally, flocs strength indexes (SI_1 and SI_2) were introduced. In particular, the index SI_1 indicated the divalent cations content in flocs divided by MLVSS content (mg g $MLVSS^{-1}$):

$$SI_1 = \frac{M_{Ca+Mg,\,flocs}}{MLVSS \cdot \left(V_{mixed\ liquor} / 1{,}000\right)} \qquad 5.30)$$

where MLVSS states for the concentration of mixed liquor volatile suspended solids (g L^{-1}). Differently, the index SI_2 indicated the percentage (equation 5.31) of low bounded divalent cations in flocs, defined as the cations that are extracted by thermal flocs break-up, as follows:

$$SI_2 = \frac{M_{Ca+Mg,\,extrated\ solution}}{M_{Ca+Mg,\,flocs}} \cdot 100 \qquad 5.31)$$

According the divalent cation bridging (DCB) theory (Sobeck and Higgins, 2002) and the polymer bridging model (PBM) theory (Wilén at al., 2003), divalent cations bridge negatively charged functional groups within the EPS, thus aggregating cells and stabilizing flocs (see section 2.5.2). Therefore, the higher the values of SI_1, the better the flocs strength is.

Differently, as for index SI_2, the higher the fraction of low bounded divalent cations, the slighter the compactness and strength of flocs are.

Evaluation of sludge filterability (method A.7). The estimation of sludge filterability, i.e. the propensity of mixed liquor to be filtered, was assessed evaluating the specific resistance to filtration (SRF), and the modified fouling index (MFI) using the procedures adopted by Christensen et al. (1993) and Schippers and Verdouw (1980), respectively. In particular, in this study, SRF and MFI were detected in series using two types of filter cut-off as shown in Figure 5.20. In particular, SRF (Wathman paper filter grade 40, 8 μm) gave an indication of sludge filterability related to the resistance to filtration offered by sludge cake (aggregation of biomass flocs mainly) forming during the test. Differently, MFI (Wathman mixed acetate-cellulose ME25, 0.45 μm) provided information about the effects of little particles and colloids forming a sort of gel structure on the filter. In this way, SRF and MFI supplied information about sludge filterability in membrane filtration since biomass flocs and colloids imply resistances to filtration as stated in chapter 2 (see section 2.4.1). The third main component implying a resistance, i.e. macromolecules causing pores restriction in MBRs, can not be assessed in such tests as it must be used a membrane filtration system instead of paper or mixed acetate-cellulose filters.

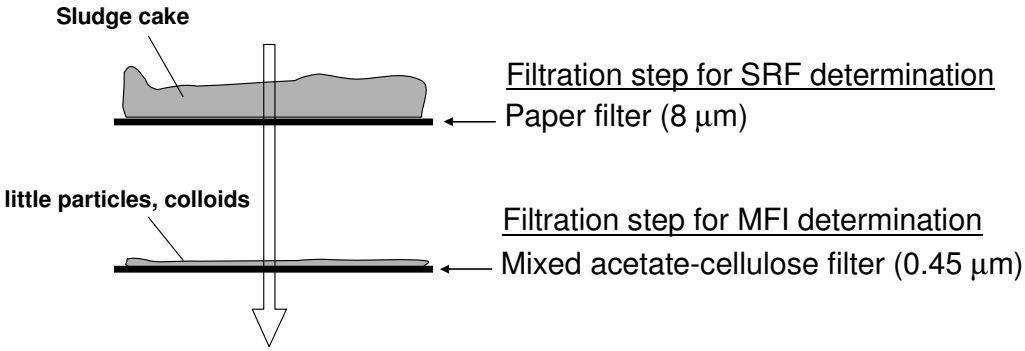

Figure 5.20. SRF and MFI in series detection.

According to Christensen et al. (1993) and Schippers and Verdouw (1980), both sludge cake and colloidal cake filtration occurring during tests can be described adopting the cake filtration theory equation (Carman, 1938; Ruth, 1946), as follows:

$$\frac{dV}{dt} = \frac{\Delta p \cdot A}{\mu_T \cdot \left(R_{deposit} + R_{filter}\right)} \qquad 5.32)$$

where V is the filtrate volume (m^3), t the time in the filtration process (s), μ_T the filtrate viscosity at temperature T (Pa s, see equation 2.4 and 2.5), A the area of the filter (m^2); ΔP

the applied pressure (Pa), whereas $R_{deposit}$ and R_{filter} (m^{-1}) represent the resistance to filtration provided by the deposit (sludge cake or colloidal cake) and the filter, respectively. Then, in the case of sludge cake filtration, $R_{deposit}$ is considered to be a function of SRF (m kg^{-1}), whereas with regards to colloidal cake formation, the parameter I (m^{-2}), that is a measure of the specific resistance due to colloids, has been introduced (Christensen et al., 1993; Schippers and Verdouw, 1980), as follows:

$$R_{deposit} = SRF \cdot w \cdot \frac{A}{V} \qquad 5.33)$$

$$R_{deposit} = I \cdot \frac{A}{V} \qquad 5.34)$$

where w is the mass of dry cake deposited per unit volume of filtrate (kg m^{-3}), that can be assumed to be approximately equal to MLSS concentration of mixed liquor.
Finally, the following equations are derived by integration at Δp constant from t = 0 to t = t:

$$\frac{t}{V} = \frac{\mu_T \cdot w \cdot SRF}{2 \cdot \Delta p \cdot A^2} \cdot V + \frac{\mu_T \cdot R_{filter}}{\Delta p \cdot A} \qquad 5.35)$$

$$\frac{t}{V} = \left(\frac{\mu_T \cdot I}{2 \cdot \Delta p \cdot A^2} \right) \cdot V + \frac{\mu_T \cdot R_{filter}}{\Delta p \cdot A} = MFI^* \cdot V + \frac{\mu_T \cdot R_{filter}}{\Delta p \cdot A} \qquad 5.36)$$

where MFI* (sec m^{-6}), defined by the term in brackets (equation 5.36), is the modified volume index at experimental conditions, i.e., temperature T and vacuum Δp. In Table 5.11 specific information is provided, particularly, with regards to different parameters and material considered for SRF and MFI determination. However, since equation 5.35 and 5.36 are very similar, also the experimental procedures and data processing were analogous from a practical point of view. In fact, experimental procedures were conducted as follows. Firstly, a proper volume of sludge/filtrate was poured into a filtering funnel. Vacuum condition was then created using a vacuum pump connected to the funnel and filtrate was collected in a graduated cylinder. Finally, data of collected filtrate volume over time was recorded.

Table 5.11. Specifics of experimental procedures for SRF and MFI determination.

	SRF	**MFI**
Volume (mL)	500 (sludge)	200 (filtrate from SRF)
Filtering device	Ceramic Buckner Funnel	Plastic Wathman funnel
Filter type	paper filter, 8 μm, 125 mm	acetate-cellulose filter, 0.45 μm, 47 mm
Applied Δp (KPa)	70	90
Temperature (°C)	20±1	20±1

Then, tests results were processed. Firstly, the ratio of the collected volume (V) and time (t) was calculated and plotted against volume (V). Linear regressions were then employed to fit equations 5.35 and 5.36 to (V/t) - V data for the determination of SRF and MFI*, respectively (Figure 5.21).

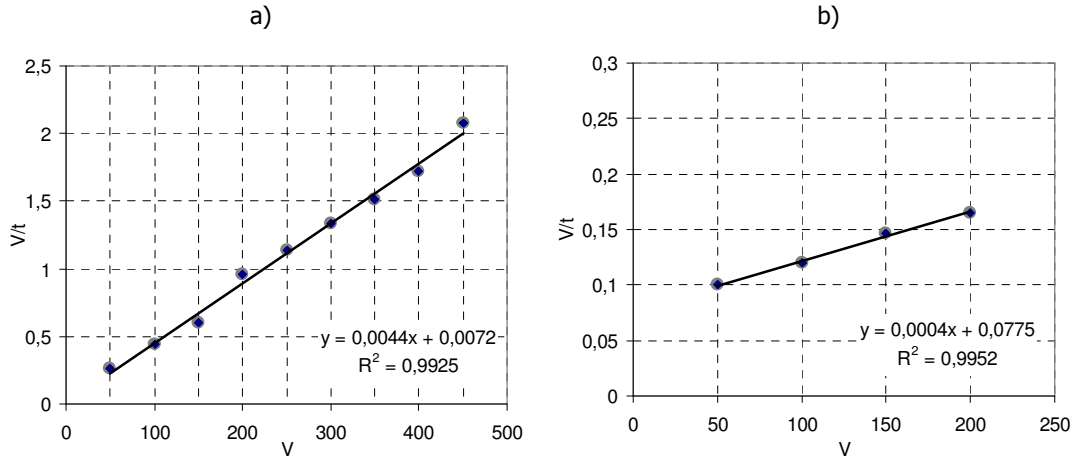

Figure 5.21. Examples of linear regressions for estimation of SRF (a) and MFI* (b); in these graphs volumes are expressed as mL instead of m^3.

Finally, with regards to MFI determination (sec L^{-2}), the value obtained by interpolation (i.e., MFI*, sec m^{-6}) was adjusted to standard conditions, i.e., 210 KPa and 20 °C, as follows (Schippers and Verdouw, 1980):

$$MFI = \frac{\mu_{20}}{\mu_T} \cdot \frac{\Delta p}{210} \cdot MFI^* \cdot 10^{-6} \qquad 5.37)$$

Evaluation of biological aerobic heterotrophic and autotrophic activity (method A.8). Aerobic heterotrophic and autotrophic activities are related to organic matter biodegradation and to ammonia oxidation into nitrate, respectively. In particular, the latter consists of two in series reactions, i.e., the ammonia oxidation to nitrite, provided by ammonia oxidising bacteria (AOB), and nitrite oxidation to nitrate, provided by nitrite oxidising bacteria (NOB), as follows:

$$NH_4^+ + 1.5\ O_2 \rightarrow NO_2^- + H_2O + 2\ H^+ \qquad 5.38)$$

$$NO_2^- + 0.5\ O_2 \rightarrow NO_3^- \qquad 5.39)$$

In order to characterize the bacteria activity, the Michaelis-Menten equation was considered in this study since it has been widely applied in modelling the biodegradation rate of biological processes:

$$\frac{dS_i}{dt} = v_{T\,i}^{max} \cdot \frac{S_i}{k_{s\,i} + S_i} \cdot x_{active\,i} \qquad 5.40)$$

where S_i (mg L^{-1}) is the concentration of the generic substrate i, i.e., organic matter (measured as COD), ammonia and nitrite, $v_{T\,i}^{max}$ and $k_{s\,i}$ are the maximum specific substrate consumption rate (mg g $VSS_{active\ biomass}^{-1}$ h^{-1}) and the semi-saturation constant for substrate i, respectively, whereas $x_{active\,i}$ is the concentration of active heterotrophic/AOB/NOB biomass (g $VSS_{active\ biomass}$ L^{-1}).

In particular, the estimation of the kinetic constants was executed adopting respirometric techniques, i.e., assessing the respiration activity of bacteria as their oxygen consumption rate or, oxygen uptake rate (OUR_i, mg OD L^{-1} h^{-1}), is correlated to the Michaelis-Menten equation, as follows:

$$OUR_i = k_i \cdot \frac{dS_i}{dt} = k_i \cdot v_{T\,i}^{max} \cdot \frac{S_i}{k_{s\,i} + S_i} \cdot x_{active\,i} \qquad 5.41)$$

where, as for heterotrophic activity the generic parameter k_i takes into account the biomass growth yield (Y_H, g VSS_H g COD^{-1}, see equation 5.42); whereas as for autotrophic activity, where growth yield is lower, k_i can be directly calculated by stoichiometry (equations 5.38 and 5.39).

$$k_i = 1 - 1.42 \cdot Y_H \qquad 5.42)$$

Moreover, the endogenous oxygen uptake rate (OUR_e) must be considered because oxygen is consumed also in absence of external substrates. In fact, substrates such as COD and ammonia are slowly released from biomass decay. Consequently the overall oxygen consumption rate (OUR) detectable using respirometers is the sum of rates related to external and endogenous substrates.

Generally, respirometers are bioreactors filled with activated sludge mixed liquor which can be classified according to two criteria defined by Spanjers et al. (1998):

- the phase (liquid or gas) where oxygen is measured;
- the presence (flowing) or absence (static) of gaseous or liquid flow.

In particular, in this study, it was adopted the Multiple Analysis Reprogrammable TItratioN Analyser (MARTINA) developed by Politecnico di Milano in cooperation with SPES (Fabriano,

AN, IT). It is a complex system including a liquid phase respirometer (i.e., the measurement of oxygen concentration occurs in the liquid phase using DO probes).

With regards to heterotrophic biological activity, the system was configured as a *gas static* and *liquid static* respirometer adopting re-aeration cycles provided by a blower and submerged diffusers. In particular, the central control unit of MARTINA switched on the blower when the OD concentration was close to a lower threshold value (4 mg L^{-1}) in order to reach rapidly the higher threshold value (7 mg L^{-1}). In this way, OUR was estimated considering the DO profile between two consecutive re-aeration cycles, as follows (Rozzi et al., 2003):

$$OUR = -\frac{dOD}{dt} \qquad 5.43)$$

Differently, with regards to autotrophic biological activity, the system was configured as a *gas static* and *liquid flowing* DO-stat titrator. In fact, MARTINA is provided with a titration unit to control the DO concentration to a constant fixed value. In particular, peristaltic pumps and automatic valves controlled by the central unit consent the addition of a hydrogen peroxide titration solution (H_2O_2, 0.08 N) to control DO around 7.0 mg OD L^{-1}. Hydrogen peroxide is rapidly decomposed to oxygen and water by catalases, an enzyme produced by most all aerobic organisms to prevent the build up of peroxides and free radicals, detrimental to living cells, and are therefore naturally present in any biomass suspension.

In this way, OUR can be estimated as follows (Rozzi et al., 2003):

$$OUR = \frac{Q_{in} \cdot DO_{in}}{V} \qquad 5.44)$$

where Q_{in} and DO_{in} are the flow rate (L h^{-1}) and the equivalent DO concentration (mg OD L^{-1}) of titration solution, whereas V is the volume of respirometer filled with sludge (L). In particular, MARTINA measured the volume dosed over time of titration solution (V_{TS}), therefore equation 5.44 can be written as follows:

$$OUR = \frac{DO_{in}}{V} \cdot \frac{dV_{TS}}{dt} \qquad 5.45)$$

In both of the cases, the system was provided with a magnetic stirrer to homogenize the medium, temperature and pH control devices to keep then at the desired constant values (20±1°C, 7.5±0.1).

In order to assess the heterotrophic activity a standard substrate, i.e., sodium acetate, was considered, whereas for the estimation of the ammonia and nitrite oxidizing activities, two

solutions of ammonium chloride (2 g $N\text{-}NH_4^+$ L^{-1}) and sodium nitrite (1 g $N\text{-}NO_2$ L^{-1}) were used as substrates, respectively.

The applied methodology to assess the main parameters of biomass activity are shown in Table 5.12. In particular, all the three types of test were considered and applied in duplicate considering 0.5 L of aerobic mixed liquor samples, previously characterized for MLSS and MLVSS concentrations. With regards to autotrophic activity, the applied methodology permits to obtain maximum substrate consumption rate specific to the MLVSS content of samples instead of active AOB and NOB mass.

Table 5.12. Tests to assess the main parameters of biomass activity and reference methodologies.

	Measured parameter	Measuring technique	Methodology
Heterotrophic activity	aerobic biomass growth yield on acetate Y_H	*gas static - liquid static*	test type 1 (Ekama et al., 1986)
	aerobic maximum growth rate $\mu_{20\,H}^{max}$	*gas static - liquid static*	test type 2 (Kappeler and Gujer, 1992)
	maximum specific substrate consumption rate $v_{20\,H}^{max}$	-	$v_{20\,H}^{max} = \frac{\mu_{20\,H}^{max}}{Y_H}$
Autotrophic activity	AOB maximum specific substrate consumption rate $v_{20\,AOB}^{max}$	*gas static - liquid flowing*	test type 3 (Artiga et al., 2005)
	NOB maximum specific substrate consumption rate $v_{20\,NOB}^{max}$	*gas static - liquid flowing*	

Evaluation of TMP, P_{20} and R (method A.9). Transmembrane pressure (TMP) was measured according to the following equation:

$$TMP = p_{atm} - p - H \qquad 5.46)$$

where p_{atm} is the atmospheric pressure (bar), p is the absolute pressure measured in the suction line of the process pump (bar) during the active phase of RX and H is the distance between the water level in the reactor and the point of the measurement in the suction line (Figure 5.22), expressed in bar (0.0978 bar/m).

Since only one pressure gauge was available, the atmospheric pressure was detected once a day disconnecting the pressure gauge from the suction line. Since 30 data per hour were collected in relation to p, whereas only 1 data per day to p_{atm}, atmospheric pressure data were estimated assuming a linear variation over time of p_{atm} between 2 consecutive collected data.

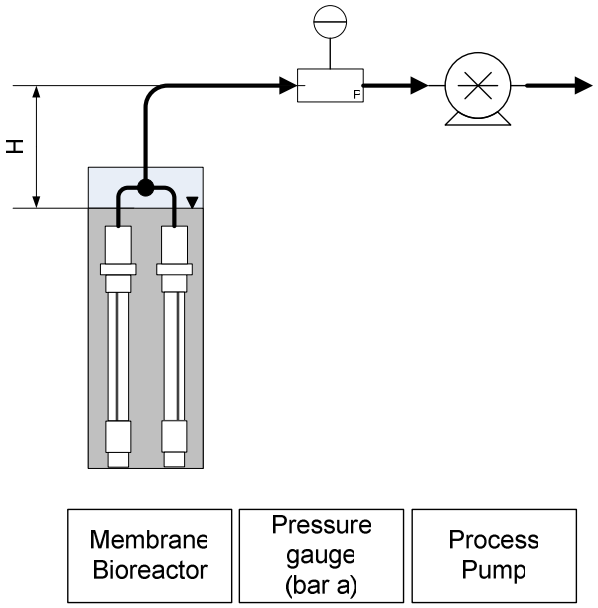

Figure 5.22. Evaluation of the transmembrane pressure (TMP).

Then, the evaluation of the permeability at 20°C (P_{20}, LMH bar^{-1}) and the total resistance to filtration (R, m^{-1}) were calculated as follows (see section 2.3.3):

$$P_{20} = \frac{J}{TMP} \cdot e^{-0.0239 \cdot (T-20)} \qquad 5.47)$$

$$R = \frac{1}{\mu_{20} \cdot P_{20}} \cdot 3.6 \cdot 10^{11} \qquad 5.48)$$

where μ_{20} is the viscosity of the permeate at 20°C, that is usually assumed to be equal to water viscosity (0.001 Pa s).

Membrane cleaning procedure (method A.10). The cleaning procedure adopted in the study was developed according to indication provided by the manufacturer. In particular, the complete procedure consisted of physical and chemical cleanings, as follows.

- Clean A (physical clean). Removal of the residual cake layer on the membranes by hand and a gentle spray of potable water over a drain, followed by a potable water filtration (10 LMH, 30 min) with high aeration flowrate (1,000 L h^{-1}).
- Clean B (1st chemical clean). Soaking of the modules in a sodium hypochlorite (NaOCl) solution at a concentration of 1,500 $mgCl_2$ L^{-1} (free chlorine) at room temperature for a soaking time calculated using equation 5.49, followed by filtration (10 LMH, 20 min) without aeration.

- Clean C (2^{nd} chemical clean). Soaking of the modules in a sodium hydroxide (NaOH) solution (pH = 9) at room temperature for a soaking time calculated using equation 5.49, followed by filtration (10 LMH, 20 min) with high aeration flowrate (1,000 L h^{-1}).
- Clean D (3^{rd} chemical clean). Soaking of the modules in a solution of citric acid (0.5% w/w) and sulphuric acid (approximately 0.05% w/w for pH adjustment to pH 2) at room temperature for a soak time calculated using equation 5.49, followed by filtration (10 LMH, 20 min) with high aeration flowrate (1,000 L h^{-1}).

$$\text{soaking time} = \max\left[3\,;7-0.2\cdot(\text{temperature in }^{\circ}\text{C})\right] \qquad 5.49)$$

Moreover, the efficacy of membrane cleaning was assessed evaluating the membrane permeability at 20°C (P_{20}) after each cleaning step (Figure 5.23). In particular, water filtration experiments at different fluxes (5, 10, 15 LMH) applied to each module separately were performed, as follows. Firstly, each flux value was applied to the membrane modules for 10 min and TMP was calculated according to equation 5.26. Then, a linear regression was employed to fit equation 5.50 (a modified Darcy equation, see section 2.3.3 for the original equation in membrane filtration) to J-TMP data. In this way, estimate of permeability P was obtained and then adjusted to 20°C, i.e., P_{20} was calculated (equation 5.51):

$$J = P\cdot TMP \qquad 5.50)$$

$$P_{20} = P\cdot e^{-0.0239\cdot(T-20)} \qquad 5.51)$$

where T is the water temperature (°C).

Finally, the overall efficiency of the cleaning procedure was then evaluated comparing P_{20} calculated in water test T.D to the original permeability at 20°C of the new membranes.

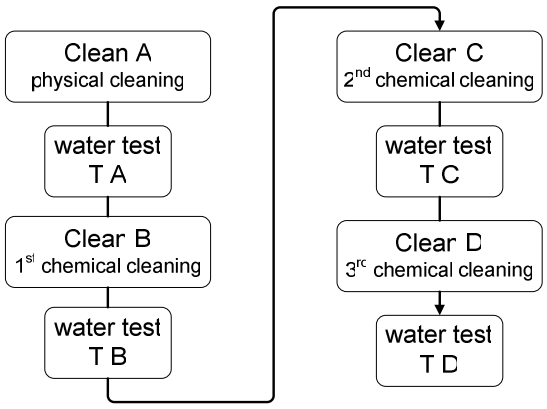

Figure 5.23. Cleans and water tests in the cleaning procedure.

Resistance to filtration apportionment (method A.11). The resistance to filtration R can be apportioned between the membrane resistance (R_m), the resistance by cake layer formed on the membrane surface (R_c) and the fouling resistance caused by pore restriction and adsorption of foulants onto the membrane pore wall or surface (R_f). In particular, the procedure considered in this study is reported by Bae and Tak (2005), whose method is based on the concept that R_m and R_f (due to irreversible fouling) can be detectable in clean water test, whereas R_c only in mixed liquor filtration, when cake layer formation occurs (due to flocs accumulation, reversible fouling). Firstly, the resistance R along the MBR operation, was evaluated and recorded as follows, where P_{20} was assessed using equation 5.51:

$$R = \frac{1}{\mu_{20} \cdot P_{20}} \cdot 3.6 \cdot 10^{11}$$

Then, R_m, R_f and R_c were evaluated using eq. 5.52, eq. 5.53 and eq. 5.54:

$$R_m = \frac{1}{\mu_{20} \cdot P_{20,\,\text{clean water}}} \cdot 3.6 \cdot 10^{11} \qquad 5.52)$$

$$R_f = \frac{1}{\mu_{20} \cdot P'_{20,\,\text{clean water}}} \cdot 3.6 \cdot 10^{11} - R_m \qquad 5.53)$$

$$R_c = R - R_m - R_f \qquad 5.54)$$

where $P_{20,\,\text{clean water}}$ is the permeability evaluated by linear regression (see above, method A.10) using clean water and new membranes, whereas $P'_{20,\,\text{clean water}}$ is the permeability evaluated using clean water (again, by linear regression) of used membranes (1) after having removed the cake layer through step A of the cleaning procedure (water test T.A), or, (2) at the end of the cleaning procedure (water test T.D) before immerging them into the mixed liquor. Consequently the resistance to filtration apportionments was evaluated in parallel with membrane main cleans, as reported in Table 5.19.

Table 5.13. Evaluation of membrane resistance (R_m), resistance by cake layer formed on the membrane surface (R_c) and fouling resistance caused by pore restriction and adsorption of foulants onto the membrane pore wall or surface (R_f) at the beginning and the end of each stage (istage 1 and stage 2.

instant of interest	R apportionment
1 - beginning of stage 1	$R_m+R_{f1}+R_{c1}$
2 - end of stage 1	$R_m+R_{f2}+R_{c2}$
3 - beginning of stage 2	$R_m+R_{f3}+R_{c3}$
4 - end of stage 2	$R_m+R_{f4}+R_{c4}$

R_m was evaluated when membranes were new before the MBR start-up during the membrane characterization with clean water after the main clean 1, using equation 5.52. Differently from all other water tests, fluxes applied to membrane modules were 5, 7.5, 10, 12.5, 15, 20 LMH. As shown in Figure 5.24, R_{f1} was determined using equation 5.53 applied to results of water test T.D of the main clean 2, whereas R_{f2} was determined using equation 5.53 applied to results of water test T.A of the main clean 3. With regards to stage 2, R_{f3} was determined using equation 5.53 applied to results of water test T.D of the main clean 3, whereas R_{f4} was determined using equation 5.53 applied to results of water test T.A of a physical cleaning, performed on purpose only for R_f detection.

Finally, in order to compare the effects of the flux enhancer addition on membrane fouling the "average irreversible fouling rate", FR (m^{-1} d^{-1}), was introduced for each stage, as follows:

$$FR_{stage\ 1} = \frac{R_{f2} - R_{f1}}{\Delta t_{stage\ 1}} \qquad 5.55)$$

$$FR_{stage\ 2} = \frac{R_{f4} - R_{f3}}{\Delta t_{stage\ 2}} \qquad 5.56)$$

where R_{f1} and R_{f2} represent the fouling resistance (m^{-1}) at the beginning and the end of stage 1, which duration is indicated by Δt_{stage1} (d), whereas R_{f3} and R_{f4} are the fouling resistance (m^{-1}) at the beginning and the end of stage 2, which duration is indicated by Δt_{stage2} (d).

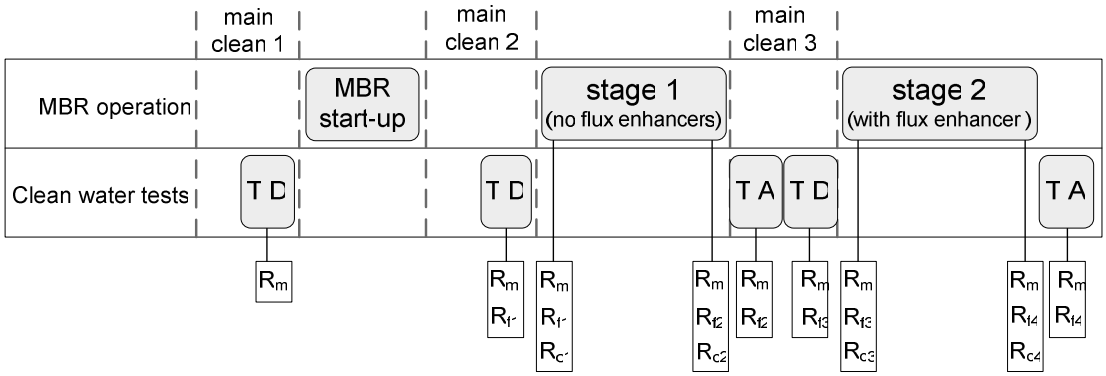

Figure 5.24. Evaluation of membrane resistance (R_m), resistance by cake layer formed on the membrane surface (R_c) and fouling resistance caused by pore restriction and adsorption of foulants onto the membrane pore wall or surface (R_f) at the beginning and the end of each stage (i.e, stage 1 and stage 2).

5.3.3 Methods applied for the best flux enhancer selection

The selection of the best flux enhancer between NORIT CA1 (a powered activated carbon), TILLMANNS TILLPAC18 (a polyaluminium chloride) and DALTON FLODAL (a cationic polyaminic flocculant with high decolouring power) was executed performing a jar test campaign, consisting in short-term batch experiments applying the procedure shown in Figure 5.25 to raw and conditioned (i.e., with the addition of flux enhancers) sludge samples. In particular, the scope of jar tests was to give an estimation of the fouling control capability and effluent quality improvement of flux enhancers. Consequently, the parameters selected to gain the required information for the best choice were considered to be:

- soluble-EPS (proteins and carbohydrates) removal, sludge filterability enhancement measuring capillary suction time (CST), specific resistance to filtration (SRF) and the modified fouling index (MFI), as for fouling control;
- TOC, COD and colour removal occurring in mixed liquor bulk liquid, as for quality enhancement.

Moreover, the specific mass (i.e., the mass per unit of filtered volume) of suspended solids collected on the filter used for bulk separation was estimated. In particular, such solids were defined as low density suspended solids (LDSS, mg LDSS mL^{-1}) as they did not settle during the centrifugation step of sludge samples for the bulk liquid separation (see method A.3).

Raw and conditioned sludge samples (600 mL) were treated according to the following procedure, performed at 20±0.5°C:

1. determination of mixed liquor suspended solids (MLSS) concentration of the raw sludge sample;
2. flux enhancer addition (conditioned samples only) applying definite doses (see over);
3. rapid mixing (150 rpm, 60 sec) to dissolve/disperse the enhancer into the sample volume rapidly;
4. flocculation (45 rpm, 90 min) to provide time for generating of interactions between sludge flocs/soluble EPS and flux enhancers;
5. partition of the sample in three fractions:
    - fraction 1, then analyzed for the CST evaluation (20 mL);
    - fraction 2, then analyzed for the determination of SVI (500 mL), and, after sample re-suspension, the determination of SRF (500 mL, see section 5.3.2) and MFI (200 mL, see section 5.3.2);
    - fraction 3, then used for bulk liquid separation (80 mL, see section 5.3.2), characterized considering selected parameters as described above (see also Figure 5.25).

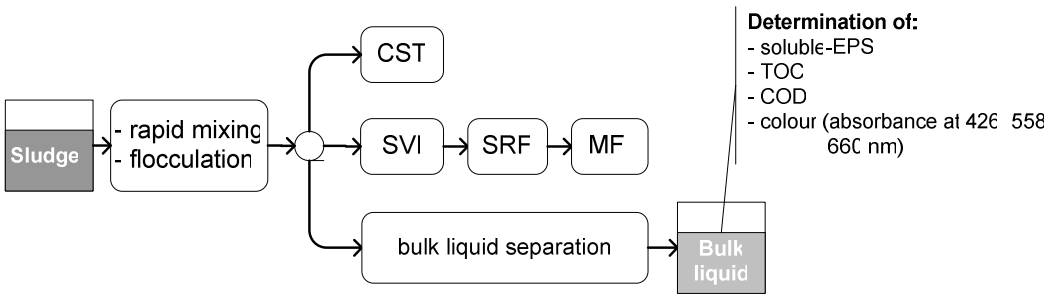

Figure 5.25. Procedure adopted in the Jar test campaign for the flux enhancer selection.

With regards to flocculation, mixing and time provided were defined and fixed at proper values in order to define comparable conditions to that of the pilot plant, particularly considering the aerobic tank. For this reason, flocculation time was extended to the highest technically practicable value (i.e., permitting to execute 4 complete jar tests a day), 90 min, that resulted to be 3÷9 times the typical flocculation duration in wastewater treatment (10÷30 min; Metcalf and Eddy, 2003).

Evaluation of SVI, CST, SRF, MFI (method A.12). The sludge volume index (SVI, mL g_{MLSS}^{-1}), an index of sludge settling propensity representing the volume occupied by 1 g of MLSS after 30 min of static settling, was evaluated according to Standard Methods for Examination of Water and Wastewater (APHA, 2005) applying the original procedure to a sample volume (V_0, L) of 0.5 L instead 1 L. The 30 min settled sludge volume (V_{30}, mL) was determined using a 500 mL glass cylinder and SVI was then calculated, as follows:

$$SVI = \frac{V_{30}}{MLSS \cdot V_0} \qquad 5.57)$$

where MLSS is the mixed liquor suspended solids concentration (g L^{-1}) of the sludge sample. With regards CST (sec), it is a quick method for characterising sludge filterability. In particular, during the CST test, the capillary suction pressure generated by standard filter paper is used to 'suck' water from the sludge. The rate at which water permeates through the filter paper varies depending on the filterability of the cake formed on the filter paper. In fact, the force generated by capillary suction is much greater than the hydrostatic head within the funnel, so the test is independent of the amount of sludge. The CST is obtained from two electrodes (A, B) placed at a standard interval from the funnel. In particular, the time (t_{AB}, sec) taken for the water front to pass between these two electrodes constitutes the CST (APHA, 2005). The equipment used was the Triton Electronics Ltd. Type 304 CST meter. The procedure was applied both on potable water (reference value) and on sludge

samples and CST was calculated subtracting the value obtained with water ($t_{AB, water}$, sec) from the sludge value ($t_{AB, sludge}$, sec), as follows:

$$CST = t_{AB,sludge} - t_{AB,water} \quad 5.58)$$

Since CST was determined considering duplicate sludge samples, the average value is shown in the results and discussion chapter. Finally, as for SRF and MFI, see section 5.3.2, method A.7.

Definition of doses to test (method A.13). Generally, the term "dose" (D) refers to the concentration in mg L^{-1} of the flux enhancer in the volume of mixed liquor (see section 2.6). Differently, in this study D was defined as the relative quantity of the flux enhancer present in mixed liquor per 1 g of MLSS (mg g $MLSS^{-1}$). In fact, it is believed that, in this way, the dose is defined more properly since, conceptually, main effects of flux enhancers are related to MLSS. For instance, considering coagulants/flocculants (category A in Table 2.7), the particle aggregation effects depends on MLSS at a given concentration of flux enhancer (in mg L^{-1}). The higher MLSS, the lower the particle aggregation and flocculation by coagulants/flocculants are. Again, with regards to adsorbents (category B in Table 2.7), since effects of particle inclusion in flocs during BAC formation can lead to an improvement in sludge filtration (see section 2.6), it is believed that such effects are related to MLSS at a given concentration of the adsorbents (in mg L^{-1}). In particular, the higher MLSS, the lower the effects are. Furthermore, soluble-EPS and bound-EPS production is proportional to biomass concentration (Laspidou and Rittmann, 2002). In particular, the higher the biomass, the higher EPS production is. As a results, in this study, doses were expressed as the flux enhancer active mass in mg per g of MLSS. As for CA1 and FLODAL the active mass of the flux enhancer corresponded to the total mass of the commercial product, whereas for TILLPAC18 the active fraction (polyaluminium chloride) was the 18% of the total commercial product mass.

As previously stated, the main goal of the thesis was the assessment of the flux enhancer effects at low sustainable dosages in MBRs, with reference to fouling control and effluent quality enhancement. Consequently the definition of the "doses to test" was executed taking into consideration economic aspects. In particular, the range of "doses to test" was defined according to a double criteria, as follows (Figure 5.26):

1. flux enhancers addition must be economical compared to a threshold value of cost;
2. flux enhancers addition must not induce negative effects detectable in short-term tests, such as the variation in pH values and the release of nitrogen in bulk liquid.

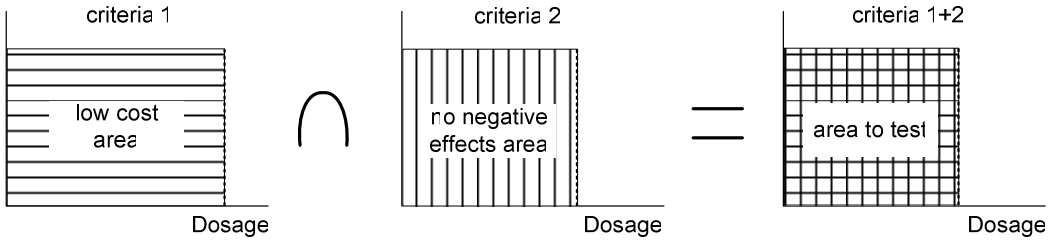

Figure 5.26. Criteria for identification of the "doses to test" range.

With regards to criteria 1, the limit value considered in the study was 0.025 € per cubic meter of wastewater treated and it was related to doses approximately of 100, 150, 220 mg g $MLSS^{-1}$ of CA1, TILLPAC18 and FLODAL, respectively (see below, method A.16). In particular, the specific cost indicated herein was fixed arbitrary at a value 3 times the specific cost disbursed in a full scale WWTP (Comodepur, Como) treating mixed domestic-textile (20% of flow), where DALTON FLODAL was adopted in a tertiary treatment for decolouring purpose only. With regards to criteria 2, negative effects detectable in batch experiments were the acidification (diminution of pH) in the case of TILLMANS TILLPAC18 and the release of nitrogen in bulk liquid for DALTON FLODAL, implying the risk that effluent quality would not have met standards for nitrogen imposed by regulation. Differently, CA1 did not present such negative effects. In particular, the minimum pH value considered to be admissible was 1 unit less the average pH of raw sludge samples (6.3 and 7.3, respectively). This limit was related to a TILLPAC18 dose of 50 mg g $MLSS^{-1}$. By comparison, the maximal admissible total nitrogen release in bulk for FLODAL was considered to be 10 mg L^{-1}, also related to a dose of 50 mg g $MLSS^{-1}$. In conclusion, the "doses to test" were fixed at:

- CA1: 0÷100 mg g $MLSS^{-1}$;
- TILLPAC18: 0÷50 mg g $MLSS^{-1}$;
- FLODAL: 0÷50 mg g $MLSS^{-1}$.

Then, four doses for each product were considered as shown in Table 5.14. Finally, the batch procedure was executed in duplicate at every dose, referring to different raw sludge samples (four samples in total) in order to take into account any possible variation of sludge characteristics.

Table 5.14. Doses considered in the jar test campaign (mg g_{MLSS}^{-1})

Flux enhancer	D1	D2	D3	D4
NORIT PAC C1	12.5	25	50	100
TILLMANS TILLPAC18	6.25	12.5	25	50
DALTON FLODAL	6.25	12.5	25	50

Criteria for the selection of the best flux enhancer (method A.14). Firstly, for every dose and chemical tested, the relative variation (%) of the parameters of interest was evaluated, as follows:

$$\text{variation} = \alpha \cdot \frac{P_c - P_r}{P_r} \cdot 100 \qquad 5.59)$$

where P_r and P_c represent the values of the parameters related to the raw sludge and the conditioned sludge, respectively; whereas α is a constant which value can be "-1" or "+1" according to the information provided by equation 5.59 as shown in Table 5.15.

Table 5.15. Information provided by equation 5.59.

Parameter	α	Information by eq. 5.59	Parameter	α	Information by eq. 5.59
SVI	+1	Variation	bulk proteins	-1	Removal rate
CST	+1	Variation	bulk carbohydrates	-1	Removal rate
SRF	+1	Variation	bulk TOC	-1	Removal rate
MFI	+1	Variation	bulk COD	-1	Removal rate
LDSS	-1	Removal rate	bulk colour	-1	Removal rate

Then, since the batch test procedure was applied in duplicate for every dose, the average value and standard deviation of variation (equation 5.59) were evaluated. In particular, the average values were plotted versus the applied doses. In this way, effects of different flux enhancers were compared and the product giving the best performances was selected and identified as the best product.

Finally, the optimal dose of the best flux enhancer, usually determined as shown in Figure 5.27 ($D_{optimal}$*), was identified using a multi criteria analysis ($D_{optimal}$), considering:

1. the relevance of effects related to fouling control and effluent quality enhancement;
2. the economic sustainability of flux enhancer addition;
3. the negative effects detectable in short-period batch tests;
4. any risks of biological activity decline.

In particular, considering criteria 1, the higher the dose, the more significant the effects are (when $D \leq D_{optimal}$*); whereas, considering criteria 2, 3 and 4, the higher the dose, the higher the costs and the risks of negative effects are. As a result, the multi criteria optimal dose ($D_{optimal}$) can be lower than $D_{optimal}$*, as shown in Figure 5.27.

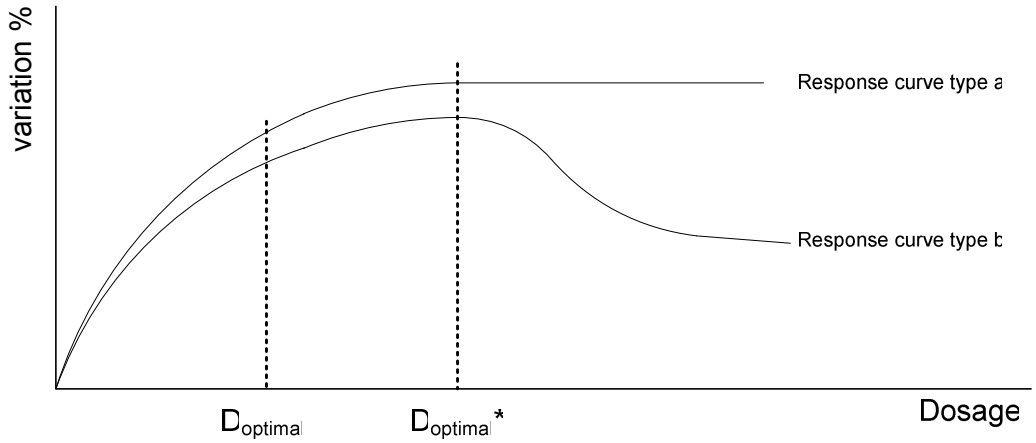

Figure 5.27. Optimal dose according to usual criteria ($D_{optimal}$*) and multi criteria used in this study ($D_{optimal}$*).

Extension of batch tests results to continuous operation of MBRs (method A.15).
The continuous flow operating of the pilot MBR plant suggested a continuous dosage of the flux enhancer into the pilot to compensate for the losses due to the excess sludge removal (Yoon et al., 2005). In continuous operating, it is necessary to refer to a continuous dosage of flux enhancers (DS) per unit time (g d^{-1}). In particular, DS was calculated on a basis of mass balances in stationary condition considering only the physical phenomena occurring in reactors. Such a modelling was also helpful to evaluate theoretically the concentration (or dose, D in mg $gMLSS^{-1}$) of the flux enhancer in the mixed liquor at the generic time t since a practical determination was not feasible.
Firstly, flux enhancers were assumed to be suspended material (solid particles > 0.45 μm) since NORIT CA1 was characterized by particle diameters > 7 μm for the 90% of its mass, and TILLMANS TILLPAC18 and DALTON FLODAL were involved in particle aggregation with flocs. Then, with regards to the generic suspended material i (i.e., MLSS and flux enhancers), it was considered that the ratio between the concentration of material i in tank j ($C_{i,j}$ in milligram or gram per litre of mixed liquor) and the concentration of material i in aerobic tank ($C_{i,2}$ in milligram or gram per litre of mixed liquor) was only due to physical phenomena occurring in reactors. In addition, since physical phenomena are more rapid than the biological phenomena they can be considered at the equilibrium. Therefore, applying mass balances at the stationary state avoiding biological kinetics, equations 5.60 and 5.61 follow.

$$\frac{C_{i,1}}{C_{i,2}} = \frac{q_{r1}}{q + q_{r1}} \qquad 5.60)$$

$$\frac{C_{i,3}}{C_{i,2}} = \frac{q + q_{r2}}{q_{r2}} \qquad 5.61)$$

where q, q_{r1} and q_{r2} (L h^{-1}) are flowrates defined in Figure 5.28, system A. Then, evaluating the flux enhancer dose for tank j (D_j) by definition, it comes out that D_j is the same for all the 3 tanks, as follows:

$$D_1 = \frac{C_{\text{flux enhancer},1}}{C_{\text{MLSS},1}} = \frac{\frac{q_{r1}}{q + q_{r1}} \cdot C_{\text{flux enhancer},2}}{\frac{q_{r1}}{q + q_{r1}} \cdot C_{\text{MLSS},2}} = \frac{C_{\text{flux enhancer},2}}{C_{\text{MLSS},2}} \qquad 5.62)$$

$$D_2 = \frac{C_{\text{flux enhancer},2}}{C_{\text{MLSS},2}} \qquad 5.63)$$

$$D_3 = \frac{C_{\text{flux enhancer},3}}{C_{\text{MLSS},3}} = \frac{\frac{q + q_{r2}}{q_{r2}} \cdot C_{\text{flux enhancer},2}}{\frac{q + q_{r2}}{q_{r2}} \cdot C_{\text{MLSS},2}} = \frac{C_{\text{flux enhancer},2}}{C_{\text{MLSS},2}} \qquad 5.64)$$

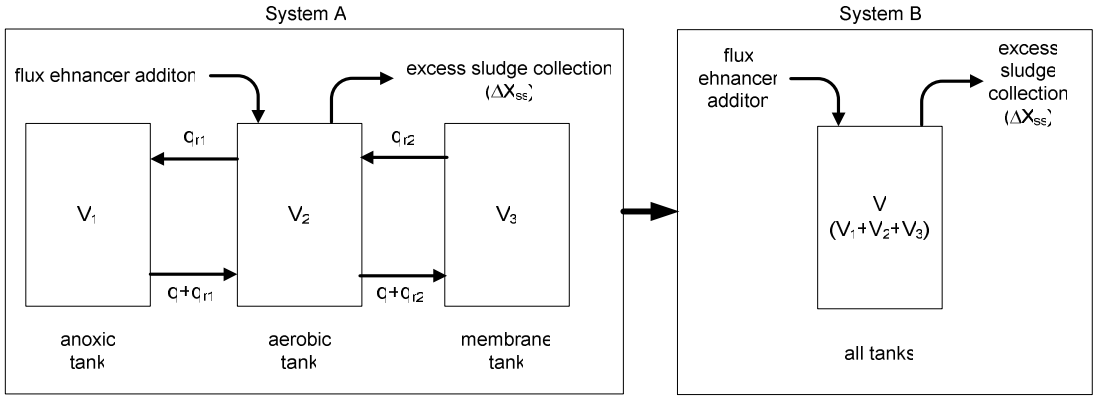

Figure 5.28. System description and simplification.

In conclusion, the system A in Figure 5.28 can be modelled as the simple system B using one differential equation only for one bigger reactor, that was considered a CFSTR reactor of a total volume V (L) at the equilibrium from a biological point of view (i.e., MLSS concentrations in tanks were considered to be constant over time), see eq. 5.65.

$$\frac{dD}{dt} = \frac{1{,}000 \cdot DS}{\overline{MLSS} \cdot V} - \frac{\Delta X_{ss}}{\overline{MLSS} \cdot V} \cdot D \qquad 5.65)$$

where D is the dose in the mixed liquor volume (mg g $MLSS^{-1}$), DS the dosage applied to the pilot plant (g d^{-1}), $\overline{MLSS}$ represent the average MLSS concentration over the three reactors (g L^{-1}), and ΔX_{ss} the excess sludge production (gSS d^{-1}).

Then, introducing the formal definition of SRT (equation 5.66) the model can be written as stated in equation 5.67.

$$SRT = \frac{\overline{MLSS} \cdot V}{\Delta X_{ss}} \qquad 5.66)$$

$$\frac{dD}{dt} = \frac{1{,}000 \cdot DS}{\overline{MLSS} \cdot V} - SRT^{-1} \cdot D \qquad 5.67)$$

Therefore, the solution at the equilibrium of the differential equation follows (equation 5.68) and daily dosage (DS) can be obtained (equation 5.69):

$$D_{\infty} = \frac{1{,}000 \cdot SRT}{\overline{MLSS} \cdot V} \cdot DS \qquad 5.68)$$

$$DS = \frac{\overline{MLSS} \cdot V}{1{,}000 \cdot SRT} \cdot D_{\infty} \qquad 5.69)$$

The latter equation was used to estimate the daily dosage (DS) fixing the equilibrium dose (D_{∞}) at the optimal value defined in the jar test campaign.

Then, the dose at the generic time t was estimated applying equation 5.70, that is the solution of equation 5.67.

$$\frac{D(t)}{D_{\infty}} = 1 - (1 - \upsilon) \cdot e^{\frac{t}{SRT}} \qquad 5.70)$$

where ν is the ratio between the initial dose (D_0) and the equilibrium dose, as follows:

$$\upsilon = \frac{D_0}{D_{\infty}} \qquad 5.71)$$

If ν had been considered equal to 1, then the actual dose D would have been equal to the optimal dose from time zero onwards. However, as stated above (see section 4.2.1), the dosing strategy was designed considering an initial dose (D_0) half the optimum value (ν=0.5). Such a dose was imposed adding instantaneously at time zero a proper amount of flux enhancer into the mixed liquor of the 3 tanks. Then the continuous dosage DS of the

flux enhancer was executed considering the aerobic tank (the core of MBR from a biological point of view) as the point of injection and using a peristaltic pulp (VELP, model 622).

Evaluation of costs related to continuous dosages (method A.16). The daily cost and specific costs of the continuous dosage can be defined as shown in Table 5.16 and evaluated according to definitions using equation 5.72, 5.73, and 5.74.

Table 5.16. Definition of daily cost and specific costs of the continuous dosage.

Cost	Symbol	Unit of measure
daily cost	Cost	€ d^{-1}
specific cost per unit of excess sludge produced	Cost'	€ t_{ss}^{-1}
specific cost per unit of treated wastewater volume	Cost''	€ $m_{waste\ water}^{-3}$

$$Cost = \frac{DS}{\%_{active}} \cdot p \cdot 10^{-3} \qquad 5.72)$$

$$Cost' = \frac{Cost}{\Delta X_{ss}} \cdot 10^{6} \qquad 5.73)$$

$$Cost'' = \frac{Cost}{q} \cdot 10^{3} \qquad 5.74)$$

where DS represents the continuous dosage applied to the pilot plant (g d^{-1}), $\%_{active}$ the percentage of active mass over the total mass of the commercial product (100% for CA1, 18% for TILLPAC18, 100% for FLODAL), which price is indicated by p (€ kg^{-1}), whereas ΔX_{ss} is the excess sludge production (g_{SS} d^{-1}) and q the wastewater flow rate treated by the pilot plant (L d^{-1}).

Specific costs provide general information that can be extended to full scale WWTPs. In particular, the following more practical equations can be obtained from the previous ones:

$$Cost' = \frac{D_{\infty}}{\%_{active}} \cdot p \qquad 5.75)$$

$$Cost'' = \left(\frac{D_{\infty}}{\%_{active}} \cdot p \right) \cdot \frac{HRT_{th}}{SRT} \cdot \overline{MLSS} \cdot 10^{-3} \qquad 5.76)$$

where D_∞ is the equilibrium dose, i.e., the optimal dose to consider (mg g $MLSS^{-1}$), $\overline{MLSS}$ represents the average MLSS concentration (g MLSS L^{-1}), HRT_{th} the theoretical hydraulic retention time (d) and SRT the sludge retention time (d).

5.3.4 Standard and modified flux step methods for critical flux determination

In this section standard and modified flux step procedures for critical flux (Jc) determination are presented, whereas indication about the criteria for Jc detection and, also, about relevant parameters for gaining important information related to sludge fouling propensity are reported and investigated in the results and discussion section (see section 6.7). Weekly working programme shown in Figure 5.32 was applied for 10 weeks, the first one at the end of stage 1 (no addition of flux enhancer) and the others during stage 2 (addition of flux enhancer). Firstly, the excess sludge collected on Wednesday was characterized for MLSS, and filterability parameters, i.e., SRF and MFI (see section 5.3.2, method A.7). After that, it was analysed by the standard flux step procedure and then by the modified one using the batch test unit described above (see section 5.2.3). Moreover, it can be seen from the chart that the membrane module was systematically cleaned prior to each critical flux test. In particular, with regards to cleaning protocol, standard procedure and the modified one, consider method A.17 and method A.18, respectively.

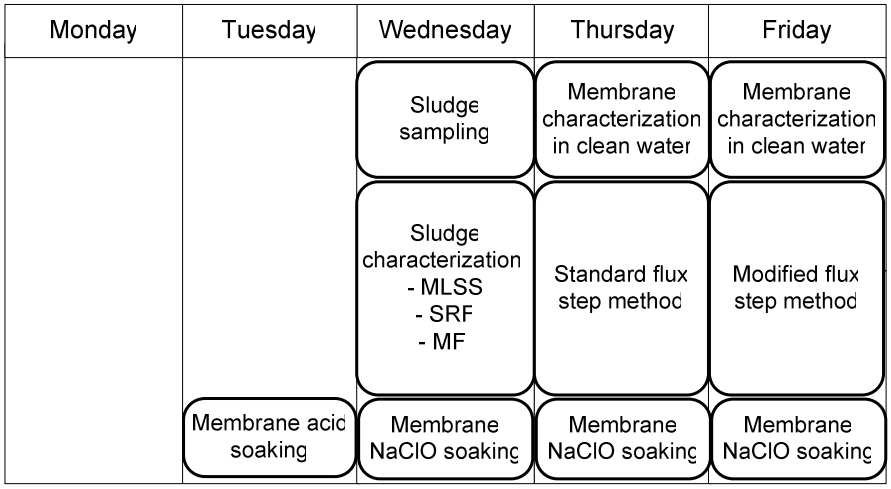

Figure 5.29. Weekly works programme chart for fouling propensity and filterability assessment.

Cleaning protocol (method A.17). The general cleaning protocol of the ZW1 module used in the batch test unit (see section 5.2.3) consisted of removing any cake apparent on

the membranes by hand and with a gentle spray over a drain and soaking the module in 200 ppm NaOCl at room temperature over night before and after each flux step procedure. Moreover, once a week an additional acid soak solution (HCl, pH=2) was perform for a minimum of 5 hours, in order to prevent inorganic fouling.

Standard and modified flux step method (method A.18). The most common practice for the experimental critical flux determination is to increase the flux step by step, each step having a fixed duration and a constant increase of flux one step after the other (standard method), giving a stable TMP at low fluxes but an ever-increasing rate of TMP increase at higher fluxes. In particular, once it is reached a max LHM value (i.e., the flux giving max admissible TMP values), steps are performed decreasing progressively flux to the initial value as shown in Figure 5.30. Variables, including step duration, step height, max flux, system hydraulics parameters (air flowrate and mixer rpm) and temperature were fixed at the arbitrary values shown in Table 5.17. In the modified method the same set values of variables were considered, but 5 min breaks were taken into account between each filtration step (Figure 5.31). This sort of RX was not aimed to obtain a filtration configuration closer to real plant operation, as introduced by De la Torre et al. (2008). In fact, brakes in real RX are about 15÷60 sec every 3÷12 min of filtration (Drews, 2010) in order not to increase too much the membrane surface requirement keeping the real flux (i.e., flux in the active filtration phase of RX) at proper values. Differently, RX in the modified method was set to 5 min, therefore adopting a security factor of 5 (i.e., adopted RX break = 5 $\times$ real RX break), in order to be sure that the cake layer, forming during filtration (reversible fouling), had been removed efficiently during the break so that a new cake formation could have been observed at each new filtration phase.

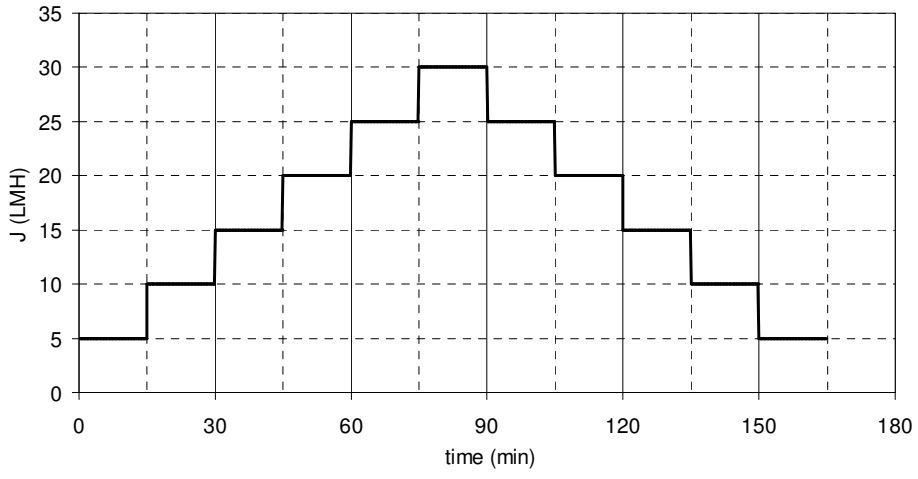

Figure 5.30. Standard method for critical flux determination adopted in this study.

Table 5.17. Parameters of the standard and modified flux step method.

Parameter	Value
step duration	15 min
step height	5 LMH
max flux	30 LMH
mixer rpm	100
air flowrate	6 LPM
temperature	20°C

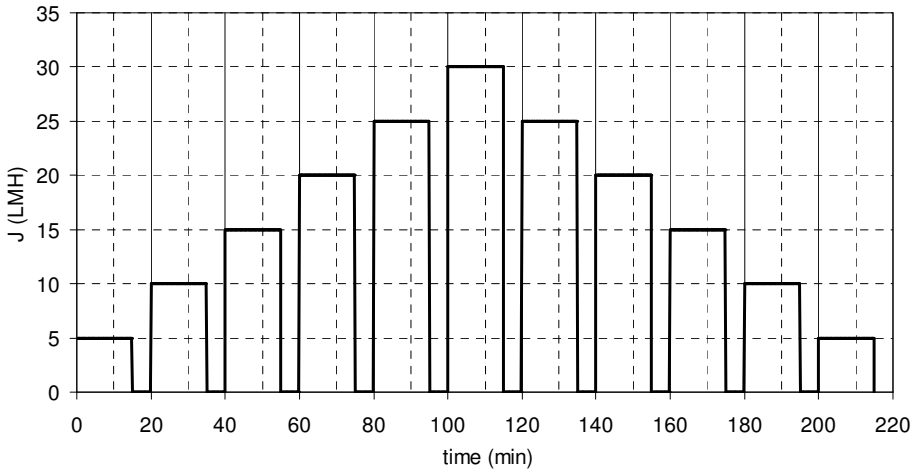

Figure 5.31. Modified method for critical flux determination adopted in this study.

In both of the methods, the batch filtration unit operated recycling the permeate to keep constant the mixed liquor level in the reactor except for the first, the central, and the last 2 minutes of each filtration step. In fact, in these three cheeking periods, flows and fluxes were evaluated using a glass cylinder (50 mL) and a stop watch and eventually adjusted to proper values. This method was effective keeping the coefficient of variation of flux values (LMH) within 10% at each flux step performed.

5.4 Experimental procedures and data processing (topic B)

5.4.1 Evaluation of biodegradability and inherent toxicity of the MWF

Three different screening assays were employed to give a preliminary estimation of the biodegradability and any toxicity inherent in the selected MFW, as follows:

1. biochemical methane potential (BMP) assays;
2. volatile fatty acids (VFAs) production assays;
3. anaerobic toxicity assays (ATAs).

All the assays were conducted at 30°C using the media and serum bottle technique reported by Owen et al. (1979). In order to remove any residual organic carbon, the anaerobic biomass (from a conventional sewage sludge digester in Mogden, UK) was first centrifuged and then re-suspended using the Owen et al. (1979) mineral media, containing nutrients, vitamins, resazurin to detect oxygen contamination (pink when oxidized) and sodium sulfide to provide a reducing environment (Table 5.18).

Table 5.18. Mineral media with a concentration of nitrogen, phosphorus, and alkalinity of: 122 mg L^{-1} as N, 19 mg L^{-1} as P, and 2.500 mg L^{-1} as $CaCO_3$ (Owen et al., 1979).

	Compound	Concentration mg L^{-1}		Compound	Concentration mg L^{-1}
	Resazurin	1.0	N/P salts	$(NH_4)_2HPO_4$	80.1
metal salts	$CaCl_2 \cdot 2H_20$	250.5		NH_4Cl	400.0
	$MgCl_2 \cdot 6H_20$	1800.0	vitamins	Biotin	0.020
	KCl	1300.5		Folic acid	0.020
	$MnCl_2 \cdot 4H_20$	20.0		Pyridoxine hydrochloride	0.100
	$CoCl_2 \cdot 6H_20$	30.0		Riboflavin	0.050
	H_3BO_3	5.7		Thiamin	0.050
	$CuCl_2 \cdot 2H_20$	2.7		Nicotinic acid	0.050
	$Na_2MoO_4 \cdot 2H_20$	2.6		Pantothenic acid	0.050
	$ZnCl_2$	2.1		$B_{1\,2}$	0.001
	$FeCl_2 \cdot 4H_20$	370.0		*p*-aminobenzoic acid	0.050
	$Na_2S \cdot 9H_20$	500.0		Thioctic acid	0.050

Then, the addition of the selected MWF at different concentrations was carried out for all the assays. With regards to VFAs production assays, also the addition of 2-bromoethanesulfonate (BES) at a concentration of 50 mM was taken into account in order to inhibit acetoclastic methanogenesis (Xu et al., 2010), whereas as for ATAs, acetic and formic acids were dosed at a concentration of 2 g COD L^{-1}.

As shown in Table 5.19, BMP assays were performed considering three different series. A first series of BMP assays was carried out at different MWF concentrations, as follows: 0.5%, 1.0%, 2.0%, keeping constant the biomass concentration (2g MLSS L^{-1}) and varying therefore the F/M ratio (2.5, 5.0, 10.0 g MWF g $MLSS^{-1}$). The concentrations considered in the first series were defined adopting a security factor (SF) applied to the minimum value recommended by the manufactured, that is, 4%, as follows:

$$\text{tested concentration} = \frac{\text{recommended concentration}}{\text{SF}} \qquad 5.77)$$

In particular, SF values were 8, 4, 2 for the coolant concentrations of 0.5%, 1.0%, 2.0%, respectively.

Due to the low methane production of the first series, a second series of BMP assays was performed considering a constant MWF concentration of 0.1% (SF=40) varying the biomass concentration (1, 5, 10 g TSS L^{-1}) and therefore the F/M ratio (1.0, 0.2, 0.1 g MWF g $MLSS^{-1}$). The conditions of the second series were defined in order to assess if the biodegradability of the selected MWF was not only dependent on the coolant concentration but also on the ratio between the coolant and biomass concentrations as discussed in results and discussion section.

With regards to ATAs, experiments were employed considering conditions close to the first series of BMB assays, whereas as for VFAs production assays, conditions close to the second series of BMB assays were considered.

All the samples were prepared in duplicate adding an appropriate volume of the mixture (i.e., anaerobic biomass, the MWF, etc.) in reagent bottles with rubber serum caps of appropriate size. In particular, 35 mL of mixture was poured into 60 mL bottles for the first series of BMP assays and ATAs, whereas 80 mL of mixture into 125 mL bottles for second series of BMP and VFA production assays. All serum bottles were flushed with 70% N_2 and 30% CO_2 gas at a flow rate of approximately 0.5 L min^{-1} for 2.5 min. Then, they were equilibrated at 30°C, and zeroed ten minutes after mixture addition. Gas-volume sampling and removal during incubation was performed with glass syringes (10 ml).

Table 5.19. Assays employed for the estimation of the biodegradability and the inherent toxicity in the selected MFW.

Assay		MWF %	TSS g TSS L^{-1}	F/M g MWF $gTSS^{-1}$
BMP assays MWF	**BMP first series** constant TSS and high MWF concentration	0	2	-
		0.5		2.5
		1.0		5.0
		2.0		10.0
	BMP second series constant and low MWF concentration	0	10	-
			5	
			1	
		0.1	10	0.1
			5	0.2
			1	1.0
VFAs production assays MWF + BES (50 mM)		0	5	0.2
		0.1	5	0.2
ATAs MWF **+** acetate acid (2 g COD L^{-1}) MWF **+** formic acid (2 g COD L^{-1})		0	2	-
		0.5		2.5
		1.0		5.0
		2.0		10.0

Cumulative methane production was detected by measuring the composition and the amount of gas produced over time in the serum bottles according the procedure described below (see method B.1). With regards to VFAs production assays, VAFs were monitored over time (see section 5.5) and also the methane production was investigated just for control purposes.

Cumulative methane production evaluation (method B.1). The cumulative methane production measured at the experimental conditions (30°C, 1 atm) was evaluated according the following equation:

$$V_t = V_{t-1} \cdot \left[(\%_t - \%_{t-1}) \cdot Vg + \%_t \cdot Vs_t \right] \qquad 5.78)$$

where V_t and V_{t-1} represents the cumulate methane production at day t and t-1; $\%_t$ and $\%_{t-1}$ represents the percentages of methane in the biogas collected at day t and t-1; Vg is the volume of the gas phase in serum bottles an Vs_t is the volume measured at day t using the glass syringe. In order to compare results of the different assays, data are shown as the

cumulate methane production divided by the liquid volume (in L) present in each serum bottle. Moreover, in the results and discussion section (section 7.2), when the coefficient of variance (COV) was within ±10% the average values are presented since each experiment was performed in duplicate. Differently, in cases of COV major than 10% results of each duplicate are shown.

Finally, in order to estimate the biodegradability of MWF in BMP assays according to the following method (see method B.2), it must be taken into account that the mass of carbon corresponding to 1 mL of CH_4 at experimental conditions (30°C, 1 atm) is 0.48 mg C.

Evaluation of MWF biodegradability (method B.2). The MWF biodegradability expressed as the percentage of organic carbon biodegraded at the conditions of the experiments was evaluated as follows.

Firstly, it was supposed that the biomass growth was negligible and it was considered that the produced methane measured as COD ($\Delta CH_{4,COD}$) was equal to the biodegraded MWF measured as COD (ΔMWF_{COD}), as follows:

$$\Delta CH_{4,COD} = \Delta MWF_{COD} \qquad 5.79)$$

Then, the selected MWF was assumed to be a homogeneous material characterized by a constant molar COD/TOC ratio (r_{MWF}). Therefore, the relation between the biodegraded MWF measured as COD (ΔMWF_{COD}) divided by biodegraded MWF measured as TOC (ΔMWF_{TOC}) follows:

$$\frac{\Delta MWF_{COD}}{\Delta MWF_{TOC}} = r_{MWF} \cdot \frac{32}{12} \qquad 5.80)$$

Thus, the biodegraded MWF measured as TOC (ΔMWF_{TOC}) can be measured by:

$$\Delta MWF_{TOC} = \frac{\Delta CH_{4,COD}}{r_{MWF}} \cdot \frac{12}{32} \qquad 5.81)$$

Finally, considering the relation between the methane production as COD ($\Delta CH_{4,COD}$) and the methane production as TOC ($\Delta CH_{4,TOC}$), equation 5.81, the percentage of organic carbon biodegraded (%MWF_{TOC}) at the conditions of the experiments can be evaluated by equation 5.82.

$$\Delta CH_{4,COD} = \Delta CH_{4,TOC} \cdot r_{CH4} \cdot \frac{32}{12} \qquad 5.82)$$

$$\%MWF_{TOC} = \frac{\Delta CH_{4,TOC} \frac{r_{CH4}}{r_{MWF}}}{\text{initial}\, MWF_{TOC}} \cdot 100 \qquad 5.83)$$

where r_{CH4} represents the methane COD/TOC molar ratio (i.e., 2) and initial MWF_{TOC} the initial amount of MWF measured as TOC.

5.4.2 SAMBR operation and monitoring

SAMBR operational information are provided in the results and discussion section as the start-up strategy was planned on the basis of the preliminary assays outcomes, performed as described above. With regards SAMBR monitoring, some information about methane production and TMP measurement follows; whereas with regards the estimation method of the MWF biodegradability see method B.2.

Evaluation of methane production (method B.3). The cumulative methane production was evaluated as the equivalent methane mass of organic carbon (g C) in the biogas collecting system (headspace 1 in Figure 5.7) and in the headspace of the reactor (headspace 2 in Figure 5.7) using the following equation:

$$CH_{4,TOC} = (n_1 + n_2) \cdot MW_{TOC} \qquad 5.84)$$

where n_1 and n_2 represent the moles of methane in the headspaces 1 and 2; MW_{TOC} is the molecular weight of carbon (12 g C mol^{-1}).
Moles in the generic headspace i (n_i) were evaluated according the ideal gas law:

$$n_i = \frac{\%_i}{100} \cdot \frac{p_i \cdot V_i}{R \cdot T_i} \qquad 5.85)$$

where $\%_i$ is the percentage of methane, p_i is the total absolute pressure (atm), V_i the volume (L), T_i the temperature (K) of the generic headspace i; R is the ideal gas constant (0.082 L atm K^{-1} mol^{-1}).
The parameters $\%_1$, V_1; T_1, $\%_2$, T_2 were directly measured. In particular, the percentages of methane ($\%_1$ and $\%_2$) was measured according to section 5.5, temperature values (T_1 and T_2) using a thermometer, and V_1 was measured through the upside-down graduated cylinder as shown in Figure 5.7.

With regards to the other parameters (p_1, p_2, V_2), they were evaluated using the following relations:

$$p_1 = p_{atm} - ha \qquad 5.86)$$

$$p_2 = p_{atm} + hb \qquad 5.87)$$

$$V_2 = const \cdot hc \qquad 5.88)$$

where p_{atm} is the atmospheric pressure (assumed to be 1.002 atm), h_a is the gap between the water level in the cylinder and the water level in the beaker (see section 5.2.2, Figure 5.7), h_b is the gap between the water level in the beaker and the terminal point of the pipe, connecting the collecting system and the reactor (see section 5.2.2, Figure 5.7), whereas h_c represents the gap between the water level and the top of the reactor (see section 5.2.2, Figure 5.7) and *const* is a number, which value is 0.069 L cm^{-1}. With regards to h_a and h_b, they were measured in cm an then converted into atm (0.097 atm/m), whereas h_c in cm.
With regards to h_b, the reactor sometimes has been in vacuum conditions. Therefore, a water/gas interface appeared inside the pipe connecting reactors to the collecting system. In such a situation, h_b represented the gap between the water level in the beaker and the water/gas interface in the pipe, and it was assumed to be a negative value.

Evaluation of TMP (method B.4). Differently from topic A, for the TMP measurement, the overpressure condition of the anaerobic bioreactor must be taken into account, as follows:

$$TMP = (p_{atm} + \Delta p) - p - H \qquad 5.89)$$

where p_{atm} is the atmospheric pressure (bar), Δp is the overpressure in the headspace of the reactor (bar), p is the absolute pressure measured in the suction line of the process pump (bar) and H is the distance between the water level in the reactor and the point of measurement in the vacuum line (Figure 5.32) expressed in bar (0.0978 bar/m).
Since only one pressure gauge was available, the atmospheric pressure was assumed to be 1.015 bar. With regards to the term Δp, it was measured daily with the equipment described in the methane production paragraph (see above, method B.3); in particular Δp corresponded to h_b measured in bar (0.0978 bar/m).

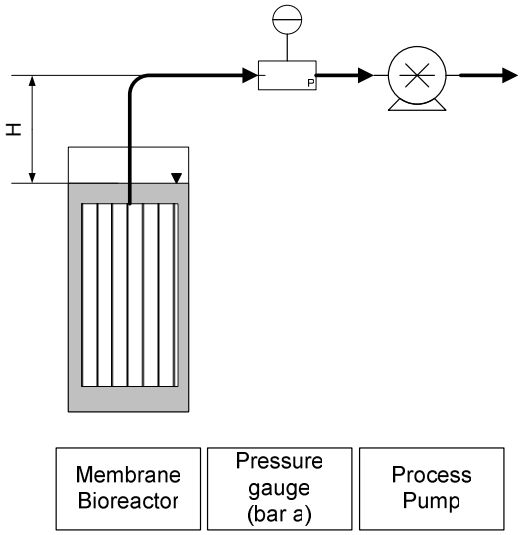

Figure 5.32. Evaluation of the transmembrane pressure (TMP).

5.5 Analytical techniques

Analytical techniques adopted in the present study (topic A and topic B) are listed in Table 5.20.

Table 5.20 Analytical techniques: methods and relevant information.

Parameter and topic		Method	Reference
biogas composition	B	biogas composition determined using a Shimadzu GC-TCD fitted with a Porapak N column (1,500 × 6.35 mm)	-
carbohydrates	A	carbohydrates content determined adopting the Dubois et al. (1956) method. D-glucose monohydrate was used as a glucose standard for method calibration	EC (2007)
COD	A	COD determined using the closed reflux titrimetric method	APHA (2005)
COD	B	COD determined using the standard closed reflux colorimetric method	APHA (2005)
colour	A	parameter analyzed as absorbance at 426 nm, 558 nm, 660 nm using a Dr. Lange spectrophotometer (model Xion 500)	AbwV (2002)
divalent cations (Ca^{2+}, Mg^{2+})	A	divalent cations detected by flame atomic absorption spectroscopy (Varian AA55); the acid digestion method 3010A, EPA was firstly executed for sludge samples	APHA (2005)
nitrogen: N-NH_4^+	A	Nitrogen compounds were measured according to Italian official methodologies (IRSA, 1994), which are quite similar to those described in Standard Methods (APHA, 2005)	IRSA (1994)
nitrogen: N-NO_2^-	A		
nitrogen: N-NO_3^-	A		
nitrogen: TKN	A	TKN determined according to the kjeldahl methods	APHA (2005)
particle size distribution	B	particle size measurements made using a Malvern Instruments (Malvern, UK, Model No. 2600C) with a helium neon laser.	-
phosphorus (total)	A	total phosphorus determined using a commercial kit (Dr. Lange LCK349)	Manufacturer's manual
proteins	A	proteins determined using the Lowry et al. (1951) method adopting a commercial kit (Sigma-Aldrich, TP0300); BSA was used as a glucose standard for method calibration	Manufacturer's manual
surfactants (anionic)	A	anionic surfactants determined using a commercial kit (Dr. Lange LCK332)	Manufacturer's manual
surfactants (non-ionic)	A	non-ionic surfactants determined using a commercial kit (Dr. Lange LCK333)	Manufacturer's manual
suspended solids (TSS, VSS, MLSS, MLVSS)	A,B	suspended solids detected according to standard methods for the examination of water and wastewater	APHA (2005)
TOC	A,B	TOC analyzed with a Shimadzu 5050 (Shimadzu, UK)	-
VFAs	B	VFAs detected on a Perkin-Elmer Series 4 high pressure liquid chromatograph with a Biorad-Aminex column, and the carrier solvent was 0.01 M H2SO4 at a flow rate of 0.7 mL min^{-1} at 60° C.	-

6 Treatment of textile wastewaters and fouling control in an anoxic-aerobic MBR

6.1 Introduction

In this chapter results related to topic A of the thesis (treatment of textile wastewaters and fouling control in an anoxic-aerobic MBR) are presented and discussed, as follows:

- wastewater characterization and operating of the pilot MBR (see section 6.2);
- selection of the best flux enhancer (see section 6.3);
- effluent quality monitoring and enhancement by the selected flux enhancer (see section 6.4);
- sludge characteristics and effects of to the selected flux enhancer (see section 6.5);
- fouling monitoring and control by the selected flux enhancer (see section 6.6);
- fouling propensity assessment using a modified flux step method for the critical flux determination (see section 6.7).

Finally, to sum up and correlate results, all the effects of the selected flux enhancer are summarized in section 6.8.

6.2 Wastewater characterization and operating of the pilot MBR

In this section, information about the wastewater characteristics and the pilot operating (stage 1 and 2) is provided, as follows:

- characterization of the mixed domestic-textile wastewater over the experimental period (see section 6.2.1);
- operating of the MBR showing the most relevant operational parameters (see section 6.2.2);

With regards experimental staging, stage 1 lasted from day 0 to day 224 (duration of 224 days, corresponding approximately to 9 SRT) and stage 2 from day 237 to day 310 (duration of 73 days, corresponding approximately to 3 SRT). The period between day 225 and day 236 was a transition period, when the third main membrane cleaning was carried out.

6.2.1 Characteristics of the mixed domestic-textile wastewater

Mixed domestic-textile wastewater characteristics are discussed herein, particularly taking into account the ordinary macro-parameters for wastewater characterization, such as COD, TSS and nutrients, and textile macro-parameters, such as colour and non-ionic surfactants

and anionic surfactants. With regards to parameters such as TOC, divalent cations, proteins and carbohydrates and other elaborated parameters (TOC apportionment and mean oxidation state of organic carbon), they are discussed in section 6.4 comparing them for the influent, the effluent, the bulk liquid and the extracted solution to investigate any possible correlation between these different media.

Figure 6.1 and Figure 6.2 show the evolution over time of COD, TSS and total nitrogen (N_{tot}), whereas in Table 6.1 and Table 6.2 statistic parameters evaluated for stage 1, stage 2 and for the entire experimental period are listed. As for COD, a high variability was observed within a wide range of values (80÷468 mg L^{-1}) with a mean value of 285±83.5 mg L^{-1} in stage 1, and a value of 164±61.5 mg L^{-1} in stage 2. Such different values were taken into account when evaluating the effect of the selected flux enhancer on effluent quality.

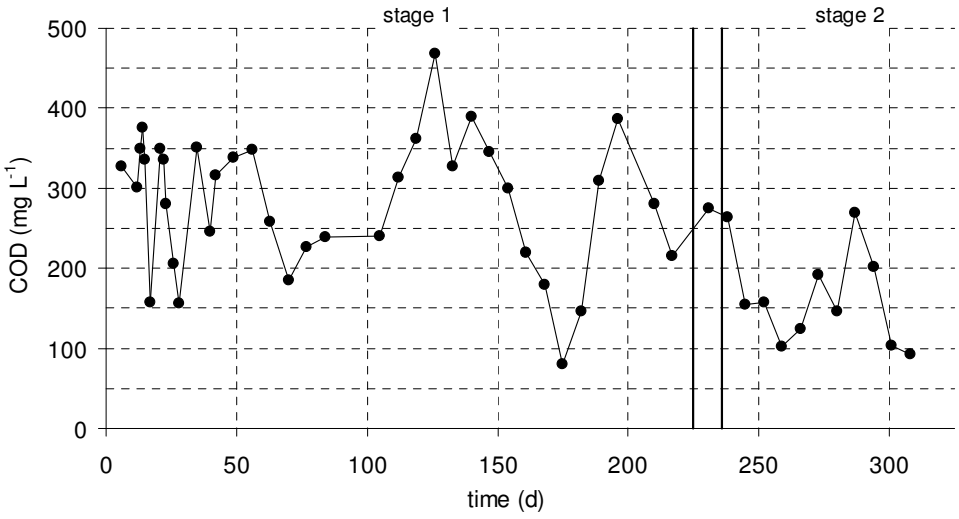

Figure 6.1. Wastewater COD evaluation over time.

In stage 1, two particular periods can be highlighted. The first period (approximately from day 50 to day 100) corresponded with the spring season (end of April, May and June), during which intensive rain episodes occurred, resulting in a dilution effect of the wastewater. Differently, the second period (approximately from day 150 to day 190) corresponded with summer holydays (August) during which both domestic and textile organic loading diminished. In fact, in this period the minimum COD value was observed (80 mg L^{-1}). With regards to stage 2, both raining episodes and winter holydays (from day 297 to day 304) affected COD data. In order to characterize the wastewater COD, soluble COD (detected after 0.45 μm paper filtration) and BOD (BOD_5 and BOD_{30}) were evaluated. In particular, soluble COD was detected weekly, whereas BOD was measured just twice taking two samples during stage 2 (day 211 and day 266). Results showed that the soluble COD accounted for 82±11.6% of the total COD, whereas BOD_5 and BOD_{30} accounted for

40±0.3% and 51±3.0% of the total COD, respectively. By comparison, typical values for domestic wastewaters are 50÷50% and 75÷82.5% for BOD_5/COD and BOD_{30}/COD, respectively (Metcalf and Eddy, 2003), therefore indicating a low degradable nature of organics in the treated wastewater. Consequently, for this reason and since the average influent COD was lower than the value considered in the pilot plant design (257 mg L^{-1} vs 400 mg L^{-1}), the addition of sodium acetate was taken into account from day 53 onwards as external readily biodegradable COD source to support microbial growth. More details about acetate addition are presented in section 6.2.2.

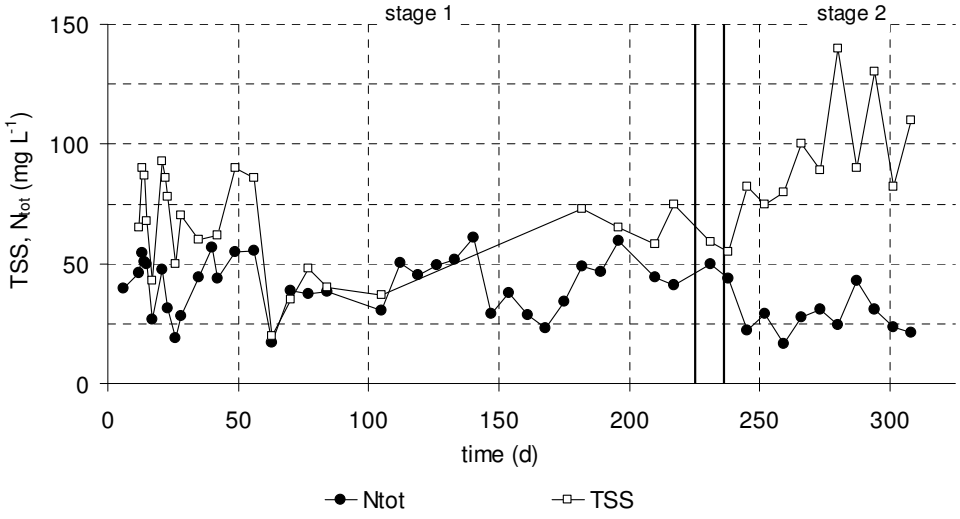

Figure 6.2. Wastewater TSS and total nitrogen (N_{tot}) evaluation over time.

With regards to total nitrogen, mean values of 42±11.6 mg L^{-1} and 28±8.6 mg L^{-1} were observed for stage 1 and stage 2, respectively. Moreover, the same consideration related to dilution effects due to raining periods and holydays can be done, particularly considering stage 2. Differently, as for TSS, values detected during stage 2 were higher than values of stage 1, with a mean of 94±24.7 mg L^{-1} and of 64±20.4 mg L^{-1}, respectively.

Table 6.1. Statistic parameters for wastewater COD and soluble COD related to stage 1 (s1), stage 2 (s2) and overall to the experimental period (o).

	COD (mg L^{-1})			**soluble COD** (mg L^{-1})		
	s1	s2	o	s1	s2	o
N	36	11	48	25	11	37
mean	285	164	257	222	136	196
st. dev.	83.5	61.5	92.7	68.7	55.0	74.5
COV	29.3%	37.4%	36.1%	30.9%	40.3%	38.0%
min	80	93	80	56	69	56
max	468	269	468	347	257	347

Table 6.2. Statistic parameters for wastewater TSS and total nitrogen related to stage 1 (s1), stage 2 (s2) and overall to the experimental period (o).

	TSS (mg L^{-1})			**N_{tot}** (mg L^{-1})		
	s1	s2	o	s1	s2	o
N	23	11	35	0	0	544
mean	64	94	73	42	28	39
st. dev.	20.4	24.7	25.4	11.6	8.6	12.3
COV	31.8%	26.3%	34.6%	27.7%	30.1%	31.6%
min	20	55	20	17	17	17
max	93	140	140	61	44	61

Table 6.3 and Figure 6.3 show the apportionment of total nitrogen in organic nitrogen (calculated as the difference between TKN and ammonia), ammonia, nitrate and nitrite. In particular, organic nitrogen and ammonia accounted for 32.3±11.66% and 65.7±11.86%, respectively, without any substantial distinction between stage 1 and stage 2. Differently, nitrate and nitrite accounted for less than 1.5%. Therefore, it can be assumed that, overall, the parameter TKN (organic nitrogen and ammonia) can represent the total nitrogen content in the wastewater. Soluble TKN (after 0.45 μm paper filtration) accounted for 65.7±11.86% of the total TKN, without any substantial distinction between stage 1 and stage 2.

Phosphorus was detected in 7 samples (2 samples at the end of stage1 and 5 samples for stage 2). Resulted showed a mean value of 3.2±0.64 mg L^{-1} and 1.2±0.52 mg L^{-1} for stage 1 and stage 2, respectively.

Overall, the nutrients content of the wastewater compared to pure domestic effluents resulted in a poor phosphorus content and a rich nitrogen content. In fact, average P/COD and N/COD ratios were about 0.008 mg P mg COD^{-1} and 0.160 mg N mg COD^{-1} for the mixed wastewater. By comparison, values related to domestic wastewaters are approximately of 0.015 mg P mgCOD^{-1} and 0.100 mg N mg COD^{-1} (Metcalf and Eddy, 2003).

Table 6.3. Statistic parameters for wastewater nitrogen apportionment in organic nitrogen, ammonia related to stage 1 (s1), stage 2 (s2) and overall to the experimental period (o).

	N_{org} (mg L^{-1})			**$N\text{-}NH_4^+$ (mg L^{-1})**		
	s1	s2	o	s1	s2	o
mean	32.1%	31.8%	32.3%	65.9%	66.0%	65.7%
st. dev.	12.23%	10.47%	11.66%	12.58%	10.45%	11.86%
COV	38.1%	33.0%	36.0%	19.1%	15.8%	18.1%
min	4.8%	16.2%	4.8%	40.3%	43.3%	40.3%
max	57.6%	54.8%	57.6%	95.1%	82.9%	95.1%

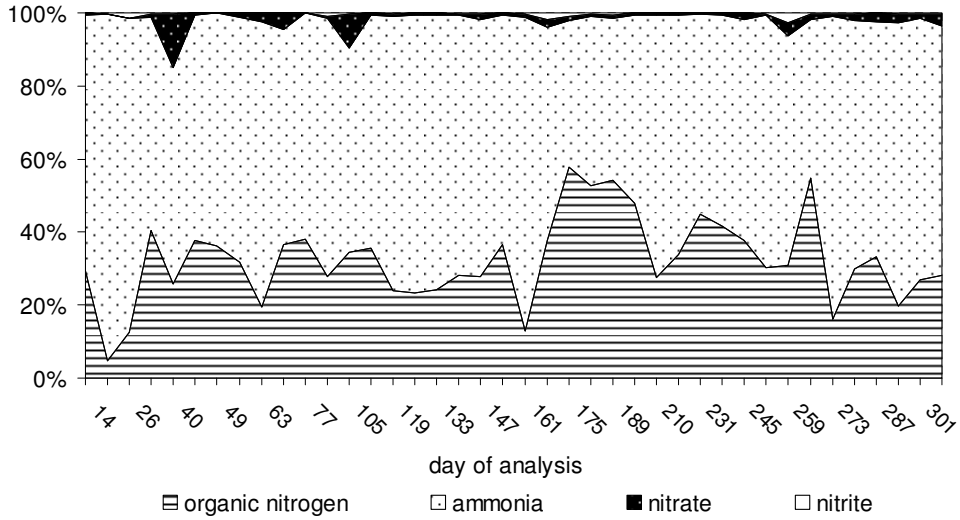

Figure 6.3. Wastewater nitrogen apportionment.

With regards to textile macro-parameters, statistics related to colour measured as absorbance at 426, 558 and 660 nm are summarized in Table 6.4. Moreover, Figure 6.4 shows the evolution over time of the absorbance at 426 nm that is considered to be the most consistent length since it showed the highest values of absorbance in the effluent and, also, according to previous experiences on the same wastewater (e.g., Malpei et al., 2003) the absorbance at 426 nm showed the lower removal efficiency. Absorbance was characterized by a high variability in a wide range of values (0.053÷0.426 cm^{-1}) with higher values (≥ 0.250 cm^{-1}) in the first days of stage 1 and between day 100 and day 150. Differently, lower values were observed during the spring raining period (day 50÷day 100) and summer holydays (day 150÷day 190) as observed for COD. Also in stage 2 absorbance values were low.

Table 6.4. Statistic parameters for wastewater colour related to stage 1 (s1), stage 2 (s2) and overall to the experimental period (o).

	abs. × 1,000 at 426 nm (cm^{-1})			**abs. × 1,000 at 558 nm (cm^{-1})**			**abs. × 1,000 at 660 nm (cm^{-1})**		
	s1	s2	o	s1	s2	o	s1	s2	o
N	27	16	44	27	16	44	27	16	44
mean	204	161	189	139	111	129	87	72	82
st. dev.	116.8	45.0	97.0	87.7	32.1	72.1	55.2	20.9	45.3
COV	57.2%	28.0%	51.5%	63.1%	28.9%	55.8%	63.5%	28.9%	55.3%
min	53	90	53	7	60	7	18	35	18
max	426	218	426	335	147	335	206	94	206

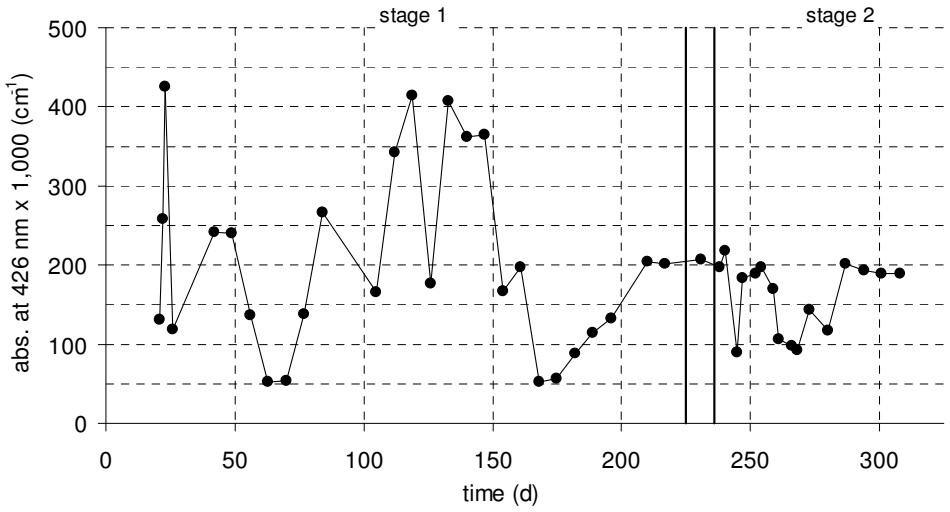

Figure 6.4. Wastewater colour (absorbance at 426 nm) evaluation over time.

Finally, surfactants concentration are presented in Table 6.5. In particular, the mean concentrations of anionic surfactants were about 3.6±0.97 mg L^{-1} and 2.4±1.04 mg L^{-1} for stage 1 and stage 2, respectively. Differently, mean values of non-ionic surfactants were 7.4±2.47 mg L^{-1} and 4.0±1.63 mg L^{-1} for stage 1 and stage 2, respectively.

Table 6.5. Statistic parameters for wastewater surfactants related to stage 1 (s1), stage 2 (s2) and overall to the experimental period (o).

	anionic surfactants (mg L^{-1})			**non-ionic surfactants (mg L^{-1})**		
	s1	s2	o	s1	s2	o
N	5	11	17	5	11	17
mean	3.6	2.4	2.8	7.4	4.0	5.1
st. dev.	0.97	1.04	1.09	2.47	1.63	2.37
COV	27.2%	43.0%	39.4%	33.6%	40.4%	46.4%
min	1.9	0.9	0.9	4.5	2.0	2.0
max	4.5	3.8	4.5	11.2	8.0	11.2

6.2.2 Monitoring of operational parameters

In this section, the evolution over time of main biological parameters is discussed. Differently, with regards to operational filtration parameters were fixed at constant values, as follows: permeate flux (J): 10 LMH; air flowrate: 400 L_N h^{-1}; relaxation: 8:1 minutes (see section 5.2.1) and therefore they did not vary over time. On the other hand, since constant flux filtration was executed, TMP varied over time, particularly between 0.018 and 0.191 bar,

because of a rise occurred in fouling resistances. Therefore, observed TMP values are discussed properly in section concerning fouling monitoring and control (see section 6.6).

At the beginning of stage 1, the pilot MBR was inoculated using biomass collected from the full scale WWTP (from the sludge recycle) because of the textile fibres presence in mixed liquor at the end of the MBR start-up phase. The initial MLSS concentrations were approximately 5.5, 4.0, 7.0 g L^{-1} in aerobic, anoxic and membrane tanks, respectively and the initial food to microorganisms ratio (F/M) was 0.1 kg COD kg SS^{-1} d^{-1}. All the operating parameters were then fixed at the values previously summarized in Table 5.4 (see section 5.2.1).

With regards to these parameters, they were imposed directly (apart from DO concentrations) and checking procedures were executed weekly to be sure such values were kept constant over time. Table 6.6 shows main parameters characterizing the operation of biological reactors and therefore they were taken into account for the biological monitoring of the MBR. As shown in Table 6.6, they can be divided in two classes, i.e., "controlled parameters" (c) and "monitored parameters" (m), however, variable within a certain range compatible with biological processes.

Table 6.6. Main biological parameters and their classification as "controlled parameters" (c) and "monitored parameters" (m).

Parameter	type	information
food to microorganisms ratio (F/M)	m	
sludge retention time (SRT)	c	SRT is controlled by sludge wastage.
biomass in reactors (as total mass)	m	biomass quantity evolves depending on F/M, SRT, kinetics and temperature.
biomass concentration in tanks	m	
temperature of mixed liquor	m	temperature is affected by atmospheric temperature as a low temperature implies a rise in heat dispersion.
OD in aerobic tank	c	OD was controlled by aeration.
pH in aerobic and anoxic tank	m	in general, pH is related to nitrification and denitrification stoichiometry, whereas redox potential in anoxic tank depends on nitrate and DO concentrations.
redox potential in anoxic tank	m	

Figure 6.5 shows the evolution of F/M along time. As it can be seen from the chart, at day 53, a dosage of a high concentrated solution of sodium acetate (daily loading as COD of 45 g d^{-1}) was introduced and carried out till the end of the study, with the aim of:

1. increase the F/M ratio to support bacterial growth and keep biomass concentration at proper values comparable with real scale applications as previously stated;
2. supply readily biodegradable COD to support denitrification (see section 6.4.2).

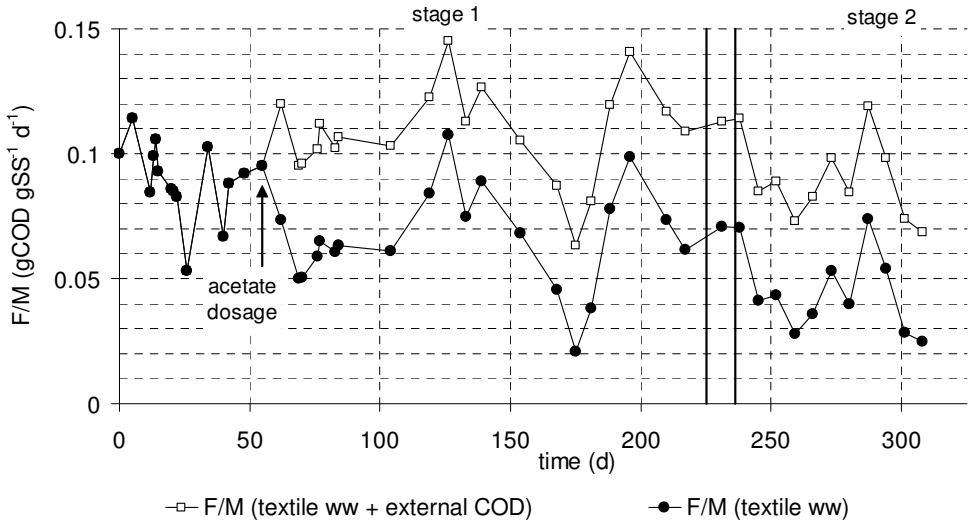

Figure 6.5. F/M evolution over time.

In particular, considering the F/M ratio related only to the mixed domestic-textile COD (named "textile ww" in Figure 6.5), it varied between 0.02 and 0.11 g COD g SS^{-1} d^{-1} with an average value of 0.07±0.02 g COD g SS^{-1} d^{-1}. Differently, considering also the contribute of acetate, the average F/M was approximately of 0.10±0.02 g COD g SS^{-1} d^{-1}. Consequently, the dosage of sodium acetate increased the food to microorganisms ratio to reach an average value equal to that considered in the MBR design, but, on the other hand, it accounted for the 44±10% of the total COD entering the reactor (Figure 6.6). However, since acetate was supplied using a high concentrate solution, the influence of the acetate flowrate was negligible compared to that of mixed domestic-textile effluent (<10%). Therefore, neither dilution effects on the other pollutants nor significant variation of membrane flux occurred. On the other hand, acetate addition could have affected sludge characteristics and fouling occurrence probably modifying bacteria metabolism, the bacterial community composition, the formation/elimination of soluble-EPS and flocs stability (McAdam et al., 2007).

It can be seen from the chart (Figure 6.5) that the F/M ratio was characterized by a certain variability, due to the variation of wastewater COD concentration. However, such changes in F/M did not affect to large extent the biomass (Figure 6.7,

Table 6.7) in tanks. The reason was related to the MBR operation at high SRT values implying a slow dynamic of MBR biological characteristics, such as biomass concentration, and because the MBR pilot was in pseudo-stationary conditions. In particular the average MLSS total mass in bioreactors was approximately of 813±70.9 g SS and the ratio of volatile suspended solids was 80±1.9%.

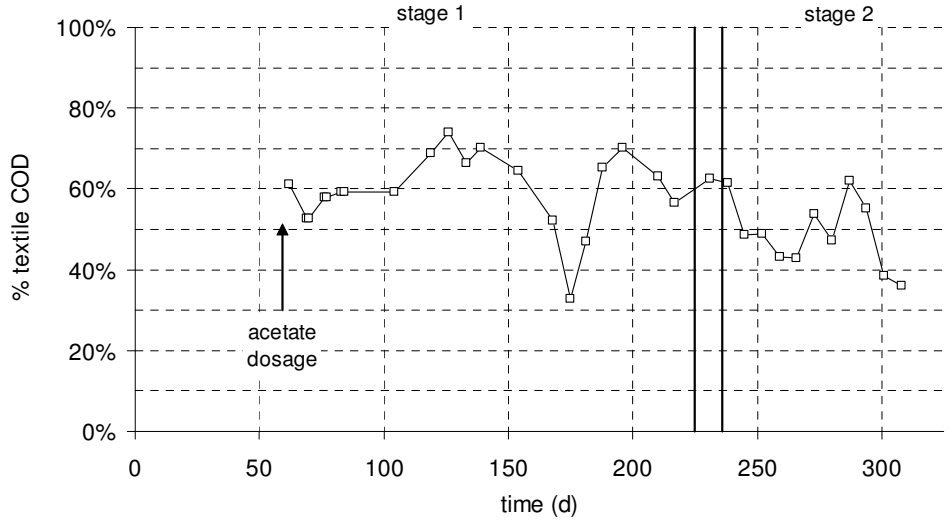

Figure 6.6. Percentage of COD daily load due to mixed domestic-textile wastewater .

In the first 120 days, the sludge wastage, executed just for sludge sampling to monitor mixed liquor characteristics, was approximately of 7 L a week (SRT~170 days). Then, from day 120, proper volumes of aerobic excess sludge were collected daily (using valve V1, see Figure 5.2) and wasted in order to maintain constant the sludge retention time (SRT) at a value of 25±2 days.

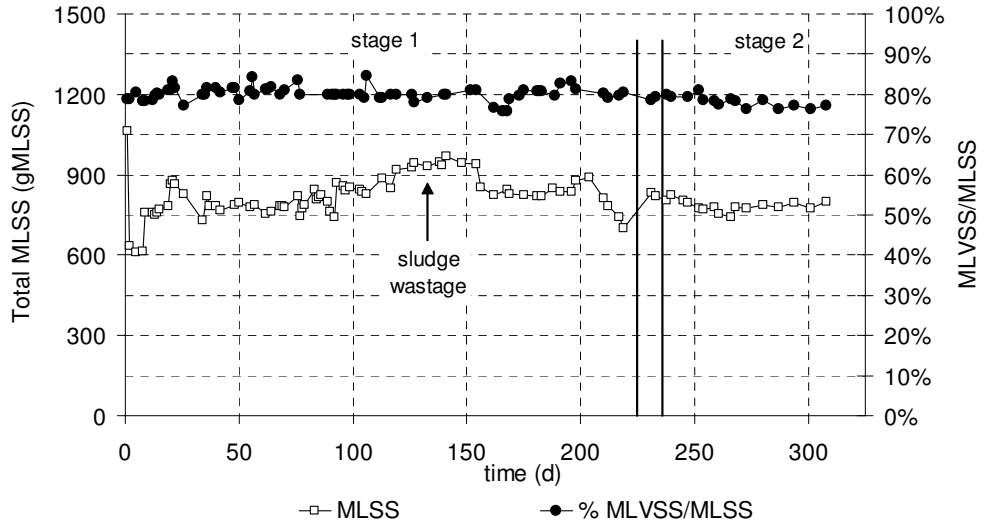

Figure 6.7. MLSS as the total mass present in bioreactors and MLVSS/MLSS ratio evolution over time.

Table 6.7. Statistic parameters for F/M, MLSS as the total mass present in bioreactors related to stage 1 (s1), stage 2 (s2) and overall the experimental period (o).

	F/M (gCOD gSS^{-1} d^{-1})			**MLSS** (gSS)		
	s1	s2	o	s1	s2	o
mean	0.10	0.09	0.10	820	783	813
st. dev.	0.020	0.016	0.019	77.2	20.2	70.9
COV	19.6%	18.2%	19.6%	9.4%	2.6%	8.7%
min	0.05	0.07	0.05	612	743	612
max	0.15	0.12	0.15	1062	826	1062

Data of MLSS concentrations in tanks are shown in Table 6.8 and Figure 6.8. Overall, MLSS concentration were 5.9±0.51, 4.4±0.67 and 7.6±0.64 g SS L^{-1} for aerobic, anoxic and membrane tanks, respectively. It can be seen from the chart that a slight increasing trend was observed after introduction of the acetate dosage reaching a peak around day 120. Then, after the introduction of sludge wastage a slight decreasing trend was observed, particularly for aerobic and anoxic tanks. Differently, in stage 2 the MLSS concentration of three tanks were almost constant as it can be seen from COV data in Table 6.8. Also, this fact justifies assumptions at the basis of equation 5.65, modelling the evolution over time of flux enhancer dose.

The MLSS dynamics in stage 1 was also affected by seasonal variation in temperature values, that showed a similar evolution over time, as discussed below.

The ratio between the average MLSS concentration in anoxic/membrane tanks and the aerobic MLSS concentration were 0.745 and 1.288, respectively for the anoxic and membrane tanks, presenting therefore very close results to the values obtained from theoretical equations 5.60 and 5.61 (0.750 and 1.250). This justifies the assumption made at the basis of equations 5.60 and 5.61. However, the slight difference between theoretical and experimental ratios observed for membrane tank could be related to the not optimal mixing of sludge as resulted from tracer studies (see section 5.3.1, method A.2), indicating the presence of a dead volume in the tank.

Table 6.8. Statistic parameters for MLSS concentrations in tanks related to stage 1 (s1), stage 2 (s2) and overall to the experimental period (o).

	MLSS in aerobic tank (gSS L^{-1})			**MLSS in anoxic tank** (gSS L^{-1})			**MLSS in membrane tank** (gSS L^{-1})		
	s1	s2	o	s1	s2	o	s1	s2	o
mean	6.0	5.5	5.9	4.5	3.9	4.4	7.5	7.9	7.6
st. dev.	0.52	0.16	0.51	0.70	0.25	0.67	0.69	0.16	0.64
COV	8.8%	3.0%	8.6%	15.6%	6.5%	15.3%	9.3%	2.0%	8.5%
min	4.4	5.2	4.4	3.1	3.5	3.1	5.5	7.6	5.5
max	7.7	5.8	7.7	5.8	4.5	5.8	9.8	8.2	9.8

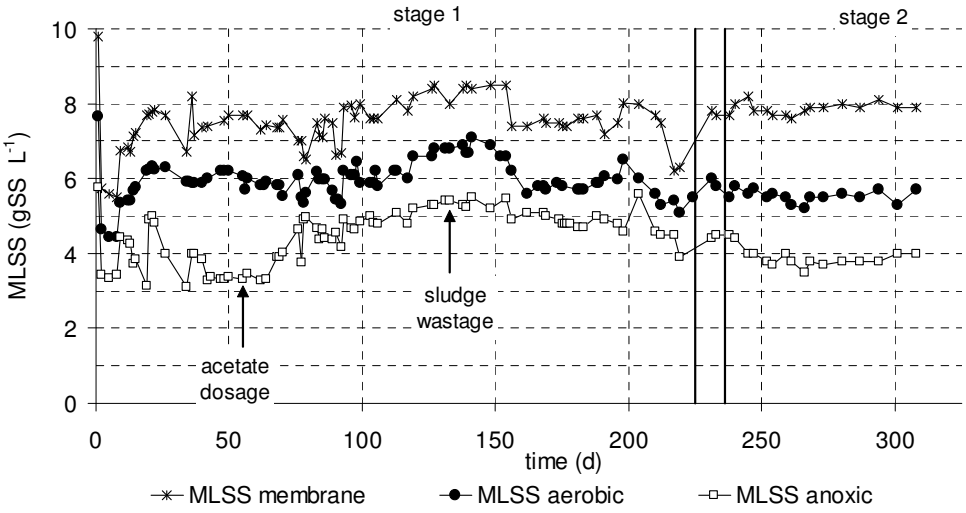

Figure 6.8. MLSS concentration in tanks.

Figure 6.9 shows the evaluation of growth and apparent yield of the MLSS (Y_{obs}) in the MBR, that was calculated on the basis of the cumulative curves of biomass increase (sum of daily increase/decrease of the MLSS plus the sludge wasted during the whole experimental period) and COD removal. Results showed a value of 0.11 and 0.31 g SS g COD^{-1} for stage 1 (R^2=0.975) and stage 2 (R^2=0.998), respectively. This discrepancy was probably due to the increase in TSS content observed for the influent wastewater in stage 2 (see section 6.2.1). By comparison, Malpei et al. (2003) found a value of 0.29 gSS $gCOD^{-1}$ for a textile effluent from a factory which manufactured and finished polyester fabric.

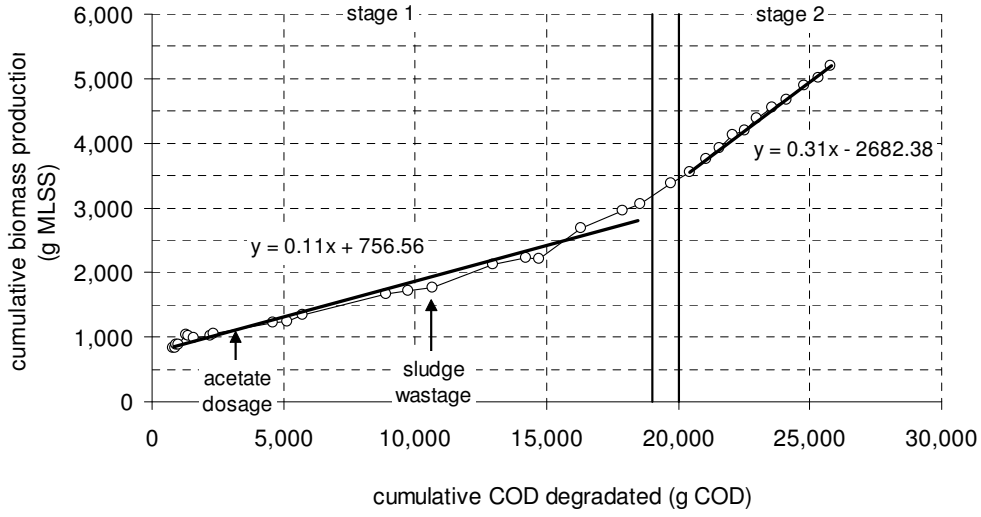

Figure 6.9. Evaluation of growth and apparent yield of the MLSS (Y_{obs}).

With regards to parameters such as temperature, pH, DO, redox potential measured in mixed liquor, results are shown in Figure 6.10, Figure 6.11, Table 6.9 and Table 6.10. With regards to aerobic tank, temperature, pH and DO were measured, whereas in anoxic tank pH and redox potential were monitored.

As for temperature, other measurements were carried out twice a day for the other tanks (anoxic and membrane) using a mercury-in-glass thermometer. Results showed deviation from the temperature in the aerobic tank within 0.5°C. Consequently it was assumed that temperature in aerobic tank was representative for all the pilot MBR.

Temperature varied noticeably during the experimental period. At the beginning of stage 1 (spring season) values of 12÷13°C were observed and then increased slightly in 120 days reaching a value of 29.9°C. Then, temperature declined and reached values of 12÷13°C at the end of stage 1. In stage 2, temperature fluctuated around 12.7°C since a heater was installed on the pilot to prevent a temperature fall due to the winter season.

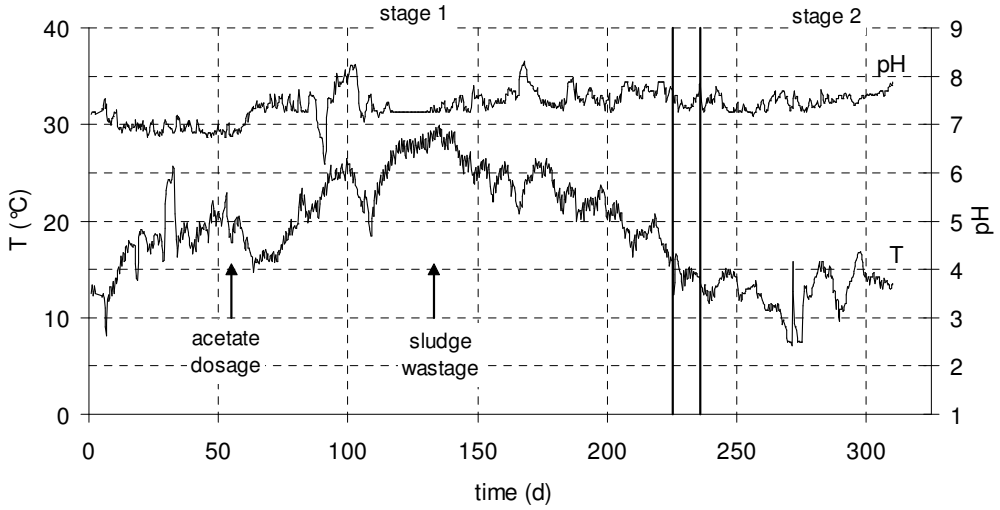

Figure 6.10. Average values over 6 h of pH and temperature (T) in aerobic tank.

With regards to pH, it increased slightly for both aerobic and anoxic tanks after the addition of acetate, because denitrification was fully developed. Overall, before the addition, it was <7 for aerobic tank and <7.5 for the anoxic tank, respectively; whereas, after the addition, pH values fluctuated around 7.4 and 7.8 for aerobic and anoxic tanks. This fact can be explained taking into account that in the nitrification process 7.14 g alkalinity (as $CaCO_3$) are consumed per g of N-NH_4^+ oxidized. Therefore, at the beginning of stage 1, the alkalinity of the wastewater did not balance properly this acidification effect resulting in a slight acid pH in the aerobic tank (<7). Then, as stated above, the addition of sodium acetate permitted full denitrification and therefore balancing H^+, since in the heterotrophic denitrification

process 3.57 g alkalinity (as $CaCO_3$) are produced per g of $N\text{-}NO_3^-$ reduced. This resulted in a optimization of pH values within the optimal range for nitrification and denitrification.

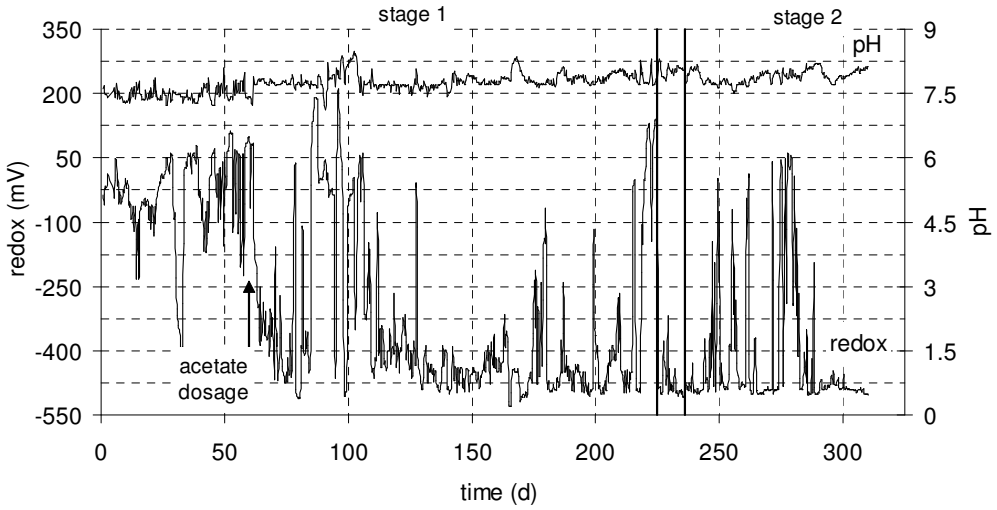

Figure 6.11. Average values over 6 h of pH and redox potential in anoxic tank.

Table 6.9. Statistic parameters for DO, pH and temperature (means over 6 h) in aerobic tank related to stage 1 (s1), stage 2 (s2) and overall the experimental period (o).

	pH			**OD (mg L-1)**			**T (°C)**		
	s1	s2	o	s1	s2	o	s1	s2	o
mean	7.4	7.5	7.4	2.4	1.4	2.2	21.5	12.7	19.1
st. dev.	0.34	0.15	0.31	2.32	1.16	2.12	4.15	2.09	5.30
COV	4.7%	2.0%	4.2%	95.2%	82.7%	97.5%	19.3%	16.4%	27.7%
min	6.2	7.2	6.2	0.0	0.2	0.0	8.2	7.1	7.1
max	8.3	7.9	*8.3*	10.9	5.7	10.9	29.9	16.9	29.9

Finally, considering redox potential, the acetate dosage resulted in a fall of redox values indicating a decrease in DO and nitrate in the anoxic mixed liquor, since redox is dependent on these parameters. In particular DO could be present in the anoxic tank because of mixed liquor recycle from the aerobic tank, where on average, DO concentration was 2.2 mg L^{-1}. The acetate dosage (external COD) implied the consumption of oxygen (through aerobic COD degradation) and nitrates (through anoxic COD degradation) as discussed in section 6.4. As a result redox fell down even if occasional rises were observed.

Table 6.10. Statistic parameters for pH and redox potential (means over 6 h) in anoxic tank, related to stage 1 (s1), stage 2 (s2) and overall the experimental period (o).

	pH			redox (mV)		
	s1	s2	o	s1	s2	o
mean	7.7	7.9	7.8	-264.4	-414.0	-308.0
st. dev.	0.23	0.15	0.22	215.34	151.43	210.29
COV	2.9%	1.9%	2.9%	-81.4%	-36.6%	-68.3%
min	7.1	7.5	7.1	-530.0	-504.2	-530.0
max	8.5	8.2	*8.5*	210.0	60.0	210.0

6.3 Selection of the best flux enhancer

6.3.1 Selection of the best flux enhancer

In this section results of the jar test campaign, carried out in order to select and identify the best flux enhancer, are discussed. In particular, as stated in material and methods sections (see section 4.2.1 and section 5.3.3), four doses of three different chemicals were investigated, as follows:

- NORIT CA1, a powdered activated carbon: 12.5 - 25 - 50 - 100 mg g $MLSS^{-1}$;
- TILLMANS TILLPAC18, a polyaluminium chloride: 6.25 – 12.5 - 25 - 50 mg g $MLSS^{-1}$;
- DALTON FLODAL, a cationic polymer: 6.25 – 12.5 - 25 - 50 mg g $MLSS^{-1}$;

The range of the doses to test was identified for each chemical according to a double criteria, taking into account both their costs and known adverse effects (see section 5.3.3). Moreover, each dose was investigated applying the jar test procedure twice. Overall, four mixed liquor samples were collected at the end of stage 1 when stationary conditions were reached after ~3 SRT from the beginning of sampling sludge and biomass was considered to be well acclimatized to MBR conditions. The MLSS content of the four "raw sludge" samples were 5.8±0.30 g L^{-1}, whereas values of parameters considered in jar test campaign are listed in Table 6.11.

In particular, SVI (see section 5.3.3, method A.12) quantifies the settling characteristics of a sludge representing the volume of 1 g of sludge after 30 min of settling. Usually, SVI values approximately of 100 mL g $MLSS^{-1}$ are associated with good settling sludge, even if, for CASPs, values below 100 are desired (Metcalf and Eddy, 2003). It is well know that the settling propensity for MBR sludge is lower than for CASPs. In fact, the average value of SVI of MBR sludge was 167.5 mL g $MLSS^{-1}$; by comparison, values above 150 are typically associated with filamentous growth in CASPs (Metcalf and Eddy, 2003).

Table 6.11. Determinations for raw sludge samples (four samples). Grey scale colour classifies coefficient of variation (COV) values according footnote 1.

Parameter	UM	Value mean ± std. deviation (COV%)
SVI	mL g $MLSS^{-1}$	167.5±9.52 (5.7%)
CST	sec	17.4±3.12 (18%)
SRF	m kg^{-1}	2.5±0.54 E13 (21.4%)
MFI	1,000 sec L^{-2}	4.8±1.18 (24.4%)
LDSS	mg SS L^{-1}	34±3.9 (11.4%)
soluble-EPS proteins	mg BSA L^{-1}	21.6±6.01 (27.8%)
soluble-EPS carbohydrates	mg glucose L^{-1}	7.6±3.33 (44%)
bulk TOC	mg L^{-1}	20.5±5.26 (25.7%)
bulk COD	mg L^{-1}	69.8±18.63 (26.7%)
bulk abs. 426 nm	cm^{-1}	0.046±0.0206 (44.6%)
bulk abs. 558 nm	cm^{-1}	0.027±0.0153 (56%)
bulk abs. 660 nm	cm^{-1}	0.015±0.0107 (72.9%)

[1] The colour legend for COV values follows:

<20%; 20÷40%; 40÷60%; 60÷80%; >80%

Parameters such as CST, SRF and MFI (see section 5.3.3, method A.12) characterize the sludge filterability and showed average values of 17.4 sec, 2.5 m kg^{-1} and 4.8·1,000 sec L^{-1}, respectively. Differently, LDSS identifies (see section 5.3.3) the low density suspended solids in mixed liquor that remain in the liquid phase after the centrifugation step of the bulk liquid separation procedure (see section 5.3.3 and section 5.3.2, method A.3). In particular, LDSS presented an average value of 34 mg L^{-1}. Soluble-EPS responsible for irreversible fouling in MBRs (see section 2.4 and section 2.5) presented values of 21.6 and 7.6 mg L^{-1} for proteins and carbohydrates, respectively. With regards to parameters related to total organics in mixed liquor bulk, TOC and COD had values of 20.5 and 68.9 mg L^{-1}, respectively. Applying the method A.5 (see section 5.3.2) it was calculated that proteins and carbohydrates accounted for 44.3 and 14.5% of the total TOC bulk content, respectively. With regards to colour it was measured as the absorbance at 426, 558 and 660 nm and presented values of 0.046, 0.027 and 0.015 cm^{-1}, respectively.

With regards to COV of data (Table 6.11), sludge characteristics appear to be highly variable, particularly for colour, that was characterized by the higher COV values (44.6, 56 and 72.9% for absorbance at 426, 558 and 660 nm, respectively) compared with the other parameters. The reason could be related to daily variations in the raw wastewater colour, inducing significant changes in bulk colour since molecules with chromophores are poorly biodegradable. Soluble-EPS carbohydrates presented also a high COV value (44%), whereas

proteins, TOC and COD were characterized by COV between 25 and 30%. Differently, physical parameters such as SRF and MFI presented COV between 20 and 25%, whereas SVI, CST and LDSS had the lowest COV (<20%).

According to method A.14 (see section 5.3.3), performances of flux enhancers were compared calculating the relative variation of each parameter, i.e., the variation between the value of the conditioned samples (where flux enhancers were added into) and the value of the raw sludge samples. In particular, the relative variation was properly calculated as a removal rate for LDSS, soluble-EPS, bulk TOC, bulk COD and bulk colour. Differently, as for SVI, CST, SRF and MFI it represents simply a variation, as follows:

- when the variation is positive, an aggravation is taking place;
- when the variation is negative, an improvement is taking place.

Average values and standard deviations (std. dev.) of relative variations are reported in Table 6.12, Table 6.13 and Table 6.14 for NORIT CA1, TILLMANS TILLPAC18 and DALTON FLODAL, respectively.

Table 6.12. Removal rates and variations of relevant parameters achieved by dosing NORIT CA1 in duplicate samples. Grey scale colour classifies standard deviation values according footnote 1.

Parameter	Removal rate/variation (mean and std. dev.) related to NORIT CA1 doses (mg g $MLSS^{-1}$)			
	12.5	25	50	100
SVI	-1.0±0%	1.0±0.01%	1.0±0.01%	1.2±0.3%
CST	-7.3±23.14%	21.6±57.05%	20.8±63.47%	8.8±51.37%
SRF	-28.4±14.15%	1.2±33.31%	-11.1%[2]	-6±41.35%
MFI	41.0±11.81%	-13.5%[2]	-42.3%[2]	25.7%[2]
LDSS	-11.2±25.93%	-68.9±38.52%	-50.9±4.85%	-43.4±59.98%
soluble-EPS proteins	41.1±19.36%	58.1±0.5%	59.5±6.47%	60.6±1.99%
soluble-EPS carbohydrates	-19.8±1.64%	0.0±7.35%	38.3±22.96%	51.9±45.92%
bulk TOC	18.8±0.00%	31.3±8.84%	24.0±25.04%	43.0±12.23%
bulk COD	29.2±0.00%	21.9%[2]	26.3±29.07%	27.5±36.21%
bulk abs. 426 nm	50.0±0.00%	87.1%[2]	85.7%[2]	90.0%[2]
bulk abs. 558 nm	50.0±7.86%	82.2%[2]	91.1%[2]	93.3%[2]
bulk abs. 660 nm	43.8±8.84%	74.1%[2]	96.3%[2]	96.3%[2]

[1] The colour legend for standard deviation follows:

<20%; 20÷40%; 40÷60%; 60÷80%; >80%

Table 6.13. Removal rates and variations of relevant parameters achieved by dosing TILLMANS TILLPAC18 in duplicate samples. Grey scale colour classifies standard deviation values according footnote 1.

Parameter	Removal rate/variation (mean and std. dev.) related to TILLMANS TILLPAC18 doses (mg g $MLSS^{-1}$)			
	6.25	12.5	25	50
SVI	-0.5±2.19%	-0.5±0.73%	-2.1±0.02%	-4.1±0%
CST	-30.4±0.69%	-42.1±39.96%	-51.1±21.03%	-91.2±12.43%
SRF	-16.5±9.39%	-35.4±0.83%	-59.2±14.94%	-87.4±5.66%
MFI	-73±8.57%	-60.9±17.2%	-91.6±4.21%	-86.5±19.04%
LDSS	-21.6±20.28%	53.5±18.76%	68.9±34.53%	82.5±9.05%
soluble-EPS proteins	35.9±22.91%	69.7±8.96%	68.3±0.00%	60.1±36.2%
soluble-EPS carbohydrates	31.8±2.75%	60.4±6.43%	57.1±18.37%	94.2±1.64%
bulk TOC	47.9±2.95%	41.7±5.89%	53.5±6.78%	64.7±1.33%
bulk COD	49±4.42%	26.9%[2]	45.5±0.96%	60.8±3.26%
bulk abs. 426 nm	57.1±4.04%	64.3%[2]	80%[2]	81.3±4.42%
bulk abs. 558 nm	67.8±4.71%	66.7%[2]	80%[2]	88.9±0.00%
bulk abs. 660 nm	83.3±2.62%	81.5%[2]	85.2%[2]	87.5±17.68%

[1] The colour legend for standard deviation follows:

<20%; 20÷40%; 40÷60%; 60÷80%; >80%

[2] Because of technical issues the determination of the parameter was performed only considering one of the two duplicate samples and therefore no standard deviation is shown.

Table 6.14. Removal rates and variations of relevant parameters achieved by dosing DALTON FLODAL in duplicate samples. Grey scale colour classifies standard deviation (std. dev.) values according footnote 1.

Parameter	Removal rate/variation (mean and std. dev.) related to DALTON FLODAL doses (mg g $MLSS^{-1}$)			
	6.25	12.5	25	50
SVI	0.5±0.73%	0.5±0.73%	-1±1.44%	-2±1.44%
CST	-7.5±30.33%	10.9±10.25%	-10.7±0.27%	-50.2±0.21%
SRF	7.8±62.01%	-7.2±12.97%	8.2±58.19%	-41.1±6.71%
MFI	46.3±10.6%	49.9±15.39%	1.8±51.58%	-69.2±0.01%
LDSS	-26.2±40.45%	-20.6±36.77%	3.3±34.07%	69.2±3.18%
soluble-EPS proteins	-7.9±4.49%	23.1±4.38%	31.1±3.14%	34.4±4.83%
soluble-EPS carbohydrates	86.5±7.17%	81.5±13%	84.9±5%	81±22.49%
bulk TOC	32.5±19.38%	9.1±30.6%	13.7±24.82%	41.3±23.12%
bulk COD	22.9±2.41%	27.5±6.77%	38.9±7.14%	21.9±35.39%
bulk abs. 426 nm	39±2.15%	55.4±5.67%	68.2±0.84%	79.8±2.03%
bulk abs. 558 nm	46.3±20.88%	65.1±10.13%	78.4±0.83%	86.7±10.96%
bulk abs. 660 nm	52.8±3.93%	70.8±5.89%	81.9±9.82%	94.4±7.86%

[1] The colour legend for standard deviation follows:

<20%; 20÷40%; 40÷60%; 60÷80%; >80%

The average performances of flux enhancers were compared directly considering most relevant parameters as indexes for fouling control and indexes for effluent quality enhancement, as follows:

- fouling control indexes: SRF, MFI, LDSS, soluble-EPS;
- effluent quality enhancement indexes: bulk TOC, bulk COD and colour (absorbance at 426 nm) .

With regards to SVI, it was not considered because it is just an indication of settling propensity of sludge and it appears that the effects of flux enhancers were negligible for this parameter. Moreover, CST was not considered because of its high variability (see standard deviations) compared to SRF, that provides similar information on sludge filterability. As for colour, only results at 426 nm were taken into account as previously discussed (see section 6.2.1).

Indexes relevant for fouling control are presented in Figure 6.12, Figure 6.13 and Figure 6.14.

With regards to SRF and MFI (Figure 6.12) the best performance was offered by TILLPAC18 at all the doses tested, realizing a variation approximately of -90% at 50 mg g $MLSS^{-1}$ for both parameters. However, considering CA1, it provided approximately the same performance observed for TILLPAC18 at a dose of 12.5 mg g $MLSS^{-1}$ for SRF (-28.4% for CA1, -35.4% for TILLPAC18), whereas for higher doses CA1 effects were negligible. FLODAL effects on SRF were negligible as well, except for the significant variation at 50 mg g $MLSS^{-1}$ (-41.1%).

Considering MFI results, both CA1 and FLODAL presented a particular outline. In fact, CA1 showed negative effects (positive variations>20%) at the lowest and the highest doses (12.5 and 100 mg g $MLSS^{-1}$), insignificant effects at 25 mg g $MLSS^{-1}$ (-13.5%) and a significant reduction at 50 mg g $MLSS^{-1}$ (-42.3%); this value was approximately equivalent to half of the value obtained with TILLPAC (-86.5%) at the same dose. FLODAL, presented negative or negligible effects at low doses (positive variations>20% at 6.25 and 12.5 mg g $MLSS^{-1}$, 1.8% at 25 mg g $MLSS^{-1}$) and a 69.2% reduction of MFI at 50 mg g $MLSS^{-1}$.

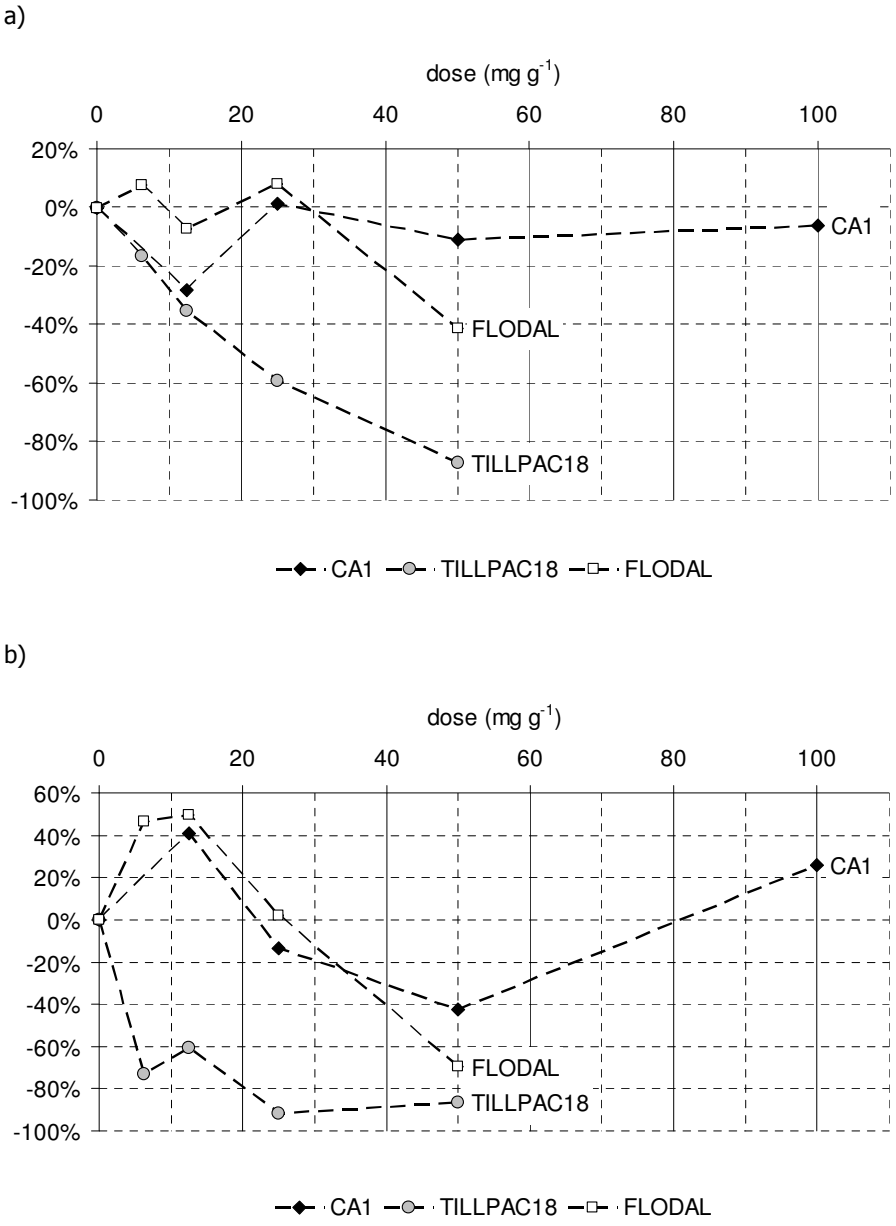

Figure 6.12. Variations of SRF (a) and MFI (b) achieved by dosing flux enhancers (average values).

With regards to soluble-EPS removal (Figure 6.14), considering proteins, TILLPAC18 and CA1 performances were superior than for FLODAL. In particular, TILLPAC18 presented a maximum removal rate at 12.5 mg g $MLSS^{-1}$ (69.7%), whereas CA1 at 50 and 100 mg g $MLSS^{-1}$ (60% approximately). By comparison, FLODAL reached a removal rate of 34.4% at 50 mg g $MLSS^{-1}$.

Differently, as for carbohydrates, FLODAL showed the overall best performance showing at all the tested doses removal rates ranging approximately from 80 to 85%. However, TILLPAC18 provided a removal of 94.2% at 50 mg g $MLSS^{-1}$, whereas at lower doses it

provided removals roughly of 60% at 12.5 and 25 mg g $MLSS^{-1}$, and 31.8% at 6.25 mg g $MLSS^{-1}$. CA1 showed negative or negligible effects at lower doses (-19.8% at 12.5 mg g $MLSS^{-1}$ and 0% at 25 mg g $MLSS^{-1}$), whereas interesting results at higher doses (38.3% at 50 mg g $MLSS^{-1}$ and 51.9% at 100 mg g $MLSS^{-1}$).

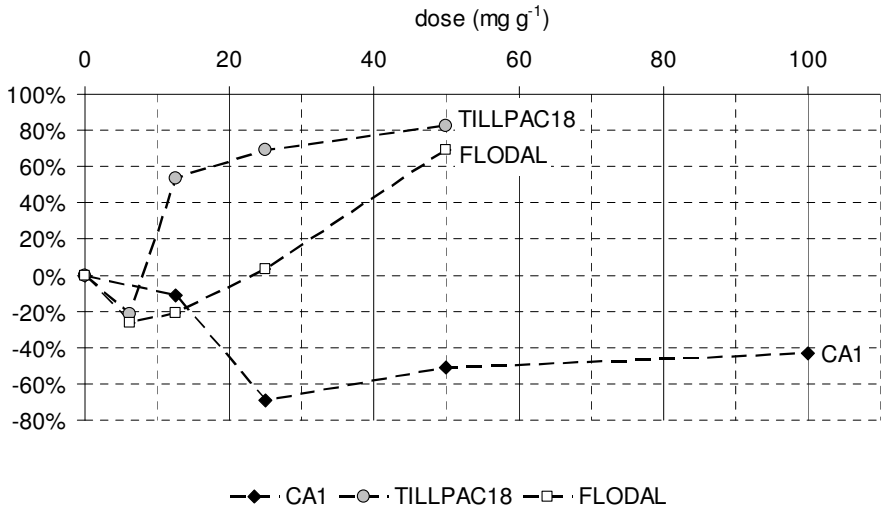

Figure 6.13. LDSS (low density suspend solids) removal rates achieved by dosing flux enhancers (average values).

With regards to indexes relevant for effluent quality enhancement, it is important to point out that such parameters were evaluated considering the bulk liquid of the aerobic mixed liquor, although in an MBR the effluent is the permeate flowing through UF/MF membranes. Therefore, it was assumed that any amelioration in bulk quality (i.e., high removal rates in batch experiments) would have been an indication of permeate quality enhancement. However, because of the presence of membranes in MBRs, in jar test campaign, it was not possible to understand how much the flux enhancers addition would have impacted on permeate quality.

Therefore, removal rates showed in Figure 6.15 and Figure 6.16 do not quantify the actual permeate quality enhancement but they represent only a qualitative indication taken into account to identify the best flux enhancer.

a)

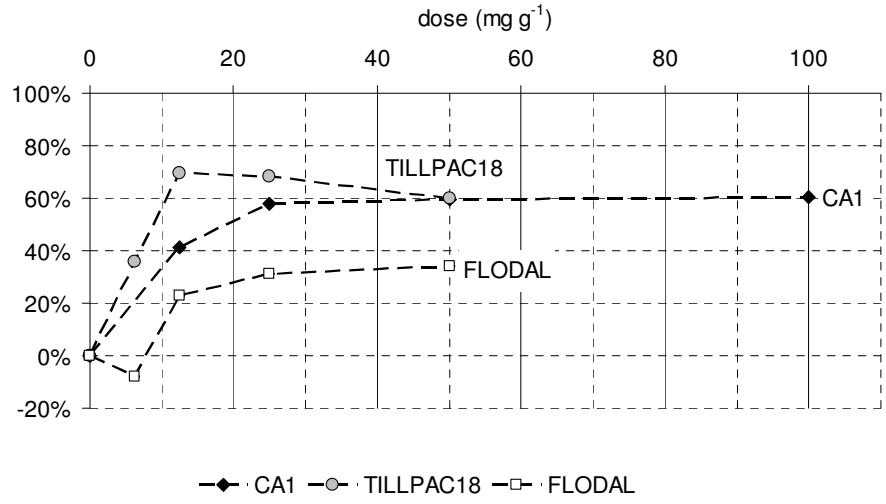

b)

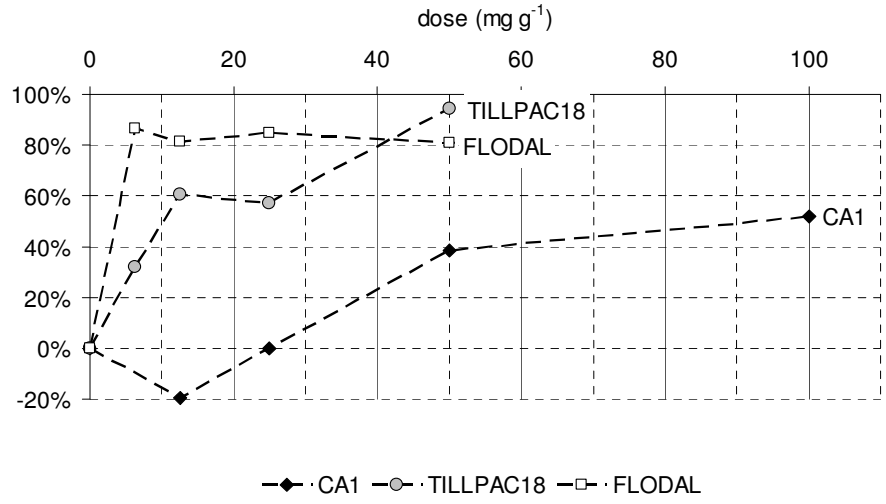

Figure 6.14. Soluble-EPS removal rates achieved by dosing flux enhancers (average values): a) proteins; b) carbohydrates.

Figure 6.15 shows removal rates of organics in bulk measured as TOC and COD. For both parameters, TILLPAC18 provided the best performance over CA1 and FLODAL. In particular, as for TOC, TILLPAC18 showed removal rates higher than 40% at all the dosed tested, whereas CA1 and FLODAL reached approximately a removal of 40% at the maximum doses, i.e., 100 and 50 mg g $MLSS^{-1}$, respectively. Moreover, TILLPAC18 showed removal rates higher than 40% for COD as well, apart from data at 12.5 mg g $MLSS^{-1}$ (26.9%), whereas CA1 and FLODAL provided removals always below 40%.

a)

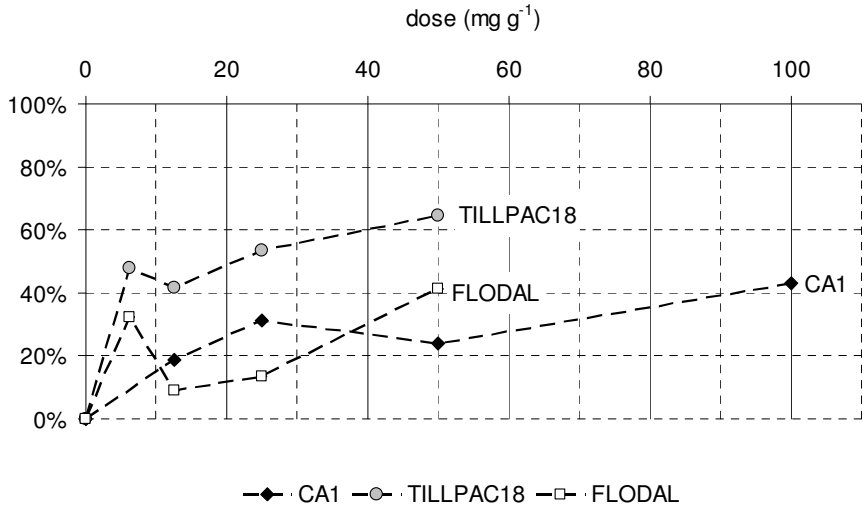

b)

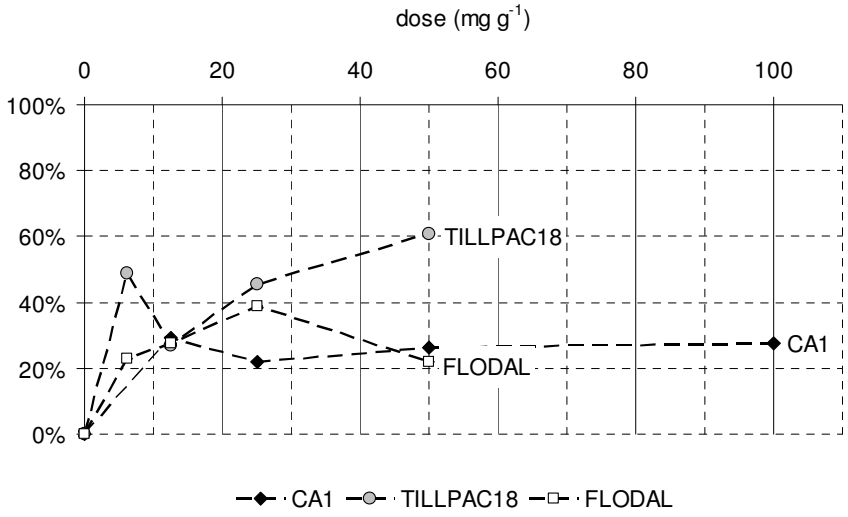

Figure 6.15. Bulk organic removal rates achieved by dosing flux enhancers (average values): a) TOC; b) COD.

Figure 6.16 shows colour removal with regards to a wavelength of 426 nm. At doses below 25 mg g $MLSS^{-1}$ TILLPAC18 and FLODAL showed the best performances. In particular, TILLPAC18 presented removals of 67.8 and 66.7% at 6.25 and 12.5 mg g $MLSS^{-1}$, whereas FLODAL removals were of 46.3 and 65.1% at 6.25 and 12.5 mg g $MLSS^{-1}$.

Differently, at doses above 25 mg g $MLSS^{-1}$ CA1 offered the highest removal rates. In particular, at 50 mg g $MLSS^{-1}$ removal rate was above 90% (91.1%), whereas at the same dose TILLPAC18 and FLODAL provided removal rate below 90% (88.9 and 86,7%, respectively).

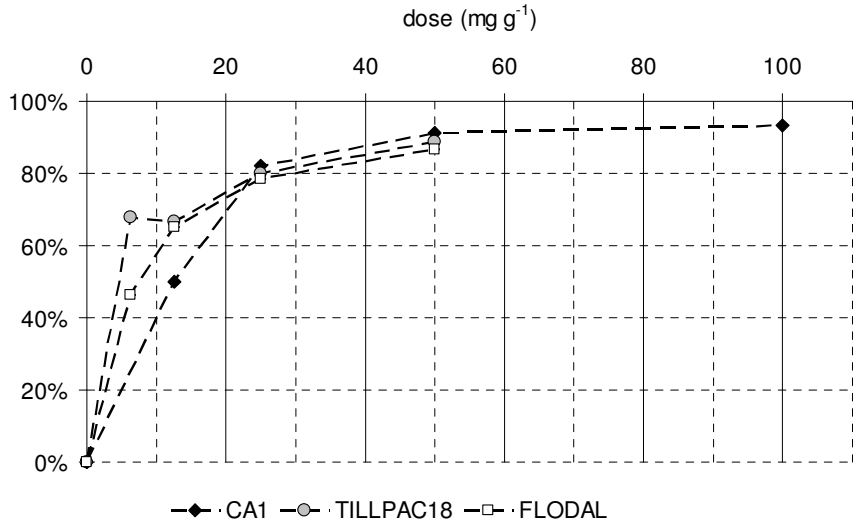

Figure 6.16. Bulk colour abatement (absorbance at 426 nm) achieved by dosing flux enhancers (average values).

Overall, Table 6.15 shows flux enhancer effectiveness with regards to fouling control and effluent quality enhancement, classifying results as worse, intermediate and best performances.

With regards to fouling control indexes, different results were achieved. Considering filterability indexes, i.e., SRF and MFI, TILLPAC18 represented the best flux enhancer, whereas CA1 the worse one.

Table 6.15. Assessment of flux enhancers effectiveness with regards to "fouling" and "quality" parameters according to symbols explains in footnote 1 next to the table.

Parameter		CA1	TILL PAC18	FLODAL
Parameters relevant for fouling control	SRF	⬩	⬩⬩⬩	⬩⬩
	MFI	⬩	⬩⬩⬩	⬩⬩
	LDSS	⬩	⬩⬩⬩	⬩⬩
	soluble-EPS proteins	⬩⬩	⬩⬩⬩	⬩
	soluble-EPS carbohydrates	⬩	⬩⬩	⬩⬩⬩
Parameters relevant effluent quality	bulk TOC	⬩⬩	⬩⬩⬩	⬩
	bulk COD	⬩⬩	⬩⬩⬩	⬩
	bulk abs. 426 nm	⬩	⬩⬩⬩	⬩⬩/⬩⬩⬩

[1] Effects of flux enhancer are classified as follows:

⬩ worse performance; ⬩⬩ intermediate performance; ⬩⬩⬩ best performance

It is believed that biological activated carbon (BAC) formation where PAC particles are included into sludge flocs providing some enhancements in sludge filterability (see section 2.6.1) probably need a long period for developing. So, such effects were not observed in these short-period batch experiments at the doses tested with the PAC NORIT CA1. With regards to FLODAL, positive effects on SRF and MFI began at the highest dose tested (50 mg g $MLSS^{-1}$). The same consideration can be made for LDSS. Moreover, with regards this parameter, TILLPAC18 showed the best performance and, again, CA1 the worse one providing negative or negligible effects mostly. Differently, positive effects of CA1 were observed for soluble-EPS removal rate, particularly for proteins. However, TILLPAC18 showed the best performance at low doses for proteins and FLODAL for carbohydrates.

With regards to effluent quality enhancement indexes, TILLPAC18 was the best flux enhancer for all the parameters. With regards to TOC and COD, FLODAL was considered the worse chemical because it is believed that low TOC and COD removal rates were related to a sort of release of the chemical in bulk. Moreover, being a cationic polyaminic flocculant, the release of nitrogen in bulk was observed (Figure 6.17).

Differently, as for colour, FLODAL showed interesting removal rates at lower doses, therefore offering an intermediate performance between TILLPAC and CA1. The latter was more effective at higher doses.

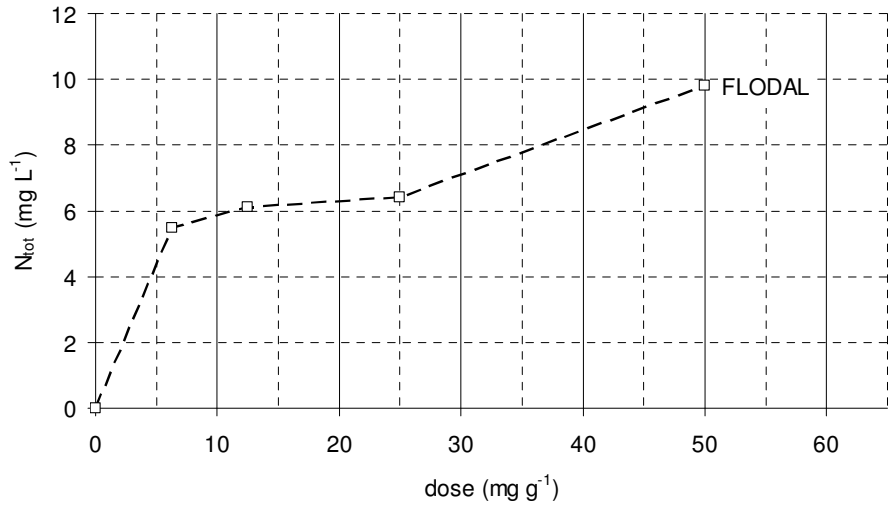

Figure 6.17. Release of nitrogen in bulk for FLODAL (average values).

According to these final considerations, TILLPAC18 was considered as the best flux enhancer, showing also consistent results as indicated by the lowest standard deviations presented above (Table 6.12, Table 6.13 and Table 6.14). In fact, standard deviations offer an idea of the removal variability and therefore the instability of flux enhancer effects.

6.3.2 Definition of the optimal dose and daily dosage for the pilot MBR

According to method A.14 (see section 5.3.3), the optimal dose was chosen considering a multi-criteria approach, taking into account:

1. the relevance of effects related to fouling control and effluent quality enhancement;
2. the economic sustainability of flux enhancer addition;
3. the negative effects detectable in short-period batch tests;
4. any risks of biological activity decline.

With regards to criteria 1, Figure 6.18 and Figure 6.19 summarized TILLPAC18 performances considering fouling control and effluent quality enhancement, respectively.

a)

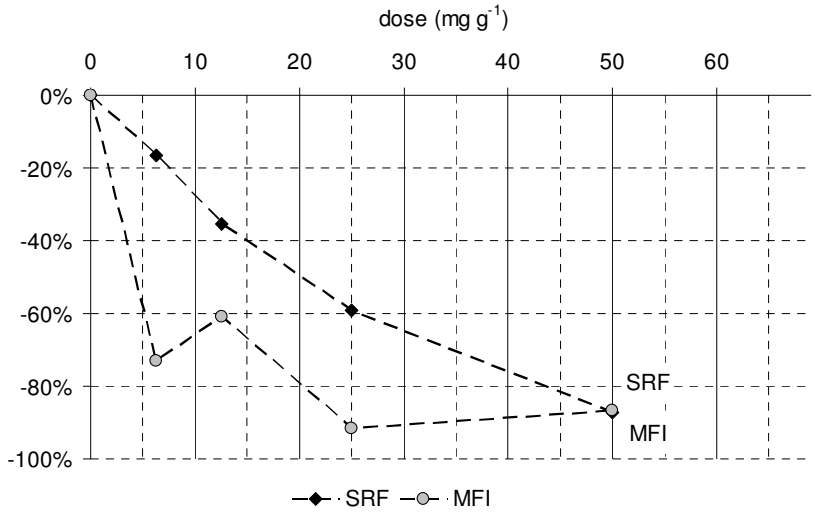

b)

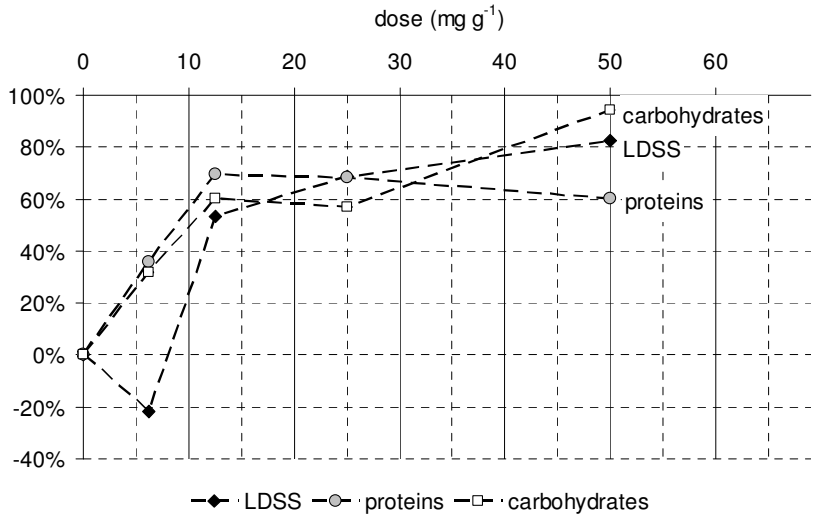

Figure 6.18. TILLPAC18 performances related to fouling control indexes (average values): a) SRF and MFI; b) LDSS, soluble-EPS (proteins and carbohydrates).

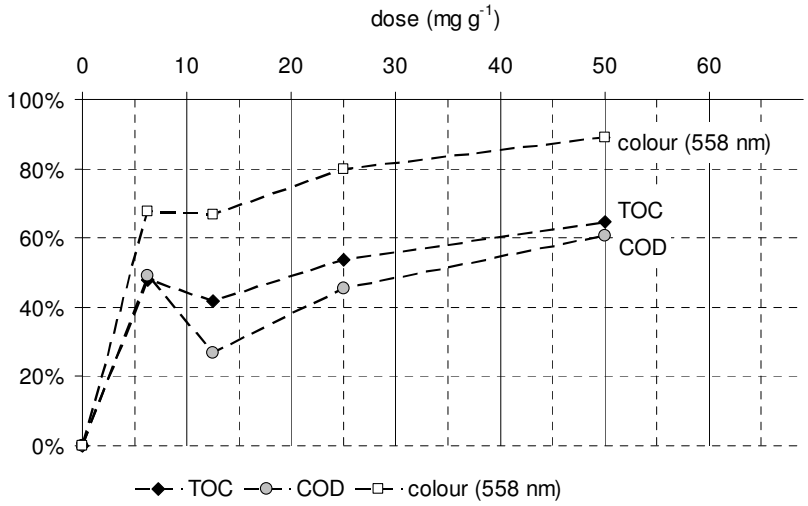

Figure 6.19. TILLPAC18 performances related to effluent quality enhancement indexes (average values): TOC, COD, colour (wavelength 426 nm).

Figure 6.18 and Figure 6.19 show that, for most of the parameters very good results were obtained at a dose of 12.5 mg g $MLSS^{-1}$ with only slight improvement at a dose of 25 mg g $MLSS^{-1}$. Moreover, as for criteria 3, Figure 6.20 shows the negative effect on mixed liquor pH at a dose major than 25 mg g $MLSS^{-1}$. In fact, pH dropped slightly at a dose of 25 mg g $MLSS^{-1}$, whereas at a dose of 50 mg g $MLSS^{-1}$ it varied considerably, of approximately 1 unit (from 7.3 to 6.3). In order to avoid any possible risks of biological activity decline, particularly considering nitrifying bacteria, and MBR performance failure due to pH, due to possible over-dosages (and also due to other unknown negative effects, criteria 4), a dose of 12.5 mg g $MLSS^{-1}$ was chosen.

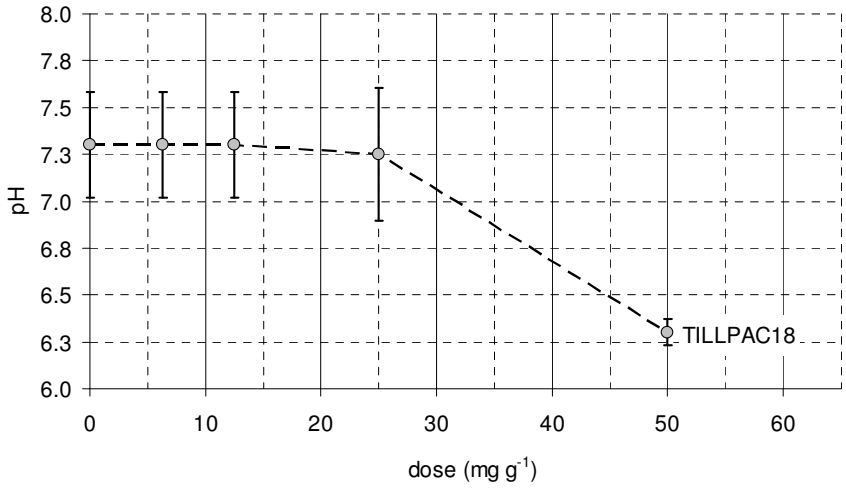

Figure 6.20. Negative effects on pH of TILLPAC18 (average values and standard deviations).

In conclusion, Table 6.16 shows all the related values of the fouling and quality indexes, the daily dosage to compensate for the losses due to the excess sludge removal (Yoon et al., 2005), calculated according to method A.15 (see section 5.3.3), and specific costs estimated according to method A.16 (see section 5.3.3).

Table 6.16. Parameters and costs related to the optimal TILLMANS TILLPAC18 dose.

Fouling control and effluent quality enhancement indexes	SRF variation	-35.4±0.83%
	MFI variation	-60.9±17.2%
	LDSS removal	53.5±18.76%
	Proteins removal	69.7±8.96%
	Carbohydrates removal	60.4±6.43%
	TOC removal	41.7±5.89%
	COD removal	26.9%
	bulk abs. 558 nm removal	66.7%
Daily dosage	daily dosage	0.4 g d^{-1}
Specific costs	specific cost per unit of excess sludge produced	15.3 € t_{ss}^{-1}
	specific cost per unit of treated wastewater volume	0.002 € $m_{wastewater}^{-3}$

6.3.3 Dosing strategy of the selected flux enhancer

Since the evaluation of TILLPAC18 in the mixed liquor was not feasible, its concentration was assessed theoretically by modelling the physical phenomena occurring in reactors (see section 5.3.3, method A.15).

Results are shown in Figure 6.21. In particular, at the beginning of Stage 2, a first spike (first arrow) was dosed to reach a concentration in mixed liquor half the optimal concentration (or dose, D) and then a continuously dosage (0.4 g d^{-1}) to reach progressively the optimal concentration (transition phase). The second arrow indicates a second spike of TILLPAC18 followed by a continuously dosage (0.4 g d^{-1}) to keep the dose constant at the optimal value.

Such a dosing strategy was developed in order to increase the dose of TILLPAC18 progressively from a lower (6.25 mg g $MLSS^{-1}$) to the optimal dose (12.5 mg g $MLSS^{-1}$). During the transition phase, attention was paid to the efficiency of MBR since a loss in effluent quality would have meant an inhibition of bacterial biomass (see section 6.4). Moreover, with this aim, heterotrophic and autotrophic activities at the beginning and at the end of stage 2 were performed (see section 6.5). Effects on fouling control are then discussed in section 6.6.

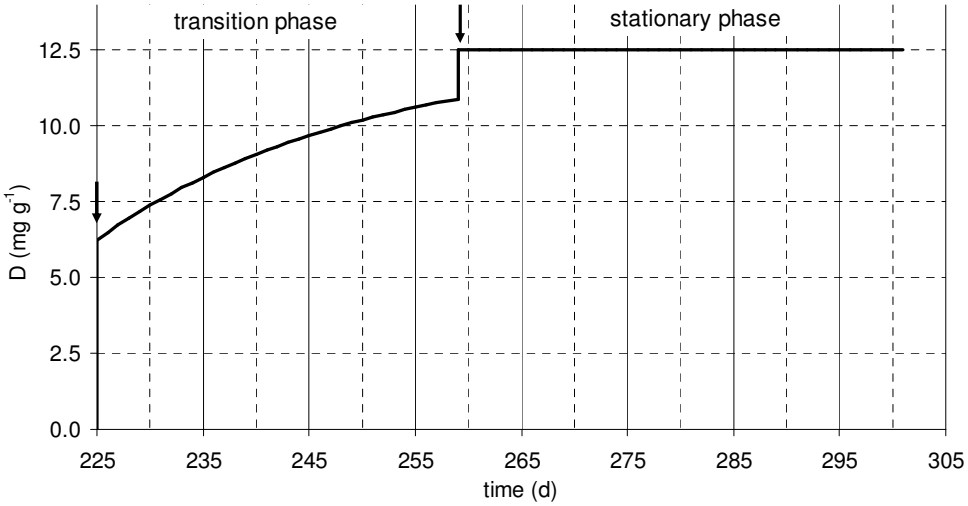

Figure 6.21. Theoretically evolution over time of the actual TILLPAC18 dose adding continuously a dosage of 0.4 g d^{-1} (black arrows indicate instantaneous additions of TILLPAC18 to reach desired doses instantaneously).

6.4 Effluent quality monitoring and enhancement by the selected flux enhancer

In this section, results of the permeate quality monitoring are presented and discussed. In particular, data collected during stage 1 (no flux enhancers) are compared with the effluent quality of the full-scale WWTP (see section 6.4.1). Then, monitoring of effluent quality in stage 1 and stage 2 is discussed in section 6.4.2, and, finally, the comparison of performances observed during these stages is carried out to give an overall estimation of the permeate quality enhancement by the selected flux enhancer (see section 6.4.3).

6.4.1 Comparison of the pilot MBR and the full scale WWTP performances

Available data of the full scale WWTP effluent were related to parameters such as COD, nitrogen compounds and colour. In particular, the full scale WWTP comprised a conventional activated sludge process in the modified Ludzack-Ettinger configuration (denitrification tanks, nitrification tanks, and settlers) and advanced wastewater treatments, including high rate clarification and ozone oxidation, as stated in section 4.2.1 (see also Figure 4.3).

Therefore, the comparison of the pilot MBR and the full scale WWTP performances was executed considering the permeate (from the pilot MBR), the biological effluent (from conventional CASPs) and the final effluent of the full scale WWTP. In particular, data from both treatment plants refer to the same time period, that was the entire duration of stage 1. Also, since the influent wastewater to treat was the same for both, the comparison was executed taking into account effluent concentrations instead of removal rates, answering in this way to goal 1 of the study.

In particular, average values and standard deviations of COD, total nitrogen and colour are presented in Table 6.17 and Figure 6.22.

Table 6.17. Effluent quality characterization for the pilot MBR and the full scale WWTP.

	pilot MBR	full scale WWTP biological effluent	full scale WWTP final effluent
COD (mg/L)	42.5±13.32	43.9±16.21	43.9±16.06
N_{tot} (mg/L)	9.1±0.6	16.3±3.45	15.8±3.71
Abs. at 426 nm x 1,000 (1/cm)	43.2±13.15	45.6±18.63	19.2±10.86

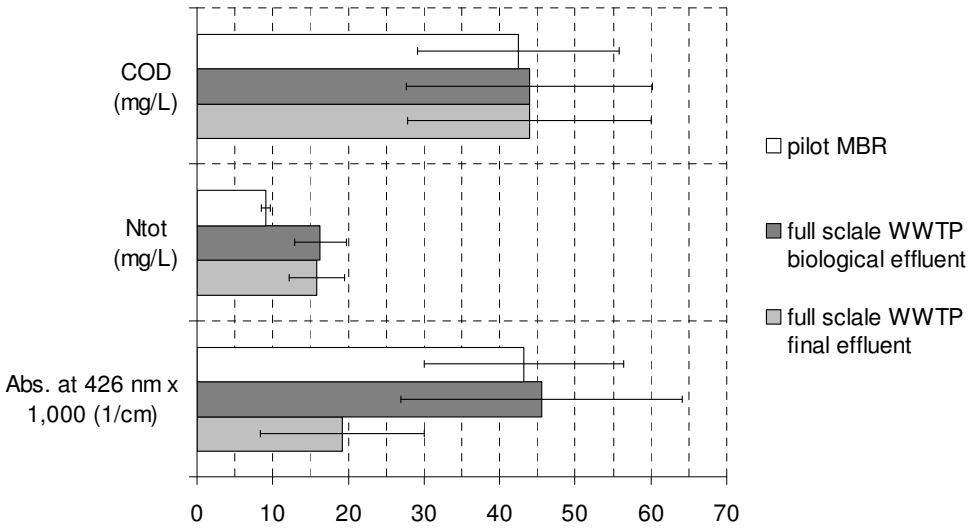

Figure 6.22. Effluent quality characterization for the pilot MBR and the full scale WWTP.

It can be seen from the chart and the table that there is a slight difference in COD concentrations between permeate and the full scale effluents. In particular, taking into account average values, the permeate was characterized by a value lower than WWTP effluents of about 3.2% (42.5 against 43.9 mg L^{-1}). Moreover, considering standard deviations, it is clear that the biological heterotrophic activity was more stable for the MBR than for the full-scale CASP having deviations of 13.32 and 16.21 mg L^{-1}, respectively. What

is more, there was no distinction between the biological and the final full scale WWTP effluents considering COD highlighting the recalcitrant nature of residual organics. Differently, advanced processes impacted on effluent colour significantly, reducing the colour (absorbance at 426 nm) of the biological effluent of about 57.9%. With regards to the pilot MBR, the absorbance (at 426 nm) of permeate was 0.043±0.0132 cm^{-1}, that, compared with absorbance of the biological effluent (0.045±0.0186 cm^{-1}) resulted in a reduction of 5.3%. Again, standard deviations were minor for the pilot, therefore giving a proof of the stability of the process. With regards to total nitrogen, statistics related to the pilot MBR were evaluated avoiding data before acetate addition, therefore referring to the optimal operating of denitrification process. The permeate was characterized by a mean value of 9.1±0.6 mg L^{-1}, whereas full scale effluents by values of 16.3±3.45 and 15.8±3.71 mg L^{-1} for the biological and the final ones, respectively. In particular, the ratio of permeate and biological effluent concentrations was about 1:1.8. Such a difference was not due to any ameliorations provided by coupling an activated sludge process and a membrane filtration in MBRs, but it was related only to different biological design parameters of the Modified Ludzack-Ettinger process. In particular the pilot was designed with a nitrate recycle of 3 (nitrogen removal rate approximately of 75%), whereas the full scale WWTP was designed with a nitrate recycle of 1 (nitrogen removal rate approximately of 50%). Therefore, it was expected that output concentrations followed a relative ratio of approximately 1:2.

6.4.2 Effluent quality monitoring

Effluent quality was monitored taking into account the ordinary macro-parameters for wastewater, such as COD and nutrients, and textile macro-parameters, such as colour and surfactants (non-ionic surfactants, and anionic surfactants). With regards to COD, N and P, results are shown in Table 6.18. Moreover, the evolution over time of COD concentration and removal rates are illustrated in Figure 6.23. COD removal rates were evaluated considering only the domestic-textile wastewater, avoiding the contribute of sodium acetate.

Table 6.18. Statistic parameters for COD, total nitrogen and total phosphorus related to stage 1 (s1), stage 2 (s2) and overall to the experimental period (o).

	COD (mg L^{-1})			**N_{tot} (mg L^{-1})**			**P_{tot} (mg L^{-1})**		
	s1	s2	o	s1	s2	o	s1	s2	o
N	31	11	43	32	11	44	2	5	8
mean	43	22	37	15	6	13	2.3	0.1	0.7
st. dev.	13.3	11.4	15.6	9.1	1.2	8.8	0.74	0.08	1.05
COV	31.3%	52.9%	42.3%	60.3%	20.5%	70.3%	32.1%	77.9%	156.8%
min	17	8	8	3	4	3	1.8	0.1	0.1
max	75	43	75	36	7	36	2.8	0.2	2.8

In particular it can be seen from the chart that effluent COD was quite variable in the range between 17 and 75 mg L^{-1} during stage 1 (43±13.3 mg L^{-1}), whereas during stage 2 the variability as well as absolute values were improved (22±11.4 mg L^{-1}). Therefore, it is clear that effluent quality was ameliorated in stage 2, but as stated above (see section 6.2.1) dilution and holyday effects on inflow wastewater COD concentration must be taken into account. In particular, the stationary phase of stage 2 (from day 260 onwards) was comparable with influent data between day 50 and day 100 and between day 150 and 200 because all these periods (grey areas in the chart) were characterized approximately by COD < 250 mg L^{-1}. However, also considering these specific control periods it came out that COD concentration was lower in the stationary phase of stage 2 and therefore such an amelioration was likely due to addition of PACl, that in the stationary phase was at the optimal concentration. Moreover, this is also highlighted by removal rates of COD. In fact, the stationary phase of stage 2 was characterized by higher values compared to other control periods as shown in Table 6.19.

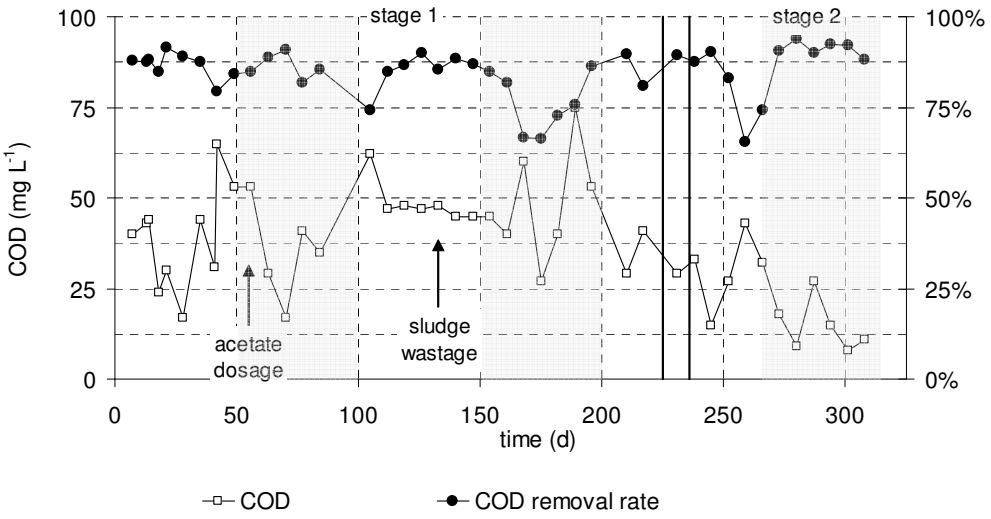

Figure 6.23. Effluent COD concentration and removal rate over time.

Table 6.19. COD removal rates during the stationary phase of stage 2 and control periods in stage 1.

	mean	st. dev.
control period 1 (day 50÷day 100)	86%	3.5%
control period 2 (day 150÷day 200)	76%	8.3%
stationary phase of stage 2 (day 260 onwards)	91%	2.1%

Figure 6.24 shows the total nitrogen concentration and removal rate over time. It can be seen from the chart that, after the dosage of sodium acetate, removal rates increased rapidly to values ranging from 70% to 90% with an average removal of 78.9% in stage 2. On the other hand, total nitrogen concentration dropped down as soon as sodium acetate was added. As previously stated (see section 6.2.2) the addition of sodium acetate was introduced to support bacterial growth and supply readily biodegradable COD to optimize the denitrification process. The latter effect can be seen properly in Figure 6.25, where nitrate concentration over time is presented.

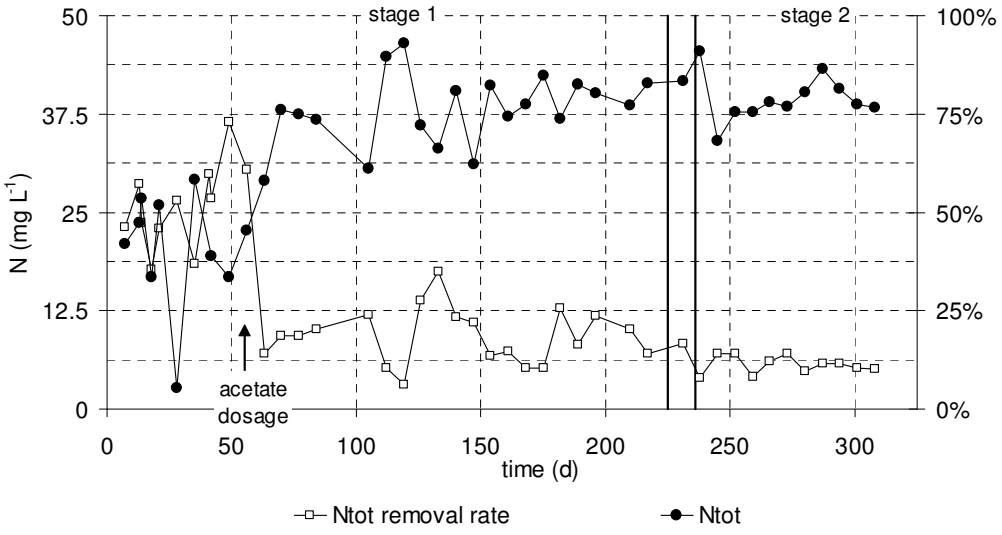

Figure 6.24. Effluent total nitrogen concentration and removal rate over time.

In particular, Figure 6.25 shows that nitrate in permeate dropped down rapidly after the addition of acetate indicating that the overall performance of the denitrification process improved significantly.

It is believed that in absence of sodium acetate the nitrate recycle of the pilot plant re-circulated also an excessive amount of oxygen into the anoxic tank, since the recycled sludge was characterized by a DO concentration of 2.2 mg L^{-1} (the same average concentration of the aerobic tank). This affected the facultative metabolism of heterotrophic denitrifying bacteria that, when oxygen is present, it is preferred for catabolic reactions instead of nitrates, as the final electrons acceptor. Adding a readily biodegradable COD into the anoxic tank (i.e., sodium acetate) implied a consumption of all the recycled oxygen because of the aerobic degradation occurred in the tank. Then, the remaining amount of readily biodegradable COD in the anoxic reactor was biodegraded through the anoxic degradation pathway of heterotrophic denitrifying bacteria, reducing therefore nitrates to molecular nitrogen.

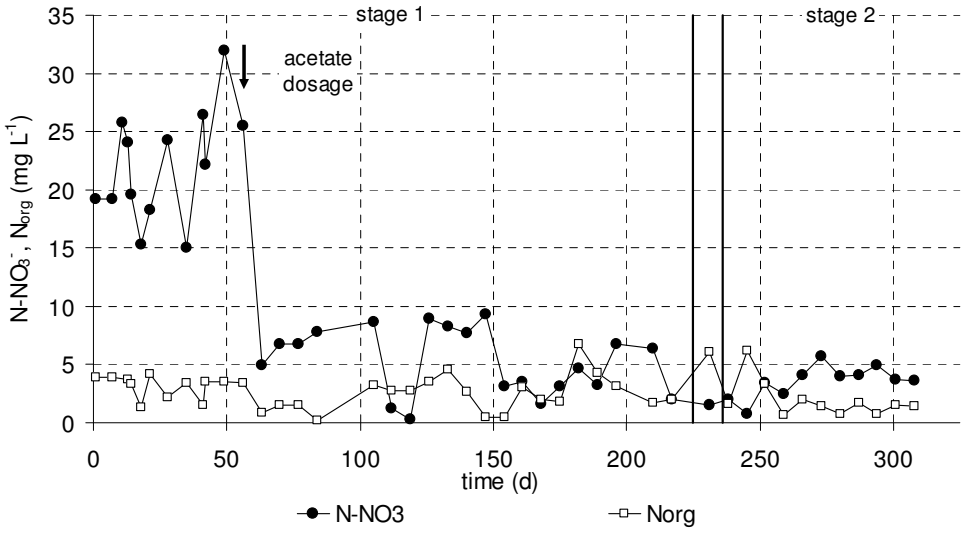

Figure 6.25. Effluent nitrate and organic nitrogen concentration and removal rate over time.

Generally, adopting a nitrate recycle ratio (r) equal to 3, it is expected that the overall nitrogen removal rates would be about 75÷80%, comprising the effect of pre-denitrification (when properly designed and performing) and nitrogen up-take due to biomass growth (Metcalf and Eddy, 2003). Therefore, since such removal rate values were observed after the addition of sodium acetate, as discussed above, it is clear that the optimization of the denitrification process was executed properly.

Considering data shown in Table 6.20 it appears that average values in stage 2 were lower than in stage 1 for all the nitrogen compounds considered. Considering the organic nitrogen, this outcome is not considered to be related to the addition of PACl but to the diluted wastewater fed during stage 2.

On the other hand, as for ammonia, the relevant diminution of average values (1.3 vs 0.1 mg L^{-1}) was probably due to a removal of some substances interfering with nitrification, and, also, these results demonstrated that the dosage of PACl did no involve any direct inhibitions of nitrification.

Table 6.20. Statistic parameters for nitrogen compounds in permeate related to stage 1 (s1), stage 2 (s2) and overall to the experimental period (o).

	N_{org} (mg L^{-1})			**$N\text{-}NH_4^+$** (mg L^{-1})			**$N\text{-}NO_3^-$** (mg L^{-1})		
	s1	s2	o	s1	s2	o	s1	s2	o
mean	2.7	1.9	2.6	1.3	0.1	1.0	11.9	3.5	9.6
st. dev.	1.41	1.58	1.55	1.17	0.16	1.12	9.13	1.36	8.70
COV	51.6%	81.4%	59.6%	92.7%	173.6%	117.4%	76.8%	38.4%	90.5%
min	0.2	0.7	0.2	0.0	0.0	0.0	0.3	0.8	0.3
max	6.8	6.2	6.8	4.7	0.4	4.7	32.0	5.7	32.0

With regards to total phosphorous, data collected during stage 1 and 2 showed (see above, Table 6.18) average values of 2.3±0.74 and 0.1±0.08 mg L^{-1}, respectively. The same result comes out considering removal rates, that were about 23.6% and 87.8%, respectively. It is believed that such an interesting outcome is related to the PACl addition during stage 2. In fact, PACl, being a cationic polymeric salt (see section 2.6), can interact with PO_4^{3-} ions, creating precipitates and removing phosphorous from the wastewater.

Finally, textile macro-parameters statistics were taken into consideration. In particular, data related to colour are presented in Table 6.21 and, also, the evolution over time of absorbance at 426 nm is shown in Figure 6.26.

Table 6.21. Statistic parameters for colour in permeate related to stage 1 (s1), stage 2 (s2) and overall to the experimental period (o).

	abs. × 1,000 at 426 nm (cm^{-1})			**abs. × 1,000 at 558 nm (cm^{-1})**			**abs. × 1,000 at 660 nm (cm^{-1})**		
	s1	s2	o	s1	s2	o	s1	s2	o
N	24	15	40	24	15	40	24	15	40
mean	43	26	36	26	17	23	13	8	11
st. dev.	13.2	7.7	14.2	10.2	5.6	9.6	4.6	2.5	4.6
COV	30.4%	30.0%	39.4%	39.2%	32.6%	42.7%	36.9%	31.4%	42.9%
min	19	14	14	4	11	4	2	5	2
max	72	44	72	48	30	48	23	13	23

It can be seen from the chart below (Figure 6.26) that colour removal rates improved significantly in stage 2, particularly considering data related to control periods, during which wastewater was affected by intensive raining episodes and holydays (grey colour in Figure 6.26). Moreover, also comparing results of the entire stage 1 and stage 2, removal rates at 426 nm were 72.0±14.0% and 83.6±6.7% for stage 1 and stage 2, respectively. Therefore, PACl addition improved colour removal of the MBR.

Taking into account surfactants, data were collected from day 180 onwards (Table 6.22). In particular, anionic surfactants showed average values of 0.8±0.68 mg L^{-1} and 0.3±0.12mg L^{-1} for stage 1 and stage 2, respectively. Differently, as for non-ionic surfactants, average values of 0.3±0.25 mg L^{-1} and 0.2±0.11 mg L^{-1} came out for stage 1 and stage 2, respectively.

Therefore, PACl addition resulted in a higher removal of anionic surfactants, whereas it did not affect non-ionic surfactant results. In particular, Figure 6.27 shows results for anionic surfactants with average removal rates of 79.2±13.4% and 84.3±13.8% for stage 1 and stage 2, respectively. In fact, PACl, being a cationic polymeric salts, can interact and remove anionic compounds such as anionic surfactants.

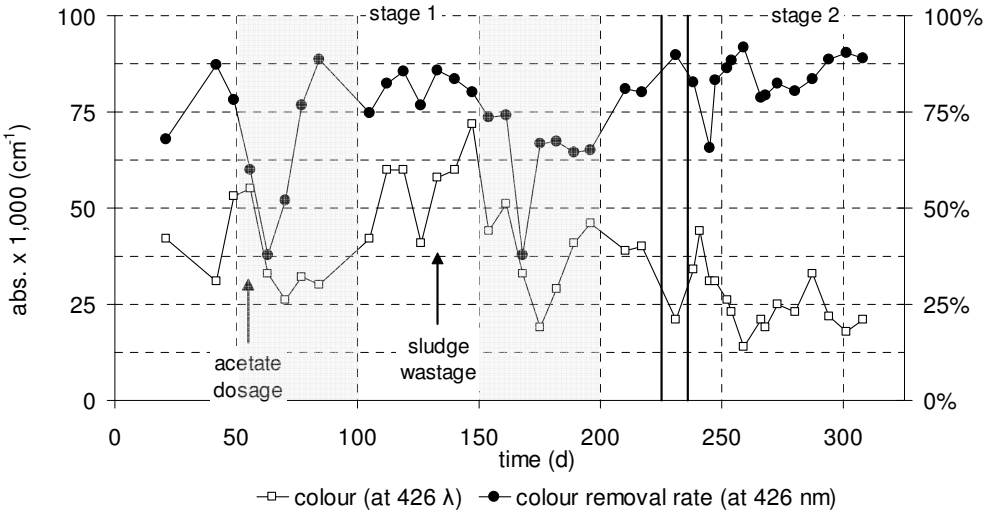

Figure 6.26. Effluent colour (absorbance at 426 nm) and removal rate over time.

Table 6.22. Statistic parameters for surfactants in permeate related to stage 1 (s1), stage 2 (s2) and overall to the experimental period (o).

	anionic surfactants (mg L^{-1})			**non-ionic surfactants** (mg L^{-1})		
	s1	s2	o	s1	s2	o
N	5	11	17	5	11	17
mean	0.8	0.3	0.4	0.3	0.2	0.3
st. dev.	0.68	0.12	0.43	0.25	0.11	0.19
COV	85.0%	42.0%	95.6%	72.3%	46.1%	63.4%
min	0.3	0.2	0.2	0.1	0.1	0.1
max	2.0	0.5	2.0	0.7	0.4	0.7

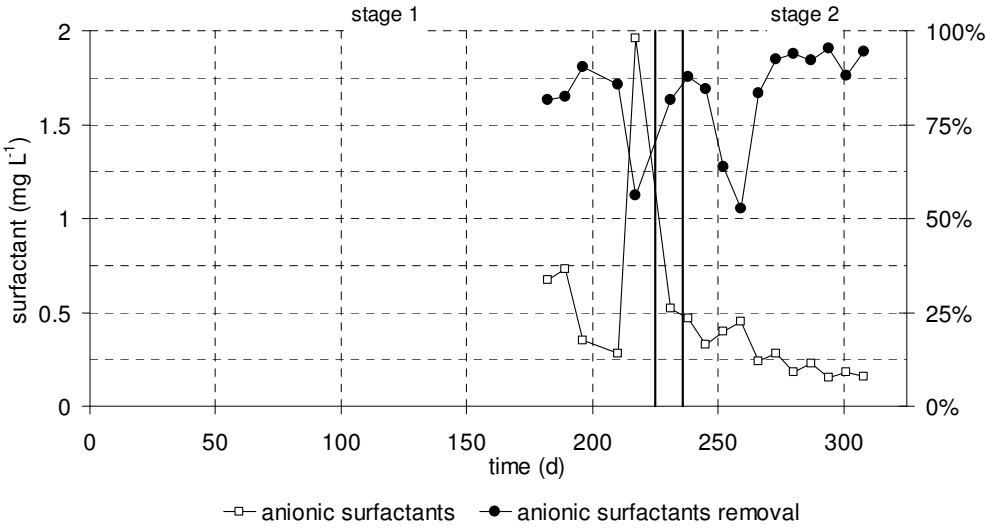

Figure 6.27. Permeate anionic surfactant concentration and removal rate over time.

6.4.3 Quality enhancement by the selected flux enhancer

Overall, the effects of PACl on the enhancement of permeate quality discussed above are summarized in Table 6.23 and Figure 6.28.

With regards to ordinary macro-parameters, the addition of PACl resulted in an improvement of removal rates and effluent quality for COD and total phosphorus. In particular, as for COD, during the stationary phase of stage 2 an average removal rate of 91±2.1% was observed, whereas in two control periods (day 50÷day 100, and day 150÷day 200) removal rates of 86±3.5% and 76±8.3% were observed, respectively. Considering, total phosphorus, since PACl, being a cationic polymeric salt (see section 2.6), can interact with PO_4^{3-} ions, creating precipitates and removing phosphorous from the wastewater, interesting results came out. In fact, removal rates were about 23.6% and 87.8% for stage 1 and stage 2, respectively.

With regards to textile macro-parameters, the addition of PACl resulted in an improvement of removal rates and effluent quality for colour and anionic surfactants, that, as for phosphorous, can be removed by PACl through ionic interactions.

In particular, removal rates at 426 nm were 72.0±14.0% and 83.6±6.7% for stage 1 and stage 2, respectively; whereas removal rates of 79.2±13.4% and 84.3±13.8% were observed for anionic surfactants in stage 1 and stage 2, respectively.

In conclusion, PACl at the low dosage considered in this study enhanced significantly both ordinary and textile macro-parameters.

Table 6.23. Assessment of PACl effectiveness on permeate quality enhancement according to symbols explains in footnote 1.

Parameter		Effect
ordinary macro-parameters	COD	+
	total nitrogen	0
	total phosphorus	+
textile macro-parameters	colour (abs. 426 nm)	+
	non-ionic surfactants	0
	anionic surfactants	+

[1] Effects of flux enhancer are classified as follows:

-	negative	0	negligible	+	positive

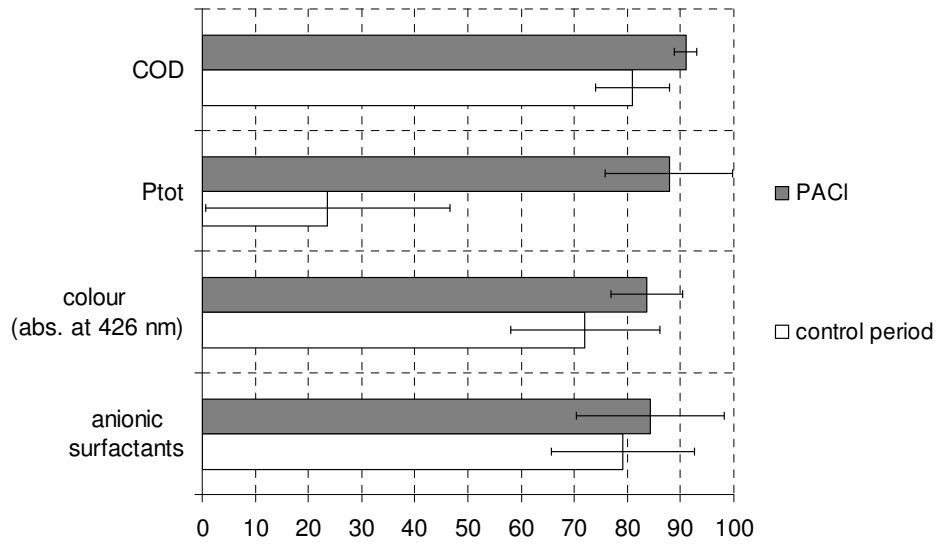

Figure 6.28. Removal rates with PACl addition and removal rates in control periods.

6.5 Sludge characteristics and effects of the selected flux enhancer

In this section, results about sludge characteristics and the effects of PACl addition are presented and discussed, considering the following aspects:

- extracellular biopolymers content of sludge suspension (see section 6.5.1).
- physical sludge characteristics, such as flocs strength and sludge filterability (see section 6.5.2);
- biological activity of heterotrophic and autotrophic bacteria (see section 6.5.3).

6.5.1 Extracellular biopolymers content of sludge suspension

The measurement of extracellular biopolymers content in sludge suspension was performed adopting the method A.3 (see section 5.3.2). In particular, soluble and bound biopolymers (soluble-EPS and bound-EPS) was extracted from sludge. For soluble-EPS, the bulk liquid of sludge suspension was separated and it contained not only extracellular biopolymers (proteins and carbohydrates) but also residual organic substrates. Differently, the bound-EPS extraction resulted in a solution where only biopolymers were present. Such biopolymers content can be named "extracted bound-EPS" or "extracted EPS" that are only a proportion of bound-EPS originally present in sludge flocs as extraction procedures are characterized by extraction efficiency below 100% (Comte et al., 2006). For soluble-EPS and extracted bound-EPS the symbol "sEPS" and "eEPS" can be use, respectively. Moreover, since proteins

and carbohydrates are the main components of biopolymers, symbols shown in Table 6.24 were also adopted.

Table 6.24. Symbols adopted for characterizing extracellular biopolymers content in sludge suspension and typical values in MBRs (see table 2.6).

Symbol	Meaning	Typical concentration in MBRs
sEPSp	soluble-EPS proteins	4.5÷34 mg L^{-1}
sEPSc	soluble-EPS carbohydrates	2÷33 mg L^{-1}
eEPSp	extracted-EPS proteins	11÷116 mg g $MLVSS^{-1}$
eEPSc	extracted-EPS carbohydrates	6÷40 mg g $MLVSS^{-1}$

Figure 6.29 and Figure 6.30 show the concentration over time of biopolymers measured as the equivalent concentration of references compounds, i.e., BSA for proteins and glucose for carbohydrates.

sEPSp showed a variation within a wide range (1.3÷24 mg L^{-1}), with an increasing trend over time in stage 1 (Figure 6.29). Differently, sEPSp dropped down in stage 2 as soon as PACl was added, from a value of 24 mg L^{-1} to values fluctuating around 10 mg L^{-1}. Then, after day 273, sEPSp increased to values between 15 and 20 mg L^{-1}. Whit regards to eEPSp, concentrations ranging from 27.2 to 64.6 mg g $MLVSS^{-1}$ were observed in stage 1, whereas in stage 2 eEPSp were lower than in stage 1 varying in a narrower and lower range (from 28.6 to 32.0 mg g $MLVSS^{-1}$) and presenting an average value of 30.6±1.30 mg g $MLVSS^{-1}$.

As for carbohydrates (Figure 6.30), in stage 1 sEPSc varied within a range from 3.2 to 12.2 mg L^{-1} with higher values at the beginning of the stage. In stage 2 the first datum observed was 15.9 mg L^{-1} (the highest value of the entire experimental period), but with the progressive increase in PACl concentration in the transition phase sEPSc dropped down and in the stationary phase of stage 2 (grey area in Figure 6.30) reached values between 7 and 7.5 mg L^{-1}. eEPSc varied between 1.9 and 4.0 mg g $MLVSS^{-1}$ in stage 1, whereas with the addition of PACl (stage 2) eEPSc presented lower values varying within a narrow range from 0.9 to 2.4 mg $gMLVSS^{-1}$.

Overall, PACl affected EPS concentration reducing proteins and carbohydrates significantly, except for sEPSp.

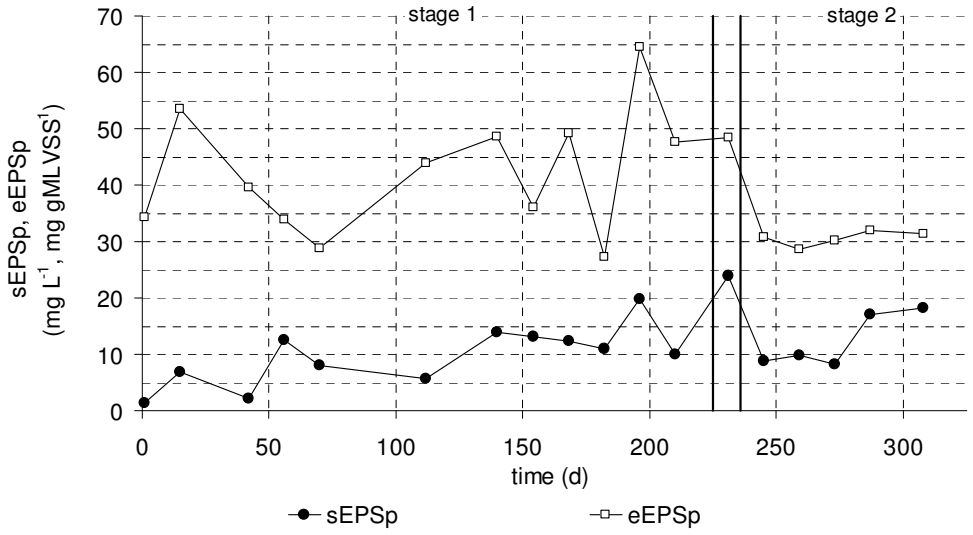

Figure 6.29. Proteins concentration in soluble-EPS (sEPSp) and extracted-EPS (e-EPSp) over time.

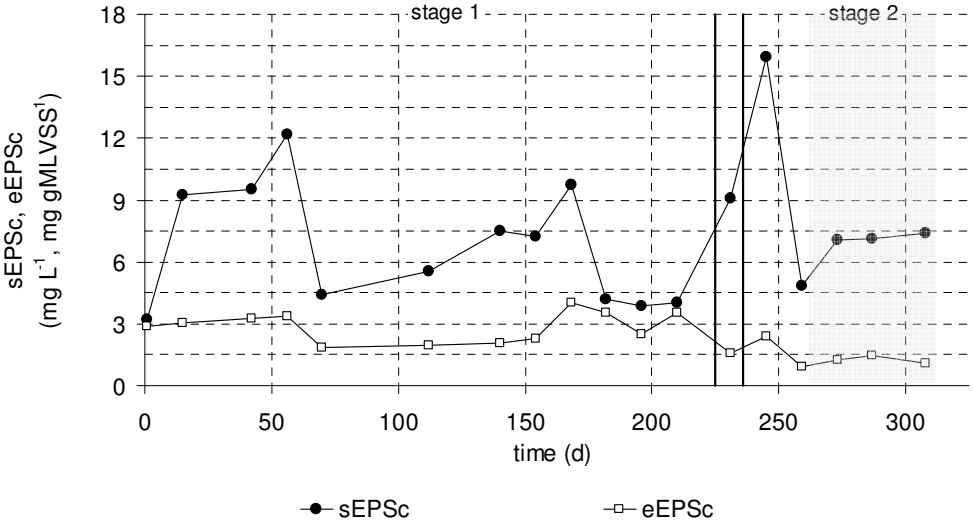

Figure 6.30. Carbohydrates concentration in soluble-EPS (sEPSp) and extracted-EPS (e-EPSp) over time.

Statistics of extracellular biopolymers concentrations are presented in Table 6.25 and in Table 6.26 for bulk liquid and extracted-EPS, whereas relative variation between stage 1 and stage 2 are shown in Table 6.27.

Moreover, in Table 6.25 and in Table 6.26, as proteins and carbohydrates were measured also in mixed domestic-textile wastewater and permeate (for control purpose), statistics for these media are shown.

Table 6.25. Proteins in bulk liquid, extracted EPS, mixed domestic-textile wastewater and permeate measured in stage 1 (s1), stage 2 (s2) and overall the experimental period (o).

	bulk liquid (mg L^{-1})			**extracted EPS** (mg $gMLVSS^{-1}$)			**wastewater** (mg L^{-1})			**permeate** (mg L^{-1})		
	s1	s2	o	s1	s2	o	s1	s2	o	s1	s2	o
N	12	5	18	12	5	18	9	5	15	9	5	15
mean	9.7	12.4	11.3	42.3	30.6	39.4	64.7	50.0	59.0	6.1	8.0	7.2
st. dev.	5.24	4.82	5.90	11.01	1.30	10.59	29.10	31.14	28.54	2.96	2.09	3.20
COV	54%	39%	52%	26%	4%	27%	45%	62%	48%	49%	26%	44%
min	1.3	8.3	1.3	27.2	28.6	27.2	25.8	17.9	17.9	2.1	5.5	2.1
max	19.7	18.3	24.0	64.6	32.0	64.6	118.6	95.6	118.6	12.2	11.0	13.6

Table 6.26. Carbohydrates in bulk liquid, extracted EPS, mixed domestic-textile wastewater and permeate, measured in stage 1 (s1), stage 2 (s2) and overall the experimental period (o).

	bulk liquid (mg L^{-1})			**extracted EPS** (mg $gMLVSS^{-1}$)			**wastewater** (mg L^{-1})			**permeate** (mg L^{-1})		
	s1	s2	o	s1	s2	o	s1	s2	o	s1	s2	o
N	12	5	18	12	5	18	9	5	15	9	5	15
mean	6.7	8.5	7.3	2.9	1.4	2.4	20.5	8.5	15.7	5.6	6.5	5.8
st. dev.	2.94	4.29	3.28	0.71	0.59	0.93	6.94	3.48	8.26	1.11	2.12	1.52
COV	44%	51%	45%	25%	41%	39%	34%	41%	53%	20%	33%	26%
min	3.2	4.9	3.2	1.9	0.9	0.9	10.3	5.7	5.7	4.0	4.1	4.0
max	12.2	15.9	15.9	4.0	2.4	4.0	30.1	14.5	30.1	7.7	9.8	9.8

It can be seen from the tables above that proteins in bulk (sEPSp) were characterized by average values of 9.7±5.24 mg L^{-1} and 12.4±4.82 mg L^{-1} in stage 1 and stage 2, respectively, whereas proteins in extracted-EPS (eEPSp) were 42.3±11.01 mg g $MLVSS^{-1}$ and 30.6±1.30 mg MLVSS L^{-1} in stage 1 and stage 2, respectively. With regards to carbohydrates, the concentrations in bulk (sEPSc) were 6.7±2.94 mg L^{-1} and 8.5±4.29 mg L^{-1} in stage 1 and stage 2, respectively, whereas carbohydrates in extracted-EPS (eEPSc) were 2.9±0.71 mg g $MLVSS^{-1}$ and 1.4±0.59 mg g $MLVSS^{-1}$ in stage 1 and stage 2, respectively.

Table 6.27. Relative variation of EPS between stage 1 and stage 2.

EPS	**Variation between stage 1 and stage 2**
sEPSp	27.8%
sEPSc	26.9%
eEPSp	-27.7%
eEPSc	-51.7%

Consequently, average values detected in this study were within the range of typical values in MBRs (see above, Table 6.24) even though very close to minimum concentration for carbohydrates (sEPSc and eEPSc) .

Considering proteins and carbohydrates in the raw wastewater, overall, average values of 59.0±28.54 mg L^{-1} and 15.7±8.26 mg L^{-1} were observed, respectively; whereas, as for permeate, overall, concentrations were about 7.2±3.20 mg L^{-1} and 5.8±1.52 mg L^{-1}, respectively.

Even if sEPSp and sEPSc were detected in bulk liquid of the aerobic tank it can be assumed that the same concentration would have been detected in bulk liquid of the membrane tank. Taking into account this assumption, membrane rejection of soluble EPS was calculated. Higher rejection was found for proteins than for carbohydrates. In fact, values of 55±11.6% and 38±20% were detected for proteins in stage 1 and stage 2, respectively; whereas, for carbohydrates, values of 21±17.2% and 19±13% were observed in stage 1 and stage 2, respectively. According to these average results, it seems that the addition of PACl reduced the protein rejection factor, whereas, for carbohydrates, no significant differences were observed between stage 1 and stage 2. However, taking into consideration the dynamic over time of the protein rejection factor (Figure 6.31) it can be seen that at the beginning of stage 2 the rejection factor dropped rapidly but, then, in the stationary phase (grey area in Figure 6.31) the factor was recovered probably due to an enhancement in the protein bridging power of the cake layer provided by PACl.

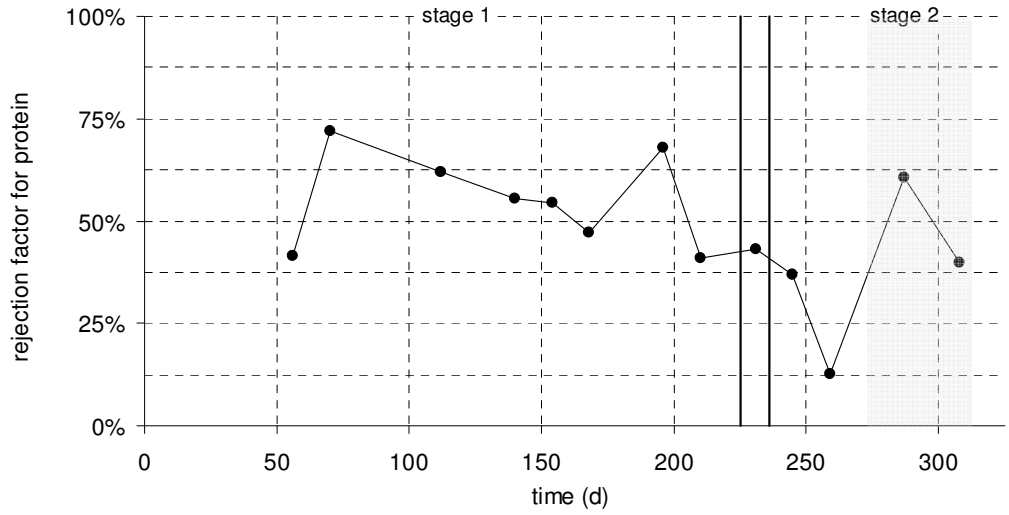

Figure 6.31. Rejection factor for protein over time.

With regards to the mean oxidation state (see method A.4, section 5.3.2), neither particular trends nor relevant differences between different media were detected. For instance, bulk organic carbon was characterized by a value of -1.8, extracted EPS carbon by a value of -1.6 and, as a reference, the soluble organic carbon in wastewater by a value of -1.6.

Differently, the TOC apportionment (see section 5.3.2, method A.5) showed interesting results. In particular, Table 6.28 presents data related to bulk and extracted-EPS. For proteins in extracted-EPS, as discussed in materials and methods section (see section 5.3.2, method A.4) two different equations were used based on the basis of two different assumptions. The first equation (eq. 5.22) takes into account the protein measurement by the Lowry method (see section 5.5), whereas the second equation (eq. 5.25) is based on the organic nitrogen content in eEPS. It can be seen from the table below that the method based on nitrogen (method 2) provides higher values that the method based on direct protein detection (method 1) giving an average percentage of proteins of 65% over a value of 55% for method 1. This fact was probably due to that organic nitrogen can be related not only to proteins but also to other organics such as humic compounds. Moreover, the composition of the eEPS amino acids pool detected by Dignac et al. (1998) did not match with the amino acids pool characterizing eEPS in this study.

In addition, standard deviations of method 1 showed a lower value than method 2 (12.3% vs 31.7%). Therefore, in general, method 1 was preferred and then considered in charts shown in Figure 6.32.

Table 6.28. TOC apportionment of bulk and extracted-EPS performed for stage 1 (s1), stage 2 (s2) and overall the experimental period (o).

	proteins			**carbohydrates**			**other organics**		
	s1	s2	o	s1	s2	o	s1	s2	o
bulk									
mean	25%	34%	29%	16%	25%	19%	59%	41%	52%
st. dev.	13.4%	13.4%	13.5%	5.3%	18.7%	11.6%	12.2%	23.6%	17.8%
eEPS									
mean	52%	57%	55%	4%	3%	3%	44%	40%	42%
st. dev.	17.4%	7.2%	12.3%	1.0%	1.2%	1.3%	18.2%	7.7%	12.7%
eEPS*									
mean	61%	74%	65%	4%	3%	3%	35%	23%	32%
st. dev.	53.0%	14.7%	31.7%	0.8%	1.2%	1.2%	53.4%	13.7%	31.7%

* Apportionment calculated on the base of organic nitrogen in eEPS (method 2).

It can be seen from Figure 6.32 (see over) than "other organics" resulted in the major fraction of TOC. In particular, as for sEPS, in stage 1, proteins, carbohydrates and "other

organics" accounted for 25%, 16% and 59%, respectively. Differently, in stage 2, such fractions resulted in 34%, 25%, and 41%, respectively. These results can be explained by the fact that probably PACl addition removed more "other organics" from the bulk liquid than sEPSp and sEPSc, from a relative point of view (i.e., considering data in percentage).

As for eEPS, no significant variations between stage 1 and stage 2 were observed for all the eEPS fractions (52 and 57% for eEPSp, 3 and 4% for eEPSc and 44 and 40% for other eEPS organics), demonstrating that PACl reduced also other eEPS organics.

Overall, the TOC apportionment for bulk and the extracted-EPS evaluated over the entire experimental period is summarized in Table 6.30.

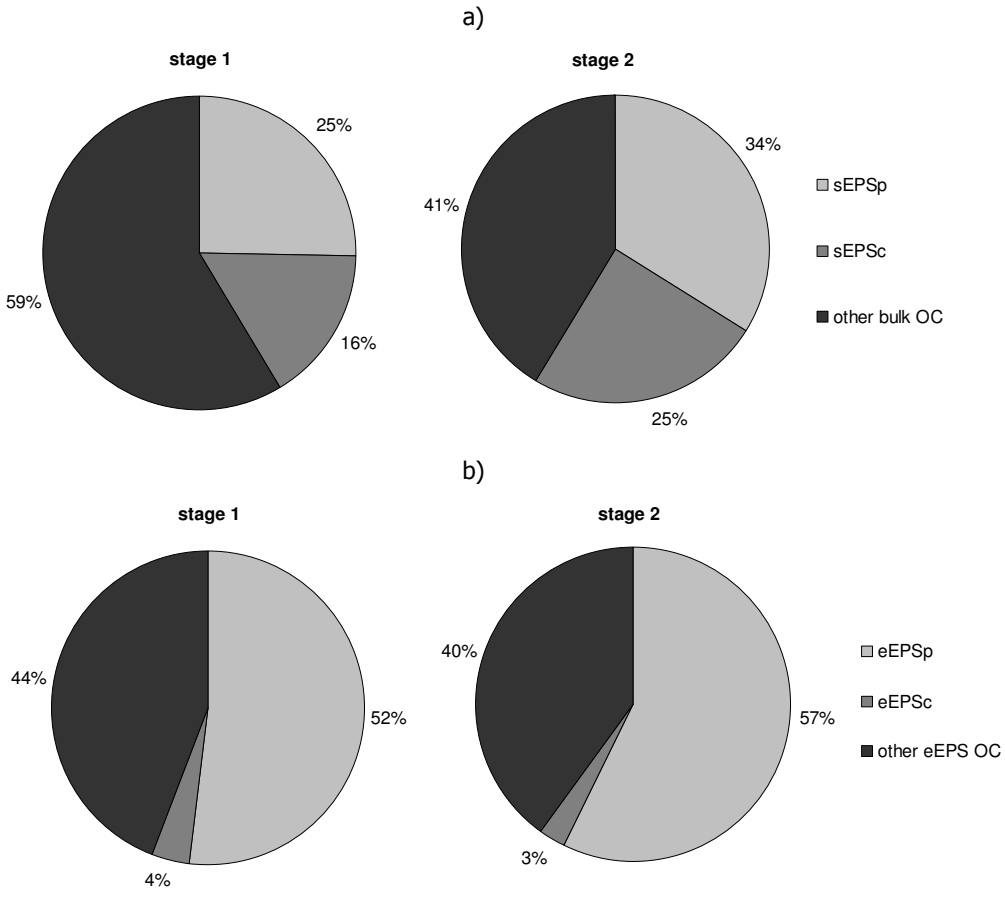

Figure 6.32. TOC apportionment of bulk (a) and extracted-EPS (b).

Table 6.29. TOC apportionment of bulk and extracted-EPS (average and standard deviations evaluated over the entire experimental period).

	proteins	**carbohydrates**	**other organics**
bulk	29±13.5%	19±11.6%	52±17.8%
eEPS	55±12.3%	3±1.3%	42±12.7%

Finally, taking into consideration the entire experimental period, TOC apportionment of bulk can be compared to TOC apportionment of influent wastewater and permeate, as shown in Figure 6.33.

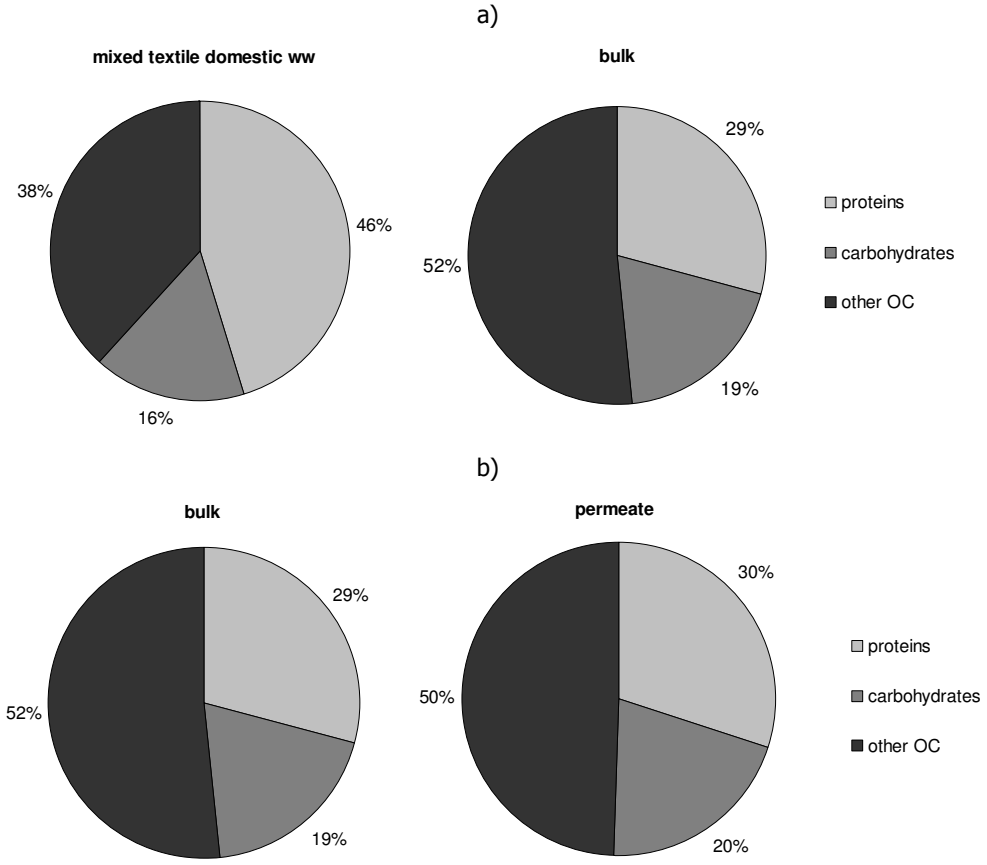

Figure 6.33. TOC apportionment of bulk against influent wastewater (a), and against permeate (b).

Influent wastewater was characterized by a relevant content of proteins and carbohydrates compared with bulk content, both considering absolute values and TOC fractionation. In particular, considering absolute values (see above, Table 6.25 and Table 6.26) the average protein content was 59.0 mg L^{-1} (bulk liquid average value=11.3 mg L^{-1}), whereas for carbohydrates an average value of 15.5 was observed (bulk liquid average value=7.3 mg L^{-1}). Moreover, with regards to TOC apportionment, proteins accounted for 46% (bulk liquid average value=29%) and carbohydrates for 16% (bulk liquid average value=19%). This high content of proteins and carbohydrates in wastewater against bulk can be explained considering two possible aspects. Firstly, proteins and carbohydrates in wastewater presented some affinities with flocs organic matrix and therefore adsorbing on it or, in general, creating chemical-physical interactions with it. However, proteins and carbohydrates in wastewater were of a different nature compared to proteins and carbohydrates detected in bulk (sEPSp, sEPSc), that were produced by bacteria for different specific purposes (see

section 2.5.1). In particular it is believed that proteins and carbohydrates in wastewater were more biodegradable than sEPSp and sEPSc because they accounted for a relevant fraction of organic pollution (62% of the wastewater TOC) which was removed effectively by the pilot MBR (see section 6.4).

6.5.2 Physical sludge characterization

Physical sludge characterization consisted of the determination of flocs strength using 2 indexes developed on purpose, i.e., SI_1 an SI_2 (see section 5.3.2, method A.6) and sludge filterability, measuring SRF and MFI (see section 5.3.2, method A.7). In particular, Figure 6.34 show the evolution over time of such parameters. As for sludge filterability, SRF and MFI were monitored only in stage 2 (grey area indicates the stationary phase).

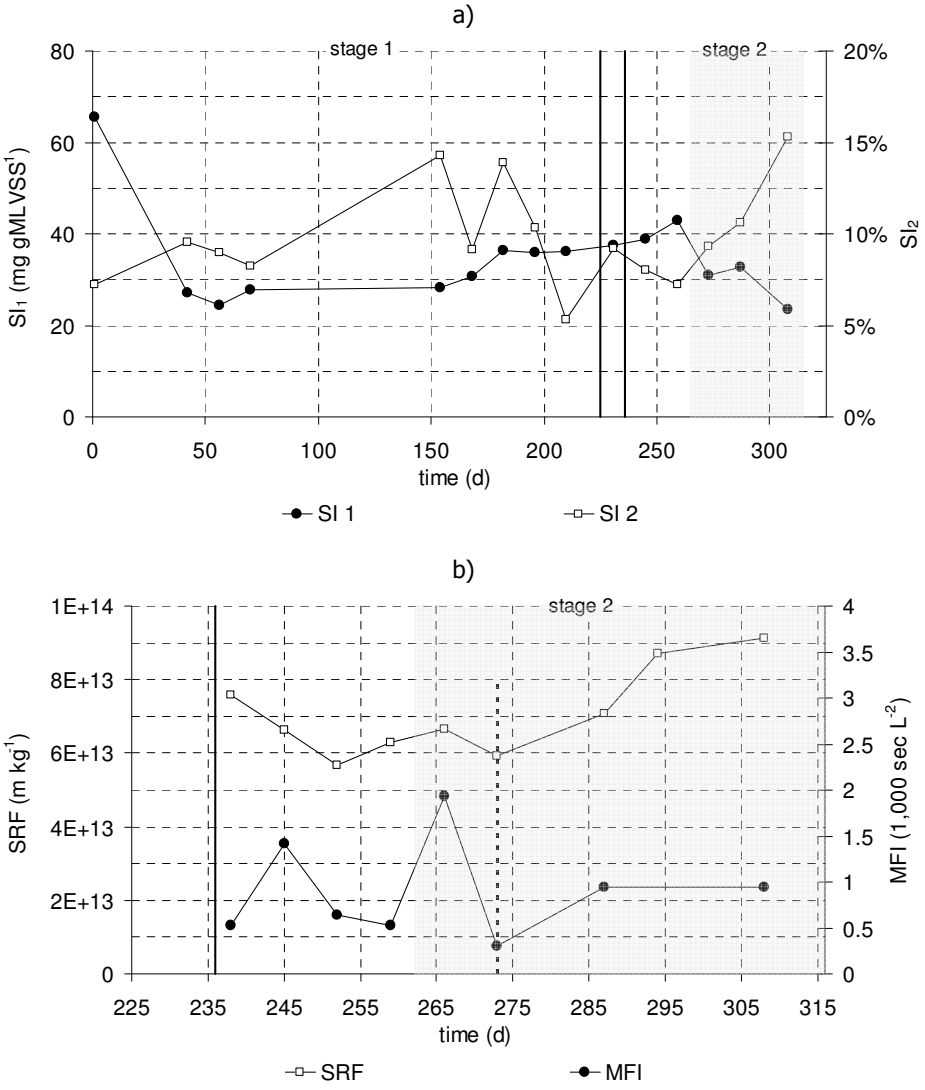

Figure 6.34. Floc strength indexes (SI_1 an SI_2, chart a) and filterability parameters (SRF and MFI, chart b) evolution over time.

With regards strength indexes, SI_1 indicates the divalent cations (sum of Ca^{2+} and Mg^{2+}) content in flocs per gram of MLVSS (mg $gMLVSS^{-1}$), whereas SI_2 indicates the percentage of low bounded divalent cations in flocs, defined as the fraction of cations extracted by thermal flocs break-up (see section 5.3.2, method A.3). According the divalent cation bridging (DCB) theory (Sobeck and Higgins, 2002) and the polymer bridging model (PBM) theory (Wilén at al., 2003; see section 2.5.2), divalent cations bridge negatively charged functional groups within the EPS aggregating cells and stabilizing flocs (see section 2.5.2). Therefore, the higher the values of SI_1, the better the flocs strength is. Differently, as for index SI_2, the higher the fraction of low bounded divalent cations, the slighter the compactness and strength of flocs are.

In stage 1, SI_1 and SI_2 varied in a wide range between 24.3 and 65.4 mg $gMLVSS^{-1}$ for SI_1, whereas for SI_2 between 5.3 and 14.3% (see above, Figure 6.34a). In particular the SI_1 highest value (65.4 mg $gMLVSS^{-1}$) was observed for the inoculum. Considering stage 2, during the transition phase, flocs strength improved slowly (a slight rise of SI_1 and a decrease of SI_2), but in the stationary phase the opposite trend was observed for both of the parameters, particularly from day 273 onwards, then reaching at the end of stage 2 the worse values observed in all the experimental period: 23.5 mg $gMLVSS^{-1}$ for SI_1 and 15.3% for SI_2. According to the DCB and PBM theories, such a behaviour can indicate a loss in flocs strength that affected also sludge filterability, particularly, SRF. In fact, Figure 6.34b (see above) shows a weak decreasing trend in SRF values for the first days of stage 2, then fluctuating around a value of $6 \cdot 10^{13}$ m kg^{-1}. But, from day 273 onwards (vertical dotted line in figure), a rise was observed and a value of $9 \cdot 10^{13}$ was reached at the end of stage 2. That corresponded to a significant variation of 50% in SRF values. Differently, with regards to MFI, it varied within a wide range but without (0.3÷1.9 1,000 sec L^{-2}) any particular trends.

In order to better understand the phenomenon of the loss in flocs strength and sludge filterability, the divalent cations content of the wastewater and of the permeate was analyzed (Figure 6.35a). It can be seen from the chart that, for almost the entire duration of the research, the dynamic over time of divalent cations showed the same pattern for wastewater and permeate, always having approximately the same value, indicating that no significant accumulation or release occurred in the pilot MBR. Differently, in the stationary phase of stage 2 (grey area in the figure), the permeate was characterized by significant lower values than the influent wastewater, indicating an accumulation of Ca^{2+} and Mg^{2+} in the reactor.

Therefore, in order to understand where divalent cations accumulated the concentration in mixed liquor and in bulk was analyzed (Figure 6.35b).

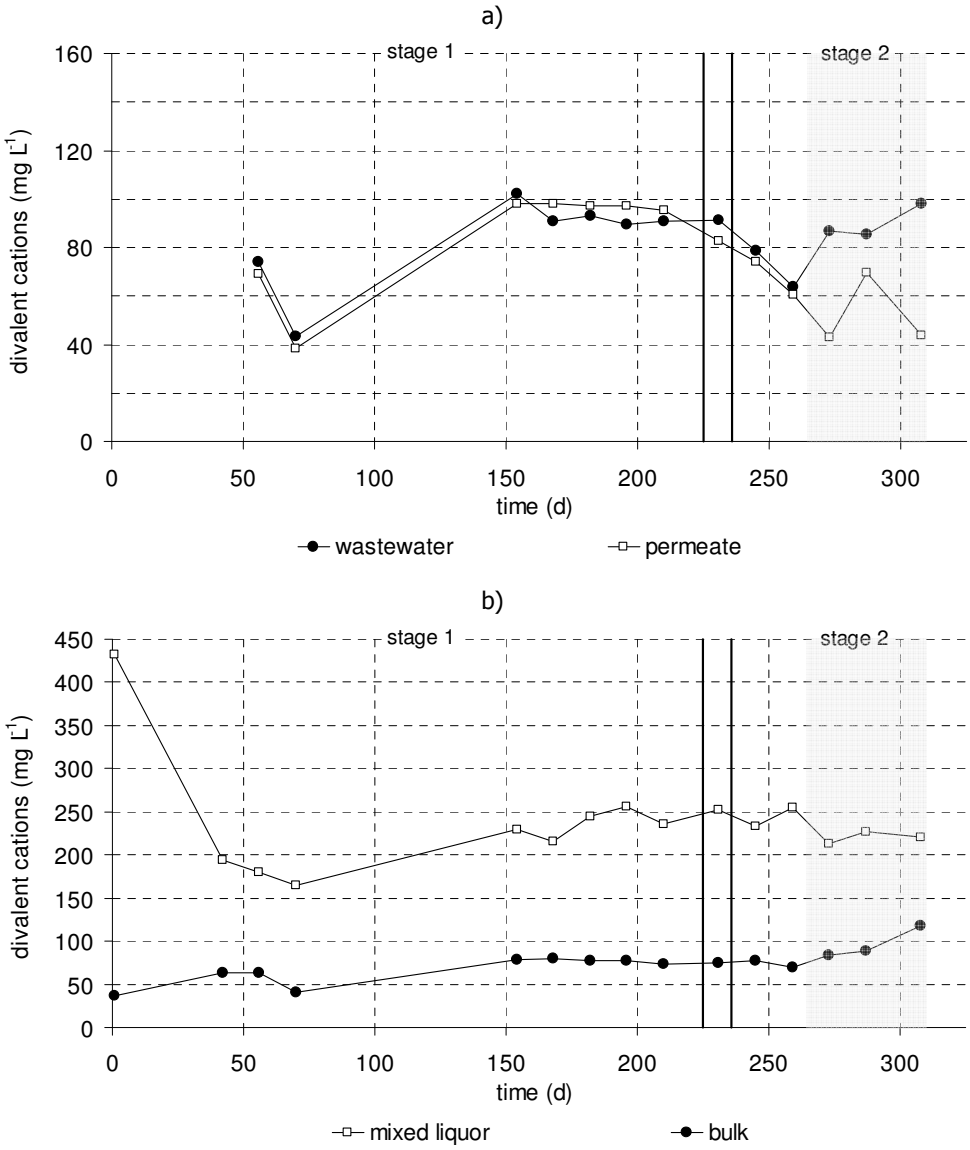

Figure 6.35. Divalent cations content (sum of Ca^{2+} and Mg^{2+}) in the influent wastewater and permeate (a), and in bulk and mixed liquor (b).

It can be seen from the chart in Figure 6.35b that in the stationary phase of stage 2 the cationic content of mixed liquor remained constant approximately at values of 225 mg L^{-1}. Differently, the bulk liquid cations showed a rise indicating a release of divalent cation from sludge flocs (difference between mixed liquor and bulk values). In particular, at the end of the transition phase of stage 2 the bulk cation content was the 27.4% (72.6% of cations within flocs) of the total mixed liquor concentration, whereas at the end of stationary phase the percentage doubled increasing to a value of 53.4% (46.6% of cations within flocs).

Moreover, correlating cations in bulk and in permeate (see below, Figure 6.36) it can be thought that, in the stationary phase of stage 2, divalent cations accumulated into the cake

or gel layer, forming on UF membranes during the operation of filtration. The effect of this phenomenon on fouling and filtration performances will be discussed in section 6.8.

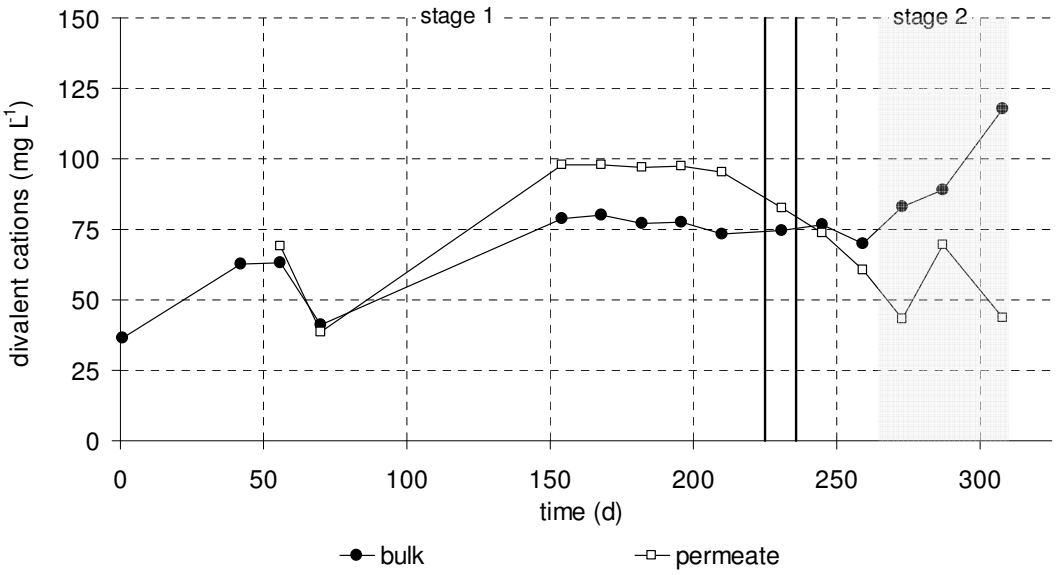

Figure 6.36. Divalent cations content (sum of Ca^{2+} and Mg^{2+}) in bulk and permeate.

6.5.3 Biological activity of heterotrophic and autotrophic bacteria

Biological activity of heterotrophic and autotrophic bacteria was assessed adopting method A.9 (see section 5.3.2).

In particular, the aim of this evaluation was the detection of eventual negative effects of PACl dosage on the heterotrophic and autotrophic bacteria. Therefore, method A.9 was applied twice, the first time at the end of stage 1 and the second at the end of stage 2.

Results presented in Table 6.30 showed values within the typical range for biological wastewater treatment (Metcalf and Eddy, 2003).

Moreover, results showed variations in kinetic constants, during the stage 2, within the COV of the methods, estimated to be approximately of 15% and therefore highlighting the absence of any drops in heterotrophic and autotrophic activities as it was also thought analyzing the MBR removal rates (see section 6.4).

Table 6.30. Results of biomass activity assessment performed at the end of stage 1 and stage 2.

	Measured parameter	end of stage 1	end of stage 2	variation
Heterotrophic activity	aerobic biomass growth yield on acetate Y_H ($g\ VSS_H\ g\ COD^{-1}$)	0.49	0.53	8%
	aerobic maximum growth rate $\mu_{20\ H}^{max}$ (d^{-1})	6.83	6.31	-8%
	maximum specific substrate consumption rate $v_{20\ H}^{max}$ ($g\ COD\ g\ VSS_H^{-1}\ d^{-1}$)	13.9	11.9	-15%
Autotrophic activity	AOB maximum specific substrate consumption rate $v_{20\ AOB}^{max}$ ($mg\ N\text{-}NH_4^+\ g\ MLVSS^{-1}\ h^{-1}$)	2.15	2.36	10%
	NOB maximum specific substrate consumption rate $v_{20\ NOB}^{max}$ ($mg\ N\text{-}NO_2^-\ g\ MLVSS^{-1}\ h^{-1}$)	2.35	2.11	-10%

6.6 Fouling monitoring and control by the selected flux enhancer

6.6.1 Filtration process and fouling monitoring

The monitoring of the filtration process was performed measuring TMP (see section 5.3.2, method A.9) over time as shown in Figure 6.37. It can be seen from the chart that TMP was characterized by a significant variability, particularly in stage 1 ranging from to 0.020 to 0.191 bar.

In the first 80 days TMP showed a progressive increasing, after that, between day 80 and day 130, a sequence of rapid decreases and increases and, then, a sort of TMP jump characterized by a very rapid variation.

The TMP jump was interrupted approximately at day 160 when some technical issues occurred (problems related to the suction performance of the process pump) and process pump was switched off for some hours, whereas membrane aeration was in operation. After that, when the pump was switched on, TMP was very low with values comparable with the first days of operation.

After day 175 the filtration process was not stable indicating a sudden rise in TMP both at day 180 and day 195. Close to the end of stage 1, in other 2 episodes the process pump was switched off because of technical issues.

Such variations in TMP values were not related to changes in temperature or MLSS concentration in the membrane tank, but they were probably due to fouling resistances as discussed below.

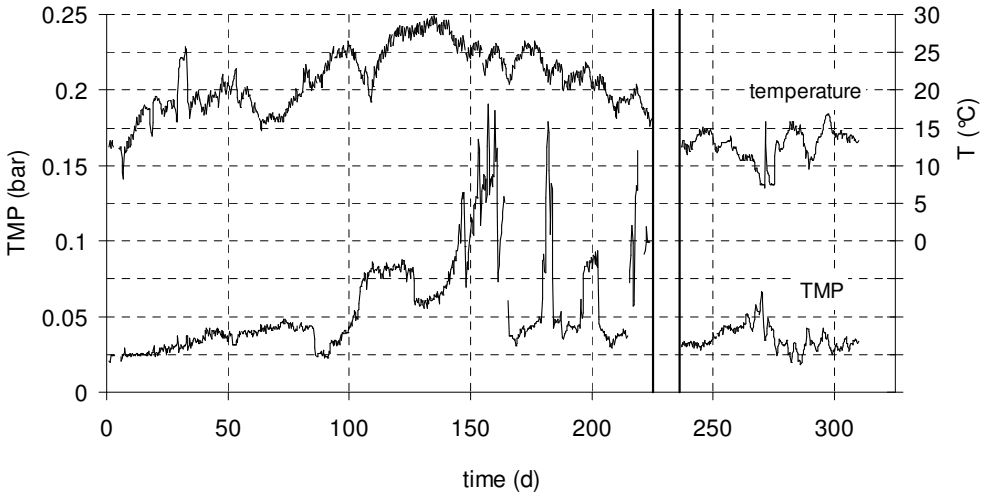

Figure 6.37. Evolution of TMP and mixed liquor temperature over time.

In stage 2, TMP values appeared to be more stable than in stage 1. Therefore, the dosage of PACl seemed to play an important role in the filtration process. However, to better understand this role, parameters such as permeability P_{20} and total resistance to filtration R were calculated and monitored over time (see section 5.3.2, method A.9), particularly to compare data at different temperature values properly and to discuss about fouling occurrence. In fact, fouling implies a rise in the resistance to filtration and a drop in membrane permeability (see section 2).

Statistic parameters for P_{20} and R related to stage 1 (s1), stage 2 (s2) and overall to the experimental period (o) are presented in Table 6.31, Figure 6.38 and Figure 6.39.

Table 6.31. Statistic parameters for TMP, P_{20} and R related to stage 1 (s1), stage 2 (s2) and overall to the experimental period (o).

	TMP (bar)			**P_{20}** (LMH bar^{-1})			**R** (m^{-1})		
	s1	s2	o	s1	s2	o	s1	s2	o
mean	0.057	0.036	0.051	223.8	349.3	255.9	2.2E+12	1.1E+12	1.9E+12
st. dev.	0.0324	0.0082	0.0297	113.03	69.49	117.21	1.34E+12	2.10E+11	1.26E+12
COV	57.1%	23.0%	57.9%	50.5%	19.9%	45.8%	61.6%	19.6%	66.4%
min	0.020	0.018	0.018	47.4	203.0	47.4	6.0E+11	5.8E+11	5.8E+11
max	0.191	0.066	0.191	600.7	621.5	621.5	7.6E+12	1.8E+12	7.6E+12

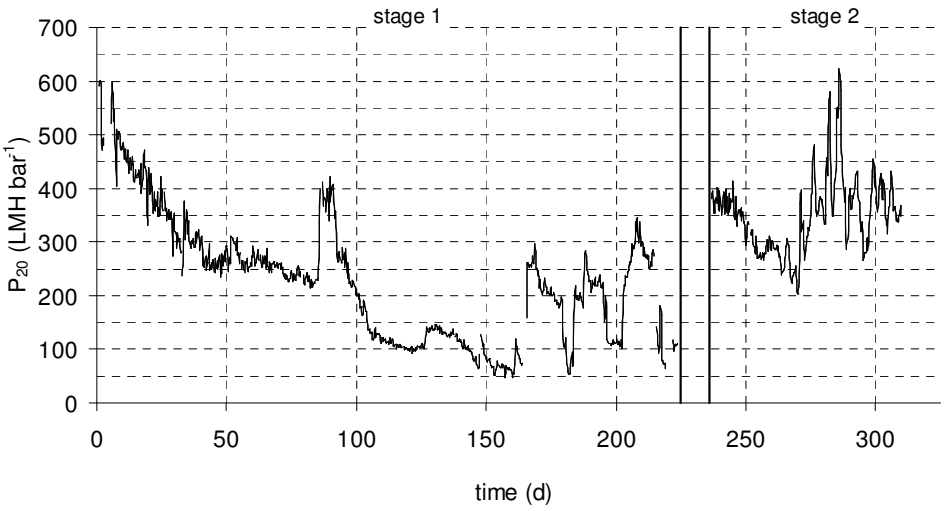

Figure 6.38. Evolution of P_{20} over time.

With regards to permeability, it is clear from the chart that stage 1 and stage 2 presented different P_{20} patterns. Overall, in stage 1, permeability showed a decreasing trend from the beginning of the stage (600 LMH bar^{-1}) to day 160 approximately (50 LMH bar^{-1}). Then, an irregular variation occurred with rapid rises and drops.

Differently, in stage 2, a decreasing trend was observed only in the transition phase (from 400 to 200 LMH bar^{-1}). In the stationary phase (from day 260 onwards) an slight increase was detected and then permeability fluctuated around 350 LMH bar^{-1}. According to these findings the PACl addition at the optimum dose resulted in a good control strategy for fouling. Additional information on the role of PACl is provided in section 6.6.3, where the R apportionment is evaluated .

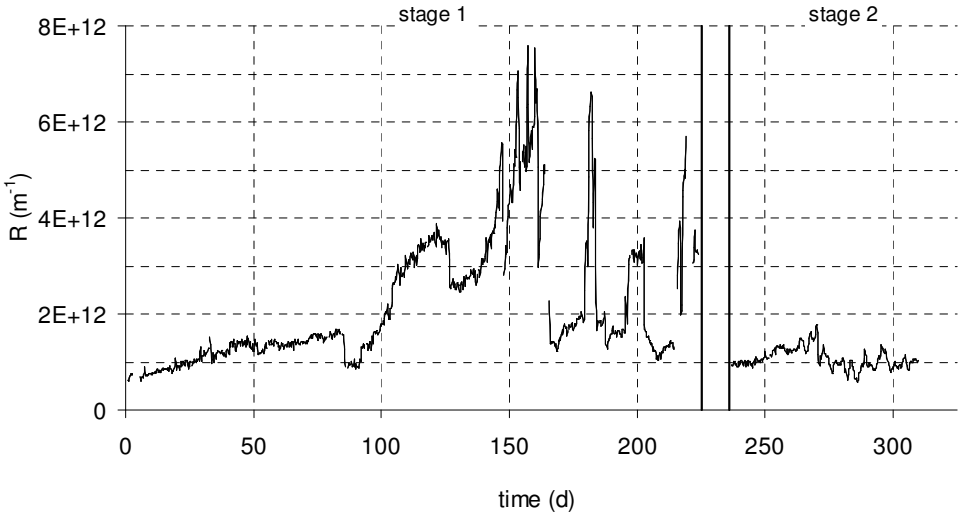

Figure 6.39. Evolution of R over time.

6.6.2 Efficiency of membrane cleanings

Main membrane cleanings were performed three times, particularly at the beginning of the research (before the MBR start-up) and before each stage (i.e., stage 1 and stage 2). In the first main cleaning, since the UF modules were new, only step B (sodium hypochlorite soaking) was performed. Differently, in the others, the complete procedure was executed (see section 5.3.2, method A.10). As discussed in the design of experiments section (see section 4.2.1), the purpose of main cleaning was not to recover membrane permeability because of severe fouling, but the purpose was to operate with clean membranes (i.e., comparable initial conditions) in each stage.

Table 6.32 shows efficiencies of the complete membranes cleanings, evaluated according to method A.10 (see section 5.3.2) and therefore considering membrane permeability measured in water tests, that is, P_{20} (LMH bar^{-1}): the higher P_{20} , the better the efficiency is. In particular, cleaning 1 and 2 are the complete cleaning performed before beginning stage 1 and stage 2, respectively.

It can be seen from the table that the two UF modules were characterized by different permeability (696 and 878 LMH bar^{-1} for module 1 and 2, respectively). Probably, this was due to little differences in UF modules, maybe related to the number of open hollow fibers. In fact, during the manufacturing, hollow fibers are fixed to the bottom and the top of the UF modules using a special glue that sometimes can occlude fibers bores.

Table 6.32. Evaluation of P_{20} (LMH bar^{-1}) during tests with water after each cleaning step.

		P_{20} module 1 (LMH bar^{-1})	**P_{20} module 2** (LMH bar^{-1})
clean modules		696	878
cleaning 1 (march 2010)	step A (physical cleaning)	268	357
	step B (NaOCl cleaning)	458	590
	step C (basic cleaning)	433	540
	step D (acid cleaning)	530	736
cleaning 2 (october 2010)	step A (physical cleaning)	359	354
	step B (NaOCl cleaning)	619	594
	step C (basic cleaning)	556	615
	step D (acid cleaning)	695	721

The efficiency of cleanings can be seen in Figure 6.40, where P_{20} data were plotted against the 4 steps of the procedure.

As for module 1 (Figure 6.40a) it can be seen from the chart that cleaning 2 was more effective than cleaning 1, particularly giving a P_{20} value after step D very close to the original value of the new membranes. Differently, with regards to module 2 (Figure 6.40b), both cleaning gave approximately the same results.

Overall, the cleaning procedures 1 resulted in P_{20} recovery factors (i.e., the ratio between P_{20} after step D and P_{20} for new membranes) of 76.1% and 83.9% for module 1 and module 2, respectively. Differently, the cleaning procedures 2 resulted in recovery factors of 99.9% and 82.2% for module 1 and module 2, respectively.

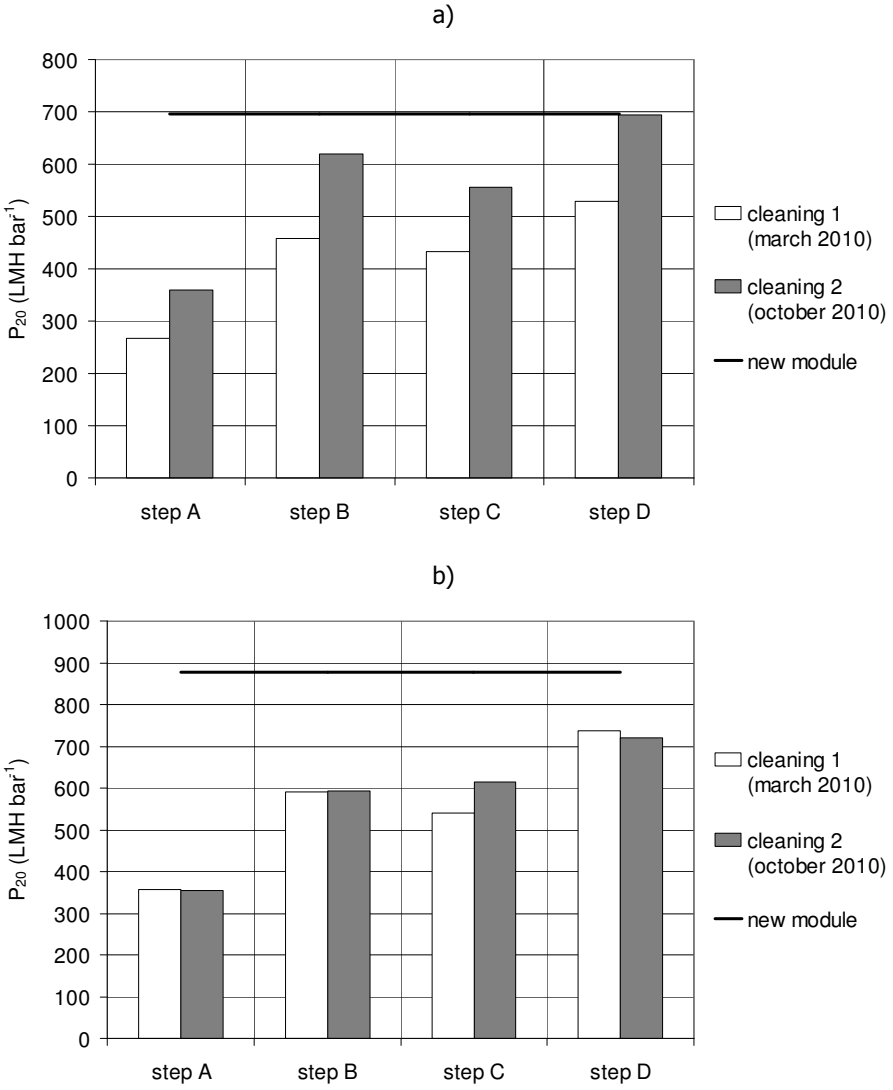

Figure 6.40. P_{20} values in water tests after each step of the cleaning procedure: a) UF module 1; b) UF module 2.

Considering the effectiveness of each step, it came out that the basic cleaning (step C) did not produce any increase in permeability values. Differently, NaOCl cleaning (step B) and acid cleaning (step D) improved P_{20} considerably. In particular, their effectiveness can be compared evaluating the increase in permeability data. In particular, the effectiveness of step B can be assessed consider the P_{20} increase against step A; whereas the effectiveness of step D can be assessed consider the P_{20} increase against step B. Results are shown in Figure 6.41.

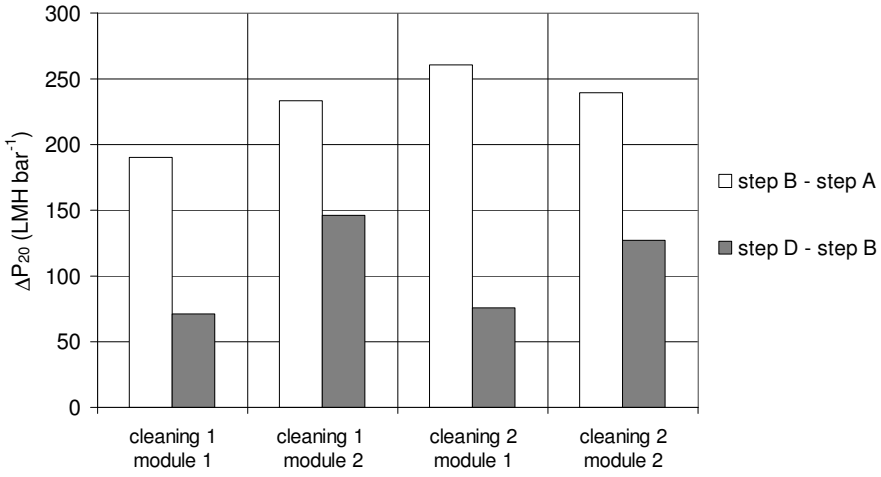

Figure 6.41. Differences in P_{20} values (ΔP_{20}) in water tests: a) UF module 1; b) UF module 2.

Overall, the NaOCl cleaning (step B) increased membrane permeability of 231±29.4 LMH bar^{-1}, whereas for the acid cleaning (step D) the increase was 105±37.3 LMH bar^{-1}. Therefore, NaOCl cleaning was the most effective step in all the procedure. However, the acid cleaning was important, particularly in the cleaning 2, where the almost complete recovering of the membrane permeability was obtained for module 1, as discussed above.

Generally, the NaOCl cleaning is considered to be related to the removal of the organic fouling, whereas the acid cleaning to the removal of inorganic fouling. Actually, since organic and inorganic fouling occur simultaneously with a synergic effect through biological precipitation[3], it is believed that both cleanings remove both fouling types. Clearly, NaClO removes more organics and acid solution removes more inorganic substances. According to Kim and Yoon (2010) the sequence NaOCl-acid cleanings is effective because the structure of organic compounds combined with calcium becomes loose by the addition of the NaOCl,

[3] Biological precipitation indicates the interaction between metal ions and the acidic functional groups of organic matter, resulting in complexes and building a compact gel layer (see section 2.4.1).

thereby releasing calcium more easily from the membrane by applying the acid cleaning agent. On the other hand, the removal of calcium can lead to a destructuration of organic precipitates related to residual organic fouling.

6.6.3 Apportionment of the total resistance to filtration

The apportionment of the total resistance to filtration was performed using method A.11. As discussed in the material and method section (see section 5.3.2), the method was applied at the beginning and the end of each stage using data from water tests performed during cleaning procedures (see above, section 6.6.2) and data from P_{20} monitoring of the pilot. Since the method can not be applied to the two UF modules separately, results shown in Table 6.33 must be considered as average values for the entire filtration system.

Table 6.33. Evaluation of membrane resistance (R_m), resistance by cake layer formed on the membrane surface (R_c) and fouling resistance caused by pore restriction and adsorption of foulants onto the membrane pore wall or surface (R_f) at the beginning and the end of each stage (stage 1 and stage 2.

	R_i	**Value** (m^{-1})
new membranes	R_m	4.6E+11
1 - beginning of stage 1	R_{f1}	1.2E+11
	R_{c1}	2.3E+10
2 - end of stage 1	R_{f2}	5.5E+11
	R_{c2}	2.2E+12
3 - beginning of stage 2	R_{f3}	4.4E+10
	R_{c3}	4.4E+11
4 - end of stage 2	R_{f4}	1.2E+11
	R_{c4}	4.5E+11

Data from Table 6.33 were then considered to investigate the effect of flux enhancer on reversible (i.e., fouling related to R_c) and irreversible fouling (i.e., fouling related to R_f).
In particular, for the latter, the "average fouling rate", FR (m^{-1} d^{-1}), was introduced and calculated (see section 5.3.2, method A.11). Values of $1.90 \cdot 10^9$ and $1.04 \cdot 10^9$ m^{-1} d^{-1} were found for stage 1 and stage 2, respectively. Therefore, it is clear that the addition of PACl, also at low doses, reduce the average build up rate of irreversible fouling. In particular, in this a study, the addition of PACl resulted in an average irreversible fouling rate approximately half the value observed in the control period (i.e., stage 1).
In order to investigate about reversible fouling, some assumptions referred to the evolution over time of R_f must be made. In particular, it is believed that R_f, generally, is characterized by a dynamic behaviour (i.e., the actual fouling rate) that can not be negative during

filtration operation because of the definition of irreversible fouling. In fact, R_f can diminished only interrupting the filtration and performing chemical cleanings and therefore the following general equation can be defined:

$$\frac{dR_f}{dt} \geq 0$$

Then, it was assumed that the dynamic could be described with a constant fouling rate equal to the average irreversible fouling rate, as follows:

$$\frac{dR_f}{dt} = FR$$

The solution of this differential equation is a linear equation where initial conditions ($R_{f,0}$) were known for each stage, as shown Table 6.33 :

$$R_f(t) = R_{f,0} + FR \cdot t$$

Finally, using the solution equation, it was possible to estimate R_f for the overall duration of stage 1 and 2, and also R_c (see section 5.3.2, method A.11) was evaluated over time as the difference among R and (R_m+R_f) (Figure 6.42).

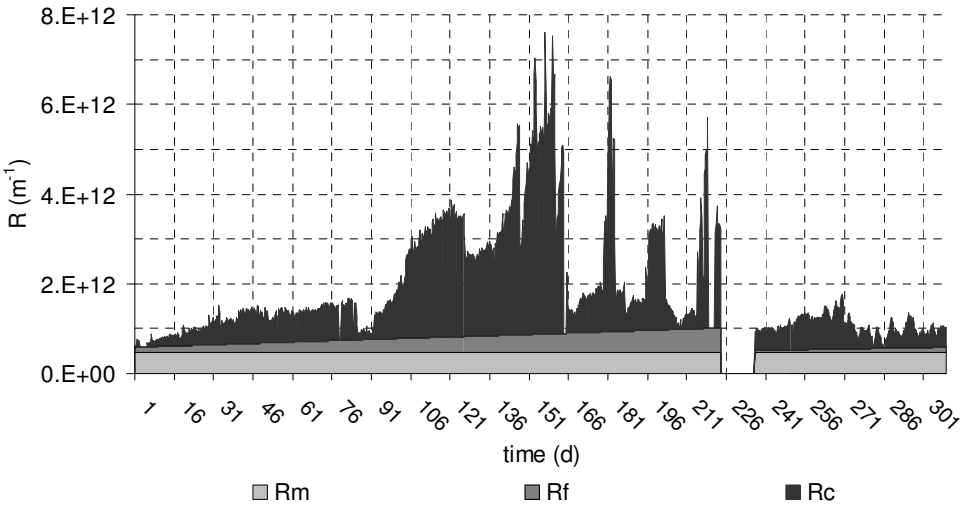

Figure 6.42. Apportionment of the total resistance to filtration over time.

It can be seen from the chart (Figure 6.42) that the so called "reversible fouling" (i.e., removable fouling by physical strategies such as relaxation, RX, or backflushing) and the related R_c values resulted in a progressive increasing tendency in the first 80 days. Then, R_c showed an outline with a rapid rise between day 80 and day 130, probably due to sludge

characteristics changes. In fact, it is believed that during stage 1 sludge characteristics varied to large extent because the inoculum was from a CASP and when in the MBR it underwent different conditions from a biological and a physical point of view. Moreover, the addition of sodium acetate into the MBR (from day 53 onwards) could have affected the bacterial community composition, the formation/elimination of soluble-EPS and sludge characteristics. For instance, McAdam et al. (2007) observed that the addition of acetic acid had a great influence on floc stability resulting in the formation of weakly flocs. On the other hand, considering physical conditions, turbulence in MBRs could be an important factor affecting the sludge structure and maybe implying a more sticky cake on membranes, difficult to be removed by aeration during the break phase of relaxation. In particular, it is believed that such a sticky cake layer was responsible for the TMP jump seen approximately around day 130 in Figure 6.37. Moreover, as discussed above, the TMP jump was then interrupted approximately at day 160 when some technical issues occurred (problems related to the suction performance of the process pump) and process pump was switched off for some hours, whereas membrane aeration was in operation. In this situation, the effect of membrane scouring was effective because when the pump was switched on, R_c values were recovered. Moreover, as discussed above, after day 175 the filtration process was not stable indicating a sudden rise in TMP both at day 180 and at day 195. In such episodes, it is thought that the sticky nature of cake layer induced a rapid increase in cake thickness till aeration became more effective in cake removing implying its detachment. However, such behaviours were not observed during stage 2, when PACl was added. In particular, R_c was controlled properly highlighting the importance of PACl at the dosage tested. Moreover, after day 273 Rc values appeared to be lower than in the first weeks of stage 2.

Finally, it is interesting to stress the fact that in this study R_c was the most relevant R fraction in decreasing membrane permeability and accounted for 52.9±19.78% and 46.9±11.39% in stage 1 and stage 2, respectively, followed by R_m with values of 28.8±14.56% and 45.0±8.95% in stage 1 and stage 2, respectively, and by R_f with values of 18.3±8.21% and 8.1±3.08% in stage 1 and stage 2, respectively (Table 6.34).

Table 6.34. Percentage of the total resistance to filtration related to stage 1 (s1), stage 2 (s2) and overall to the experimental period (o).

	R_m (m^{-1})			**R_f** (m^{-1})			**R_c** (m^{-1})		
	s1	s2	o	s1	s2	o	s1	s2	o
mean	28.8%	45.0%	33.0%	18.3%	8.1%	15.7%	52.9%	46.9%	51.3%
st. dev.	14.56%	8.95%	15.10%	8.21%	3.08%	8.51%	19.78%	11.39%	18.19%

In conclusion, the addition of PACl resulted in (see also Figure 6.43, showing average percentage values of the different fractions of the total resistance of filtration):

1. a more stable operation of UF modules;
2. the reduction of R_f and the irreversible fouling rate FR, the latter being half the value observed in the control period (i.e., stage 1);
3. the reduction of R_c having an average value comparable to that of the new membrane R_m.

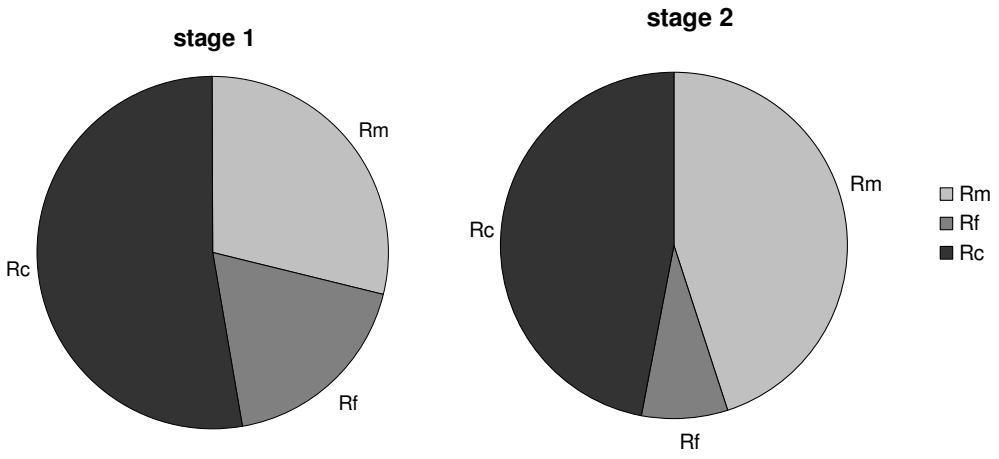

Figure 6.43. Average apportionment of the total resistance to filtration during stage 1 and stage 2.

6.7 Fouling propensity assessment using a modified flux step method for the critical flux determination

6.7.1 Comparison of the standard and modified procedure

Figure 6.44 shows results of the flux-step standard and modified procedures for the critical flux determination. It can be seen from the chart that the modified method was characterized by:

- low values of TMP, particularly at high fluxes;
- a linear variation of TMP over time in each flux-step both in the ascending and descending phases (linear correlation coefficient > 0.99);
- a more symmetric profile, indicating a higher reversibility of the TMP during the test.

These differences were related to the introduction of relaxation (15:5) in the modified procedure, that removed and then permitted a new formation of the cake layer in each flux-

step. In this way, the resistance of the cake layer formed was independent from the previous flux-steps.

Differently, in the standard procedure the sudden increase of flux between two consecutive steps could imply a compression of the cake layer formed in the previous step and then an increase in its thickness resulting in higher cake resistances and higher TMP values for the standard procedure compared to the modified one.

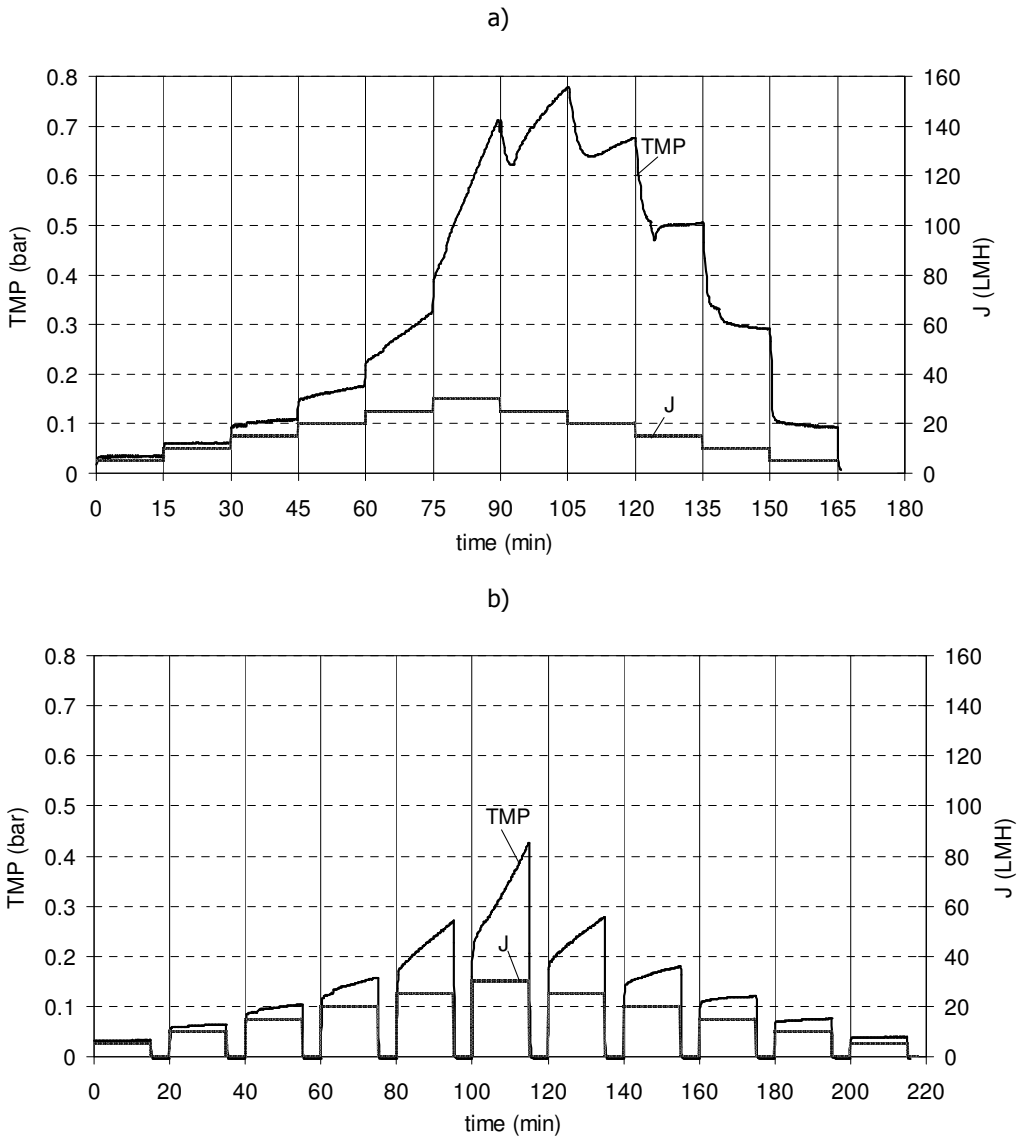

Figure 6.44. Results of the standard (a) and the modified flux step method (b).

With regards to the modified method, the TMP profile of each flux step was modelled. Firstly, the general equation of UF/MF membrane filtration (see section 2.3.3, eq. 2.3) and the resistance in series model (see section 2.4.1, eq 2.10) were taken into account, as follows:

$$J = \frac{TMP}{\mu_T \cdot R}$$

$$R = R_m + R_c + R_f$$

where J is the flux (m s^{-1}), TMP is the transmembrane pressure (Pa), μ_T the dynamic viscosity of the permeate at temperature T (Pa s^{-1}), R the total hydraulic resistance to filtration (m^{-1}), R_m the membrane resistance (m^{-1}), R_c the cake layer resistance (m^{-1}), and R_f the fouling resistance caused by pore restriction and adsorption of foulants onto the membrane pore wall or surface (m^{-1}).

Then, as in short term experiments the fouling phenomenon can be described taking into consideration only the reversible fouling, i.e., the cake layer formation (see section 2.5.1), the cake layer resistance (R_c) equation from the conventional cake filtration theory (see section 2.5.1, equation 2.11) was also considered:

$$R_c = \alpha \cdot \frac{V \cdot C_b}{S}$$

where α is the specific cake resistance (m kg^{-1}), V the permeate volume (m^3), S the membrane surface area (m^2), whereas C_b represents MLSS concentration (kg m^{-3}).

A parameter, f, was also introduced in the cake layer resistance equation since the conventional cake filtration theory does not consider the effect of aeration adopted in MBRs. In particular, f represents the ratio of the cake mass forming on membrane surface in aerated conditions over the cake mass forming without aeration (0÷1):

$$R_c = \alpha \cdot \frac{f \cdot V \cdot C_b}{S} \qquad 6.1)$$

In particular, the value of f (0÷1) is related to balance of the convective (due to J) and back transport (provided by aeration). As the air flowrate employed was constant in each flux step, f can be 0 with low fluxes, between 0÷1 at intermediate fluxes and 1 with very high fluxes.

However, taking into consideration that the volume V of the permeate collected over time within a cycle is the product of the flow rate ($m^3\ s^{-1}$) and the filtration time t (s), and also considering the definition of J (see section 2), equation 6.2 follows.

$$R_c = (\alpha \cdot f \cdot C_b) \cdot J \cdot t \qquad 6.2)$$

Moreover, assuming α constant within a generic flux step, the differential equation describing the R_c evolution over time can be developed (eq. 6.3) and the parameter α' ($\alpha \cdot f \cdot C_b$) can be introduced, as follows:

$$\frac{dR_c}{dt} = (\alpha \cdot f \cdot C_b) \cdot J = \alpha' \cdot J \qquad 6.3)$$

Then, taking into account the general equation of UF/MF membrane filtration and the resistance in series model (see above) at constant flux, it comes out equation 6.4:

$$TMP = \mu_T \cdot J \cdot (R_m + R_c + R_f) \qquad 6.4)$$

Being R_m and R_f constant in short filtration tests, the differential equation describing TMP variation over time within a flux step can be evaluated and combined with eq. 6.3, as follows:

$$\frac{dTMP}{dt} = \mu_T \cdot J \cdot \frac{dR_c}{dt} \qquad 6.5)$$

$$\frac{dTMP}{dt} = \alpha' \mu_T J^2 \qquad 6.6)$$

Finally, the solution of eq. 6.6 can be calculated easily (eq. 6.7) and, for each flux step, linear regressions can be employed to fit eq. 6.7 to experimental TMP data. In this way, estimates of α' ($\alpha' = \alpha \cdot f \cdot C_b$, m^{-2}) can be obtained, where α' is an index of the cake specific resistance to filtration, as correlated to α, at the experimental conditions, i.e., C_b (5.5÷6 g MLSS L^{-1}) and f.

$$TMP = (\alpha' \cdot \mu_T \cdot J^2) \cdot t + TMP_0 \qquad 6.7)$$

6.7.2 Definition of relevant parameters describing fouling propensity

In order to evaluate the fouling propensity of an MBR sludge, three relevant parameters were defined and then calculated, as follows:

- critical flux, Jc (LMH);
- the irreversibility factor, IF (-);
- the compressibility factor, CF (m^{-2} bar^{-1}).

In particular, critical flux and IF were evaluated for both of the procedures, whereas CF was estimated only for the modified method.

Critical flux determination. The evaluation of critical flux was executed according to the approach proposed by Le-Clech et al. (2003a). In particular, for each flux-step, two TMP values were reported: the initial TMP (TMP_i), defined as the TMP obtained after the initial sudden increase in filtration resistance following the step increase in flux, and the final TMP (TMP_f), defined as the TMP at the end of the step. Practically, the TMP_i was taken arbitrary as the TMP value 30s after the beginning of the flux-step. Then, for each flux-step, the average rate of TMP increase was calculated using equation 6.8:

$$\frac{dTMP}{dt} = \frac{TMP_f - TMP_i}{\Delta t} \qquad 6.8)$$

where Δt represents the duration of each flux-step (15 min).
Finally, the Jc value was defined from an arbitrary dTMP/dt limit, fixed at 2 mbar min^{-1}, as shown in Figure 6.45.

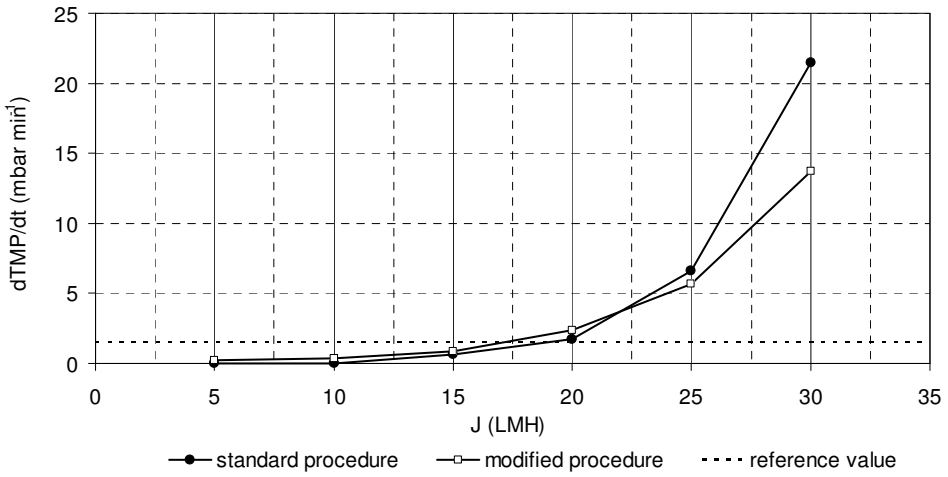

Figure 6.45. TMP rate against flux J for each step (5 LMH to 30 LMH).

IF determination. The irreversibility factor is defined by equation 6.9 and it represents the ratio of the average TMP values calculated for the last flux-step and the first flux-step, both referring at a flux of 5 LMH but in the descending and the ascending phases, respectively:

$$IF = \frac{\overline{TMP}_{last\ step}}{\overline{TMP}_{firtsl\ step}} \qquad 6.9)$$

Figure 6.46 shows average TMP values for each flux-step plotted against flux. In this chart, the standard procedure was characterized by a significant hysteresis loop, due to elevated differences between average TMP in the descending and the ascending phases. Differently, the modified procedure showed a very narrow loop indicating a more reversible behaviour of

sludge filtration. The parameter IF provides an idea of the TMP recovery of the hysteresis loop. In particular, the higher IF, the lower the TMP recovery is. Therefore, high values of IF indicate an elevated degree of the TMP irreversibility at the end of the test.

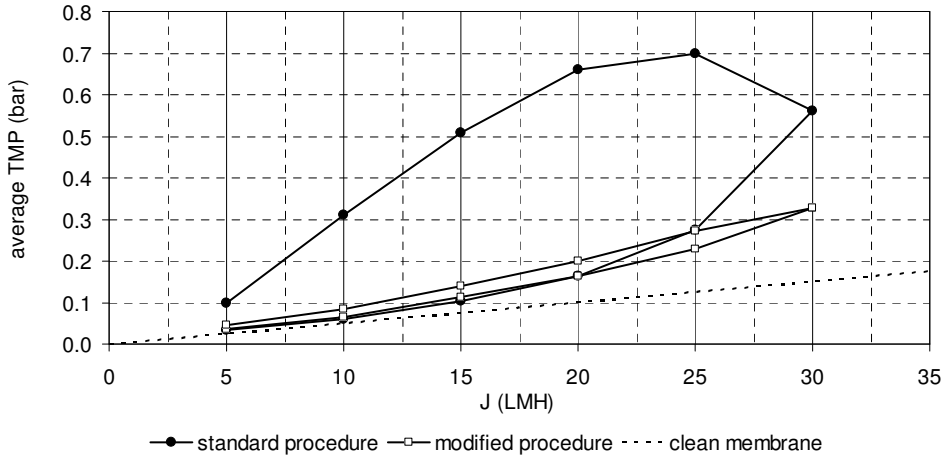

Figure 6.46. Average TMP value against flux J for each step (5 LMH to 30 LMH and 30 LMH to 5 LMH).

CF determination. The compressibility factor was evaluated only for the modified method. Firstly, for each flux-step linear regressions were employed to fit equations 6.7 to the TMP profiles for the determination of α', as discussed above. Then, α' was plotted against the average TMP values of each flux-step, as shown Figure 6.47. Finally, a linear regression was carried out and the compressibility factor CF was defined as the slope of the best fitting equation. Therefore CF factor is an index of the increasing tendency in cake resistance due to cake compressibility at the experimental condition.

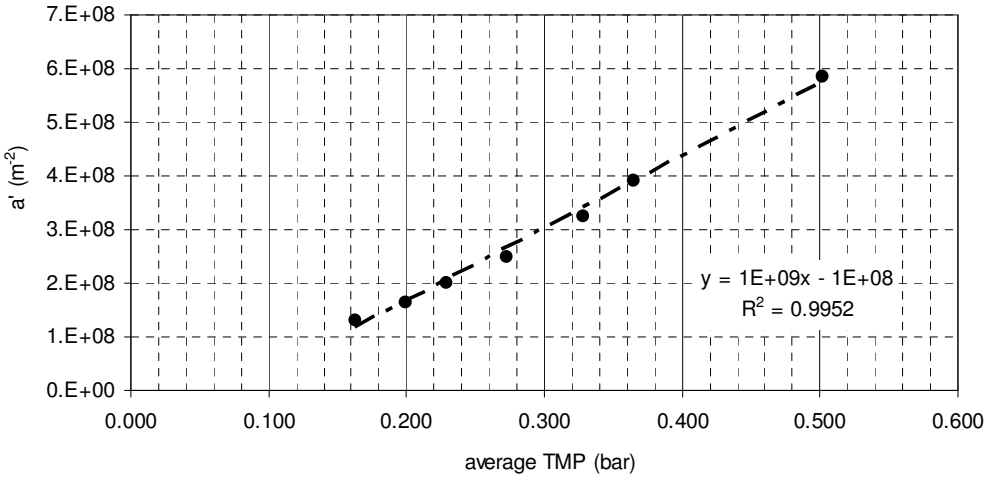

Figure 6.47. α' against the average TMP value for each step (5 LMH to 30 LMH and 30 LMH to 5 LMH).

6.7.3 Application of the method on a weekly basis to describe sludge fouling propensity

The evolution over time of the relevant parameters defined in the previous section are presented herein. In particular, Figure 6.48 shows Jc values according to the "standard" and "modified" procedures. Since Jc detection regards data collected in the first steps of the flux step methods, the two procedures did not present significant differences. However considering the modified procedure, Jc fluctuated around a value of 18 LMH from day 231 to day 266 without any particular trend. Differently, it can be seen from the chart that at day 273 Jc showed a peak reaching a value close to 20 LMH indicating therefore a decrease in the fouling propensity of the sludge. In fact, the higher the Jc value, the wider the sub critical range is. However, Jc data showed a drop from day 286 onwards reaching the minimum value (15.2 LMH) overall observed at day 294. The critical flux procedure therefore showed a higher fouling propensity of the mixed liquor after day 273. No sign of these effects was however detectable in the pilot plant operation, as TMP and Rc remained stable (see section 6.6.1, Figure 6.37 and Figure 6.39). The reduction of Jc after day 286 was consistent with data related to sludge filterability and flocs strength (see section 6.5.2).

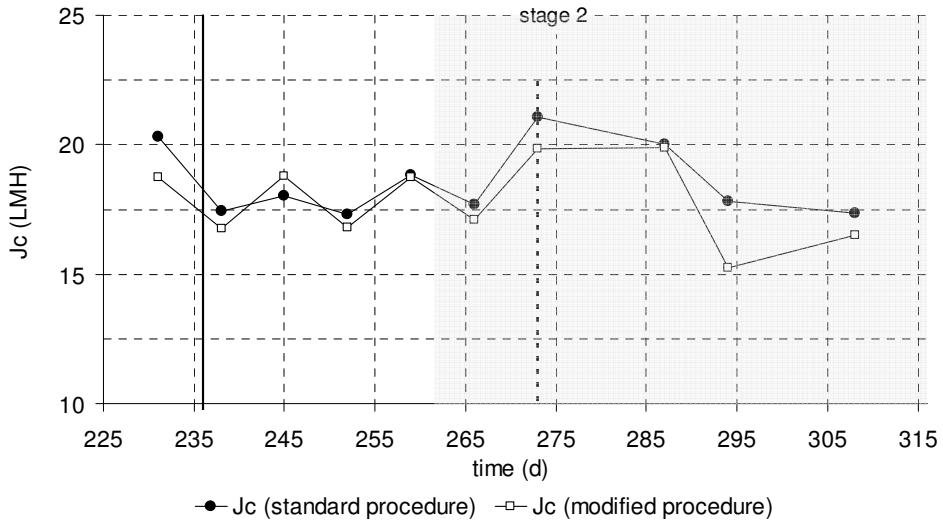

Figure 6.48. Critical flux values according to the "standard" and "modified" procedure in stage 2.

With regards to factors IF, indicating the degree of the TMP irreversibility in the test for the standard procedure and the modified one, results are shown in Figure 6.49 (see over). Firstly, it can be seen from the chart that the outcomes of two procedure were very different. In fact, the IF parameter, contrary to Jc, is not related only to the first steps of the flux step methods, but it provides information on the overall test being the ratio of the

average TMP in the last step over the average TMP of the first step, both of them at 5 LMH. The higher the ratio (i.e., IF), the higher the TMP irreversibility.

In particular, the standard method showed approximately IF values double that of the modified one. In fact, it always was between 2 and 4, whereas the modified IF was between 1 and 1.5. Since fouling in short batch test is related to the reversible fouling, i.e., the formation of the cake layer, the irreversibility in TMP values along the flux step methods are due to the characteristics of the cake. The modified method permitted a more complete regeneration of the cake layer at each step because of the relaxation performed. Differently, the standard method do not provide this possibility and therefore the cake became thicker and compressed along the procedure, therefore implying higher values of IF. However, IF provided the same information of Jc indicating an increase in values from day 273 and day 286.

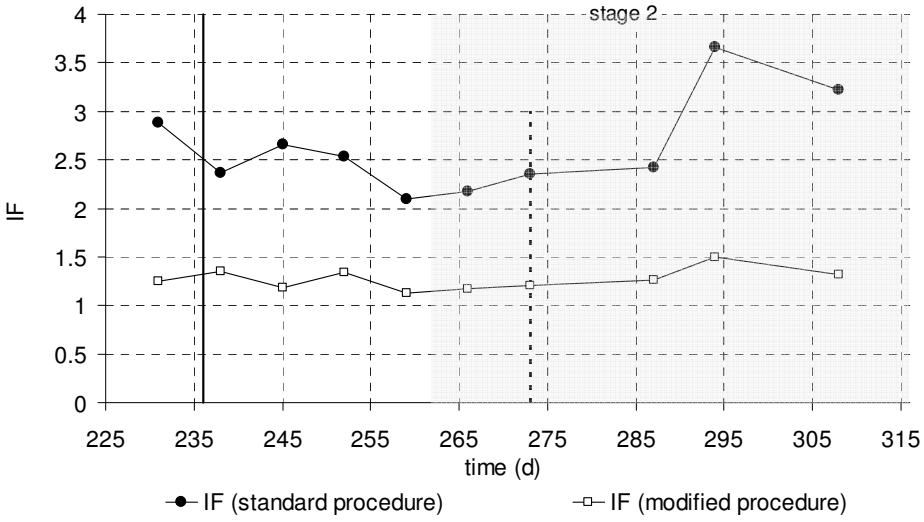

Figure 6.49. Evaluation of IF for the "standard" and "modified" procedure in stage 2.

Finally, taking into consideration the CF factor, being an index of the increase in cake compressibility, results are shown in Figure 6.50. It can be seen from the chart that in the transition phase of stage 2 there was a decrease in CF factor indicating a less compressible cake formation as also it was found observing strength indexes (see section 6.5.2, Figure 6.34).

Then, from day 273 onward CF showed a rise from a value of $1.25 \cdot 10^9$ bar^{-1} m^{-2} to approximately a value of $3.5 \cdot 10^9$ bar^{-1} m^{-2}, at the end of stage 2.

Again, such results are consistent with previous relevant parameters of the flux step methods, flocs strength indexes and sludge filterability, as discussed in section 6.5.2.

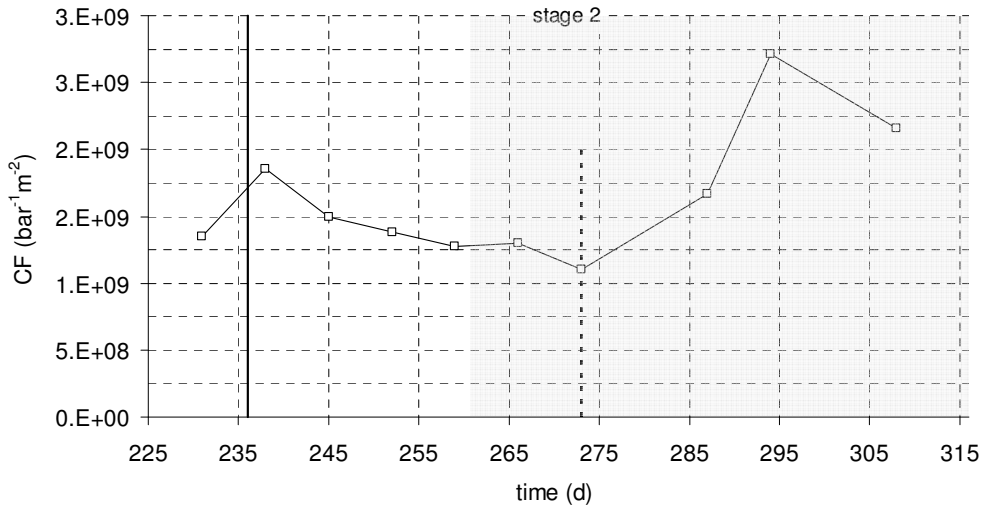

Figure 6.50. Evaluation of CF for the "modified" procedure in stage 2.

6.8 Main conclusions about the effects of the selected flux enhancer addition

Table 6.35 summarizes the effects of PACl added at a dose of 12.5 mg $gMLSS^{-1}$ on permeate quality, biomass characteristics, sludge fouling propensity and fouling control.

As for permeate quality, considering the ordinary macro-parameters, the addition of PACl resulted in a quality improvement for COD (removal rate with PACl of 91% vs removal of 86% and 76% during control periods) and total phosphorus (87.8% vs 23.6%). With regards to textile macro-parameters, PACl improved removal rates for colour, as the absorbance at 426 nm (83.6% vs 72.0%), and anionic surfactants (84.3% vs 79.2%). Considering sludge characteristics, particularly soluble EPS, strength indexes and sludge filterability, it appeared that in the transition phase of stage 2 such characteristics were improved considerably. However, after day 273, in the stationary phase of stage 2, it was observed an increase of proteins in soluble EPS and a decline in flocs strength (SI_1 and SI_2) and sludge filterability (SRF). Moreover, also the evaluation of parameters such as Jc, IF, and CF indicated an increase in fouling propensity after day 273.

On the other hand, both of the irreversible and the reversible fouling in the pilot MBR did not show any rises in resistances to filtration after day 273. In particular, overall, the average irreversible fouling rate FR presented a value of $1.04 \cdot 10^9$ m^{-1} d^{-1} with PACl, whereas in the control period (stage1), a value of $1.90 \cdot 10^9$ m^{-1} d^{-1} was detected. With regards to reversible fouling, PACl gave a significant reduction in $R_{c,}$ overall, in stage 2, presenting an average

value comparable with that of the new membrane (R_m). Moreover, it appeared that after day 273 R_c values was lower than in the first weeks of stage 2.

Table 6.35. Effects of PACl on permeate quality, biomass characteristics, sludge fouling propensity and fouling control; grey cells show effects detected in stage 2 before and after day 273.

Parameter			Effect [1)]	
Permeate quality enhancement	ordinary macro-parameters	COD	+	
		total nitrogen	0	
		total phosphorus	+	
	textile macro-parameters	colour (ads. 426 nm)	+	
		non-ionic surfactants	0	
		anionic surfactants	+	
Sludge characteristics	soluble EPS	sEPSp	+	-
		sEPSc	+	
		rejection of protein	-	+
		rejection of carbohydrates	0	
	flocs strength indexes	SI_1, SI_2	+	-
	sludge filterability	SRF	+	-
		MFI	0	0
	sludge fouling propensity	Jc	0/+	-
		IF	0	-
		CF	+	-
	biomass activity	heterotrophic bacteria	0	
		autotrophic bacteria	0	
Fouling control	irreversible fouling	R_f, FR	+	
	reversible fouling	R_c	+	

[1] Effects of flux enhancer are classified as follows:

-	negative	0	negligible	+	positive

Apparently results related to biomass characteristics and fouling monitoring did not match. In fact, it was expected that a loss in sludge strength and filterability would have affected R_c values (see section 2.5). However, an explanation of this phenomenon, occurred after day 273, can be the following one (Figure 6.51). Firstly, it was observed a release of divalent cations from sludge flocs into bulk liquid (see section 6.5.2) and, at the same time, an increase of proteins concentration in bulk (see section 6.5.1). One hypothesis can be related to the NaCl usage during winter season to prevent car-crashes occurring because of snow or ice presence on roads. In fact, NaCl can be dissolved by snow and rain and reach a WWTP thought the sewer system. It has been reported that such a phenomenon can lead to sludge

floc break-up and strength loss since monovalent cations at high concentrations can compete with divalent and polyvalent cation in binding the organic floc matrix (Bruus et al., 1992). According to this, it can be also thought that PACl was released into the bulk liquid and, overall, this phenomenon impacted negatively on sludge filterability and fouling propensity. Moreover, after such episodes, also with a drop in NaCl concentration, sludge takes time to re-structure itself (Bruus et al., 1992).

Also a second supposition can be made. In particular, comparing cations and proteins content in bulk and permeate (see section 6.5.1 and 6.5.2) it came out that there was a progressive accumulation of such compounds in the cake or gel layer, forming on membrane during filtration. Since irreversible fouling (due to gel layer) did not show a severe increase of resistance R_f, it is believed that the accumulation of cations and proteins occurred in the cake layer. Moreover, the same assumption can be made for PACl, and, as a result, since cations and PACl improve cake filterability, R_c was under control and, also slightly minor after day 273 than before in stage 2. Moreover, proteins were bound in the cake layer and therefore they not affected the gel layer resistance.

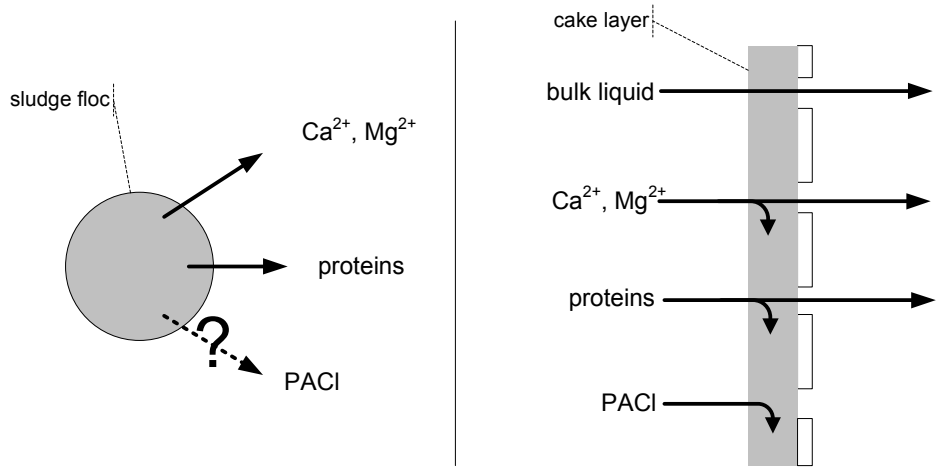

Figure 6.51. Scheme of the release of cations, proteins and PACl from flocs to bulk liquid (on the left side) and accumulation of such compounds into the cake layer (on the right side).

In conclusion, PACl addition into the MBR enhanced the permeate quality and controlled fouling occurrence also in case of floc destructuration. Moreover, no decline in the MBR biological activity was observed during PACl dosing.

Therefore, the MBR technology combined with PACl addition can be considered as an effective option for the treatment of industrial wastewater like textile effluents.

7 Start-up of a submerged anaerobic MBR (SAMBR) treating a synthetic metalworking effluent

7.1 Introduction

In this chapter, results related to topic B of the thesis (start-up of a submerged anaerobic MBR treating a synthetic metal working effluent) are presented and discussed, as follows:

- preliminary assays to characterize the coolant:
  - evaluation of macro-parameters and direct filtration test[4] results (see section 7.2.1);
  - results of the particle size distribution analysis (see section 7.2.2);
  - evaluation of coolant biodegradability: biochemical methane potential (BMP) and VFAs production assays (see section 7.2.3);
  - evaluation of coolant inherent toxicity: anaerobic toxicity assays (ATAs) (see section 7.2.4);
- start-up of a two phase SAMBR (see section 7.3).

7.2 Preliminary assays to characterize the synthetic effluent

7.2.1 Evaluation of relevant macro-parameters and direct filtration test

The characteristics of the coolant emulsion (0.1% m/m) were evaluated before and after filtration through the Kubota flat sheet module (direct filtration test performed at 10 LMH constant flux, 2.5 LPM gas sparging flow and 20 min of duration), then installed in the SAMBR pilot. Results are shown in Table 7.1.

Table 7.1. Characterization of the coolant emulsion (0,1% m/m) before and after filtration.

	Fresh coolant emulsion	**Filtered coolant emulsion**	**Reduction**
TOC (mg/L)	726	57	92.1%
COD (mg/L)	2,833	1,007	64.5%
COD/TOC (mol/mol)	1.5	6.6	-
pH	8.0	-	-

[4] The term "direct filtration test" means a filtration test without biomass in the tank, where only the synthetic effluent was present.

The fresh emulsion had a high organic content: 726 and 2,833 mg L^{-1} for TOC and COD, respectively. In particular, considering that a concentration of 0.1% m/m corresponded to 1,000 mg L^{-1}, the organic carbon accounted for the 72.6% of the total coolant mass.
With regards to the filtered emulsion, TOC and COD were about 57 and 1,007 mg L^{-1}, respectively. As a consequence, the molar COD/TOC ratio for the filtered emulsion was 6.6, whereas the maximum admissible value is for the methane with a value of 2 (Stumm and Morgan, 1996). Differently, the ratio for the fresh emulsion was 1.5 and therefore it is believed that in the permeate some interfering substances with the COD measurement were present and, as a result, COD was a poor indicator of organic in permeate. Therefore, in this study, TOC was preferred to COD and considered as a consistent indicator of organics both for fresh and filtered effluent.

With regards to membrane performance in the direct test, both from a removal and a hydraulic point of view (Figure 7.1) some considerations follow.

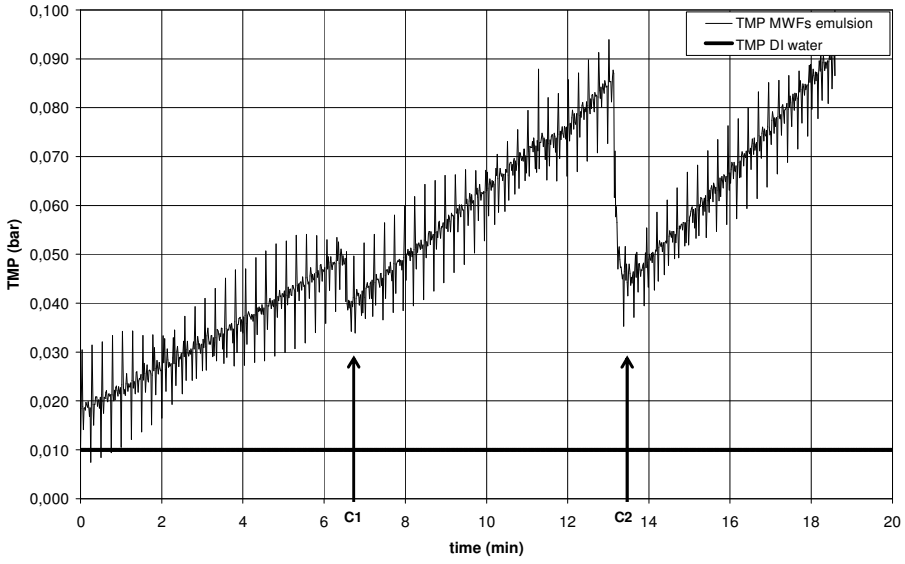

Figure 7.1. Transmembrane pressure (TMP) evolution during the direct filtration test (10 LMH, 2.5 LPM, 20 min).

The membrane rejection of TOC was high (92.1%) because of the presence of coolant-membrane interactions. In particular, it is believed that the material of Kubota membranes (i.e., polyethylene) played an important role in these interactions. In fact, the fresh emulsion was also analyzed after a filtration step performed using mixed cellulose esters 0.45 μm filters (Millipore Millex-HA filters, 33 mm). Results (not shown) demonstrated that Millipore filters did not affect TOC and COD even thought filter porosity was similar to that of Kubota

membranes, i.e., 0.4 μm. The importance of membrane material was also confirmed from results of the particle size distribution analysis (see section 7.2.2).
However, coolant-membrane interactions seemed to be mostly reversible. In fact, even thought TMP was partially recovered after two handmade physical cleans (C1: weak cleaning, C2: vigorous cleaning, see Figure 7.1), after the test, cleaning the membrane with tap water recovered completely the initial membrane permeability and TMP values in water filtration.

7.2.2 Particle size distribution analysis

Figure 7.2 shows results of the particle size distribution (PSD) analysis. It can be seen from the chart (Figure 7.2a) that the PSD of the fresh emulsion presented a bimodal outline and all the particles were between 0.1 and 30 μm. The first higher peak was approximately at 0.2 μm (8.5%) whereas the second peak was between 1 and 2 μm (4%).
In theory, knowing the PSD of an effluent to treat, it is possible to find out the relation between the pore sizes of an hypothetic membrane process applied directly to the effluent and the removal rate of particles, by calculating the cumulative distribution function (CDF) and then applying the equation 7.1, as follows:

$$\text{removal} = 1 - \text{CFD} \qquad 7.1)$$

Results are shown in Figure 7.3; according to the chart, considering a membrane pore size of 0.4 μm, the same size of Kubota flat sheet modules used in the study, it would be expected a removal rate approximately of 50%. By comparison, in direct filtration test, TOC was removed with an efficiency of 92.1% as stated above. Therefore, also particles with sizes smaller then pores were retained by the membrane and consequently the material of Kubota membranes (i.e., polyethylene) it is thought to play an important role in the rejection of the coolant, as previously supposed and discussed.
Comparing the PSD of the anaerobic biomass (Figure 7.2b) and the coolant one (Figure 7.2a), completely different outlines appeared. In particular, differently from the coolant, the anaerobic biomass did not present any particles in the range 0÷0.45 μm, covering a range from 0.45 to 800 μm with a unique significant peak. The PSD of the mixture (coolant + biomass) presents an outline (Figure 7.2c) quite similar to the biomass one, ranging from 0.45 to 800 μm with a peak at 10 μm. It was supposed that the coolant particles were attached to biomass, particularly, in the range of little flocks, i.e., 1÷30 μm, because the outline of biomass PSD changed shape in this range.

a)

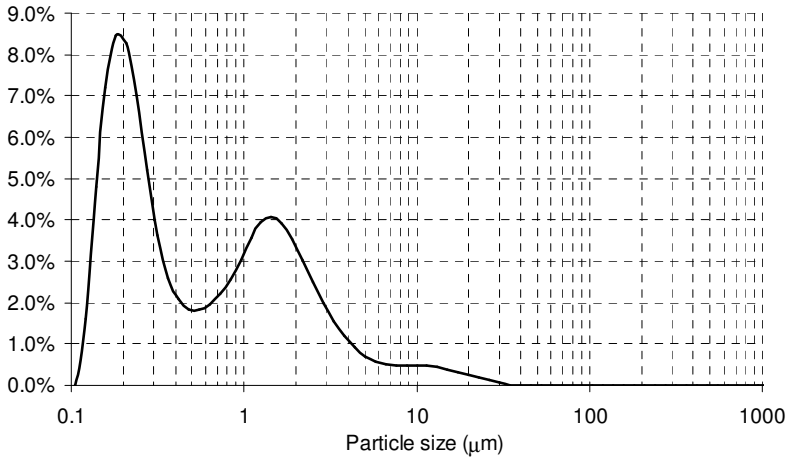

b)

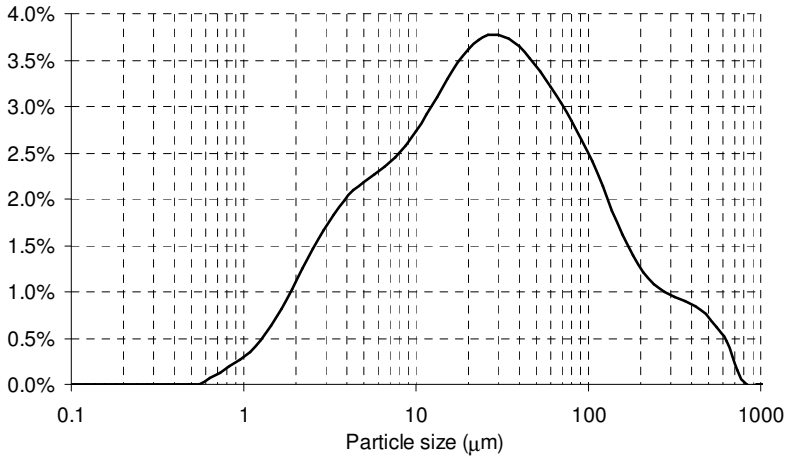

c)

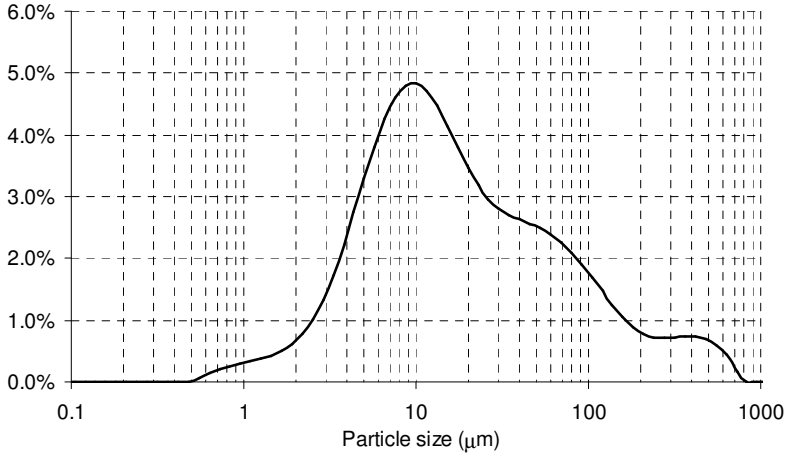

Figure 7.2. PSD analysis: a) 0.1% fresh coolant emulsion, b) anaerobic biomass, b) mixture of anaerobic biomass and coolant (0.1%).

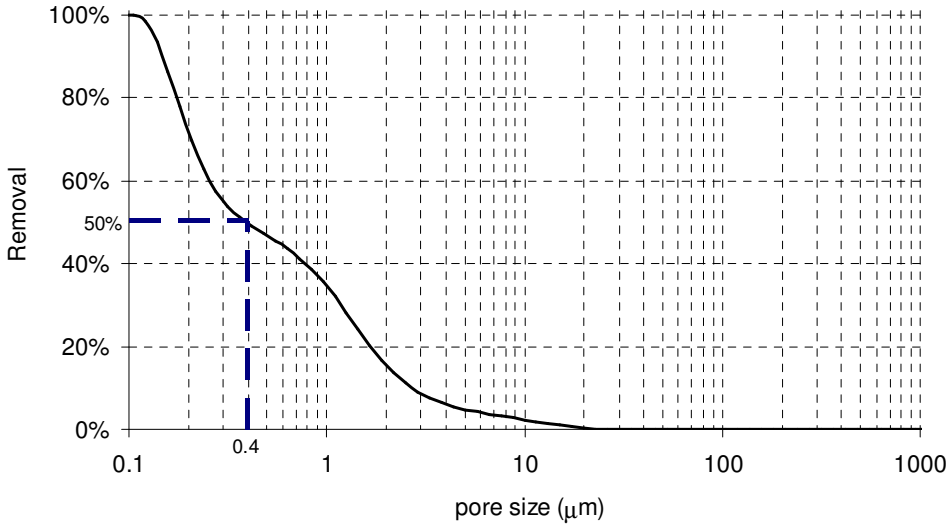

Figure 7.3. Removal rate as a function of membrane pore size.

To validate the deduction of coolant attachment propensity on biomass, TOC was evaluated in the bulk liquid of a biomass sample (40 mg L^{-1}) and in the bulk liquid of a mix biomass-coolant sample (70 mg L^{-1}). The latter would have been expected to be one order of magnitude higher. In fact, if attachment on biomass had not occurred, the bulk TOC in presence of the coolant (at a concentration of 0.1%) would have been approximately of 700 mg L^{-1}.

In conclusion, the fresh MWF selected for the study had a high propensity to attach on biomass. With regards to the nature of biomass-coolant interaction no particular supposition can be made (adsorptions? reversible? etc.). But, attachment on biomass can imply a sort of wrapping effect of flocs leading to a possible limitation of the transport of soluble substrates and therefore reducing the substrate conversion rate (Cammarota and Freire, 2006).

7.2.3 Evaluation of coolant biodegradability: biochemical methane potential (BMP) and VFAs production assays

Methane cumulative production (see method B.1, section 5.4.1) in the first series of BMB assays is shown in Figure 7.4. In the first series, only one serum bottle at 0.5% MWF produced methane over a period of 150 days. In particular, the sample started to produce methane after a lag phase of approximately 70 days and the cumulate methane production reached the maximum value of 65 mL CH_4 L^{-1} at day 85. The control sample (biomass only sample) produced approximately 20 mL CH_4 L^{-1}. Consequently, the net methane production

related to coolant degradation was 45 mL CH_4 L^{-1}, corresponding to 21,7 mg TOC L^{-1}. By comparison, the TOC corresponding to a coolant concentration of 0.5% was assumed to be approximately 3,630 mg TOC L^{-1}. As a result, the biodegradation was equal to 0.8% (see method B.2, section 5.4.1, coolant COD/TOC ratio = 1.5 mol/mol).

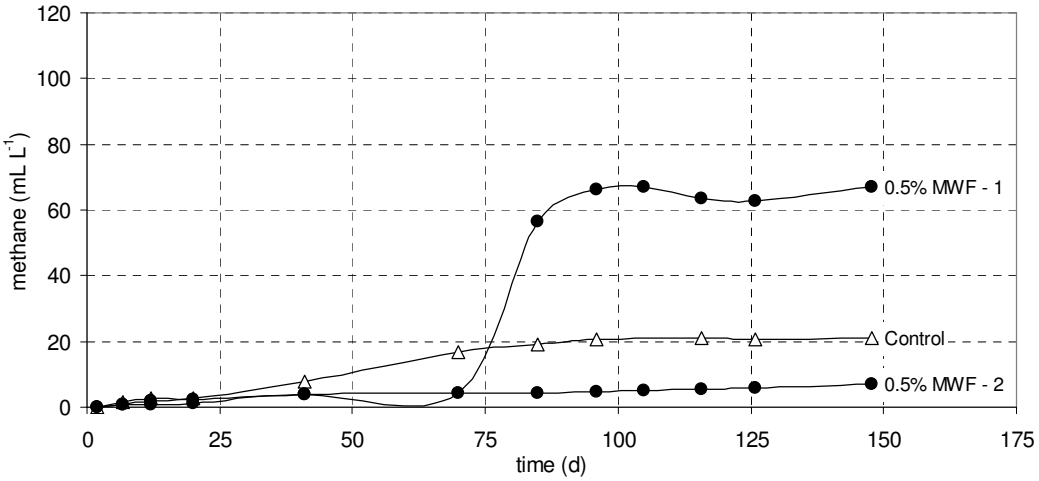

Figure 7.4. BMP assays - first series.

These first findings showed that at a MWF concentration of 0.5% and an F/M ratio of 2.5 g MFW g $MLSS^{-1}$ the anaerobic biomass used in the study needed a long acclimatization period (in batch condition) to degrade just a small amount of the coolant (less than 1%). Consequently, the second BMP series (Figure 7.5) was conducted at a lower concentration (0.1%) and F/M ratios (0.1, 0.2, 1 g MFW g $MLSS^{-1}$) as previously described (see section 5.4.1).

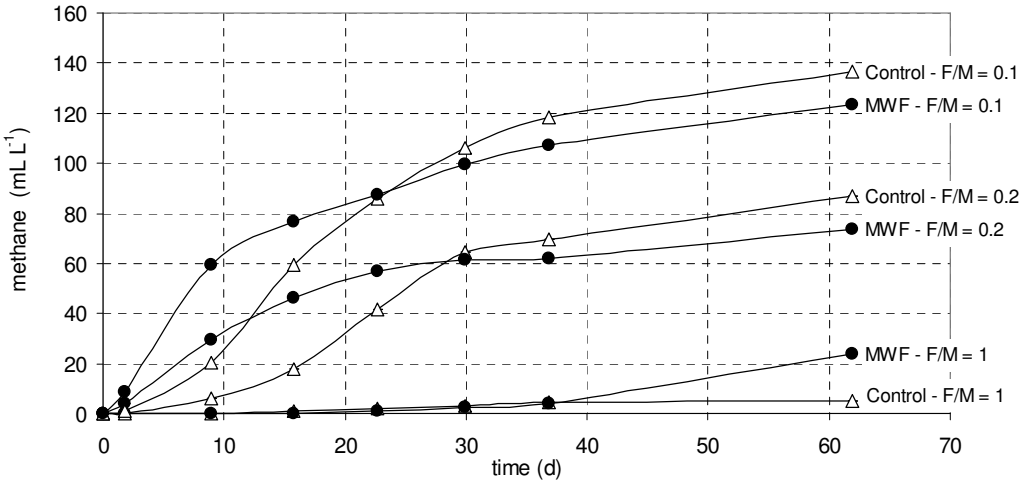

Figure 7.5. BMP assays - second series (average values are shown, COV is within ±10%).

In the second series, taking into account samples with F/M = 0.1 and 0.2 g MFW g $MLSS^{-1}$, the methane production of controls (biomass only samples) and samples with the coolant, showed an out of the ordinary pattern. In fact, the initial rate of methane production (between day 0 and day 10) in samples with the coolant was approximately double compared to controls. Differently, the total amount of methane of controls exceeded the methane produced in samples with coolant at day 30.

This result can be explained only considering that MWFs are a complex mixture of different compounds. As a result, they can inhibit some pathways of biodegradation, such as methane bio-conversion from decay, and do not affect others. Moreover, it is believed that, in all probability, the coolant contained a minute amount of simple molecules that could be degradated and converted into methane more rapidly than for the organic matter from biomass decay, but only when the F/M ratio was low (0.1 and 0.2 g MFW g $MLSS^{-1}$). In fact, the F/M ratio can be an important parameter, been an index, in the case of MWFs, of eventual inhibition due to attachment of MWFs to biomass (see above). In particular, the higher the F/M ratio (i.e., the ratio between the coolant and the biomass), the higher the possible adverse effects (due thicker oily layer attached on biomass flocs) are.

Since all the second series tests were performed at the same concentration of the coolant (0.1% m/m) but at different biomass concentrations (10, 5, 1 g MLSS L^{-1}) it was thought that the initial methane production rate (slope of methane production) would have followed ratios of 10:5:1 for tests at F/M equal to 0.1, 0.2, 1 g MFW g $MLSS^{-1}$, respectively, being kinetic proportional to biomass concentration. But, at F/M =1 g MFW g $MLSS^{-1}$ the initial rate was 0 and the total production was negligible till to day 37. Therefore, at the highest F/M tested, the degradation of the coolant need an acclimatization period before occurring.

Finally, the methane conversion from dead biomass (i.e., biomass decay), that consists of complex organic material, was inhibited to certain extent (unknown). Therefore, the evaluation of the removal rate of the coolant considering net methane production is underestimated. On the other hand, considering the gross production may lead to an overestimation. However, because of poor biodegradability of the coolant, considering net or gross production does not affect to a large extent final results and conclusions. As a consequence, herein, it is preferred to consider the more usual approach taking into account the net production.

In Figure 7.6 and Figure 7.7 VFAs production due to the coolant biodegradation (MWF = 0.1%, MLSS = 5 g/L, F/M = 0.2 g MFW g $MLSS^{-1}$) is shown. As previously discussed (see section 4.2.2), BES was added in order to inhibit the acetoclastic methanogenesis and therefore the consumption of VFAs. The differences between controls and samples with the

coolant were very close at day 20: approximately 5 mg OC L^{-1} of formic and acetic acids and approximately 2.5 mg OC L^{-1} of propionic, n-butirric and iso-buttiric acids. By comparison, MWF added to samples as TOC were about 726 mg L^{-1}.

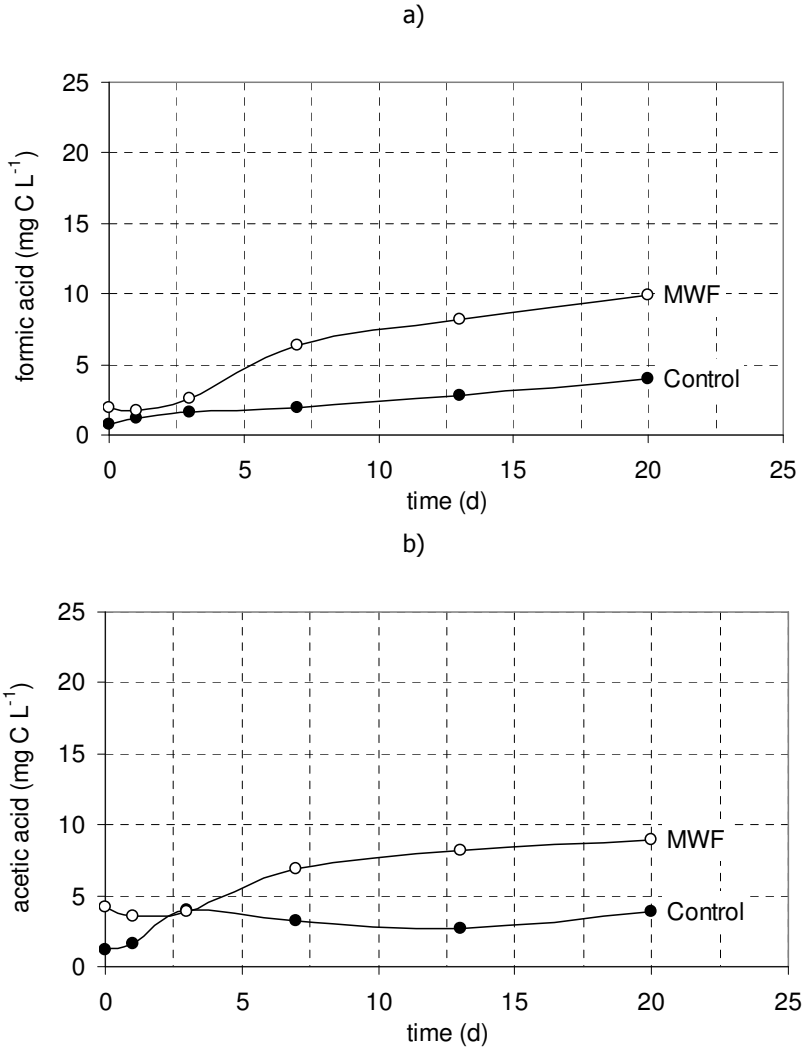

Figure 7.6. VFAs production measured as organic carbon (OC) in experiments with BES (MWF = 0.1%, MLSS = 5 g/L): a) Formic Acid; b) Acetic Acid.

These results suggest that the adaptation of the hydrolytic/heteroacetogenic biomass did not occur in a significant manner during the assays, as only a total VFAs production of approximately 17.5 mg C/L was observed (~2.5% of the initial TOC). Moreover, the methane production was negligible indicating that the methane conversion pathway through hydrogenotrophic methanogenesis (not affected by BES addition) was not relevant or almost absent for the coolant.

a)

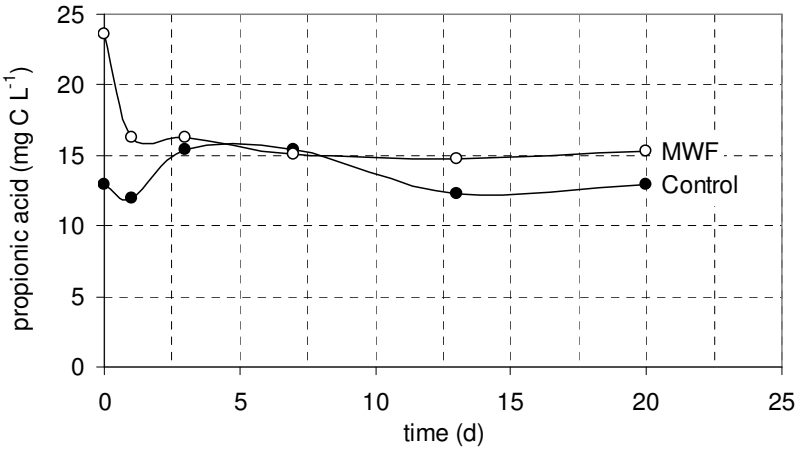

b)

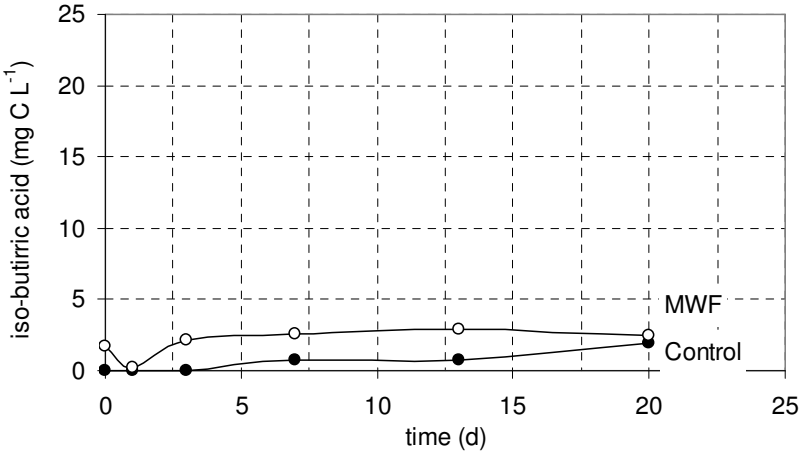

c)

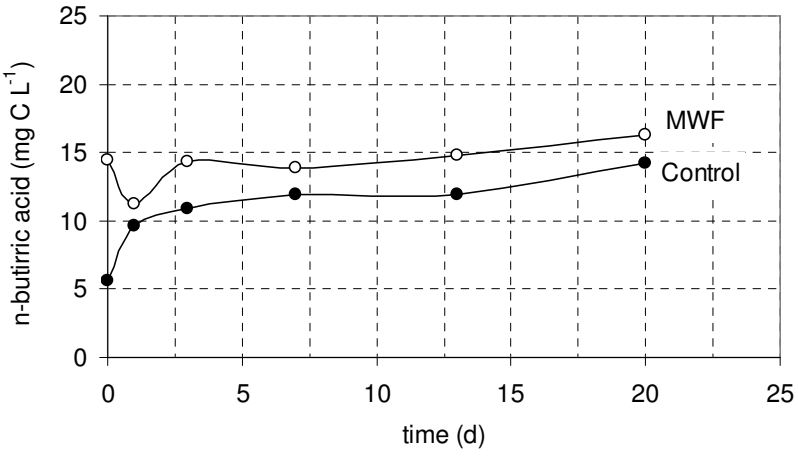

Figure 7.7. VFAs production measured as organic carbon (OC) in experiments with BES (MWF = 0.1%, MLSS = 5 g/L): a) propionic acid; b) iso-butirric acid; c) n-valeric acid.

7.2.4 Evaluation of toxicity inherent in the coolant: anaerobic toxicity assays (ATAs)

Figure 7.8 shows cumulative methane production (see method B.1, section 5.4.1) evaluated during anaerobic toxicity assays (ATAs). Such results can be discussed taking into account two different aspects, as follows:

1. the duration of the lag phase, i.e., the time bacteria community needs to get acclimatized to organic substrate at experimental conditions;
2. the whole methane production reached during tests compared to controls and to the maximal values calculated by stoichiometry.

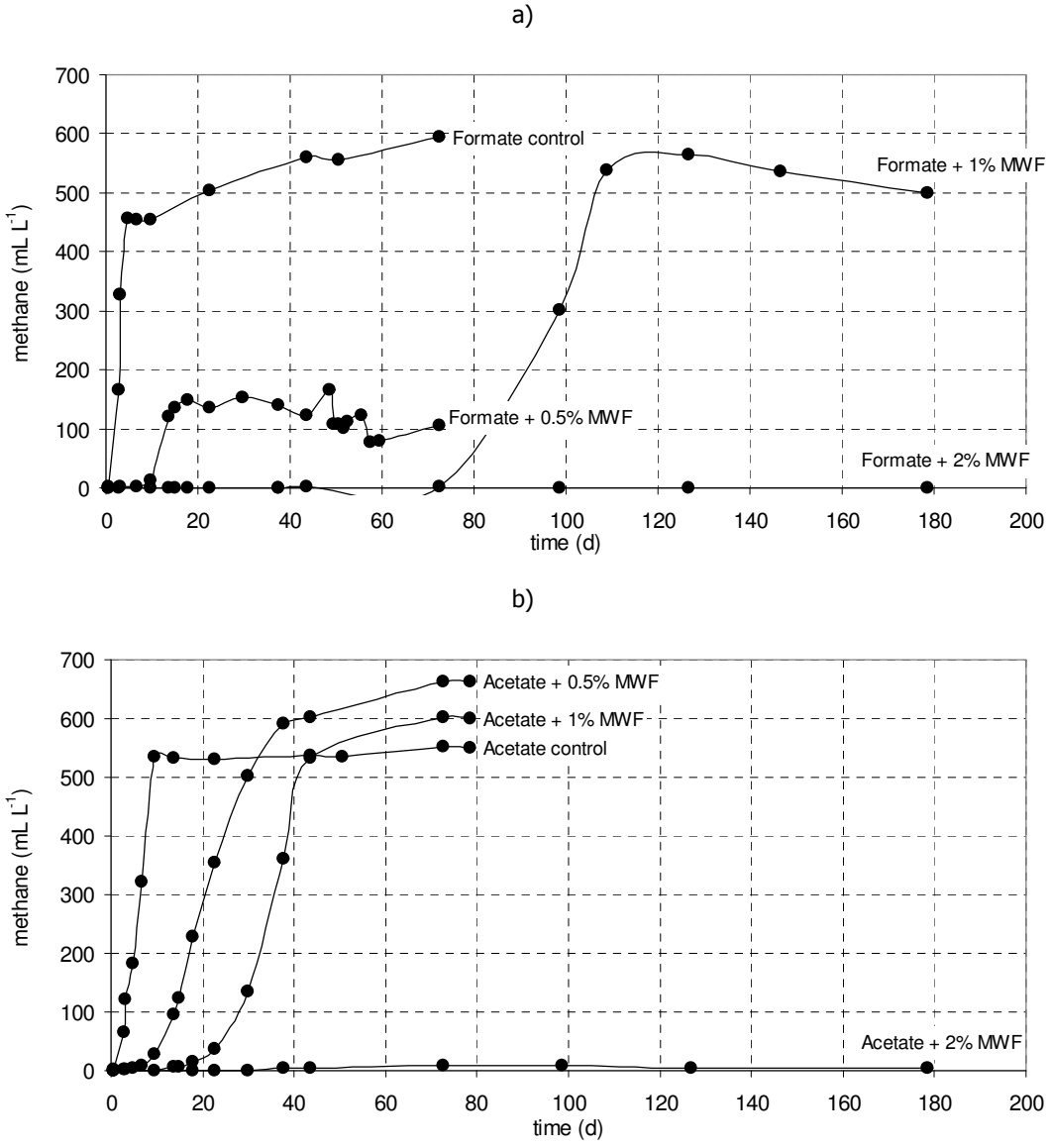

Figure 7.8. Methane production in ATAs performed at different MWF concentrations: a) formate, b) acetate (average values are shown, COV is within ±10%).

With regards to the first aspect, the lag phases were present both for acetate than formate and, particularly, they were major than the entire experimental duration (duration of approximately 150 days) for a coolant concentration of 2%. Apart from these data, lag phases were more extended for formate, principally at a coolant concentration of 1%. In fact, samples fed with acetate started to produce methane approximately at day 7 and day 15 as for 0.5% and 1%, respectively. Differently, samples with formate began to produce methane at day 10 and day 75 as for 0.5% and 1%, respectively. By comparison, control samples (no coolant) produced methane from day 1 onward as for both acetate and formate. These results suggest that methane conversion from acetate and formate was inhibited with relation to the coolant concentration. In fact, in the presence of the coolant, overall, the methanogens community needed time to get acclimatized to acetate and formate substrates because of one or more of the following possible explanations:

- the presence of coolant inhibited the pathway that was successful in control samples (absence of coolant), and, to overcome this problem, the methanogens community needed time to produce new enzymes for a different pathway;
- the presence of coolant inhibited the overall metabolic activity of the bacterial community, that started to produce a sort of detoxification enzymes and/or to convert gradually inhibitors (in the coolant) into intermediate molecules compatible with their activities;
- the attachment propensity of the coolant (resulting in a wrapping effect of biomass flocs and a reduction of diffusion phenomena) was reduced slowly because of partial bio-conversion of attached organics in soluble molecules not affecting anymore the diffusion of substrates.

With regards to whole methane production, two considerations came out. Firstly, the methane production of samples fed with acetate and coolant presented higher values compared to controls (acetate only). It is believed that the extra CH_4 amount was related to coolant complete degradation. In particular, the differences in the methane production were approximately of 113 and 49 mL CH_4 L^{-1} for 0.5% and 1% samples, respectively. This corresponds to 54.5 and 23.7 mg TOC L^{-1}, respectively. By comparison, the coolant concentrations as TOC were 3,630 and 7,260 mg COD/L, for 0.5% and 1%, respectively. As a result, the biodegradation was approximately of 4.2% (0.5% samples) and 0.9% (1% samples; see method B.2, section 5.4.1, coolant COD/TOC ratio = 1.5 mol/mol). Comparing these findings with BMP results at the same conditions (biodegradation of 0.8% and 0% for samples at a coolant concentration of 0.5% and 1%, respectively) it appears that acetate enhanced the coolant biodegradability.

Differently, the second relevant aspect is related to formate, particularly considering the methane production at a coolant concentration of 0.5%. Taking into account only the first 15 days, both the total amount of the methane and the rate of production were almost comparable to samples with acetate. Differently, after day 15, samples with formate did not produce further methane. It is believed that the reason of this phenomenon could be related to a particular toxicity inherent in the coolant due to changes in pH maybe related to the pH-dependence of the biocides effectiveness (see section 3.3), as follows.

Firstly, as the pH can not be measured in a serum bottle without opening it, it was identified a measurable index correlated to pH by a biunivocal relation. In particular, according to the chemical equilibrium theory applied to inorganic carbon (C), in a dual phase liquid-gas system a relation between the percentage of inorganic C as $CO_{2,gas}$ and pH can be developed. Such a biunivocal relation, calibrated to serum bottle conditions, is presented in Figure 7.9. For instance, the graph shows that varying the pH from 7.35 to 8.15, the percentage of CO_2 in gas phase drops of 5.4 times, from 11.9% to 2.2%.

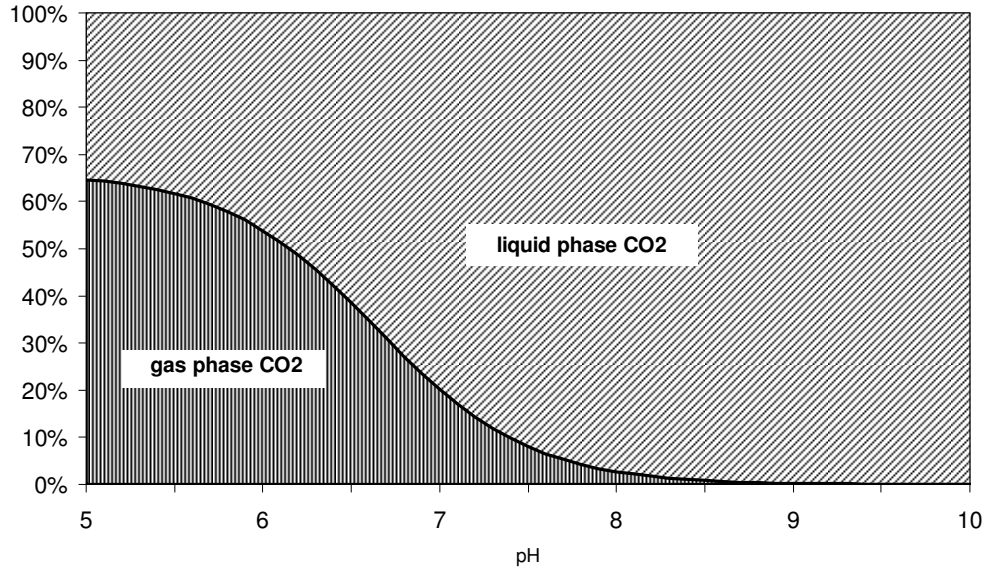

Figure 7.9. CO_2 fractionation in the liquid phase and in the gas phase in a closed system.

Differently, Figure 7.10 shows the partial volume of $CO_{2,gas}$ over time, whereas Table 7.2 also the pH value measured directly at day 0, day 45 (opening just one serum bottle of each duplicate) and at the end of experiments (day 80). These results shows that the partial volume of $CO_{2,gas}$ dropped down, particularly, at day 45 of 4.3 (control), 6.9 (0.5%), 5 (1%) times, respectively with variation of pH from 7.35 to approximately 8.15÷8.22, therefore validating the biunivocal relation between pH and the percentage of CO_2 in gas phase shown in Figure 7.9.

a)

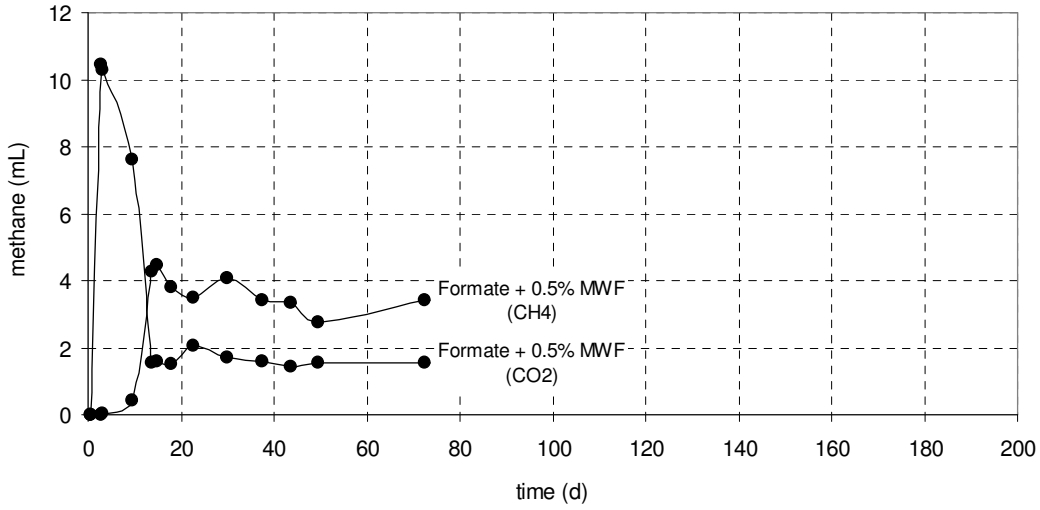

b)

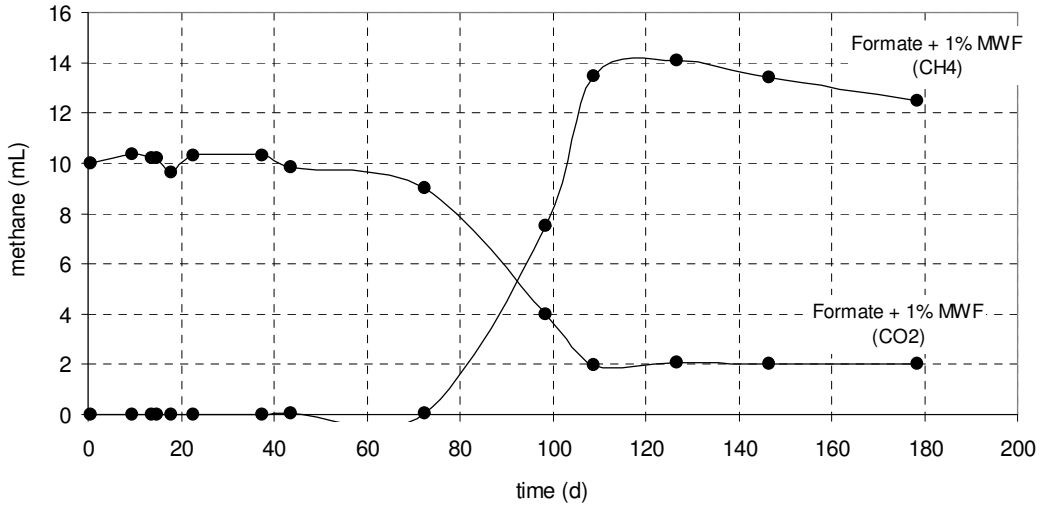

Figure 7.10. Methane production and CO_2 adsorption in ATAs with formate as substrate: a) 0.5% MWF, b) 1% MWF.

Table 7.2. pH of formate samples.

Sample	**day 0**		**day 45**		**day 80 (end)**	
	gas phase CO_2	pH	gas phase CO_2	pH	gas phase CO_2	pH
control	10.3 mL	7.35	2.0 mL	8.15	2.4 mL	8.17
0.5% MWF	10.4 mL	7.35	1.5 mL	8.22	1.5 mL	8.20
1% MWF	10 mL	7.35	10.3 mL	7.40	2 mL	8.15

By comparison, in acetate samples no CO_2 decrease was observed and pH was stable over time (approximately 7.35÷7.40). The reason was due to the fact that formic acid is a stronger avid (pK_A=3.74) than acetic acid (pK_A=4.76), and therefore a major amount of $Na(HCO)_3$ was used at the beginning to re-equilibrate pH to proper values (7.35÷7.40). As soon as formic acid was degraded, the excess of $Na(HCO)_3$ in formate samples led to the increase in pH and resulting in a drop in the gas phase CO_2. In Figure 7.10 gas phase CO_2 and CH_4 reached relative plateaus at the same time. For unknown reason in the 0.5% sample the CO_2 plateau was reached before the completion of the formate biodegradation. Therefore, it is believed that also a basic pH was reached before the completion of the biodegradation, leading to an inhibition of bacteria activity as higher pH enhances biocide activity (Rossmoore, 1981; Sandin et al., 1990).

Finally, in order to verify any adaptation of the coolant, after 80 days, controls and 0.5% samples were re-fed. In particular, in order to remove any metabolites and not degraded coolant, the mixed liquor of the serum bottles was firstly centrifuged at 7,500 rpm (10 min); the supernatant was then discharged and the pellet was re-suspended in a new media composed by acetate/formate, minerals and coolant.

In Figure 7.12 results are presented, suggesting that no adaptation was developed by the anaerobic biomass in samples with coolant. In fact, all the re-fed samples had a longer initial lag phase. As suggested by PSD analysis (see section 7.2.2) MWFs have the propensity to attach on biomass. Therefore, it is believed that in the re-feeding procedure the old coolant was not removed properly and consequently the real concentration of re-fed serum bottles higher that the previous one and unknown.

a)

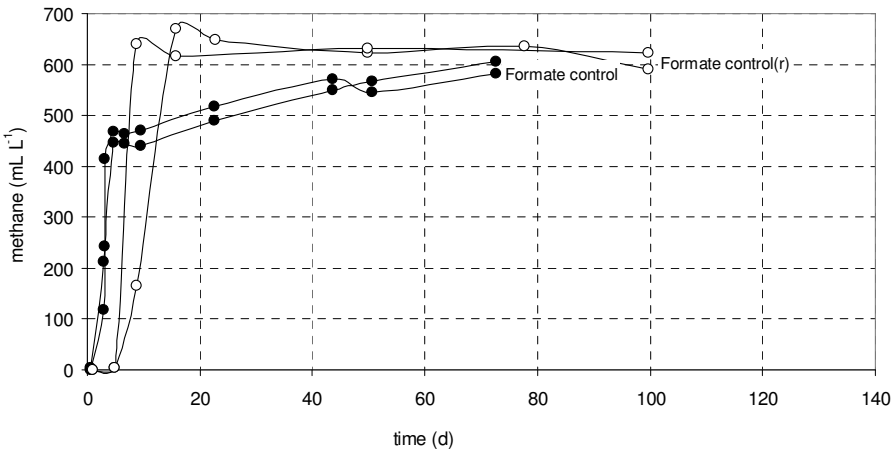

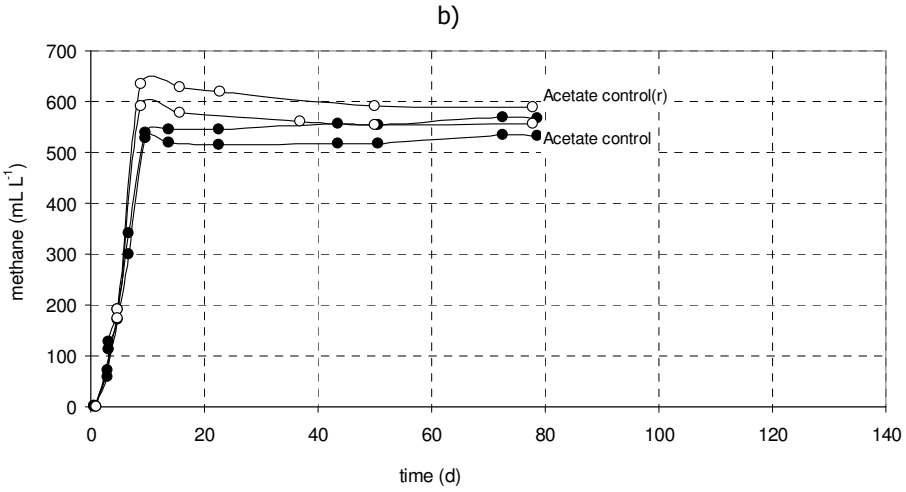

Figure 7.11. Re-feeding of ATAs: a) formate controls; b) acetate controls.

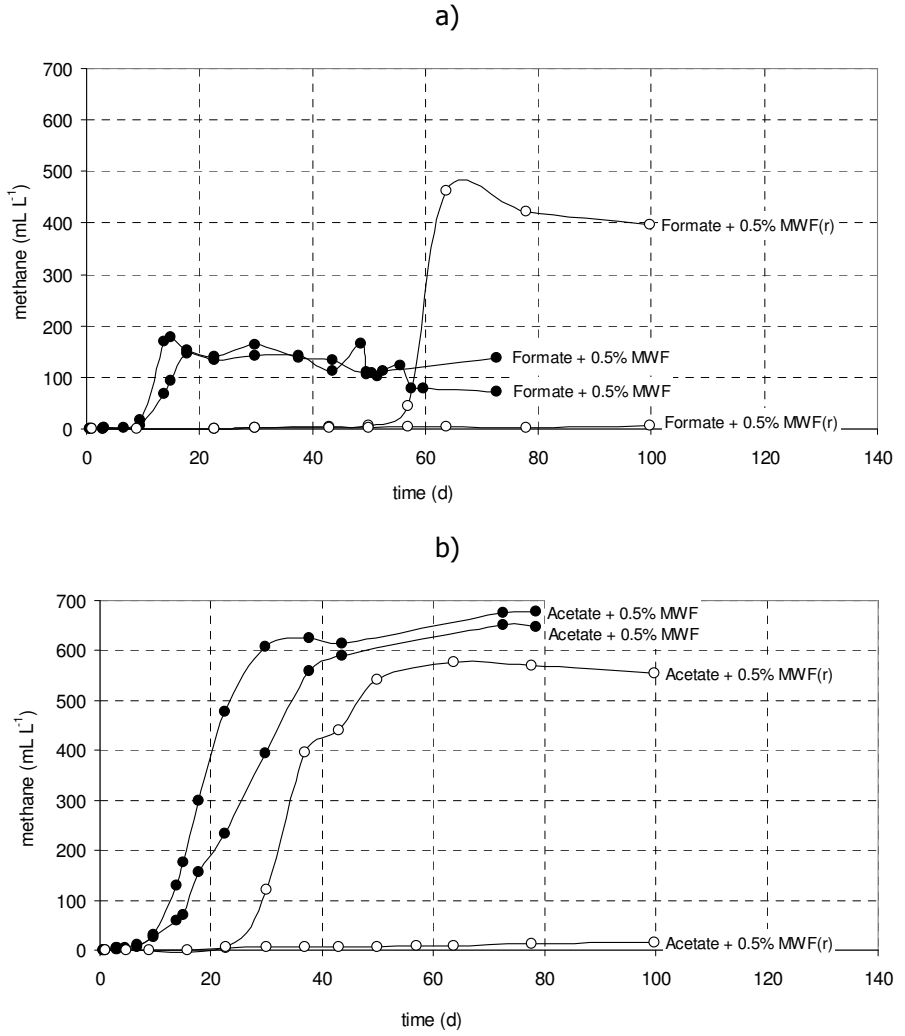

Figure 7.12. Re-feeding of ATAs: a) formate and 0.5% coolant; b) acetate and 0.5% coolant.

7.3 Start-up of a two phase SAMBR

Two submerged anaerobic bioreactors (SAMBRs) were set up as described in section 5.2.2 and placed into a water bath maintained at 33±1°C. The SAMBR start-up was planned in three stages (Figure 7.13). In particular, stage 1 and stage 2 were batch conditions, whereas during stage 3 reactors were fed continuously.

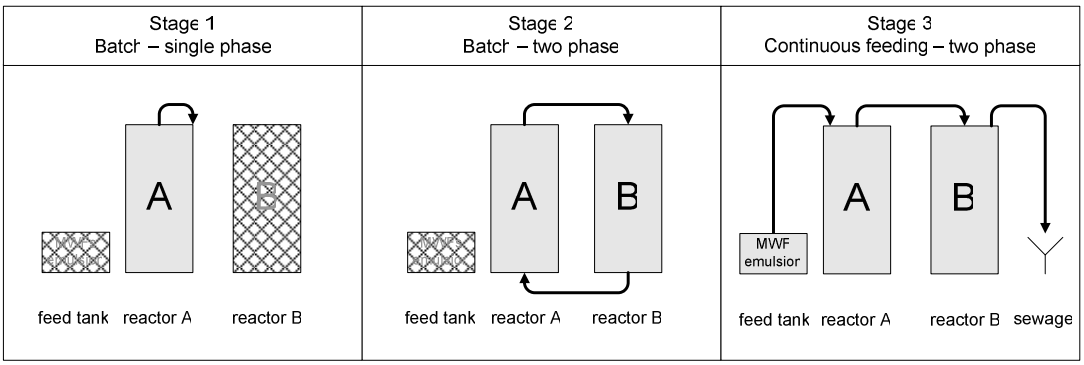

Figure 7.13. Stages of the SAMBRs start-up.

At the beginning of the experiment, reactor A was seeded with a mixture of stock solutions for the preparation of the mineral media (Owen et al., 1979), the fresh coolant and anaerobic biomass (from a conventional sewage sludge digester in Mogden, UK). Differently, reactor B was seeded with the mineral media and anaerobic biomass only (Table 7.3). Concentrations of vitamins, metals and N/P salts in the final mixture were the same indicated in Table 5.18 for BMP and ATAs.

At stage 1 only the reactor A was in operation and the filtration was executed in a re-cycle mode, whereas the reactor B was in a stand-by condition. Differently, at stage 2 the reactors were connected together, particularly the effluent of reactor A was the feed of the reactor B and the effluent of reactor B was the feed of the reactor A (Figure 7.13). With regards to stage 3, a fresh emulsion of the coolant (0.1% m/m) was added continuously to reactor A and the permeate collected was fed to reactor B. Also the mineral media (Table 5.18) was added to reactor A, but in a separate way, in order to do not break the coolant emulsion that would have lead to technical problems because of the tendency of the coolant to attach on glass and plastic surfaces (influent tank, pipes etc.).

The configuration at stage 3 was a two phase anaerobic digestion, where the first reactor was thought to be a fermentation phase mainly, whereas the second phase a methanogenic phase (Speece, 1996). In the case of MWFs treatment it was believed that the first reactor could have worked as a protective barrier for methanogens bacteria in reactor B, that usually are more sensible to inhibition (Speece, 1996). In fact, ATAs showed that

acetoclastic methane production was inhibited in presence of the coolant principally at high concentration. The presence of the first reactor could have blocked effectively the not-degraded coolant because of its propensity to attach on biomass and on membranes as well. Also, it would have been possible that biocides existing in MWFs were partially removed by filtration. Although it is known that only UF and NF membranes can retain part of the biocides (Hilal et al., 2004) it is believed that in an MBR reactor with MF membranes biocides can be retained as well. In fact the cake and gel layers act as secondary membranes improving the overall performance of the filtration system also reducing the membrane pore size (see chapter 2). As a result, fresh coolant and biocides could have been retained in the first reactor till the partial degradation would have occurred due to hydrolysis and fermentation. However, bacterial community in the first reactor would have required time to get used to coolant because its complex composition and/or its propensity to attach on biomass. In particular, it is believed that the latter can lead to a possible limitation of the transport of soluble substrates, therefore reducing the substrate conversion rate (Cammarota and Freire, 2006).

Table 7.3. Preparation of the initial mixture for the start up of the reactors.

		Specific amount per litre of final mixture	
		A	**B**
Mineral media *	Stock solution S3 of the Owen media	2.7 mL	2.7 mL
	Stock solution S4 of the Owen media	13.5 mL	13.5 mL
	Stock solution S5 of the Owen media	0.9 mL	0.9 mL
	Stock solution S6 of the Owen media	0.9 mL	0.9 mL
	Stock solution S7 of the Owen media	9 mL	9 mL
Fresh coolant +		1 g MWF	-
Anaerobic Biomass		5 g MLSS	1 g MLSS

* The mineral media was prepared using the stock solution S3, S4, S5, S6, S7 of the defined media of

+ An amount of 1 g fresh MWF per litre of final mixture corresponds to a final emulsion of 0.1% m/m.

In Table 7.4 the operating parameters are shown. With regards to the sludge retention time (SRT), it was controlled through a proper sludge sampling strategy and it was kept above 200 days for both reactors. Therefore, no washing out of methanogens occurred in reactor A leaving them the possibility of growing up and producing methane if not inhibited. As concerns the filtration parameters, information from results of the direct filtration experiment (see section 7.2.1) was taken into account and therefore operating in more "safe" conditions

was performed. In particular, the permeate flux was set at 5 LMH (half the value applied during the direct test) and the gas flow rate at 5 LPM (twice the value applied during the direct test). With regards to physical cleanings, neither relaxation nor permeate backwashing were performed.

Table 7.4. Operating parameters.

	Stage 1 day 0 – day 8		**Stage 2** day 8 – day 22		**Stage 3** day 22 – day 40	
	A	B	A	B	A	B
F/M (g MWF g $MLSS^{-1}$ d^{-1}) *	0.2	-	0.2	-	0.1	-
Initial MLSS (g MLSS L^{-1})	5	1				
HRT (h)	-	-	-	-	48	48

* In the batch phases (Stage 1 and Stage 2) the F/M ratio is expressed as g MWF g $MLSS^{-1}$ and represents the ratio of MWFs amount versus the biomass amount in the reactor A at day 0.

Parameters, such as temperature and pH, are shown in Table 7.5. With regards to temperature, the average value in the first two stages was 38°C whereas in the third stage it was 33°C. The reason was due to some technical issues related to the heater effectiveness, that was replaced with a new one at the beginning of stage 3, reaching proper mesophilic conditions.

Table 7.5. Temperature and pH values for SAMBRs.

	Stage 1 day 0 – day 8		**Stage 2** day 8 – day 22		**Stage 3** day 22 – day 40	
	A	B	A	B	A	B
Temperature (°C)	38±0.5	38±0.5	38±0.5	38±0.5	33±0.5	33±0.5
pH	6.9±0.1	7.0±0.1	7.1±0.1	7.2±0.1	7.3±0.1	7.4±0.1

Methane production. The methane production of reactor A is shown in Figure 7.14 (method B.3, section 5.4.2); as concerns reactor B methane production was negligible, so that no results are illustrates. Comparing the cumulative production (measured as mass of organic carbon) and the coolant fed to the reactor A as the equivalent mass of organic carbon, it appears that only a small amount of MWF was converted to methane. For instance, at the begging of Stage 1, 2.3 g C of coolant were added to the reactor and after 10 days a CH_4 production of 0.04 g C was observed.

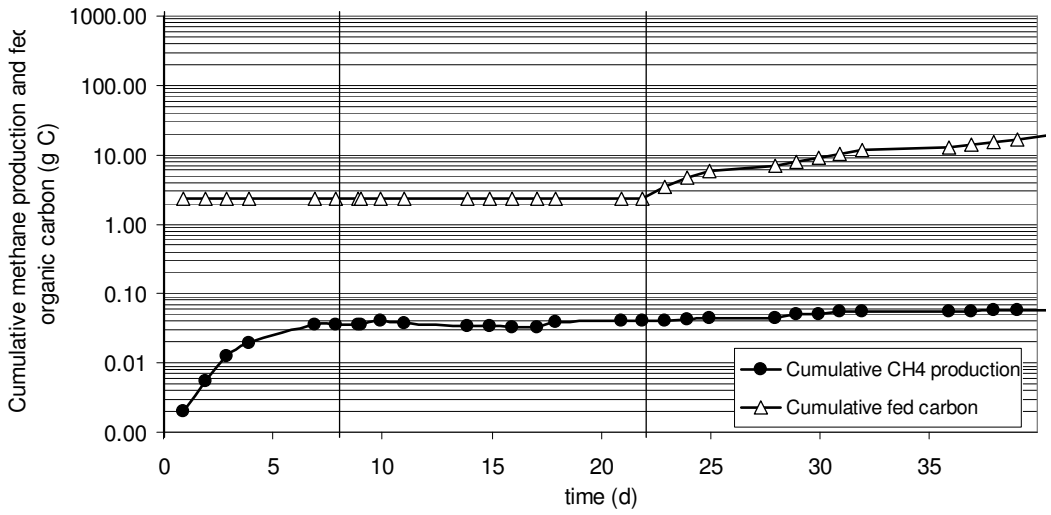

Figure 7.14. Cumulative methane production and organic carbon fed to reactor A (data are shown as the equivalent mass of organic carbon in gram).

In order to assess if the biodegradation of MWF was affected by the fact that it took place in the reactor (possible no optimal sealing condition), the methane production of the reactor A during stage 1 and stage 2 was compared to the production evaluated in 2 serum bottles (optimal sealing condition) seeded with the mixer liquor from the reactor at day 0. In particular, one serum bottle was seeded with a sample collected 30 min before the coolant addition and the other with a sample collected 30 min after. In order to compare data of the reactor A to serum bottles production, the methane production (mass of carbon in mg C) was divided by the volume of the reactor (3.2 L) and the serum bottles (35 mL), respectively. As a consequence, results are shown as the mass of methane produced in mg C per litre of reactor/serum bottle.

Results suggest that between day 0 and day 7 methane production of reactor A was comparable to methane produced in serum bottles "after". On the contrary, the methane production in reactor failed from day 8. Results of the serum bottles trials suggest that at day 9 only the 70% of methane production was related to MWF degradation (data obtained comparing production in two serum bottles). In accordance with this hypothesis the coolant biodegradation in the batch phases (stage 1 and stage 2) of rector A consisted of 1.65% (method B.2, section 5.4.1).

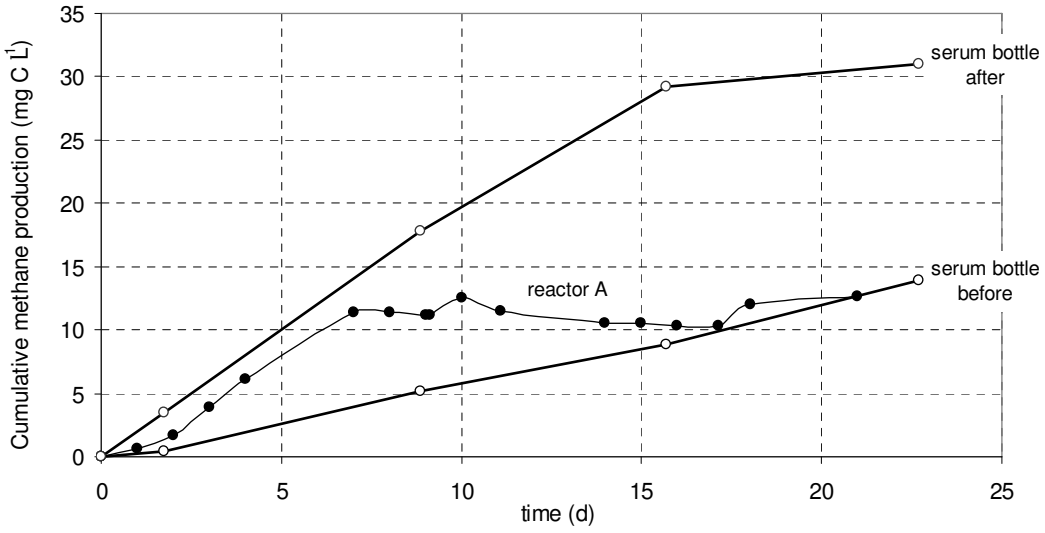

Figure 7.15. Cumulative methane production of reactor A and two serum bottles; one serum bottle was seeded with a sample collected 30 min before the coolant addition and the other with a sample collected 30 min after.

TOC and VFAs production. TOC and VFAs data are shown in Figure 7.16, Table 7.6 and Figure 7.17. With regards to TOC, values at day 0 before and after the addition of MWF were respectively 43.6 mg C/L and 71.7 mg C/L. This first result confirms that the coolant were prone to attach on biomass. In fact, if the coolant had remained in the bulk liquid, the TOC value after the addition would have been approximately 760 mg C/L, a value ten times higher the observed one. In stage 2, after the connection of two reactors it was observed a dilution effect of the total organic carbon. As a result, TOC decreased in reactor A and increased in reactor B. In stage 3, a steady value was observed for both reactors justifying again the assumption of the attachment propensity of MWFs on biomass. Moreover, comparing bulk liquid and permeate TOC, it can be assumed that the retention of organic carbon on the membrane surface did not occur in a significant way.

With regards to VFAs data, total VFAs (sum of propionic acid, isobutirric acid and n-butirric acid) accounted for 90-100% of TOC in stage 1 and stage 2, except for the first datum (64%) after the coolant addition. Therefore, the 36% of TOC after the addition could be related to that coolant which was not attached on biomass. In stage 2 the dilution effect observed for TOC affected VFAs data as well.

The quantification of formic and acetic acids was not possible to perform because of an interference in the HPLC results, hiding the formic and acetic acids peaks. However results shown in Table 7.6 suggest that propionic acid, isobutirric acid and n-butirric acid were the most significant VFAs in bulk.

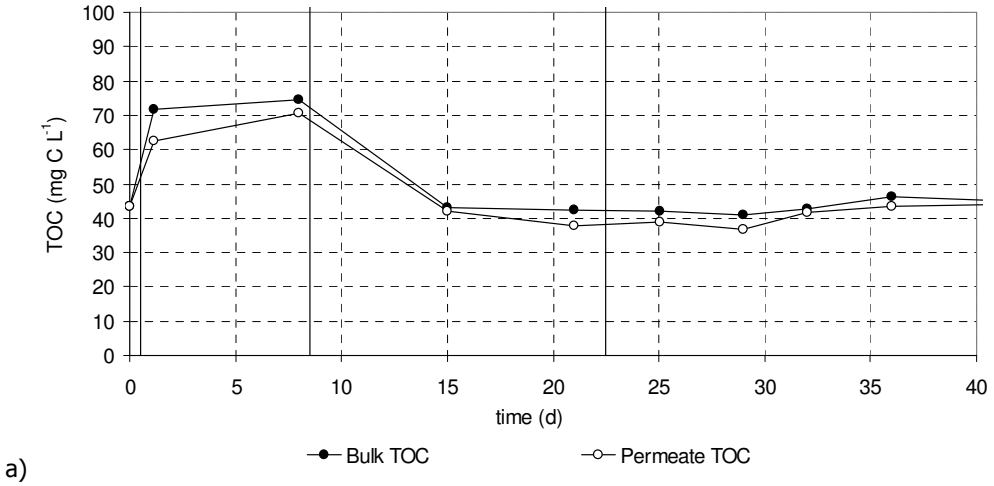

a)

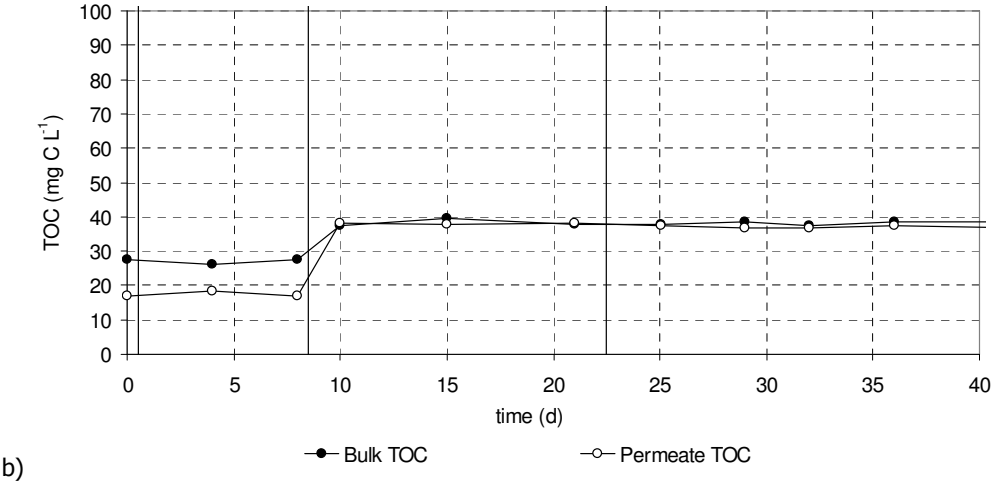

b)

Figure 7.16. Total organic carbon in bulk and permeate: a) reactor A, b) reactor B.

Table 7.6. Ratio of Total VFAs (measures as organic carbon) divided by TOC.

Sample		Total VFAs/TOC	
		A	B
Stage 1	0 before MWF addition	100%	92%
	0 after MWF addition	64%	-
	day 8	100%	81%
Stage 2	day 10	-	-
	day 15	92%	82%
	day 21	92%	83%
Stage 3	day 25	31%	61%
	day 29	42%	42%
	day 32	13%	13%
	day 36	19%	19%

a)

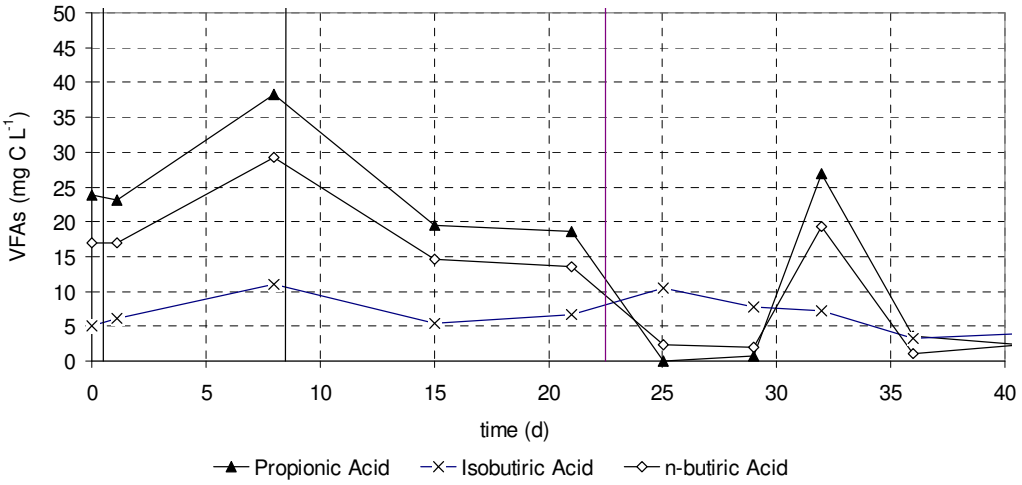

b)

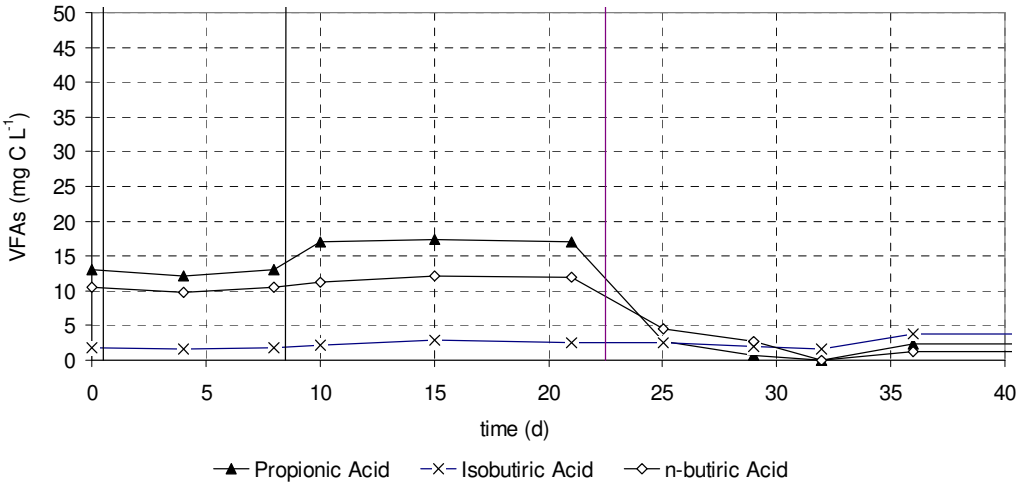

Figure 7.17. Volatile fatty acids measured as the equivalent concentration of carbon (mg C/L) in bulk: a) reactor A, b) reactor B.

Concentration and particle size distribution of biosolids. The solids concentration of mixed liquor are shown in Figure 7.18. MLSS in reactor A were approximately 4.5÷5.0 g L^{-1} whereas in reactor B, MLSS were around 0.7÷1.0 g MLSS L^{-1}. In particular, MLSS concentration in reactor B was set to such a low value because it was supposed that 1 g L^{-1} was sufficient to convert the products of fermentation into methane in the start-up phase of SAMBR. Differently, MLSS in reactor A was higher in order to work with a proper value of the F/M ratio to limit the adverse effects of fresh coolant covering of biomass.

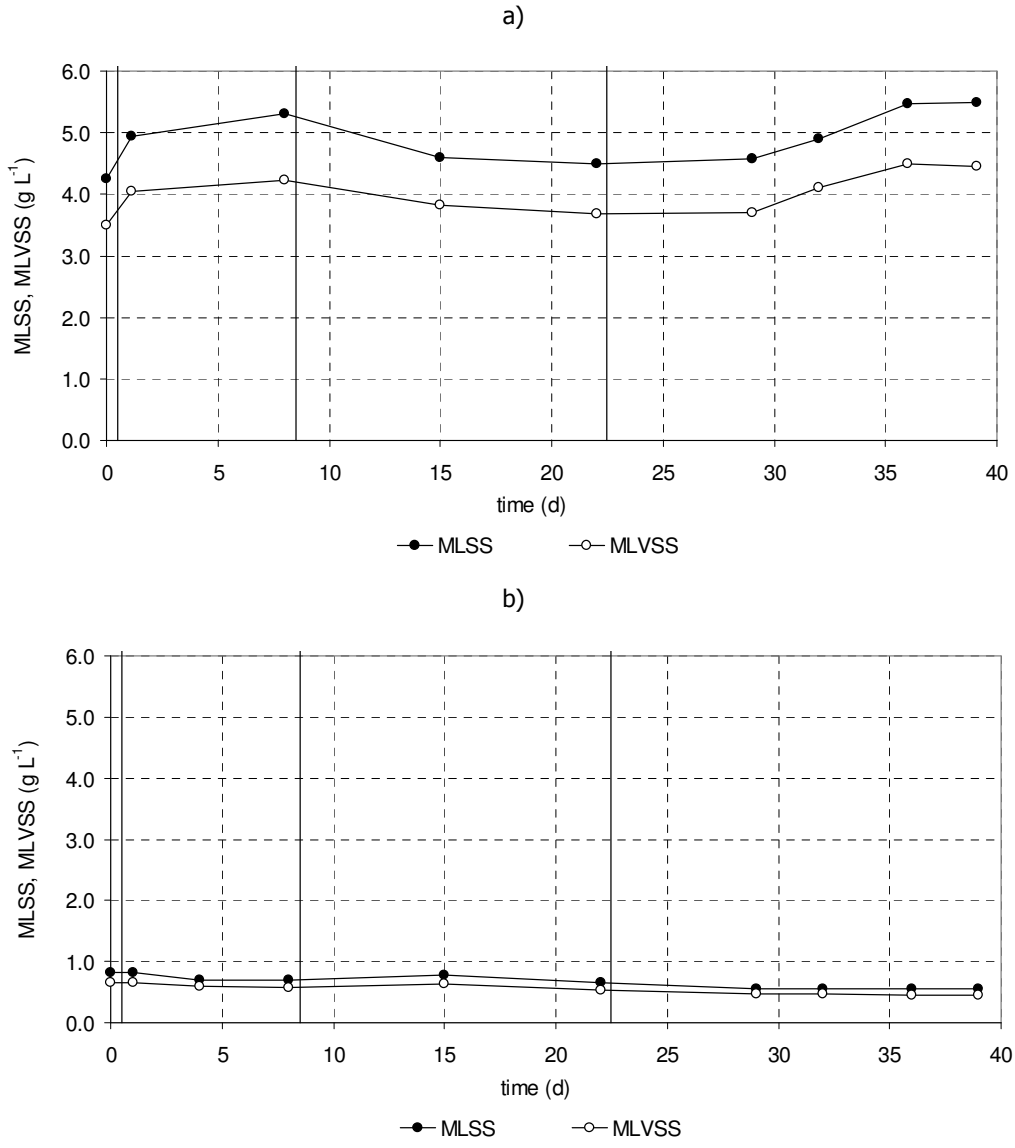

Figure 7.18. Mixed liquor solids concentration: a) Reactor A, b) Reactor B.

Particle size distribution of mixed liquor samples of reactor A are shown in Figure 7.19. In particular, original data were multiplied by the MLSS concentration of samples[5].

These results indicated that coolant attachment on biomass showed a complex dynamic behaviour over time and that coolant did not cover uniformly biomass, attaching mainly on little flocs ranging from 1 to 30 μm. However, these little flocs accounted for approximately the 55% of total biomass.

[5] With regards to samples collected before the MWF addition, the measured value of TSS was taken into account (4.3 g/L), whereas TSS and MWF added were considered for samples collected after the MWF addition (4.3 + 1.0 = 5.3 g/L).

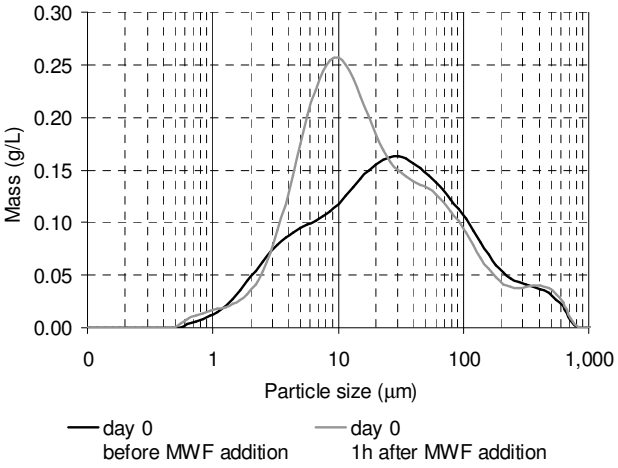

a)

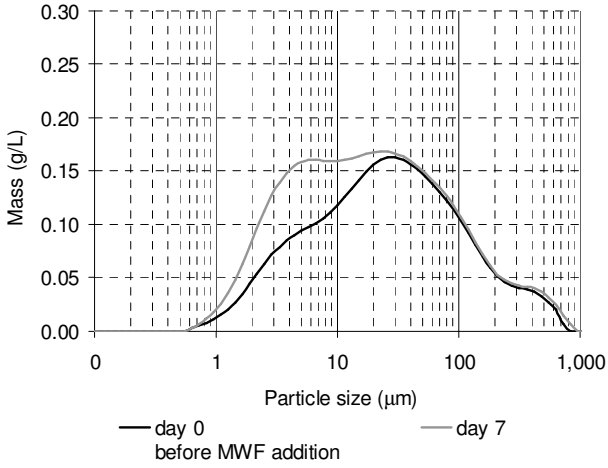

b)

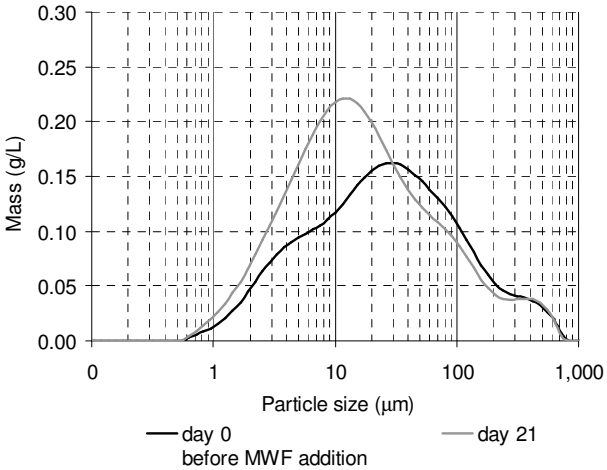

c)

Figure 7.19. Particle size distribution of mixed liquor samples of reactor A (the original output was multiplied by the MLSS concentration of samples): a) day 0 after coolant addition versus day 0 before coolant addition, b) day 7 versus day 0 before MWF addition, c) day 21 versus day 0 before MWF addition.

Hydraulic performance of Kubota modules. The evolution of TMP over time is shown in Figure 7.20 (method B.4, section 5.4.2). The results suggest that no significant membrane fouling appeared in 40 days. In fact, TMP varied between 0 and 0.010 bar in Reactor A and it showed a pick of approximately 0,020 bar at day 20. In Reactor B, TMP varied between 0 and 0.020 bar and presented a pick of approximately 0,040 bar at days 20 and 33. Comparing these results to the short permeation test (paragraph 4.3.1), it appears that the adopted filtration parameters (5 LMH flux, 5 LPM gas sparging) were properly set. Moreover, from these results, it can be supposed that the coolant was more prone to attach on biomass than on membrane surface, probably as long as the attachment on biomass was not saturated.

a)

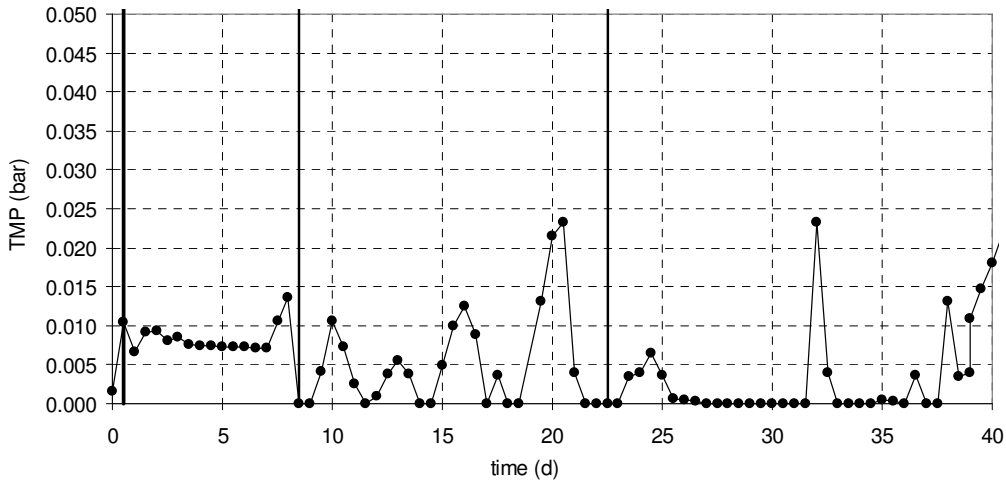

b)

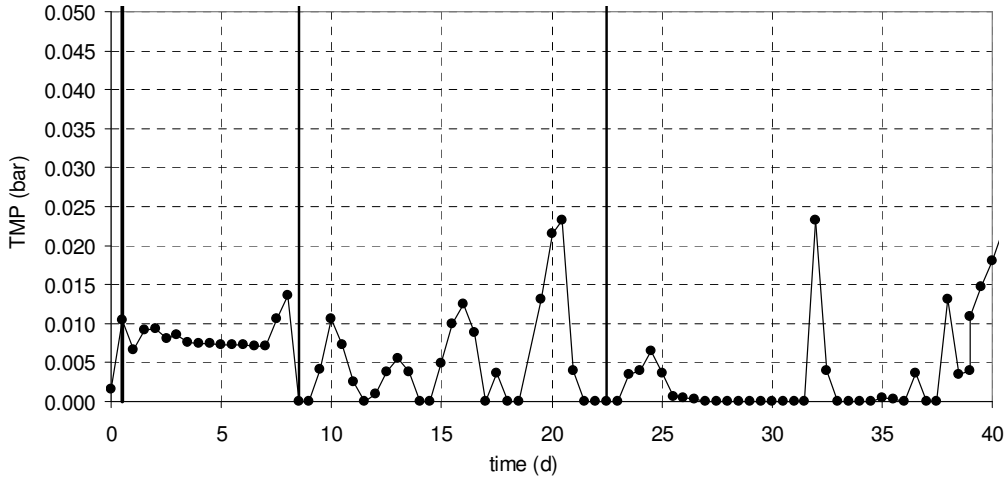

Figure 7.20. Transmembrane pressure: a) reactor A, b) reactor B.

8 Conclusions

8.1 Introduction

In the present dissertation, the application of the MBR technology to industrial wastewaters was investigated with reference to two different applications. The fist application (topic A) regarded the treatment of textile wastewaters and fouling control in an anoxic-aerobic MBR. In particular, the main aim considered was the evaluation of the effectiveness of flux enhancers addition at low dosages into a pilot scale MBR fed with a mixed domestic-textile wastewater in terms of permeate quality enhancement and fouling control. Differently, the second application (topic B) regarded the start-up of a two phases submerged anaerobic MBR (SAMBR) treating a synthetic metal working effluent. In particular, the long term aim was to achieve a biomass acclimatized to MWFs, with effective biodegradation features and methane conversion capability. In Table 8.1 main goals for both of the topics are recalled, whereas in the following sections main conclusions are drawn and relevant suggestion for further research are proposed.

Table 8.1. Topics and main goals of the thesis.

Topic	Main goals
A	1. assessment of the MBR process performances and comparison with the full scale WWTP where the pilot MBR was set; 2. screening of 3 flux enhancers by lab-scale tests to select the best chemical and define the optimal dosage; 3. continuous dosage of the selected flux enhancers and evaluation of its effects on fouling control and permeate quality enhancement. 4. development of a new methodology for the evaluation of sludge fouling propensity to monitor the effects of flux enhancer.
B	1. evaluation of biodegradability and the inherent toxicity of MWFs using not acclimatized anaerobic biomass. 2. start-up of a two phases SAMBR.

8.2 Treatment of textile wastewaters and fouling control in an anoxic-aerobic MBR (topic A)

Main results and conclusions of topic A are summarized herein. In particular, as for goal 1, the pilot MBR showed good performances considering both ordinary macro-parameters (i.e., COD and nutrients) and textile macro-pollutants (i.e., colour and surfactants). Moreover, the comparison of the MBR efficiency with the full scale WWTP performance, executed taking

into account COD, total nitrogen, and colour (data available for the full scale WWTP) showed a slight amelioration in the effluent quality (considering average values) but confirmed the higher stability of the biological process in MBRs than in CASPs. In particular, the average COD concentration was lower in permeate than in both the biological and the final full scale WWTP effluents (output of advanced treatments, comprising high rate clarification and ozone oxidation) of about 3.2%. Since advanced process did not affected COD quality at all, it can be assumed that a better performance of the MBR would not have been possible to achieve. As for total nitrogen, the pilot MBR gave lower values because it was designed to respect more strict limits[6] (<10 mg N_{tot} L^{-1}) respect to the full scale WWTP (average value of 16.3±3.45 mg N_{tot} L^{-1} in the biological effluent). Therefore, such an amelioration was not related to any improvement of biological process but it was due to a different criteria applied in WWTP design. However, it must be stressed that such a result was achieved when the denitrification performance was optimized by adding acetate that corresponded to the 44% of the total COD entering the reactor. On the other hand, acetate addition could have affected sludge characteristics and fouling occurrence probably modifying bacteria metabolism or affecting the bacterial community composition. However, an external COD source was necessary for nitrogen control because the wastewater was poor in terms of readily biodegradable COD. As for colour, the pilot MBR showed absorbance values at 426 nm lower than the WWTP biological effluent of about 5.3%. By comparison, the final WWTP effluent showed a reduction of about 57.9% in absorbance respect to the biological effluent, therefore highlighting the not biodegradable nature of dyes. To sum up, with regards to goal 1, a slight amelioration was observed for COD and colour in permeate compared to biological effluent of the full scale WWTP due to the recalcitrant nature of residual organics. But, for all the parameters, standard deviations were minor for the pilot MBR, therefore giving a proof of the stability of the biological process in MBRs compared to CASPs, as reported in literature.

With regards to the main aim of topic A, i.e., the evaluation of the effectiveness of flux enhancers in terms of permeate quality enhancement and fouling control, low dosages were considered to limit any detrimental effect to the biological process, resulting in a loss of bacterial activity as reported in literature, and to guarantee economic sustainability for a possible implementation in full scale MBRs. Firstly, polyaluminium chloride (PACl) was selected as the best flux enhancer on the basis of a jar test campaign (goal 2). Then, a specific dosing strategy was implemented to increase progressively PACl concentration from

[6] This standard was set in the Urban Waste Water Treatment Directive (91/271/EEC) for eutrophication sensitive areas and WWTPs greater than 100,000 p.e.

an initial value of 6.25 mg g $MLSS^{-1}$ to the optimum value of 12.5 mg g $MLSS^{-1}$ defined during the jar test campaign. In this phase, attention was paid to possible losses in MBR performances indicating the occurrence of bacteria inhibition, but no failure of the process was observed and therefore PACl dosage was kept constant at the optimum concentration. Moreover, to verify the absence of any inhibition, heterotrophic and autotrophic activities were assessed employing respirometric techniques. In particular, heterotrophic and autotrophic kinetic constants were evaluated before the addition of PACl and the end of experimental period, showing variation within the COV of the respirometric techniques (15%) and therefore highlighting the absence of inhibitions.

With regards to goal 3, the addition of PACl resulted in a significant improvement in permeate quality and fouling control. In fact, as for permeate quality, considering the ordinary macro-parameters, considerable improvements for COD (removal rate with PACl of 91% vs removal of 81% during control periods) and total phosphorus (87.8% vs 23.6%) were detected. With regards to textile macro-parameters, PACl improved removal rates for colour (absorbance at 426 nm: 83.6% vs 72.0%), and anionic surfactants (84.3% vs 79.2%). As for fouling, the average irreversible fouling rate FR presented a value of $1.04 \cdot 10^{9}$ m^{-1} d^{-1} with PACl, whereas in the control period a value of $1.90 \cdot 10^{9}$ m^{-1} d^{-1} was observed. With regards to reversible fouling, PACl gave a significant reduction in $R_{c,}$ overall presenting in stage 2 absolute values comparable with that of the new membranes (R_m). It is important to point out that this result was achieved even if a collapse in flocs strength and structure occurred, probably due to NaCl usage during winter season to prevent car-crashes occurring because of snow or ice presence on roads. In fact, NaCl can be dissolved by snow and rain, reach the WWTP through the sewer system, and lead to sludge flocs break-up and strength collapse since monovalent cations compete and substitute divalent and polyvalent cations in binding the organic flocs matrix. Parameters such us strength indexes (SI_1, SI_2), introduced and investigated firstly in this thesis, and SRF gave a proof of such a collapse in flocs strength and sludge filterability. In fact, it was observed that, from day 273 onwards, all the above parameters showed variations indicating the loss in strength phenomenon. In particular, SI_1, representing the divalent cations (sum of Ca^{2+} and Mg^{2+}) content in flocs per gram of MLVSS, showed a variation from 42.5 to 23.5 mg g $MLVSS^{-1}$, whereas SI_2, indicating the percentage of low bounded divalent cations in flocs, presented a variation from 7.5 to 15%. In particular, according to the divalent cation bridging (DCB) theory (Sobeck and Higgins, 2002) and the polymer bridging model (PBM) theory (Wilén at al., 2003), the higher the values of SI_1, the better the flocs strength is. Differently, as for index SI_2, the higher the fraction of low bounded divalent cations, the slighter the compactness and strength of flocs are. With regards to SRF, it showed a variation from $6 \cdot 10^{13}$ to a value of $9 \cdot 10^{13}$ m kg^{-1}. Also,

the definition and the implementation of a new flux-step method for the evaluation of the fouling propensity (goal 4) indicated a deterioration in all the relevant parameter giving information on fouling propensity from day 273 onwards, i.e., critical flux (Jc), the irreversibility factor and the compressibility factor (CF). In particular, Jc varied from a value close to 20 LMH to a value of 15.2 LMH and CF showed a rise from a value of $1.25 \cdot 10^9$ bar^{-1} m^{-2} to a value of $3.5 \cdot 10^9$ bar^{-1} m^{-2}.

Apparently, results related to biomass characteristics and fouling monitoring did not match. In fact, it was expected that a loss in sludge strength and filterability would have affected R_c negatively. However, a possible explanation of this phenomenon was proposed in the thesis. Firstly, since it was observed a release of divalent cations and sEPS proteins from sludge flocs into bulk liquid, it can be also thought that PACl was released into the bulk liquid and, overall, this phenomenon impacted negatively on sludge filterability and fouling propensity. However, comparing cations and proteins content in bulk and permeate it was found that there was a progressive accumulation of such compounds in the cake layer. Moreover, the same assumption can be made for PACl. As a consequence, since cations and PACl can improve cake filterability, this accumulation into the cake layer permitted that R_c was under control and, moreover, presented slightly minor values after day 273 than before.

Anyway, the fact that biomass characteristics and fouling monitoring did not match highlights the complexity of fouling which depends on numerous autonomous factors. Moreover, such factors can present synergic or opposing effects, that are specific for each application. Therefore, to better understand fouling, it necessary to consider a pool of selected indicators related to its occurrence and governing factors, and not to measure only single parameters because of poor reliability.

In conclusion, PACl addition into the MBR enhanced significantly the permeate quality and controlled fouling occurrence properly also when a loss in flocs compactness and strength occurred. Moreover, since no decline in the MBR biological activity was observed during PACl dosing, the MBR technology combined with PACl addition can be considered as an effective option for the treatment of textile wastewater and, in general, an option for industrial effluents. However, further research is necessary, particularly with regards to the selection criteria of flux enhancers and the definition of the optimal dose, investigating the quality and the criticism of the flux enhancers selection on the basis of jar test campaigns. Moreover, other suggestions for further research follow:

- the relation between biomass characteristics and fouling occurrence should be studied deeply to better investigate the reason of the discordance between the parameters monitored in this study, introducing also investigations of sludge rheology and dewaterability;

- considering the necessity of the optimization of denitrification in the case of poor readily degradable COD effluent, the selection and comparison of different external carbon source should be investigated properly; in fact, it has been reported that the carbon source type can affect the formation and elimination of soluble-EPS and flocs stability (McAdam et al., 2007) and therefore the selection of the best carbon source could result in a less fouling and better performances of an eventual addition of PACl also working at lower doses implying lower costs and lower risks of inhibition;
- long run assessment (years) of PACl addition in two or more pilot MBR plants in parallel could be executed not only to investigate the quality enchantment and fouling control but also taking into consideration the effects on the bacteria community composition (does PACl induce in the long run a more effective community in terms of biodegradation?) and the effects on membranes life (does PACl increase the membranes life?).

8.3 Start-up of a submerged anaerobic MBR treating a synthetic metal working effluent (topic B)

Main results and conclusions of topic B are summarized herein. In particular, considering goal 1, the evaluation of the biodegradability and the inherent toxicity using anaerobic biomass not acclimatized to MWFs was performed executing BMP, VFAs production, and anaerobic toxicity assays (ATAs). In particular, in BMP at high F/M ratios (>1 g MFW g $MLSS^{-1}$), the production of methane was detected only at a coolant concentration of 0.5% over a period of 150 days showing a biodegradation approximately of 0.8% of the total coolant organic carbon. At the same conditions, the addition of acetate (performed during ATAs) implied an amelioration in the biodegradation showing a value of 4.2%. Differently, in BMP at low F/M ratios (<1 g MFW g $MLSS^{-1}$), the total amount of methane of controls exceeded the methane produced in samples with coolant at a concentration of 0.1%, suggesting that MWFs can inhibit some pathways of biodegradation, such as methane bio-conversion from decay.

VFAs production assays suggested that the adaptation of the hydrolytic/heteroacetogenic bacteria (upper pathway of anaerobic digestion) did not occur significantly during the tests. Moreover, anaerobic toxicity assays showed the acetoclastic methanogenesis and the methane production from formate (lower pathway of anaerobic digestion) were inhibited to a certain degree related to the coolant concentration.

It is believed that the inhibitory propensity and the low biodegradability of MWFs was due both to biochemical and physical reasons. The former can be related to the necessity of a

more rich enzymatic poll of the bacteria community, that, in not acclimatized biomass used, maybe was characterized by a lack of enzymes for complex molecules degradation or detoxification enzymes to convert inhibitors into innocuous compounds. Differently, the latter can be related to the coolant attachment propensity on sludge flocs observed by particle size distribution analysis. In fact, this can result in a wrapping effect of biomass flocs leading to a possible limitation of the transport of soluble substrates, therefore reducing the substrate conversion rate. Moreover, the occurrence of basic pH values can also affect and inhibit the metabolic activity of anaerobic biomass as though it was happened in ATAs with formate at a coolant concentration of 0.5%. In particular, basic pH enhances the biocide activity, present in MWFs.

Considering these possible reasons of the inhibitory propensity and the poor biodegradability of MWFs, the start-up the two phase SAMBR was executed (goal 2), where the first reactor was thought to be a protective barrier for the growth of methanogens bacteria (present in the second reactor), usually more sensible to inhibition. However, methane production was observed in the first days of SAMBR operation (batch phases) showing a degradation of MWF of 1.65% after approximately 7 days at an initial coolant concentration of 0.1% in mixed liquor. After day 7 the methane production failed, whereas control serum bottles seeded with the same mixed liquor composition continued to produce biogas. This fact highlighted the difficulties in operation bioreactors treating MWFs.

The attachment propensity of the coolant on biomass resulted in a stable filtration operation (5 LMH, 5 LPM gas sparging) showing a TMP variation between 0 and 0.020 bar in 40 days. Differently, a previous short filtration test without biomass (10 LMH, 2.5 LPM gas sparging) showed a rapid rise in TMP reaching a value of 0.100 bar in 20 min. Therefore, it can be supposed that the coolant was more prone to attach on biomass than on membrane surface, probably as long as the attachment on biomass was not saturated.

In conclusion, results related to topic B showed that the synthetic effluent considered in the study was characterized by a low anaerobic biodegradability both in batch preliminary tests and also during the start-up of the two phases SAMBR. On the other hand, as stated above, the aim of topic B was to achieve a biomass acclimatized to MWFs (with effective biodegradation features and methane conversion capability) in the long run. In particular, to achieve this goal the following strategies could be considered for further research:

- spent MWFs could be used instead of fresh ones since spent MWFs could be biodegraded more easily because of organics alterations occurring during the machining processing;
- the co-substrate addition could be considered to support microbial growth, or, in order to generate co-metabolism, i.e., the simultaneous degradation of two compounds (co-

substrate and organics in MWFs in this case), in which the degradation of the second compound (organics in MWFs) depends on the presence of the first compound (co-substrate) because of the induction in the production of enzymes able to degrade (partially) also the second compound (organics in MWFs);

- different sources of anaerobic biomass treating similar effluents could be added systematically into the SAMBR to enrich the bacteria community and its enzymatic pool.

9 References

Abwasserverordnung (AbwV) vom 15. Oktober 2002, Anhang 38.

Ahmed Z., Cho J., Lim B.R., Song K.G., Ahn K.H. (2007). Effects of sludge retention time on membrane fouling and microbial community structure in a membrane bioreactor. Journal of Membrane Science, 287(2), 211-218.

Ahn Y.T., Kang S.T, Chae S.R., Lim J.L., Lee S.H., Shin H.S. (2005). Effect of internal recycle rate on the high-strength nitrogen wastewater treatment in the combined UBF/MBR system. Water Science and Technology, 51, 241-247.

Akram A., Stuckey D.C. (2008). Flux and performance improvement in a submerged anaerobic membrane bioreactor (SAMBR) using powdered activated carbon (PAC). Process Biochemistry, 43(1), 93-102.

Al-Halbouni D., Traber J., Lyko S., Wintgens T., Melin T., Tacke D., Janot A., Dott W., Hollender J. (2008). Correlation of EPS content in activated sludge at different sludge retention times with membrane fouling phenomena. Water Research, 42, 1475-1488.

Allen W., Prescott W.B., Derby Jr R.E., Garland C.E., Peret J.M., Saltzman M. (1972). Determination of color of water and wastewater by means of ADMI color values, in: Proceeding of 28th Ind. Waste Conf., Purdue University, Lafayette, IN, pp. 661-6 75.

APHA, AWWA, WEF (2005). Standard methods for the examination of water and wastewater 19th ed. American Public Health Association, American Water Works Association, and Water Environment Federation, Washington, DC.

Arabi S., Nakhla G. (2008). Impact of calcium on the membrane fouling in membrane bioreactors. Journal of Membrane Science, 314, 134-142.

Artiga P., Gonzalez F., Mosquera-Corral A., Campos J.L., Garrido J.M., Ficara E., Méndez R. (2005). Multiple analyses reprogrammable titration analyser for the kinetic characterisation of nitrifying and autotrophic denitrifying biomass. Biochemical Engineering Journal, 26, 176-183.

ASCE (1993). Measurement of oxygen transfer in clean water, second edition, ASCE Standard n. ANSI/ASCE 2-91.

Bacchin P., Aimar P., Field R.W. (2006). Critical and sustainable fluxes: theory, experiments and applications. Journal of Membrane Science, 281, 42-69.

Badani Z., Ait-Amar H., Si-Salah A., Brik M., Fuchs W. (2005). Treatment of textile waste water by membrane bioreactor and reuse. Desalination, 185, 411-417.

Bae T.H., Tak T.M. (2005). Interpretation of fouling characteristics of ultrafiltration membranes during the filtration of membrane bioreactor mixed liquor. Journal of Membrane Science, 264, 151–160.

Bailey J., Bemberis I., Presti J. (1971). Phase I Final Report – Shipboard sewage treatment system, General Dynamics Electric Boat Division, NTIS.

Baker C.A., Claus G.W., Taylor P.A. (1983). Predominant bacteria in an activated sludge reactor for the degradation of cutting fluids. Applied Environmental Microbiology, 46, 1214-1223.

Baker R.J., Fane A.G., Fell C.J.D., Yoo B.H. (1985). Factors affecting flux in crossflow filtration. Desalination, 53, 81-93.

Barker D.J., Stuckey D.C. (1999). A review of soluble microbial products (SMP) in wastewater treatment systems. Water Research, 33, 3063-3082.

Baumgarten S., Schroder H.Fr., Pinnekamp J. (2009). Performance of membrane bioreactors used for the treatment of wastewater from the chemical and textile industries. Water Science and Technology, 53(3), 61-67.

Bemberis I., Hubbard P.J., Leonard F.B. (1971). Membrane sewage treatment systems – potential for complete wastewater treatment. American Society of Agricultural Engineers Winter Meeting, 71-878, 1–28.

Bienati B., Bottino A., Capannelli G., Comite A. (2008). Characterization and performance of different types of hollow fibre membranes in a laboratory-scale MBR for the treatment of industrial wastewater. Desalination, 231, 133-140.

Bin C., Xiaochang W., Enrang W. (2004). Effects of TMP, MLSS concentration and intermittent membrane permeation on a hybrid submerged MBR fouling, in: Proceedings of the Water Environment-Membrane Technology Conference, Seoul, Korea.

BLF (British Lubricants Federation), (2003). Boric Acid in Metalworking Fluids. Information sheet Meatlworking

Brik M., Chamam B., Schöberl P., Braun R., Fuchs W. (2004). Effect of ozone, chlorine and hydrogen peroxide on the elimination of colour in treated textile wastewater by MBR. Water Science and Technology, 49(4), 299-303.

Brik M., Schoeberl P., Chamam B., Braun R., Fuchs W. (2006). Advanced treatment of textile wastewater towards reuse using a membrane bioreactor. Process Biochemistry, 41(8), 1751-1757.

Bromley-Challenor K.C.A, Knapp J.S., Zhang Z., Gray N.C.C., Hetheridge M.J., Evans M.R. (2000). Decolorization of an azo dye by unacclimated activated sludge under anaerobic conditions. Water Research, 34(18), 4410–4418.

Brookes A., Jefferson B., Guglielmi G., Judd S.J. (2006). Sustainable flux fouling in a membrane bioreactor: impact of flux and MLSS. Separation Science and Technology, 41, 1279-1291.

Brookes A., Jefferson B., Judd S.J. (2004). Sub-critical fouling in a membrane bioreactor: impact of flux and MLSS, in: Proceeding of IWA 4th Word Water Congress, Marrakech.

Brookes A., Judd S., Reid E., Germain E., Smith S., Alvarez-Vazquez H., Le-Clech P., Stephenson T., Turra E., Jefferson B. (2003). Biomass characterisation in membrane bioreactors, in: Proceedings of the IMSTEC, Sydney, Australia.

Brown M.J., Lester J.N. (1980) Comparison of bacterial extracellular polymer extraction methods. Applied and Environmental Microbiology, 40(2), 179-185.

Bruus J.H., Nielsen P.H., Keiding K. (1992). On the stability of activated sludge flocs with implications to dewatering. Water Research, 26, 1597-1604.

Bruze M., Hradil E., Eriksohn I.L., Gruvberger B., Widstrom L. (1995). Occupational allergic contact dermatitis from alkanolamineborates in metalworking fluids. Contact Dermatitis, 32, 24-27.

Burke J.M. (1991). Waste treatment of metal working fluids, a comparison of three common methods. Lubrication Engineering, 47, 238-246.

Cabassud C., Masse A., Espinosa-Bouchot M., Spérandio M. (2004). Submerged membrane bioreactors: interactions between membrane filtration and biological activity, in: Proceedings of the Water Environment-Membrane Technology Conference, Seoul, Korea.

Calvert G.M., Ward E., Schnorr T.M., Fine L.J. (1998). Cancer risks among workers exposed to metalworking fluids: a systematic review. American Journal of Industrial Medicine, 33, 282-292.

Cammarota M.C., Freire D.M.G. (2006). A review on hydrolytic enzymes in the treatment of wastewater with high oil and grease content. Bioresource Technology, 97, 2195-2210.

Carliell C.M., Barclay S.J., Shaw C., Wheatley A.D., Buckley C.A. (1998). The effects of salts used in textile dyeing on microbial decolourisation of a reactive azo dye. Environmental technology, 19(11), 1133-1137.

Carman P.C. (1938). Fundamental principles of industrial filtration (a critical review of present knowledge). Transactions of the Institution of Chemical Engineers, 16, 168-188.

Chang I.S., Bag S.O., Lee C.H. (2001). Effects of membrane fouling on solute rejection during membrane filtration of activated sludge. Process Biochemistry, 36, 855-860.

Chang I.S., Kim S.N. (2005). Wastewater treatment using membrane filtration—effect of biosolids concentration on cake resistance. Process Biochemistry, 40, 1307-1314.

Chang I.S., Le-Clech P., Jefferson B., Judd S. (2002). Membrane fouling in membrane bioreactors for wastewater treatment. Journal of Environmental Engineering, 128(11), 1018–1029.

Chazal P.M. (1995). Pollution of modern metalworking fluids containing biocides by pathogenic bacteria in France. Reexamination of chemical treatments accuracy. European Journal of Epidemiology, 11, 1-7.

Cheng C., Phipps D., Alkhaddar R.M. (2005). Treatment of spent metalworking fluids. Water Research, 39, 4051-4063.

Cheng C., Phipps D., Alkhaddar R.M. (2006). Thermophilic aerobic wastewater treatment of waste metalworking fluids. Water and Environment Journal, 20, 227–232.

Cheng C., Phipps D.A., Alkhaddar R.M. (2004). Treatment of waste metalworking fluids, in: Proceedings of the Fifth IWA UK Young Researchers Conference, University of Southampton.

Cho B.D., Fane A.G. (2002). Fouling transients in nominally sub-critical flux operation of a membrane bioreactor. Journal of Membrane Science, 209(2), 391-403.

Cho J., Song K.G., Yun H., Ahn K.H., Kim J.Y., Chung T.H. (2005). Quantitative analysis of biological effect on membrane fouling in submerged membrane bioreactor. Water Science and Technology, 51(6-7), 9-18.

Choi H., Zhang K., Dionysiou D.D., Oerther D.B., Sorial G.A. (2005). Influence of cross-flow velocity on membrane performance during filtration of biological suspension. Journal of Membrane Science, 248, 189-199.

Choo K.H., Lee C.H. (1998). Hydrodynamic behavior of anaerobic biosolids during crossflow filtration in the membrane anaerobic bioreactor. Water Research, 32(11), 3387-3397.

Christensen J.R., Sorensen P.B., Christensen G.L., Hansen J.A. (1993). Mechanisms for overdosing in sludge conditioning. Journal of Environmental Engineering, 119, 159-171.

Chu H.P., Li X.Y. (2005). Membrane fouling in a membrane bioreactor (MBR): sludge cake formation and fouling characteristics. Biotechnology and Bioengineering, 90(3), 323-331.

Cicek N., Franco J.P., Suidan M.T., Urbain V., Manem J. (1999). Characterization and comparison of a membrane bioreactor and a conventional activated- sludge system in the treatment of wastewater containing high-molecular- weight compounds. Water Environment Research, 71, 64-70.

Colour Index, 3rd Revision (1987).Society of Dyers and Colourists (UK) and the American Association of Textile Chemists and Colourists (USA).

Comte S., Guibaud G., Baudu M. (2006) Relations between extraction protocols for activated sludge extracellular polymeric substances (EPS) and EPS complexation properties. Part I. Comparison of the efficiency of eight EPS extraction methods. Enzyme and Microbial Technology. 38, 237–245.

Cooper S.G. (1978). The textile industry, environmental control and energy conservation. Noyes Data Co., Park Ridge, NJ.

Correia V.M., Stephenson T., Judd S.J. (1994). Characterisation of textile wastewater – a review. Environmental technology, 15(10), 917-929.

De la Torre T., Lesjean B., Mottschall M., Drews A., Iheanaetu A., Kraume M. (2008). Filterability assessment in membrane bioreactors using an in-situ filtration test cell, in: Proceedings of the Aquatech, 1-3 October, 2008, Amsterdam.

De Wever H., Van Roy S., Dotremont C., Muller J., Knepper T. (2004). Comparison of linear alkylbenzene sulfonates removal in conventional activated sludge systems and membrane bioreactors. Water Science and Technology, 50(5), 219-225.

Deepak D., Anand K.V., Bhargava R. (1994). Biodegradation kinetics of metal cutting oil: evaluation of kinetic parameters. Chemical Engineering Journal, 56, B91-B96.

Defrance L., Jaffrin M.Y. (1999). Reversibility of fouling formed in activated sludge filtration. Journal of Membrane Science, 157, 73-84.

Delée W., O'Neill C., Hawkes F.R., Pinheiro H.M. (1998). Anaerobic treatment of textile effluents: A review. Journal of Chemical Technology and Biotechnology, 73(4), 323–335.

Di Bella G., Mannina G., Viviani G. (2008). An integrated model for physical-biological wastewater organic removal in a submerged membrane bioreactor: Model development and parameter estimation. Journal of Membrane Science, 322, 1-12.

Dignac M.-F, Urbain V., Rybacki D., Bruchet A., Snidaro D., and Scribe P. (1998) Chemical description of extracellular polymers: Implication on activated sludge floc structure. Wat. Sci. Tech., 38, 45-53.

Doble M., Kumar A. (2005). Biotreatment of Industrial Effluents. Elsevier, Oxford.

Drews A. (2010). Membrane fouling in membrane bioreactors—Characterisation, contradictions, cause and cures. Journal of Membrane Science, 363(1-2), 1-28.

Drews A., Evenblij H., Rosenberger S. (2005). Potential and drawbacks of microbiology–membrane interaction in membrane bioreactors. Environmental Progress, 24(4), 426–433.

Drews A., Mante J., Iversen V., Vocks M., Lesjean B., Kraume M. (2007). Impact of ambient conditions on SMP elimination and rejection in MBRs. Water Research, 41(17), 3850-3858.

Drews A., Vocks M., Bracklow U., Iversen V., Kraume M. (2008). Does fouling in MBRs depend on SMP? Desalination, 231, 141-149.

Drews A., Vocks M., Iversen V., Lesjean B., Kraume M. (2006). Influence of unsteady membrane bioreactor operation on EPS formation and filtration resistance. Desalination, 192, 1-9.

DTI (The Department of Trade and Industry), (1998). Development of an integrated membrane bioreactor system for the treatment of used cutting fluids and other oily wastes in the engineering industry. DTI/BMB/39/1500/98/10.

Dubois M., Gilles K.A., Hamilton J.K., Rebers P.A., Smith P. (1956). Colorimetric method for determination of sugars and related substances. Analytical Chemistry, 28, 350-356.

EC (2007). Deliverable Report D13: Characterization and comparison of monitoring techniques applied to the selected MBRs operated by involved partners EUROMBRA project, Contract No. 018480.

EC (2009). Deliverable Report D12. Project AMADEUS.

Ekama G.A., Dold P.L., Marais G.v.R. (1986). Procedures for determining influent COD fractions and the maximum specific growth rate of heterotrophs in activated sludge systems. Water Science and Technology, 18(6), 91-114.

EPA (1982). The Textile Mills Point Source Category effluent guidelines, 40 CFR Part 410.

Evenblij (2006). Filtration characteristics in membrane bioreactors. PhD Thesis. Technical University of Delft.

Evenblij H., Geilvoet S., van der Graaf J., van der Roest H.F. (2005a). Filtration characterisation for assessing MBR performance: three cases compared. Desalination, 178, 115-124.

Evenblij H., van der Graaf J. (2004). Occurrence of EPS in activated sludge from a membrane bioreactor treating municipal wastewater. Water Science and Technology, 50, 293-300.

Evenblij H., Verrecht B., van der Graaf J., Van der Bruggen B. (2005b). Manipulating filterability of MBR activated sludge by pulsed substrate addition. Desalination, 178, 193-201.

Fan F., Zhou H., Husain H. (2006). Identification of wastewater sludge characteristics to predict critical flux for membrane bioreactor processes. Water Research, 40, 205-212.

Fan F.S., Zhou H.D. (2007). Interrelated effects of aeration and mixed liquor fractions on membrane fouling for submerged membrane bioreactor process in wastewater treatment. Environmental Science and Technology, 41, 2523-2528.

Fane A.G., Yeo A., Law A., Parameshwaran K., Wicaksana F., Chen V. (2005). Low pressure membrane processes – doing more with less energy. Desalination, 185(1-3), 159-165.

Fang H.H.P., Shi X., Zhang T. (2006). Effect of activated carbon on fouling of activated sludge filtration. Desalination, 189(1-3), 193-199.

Fawehinmi F., Lens P., Stephenson T., Rogalla F., Jefferson B. (2004). The influence of operating conditions on extracellullar polymeric substances (eps), soluble microbial products (smp) and bio-fouling in anaerobic membrane bioreactors, in: Proceedings of Water Environment – Membrane Technology Conference, Seoul, Korea.

Field R.W., Wu D., Howell J.A. (1995). Critical flux concept for microfiltration fouling. Journal of Membrane Science, 100(3), 259-272.

Flemming H.C., Wingender J. (2001). Relevance of microbial extracellular polymeric substances (EPSs). Part I. Structural and ecological aspects. Water Science and Technology, 43, 1-8.

Frechen F.B. , Schier W., Wett M. (2006). Pre-Treatment of Municipal MBR Applications in Germany - Current Status and Treatment Efficiency. Water Practice and Technology, 1(3).

Frolund B., Palmgren R., Keiding K., Nielsen P.H. (1996). Extraction of extra-cellular polymers from activated sludge using a cation exchange resin. Water Research, 30, 1749-1758.

Fuchs, W., Resch, C., Kernstock, M., Mayer, M., Schoeberl, P. and Braun, R. (2005) Influence of operational conditions on the performance of a mesh filter activated sludge process. Water Res., 39, 803–810.

Gander M., Jefferson B., Judd S. (2000). Aerobic MBRs for domestic wastewater treatment: a review with cost considerations. Separation and Purification Technology, 18, 119-130.

Gao M., Yang M., Li H., Yang Q., Zhang Y. (2004). Comparison between a submerged membrane bioreactor and a conventional activated sludge system on treating ammonia-bearing inorganic wastewater. Journal of Biotechnology, 108, 265-269.

Geilvoet S.P., van Nieuwenhuijzen A.F., van der Graaf J.H.J.M., Moreau A.A., Lousada Ferreira M.C. (2007). MBR activated sludge filterability and quality alteration, in: 6th International Membrane Science and Technology Conference (IMSTEC 07), Sydney, 5-9 November.

Geng Z., Hall E.R. (2007). A comparative study of fouling-related properties of sludge from conventional and membrane enhanced biological phosphorus removal processes. Water Research 41(19), 4329-4338.

Glover B., Hill L. (1993). Waste minimization in the dyehouse. Textile Chemist and Colorist, 25, 15.

Goldstein J.F., Mallory L.M., Alexander M. (1985). Reason of possible failure of inoculation to enhance biodegradation. Applied and Environmental Microbiology, 50(4), 977-983.

González S., Petrovic M., Barceló D. (2007). Removal of a broad range of surfactants from municipal wastewater-comparison between membrane bioreactor and conventional activated sludge treatment. Chemosphere, 67(2), 335-43.

Gonzalez S., Petrovic M., Barcelo D. (2008). Evaluation of two pilot scale membrane bioreactors for the elimination of selected surfactants from municipal wastewater. Journal of Hydrology, 356, 46-55.

Gori R., Cammilli L., Petrovic M., Gonzalez S., Barcel D., Lubello C., Malpei F. (2010). Fate of surfactants in membrane bioreactors and conventional activated sludge plants. Environmental Science and Technology, 44(21), 8223-8229.

Gorner T., de Donato P., Ameil M.H., Montarges-Pelletier E., Lartiges B.S. (2003). Activated sludge exopolymers: separation and identification using size exclusion chromatography and infrared micro-spectroscopy. Water Research, 37, 2388-2393.

Grace H.P. (1956). Structure and performance of filter media. I. The internal structure of filter media. AIChE Journa, 2(3), 307-315.

Grelier P., Rosenberger S., Tazi-Pain A. (2005). Influence of sludge retention time on membrane bioreactor hydraulic performance, in: Proceedings of the International Congress on Membranes and Membrane Processes (ICOM), Seoul, Korea.

Guglielmi G., Saroj D.P., Chiarani D., Andreottola G. (2007). Sub-critical fouling in a membrane bioreactor for municipal wastewater treatment: experimental investigation and mathematical modelling. Water Research, 41, 3903-3914.

Han S.S., Bae T.H., Jang G.G., Tak T.M. (2005). Influence of sludge retention time on membrane fouling and bioactivities in membrane bioreactor system. Process Biochemistry, 40(7), 2393-2400.

Harris C.B., Alkhaddar R., Phipps D.A. (2001). Evaluation of solid media support characteristics favourable for immobilised microbial growth and three phase fluidised bed reactor performance, in: Proceedings of the IWA Second World Water Congress, Berlin, Germany.

Hernandez Rojas M.E., Van Kaam R., Schetrite S., Albasi C. (2005). Role and variations of supernatant compounds in submerged membrane bioreactor fouling. Desalination, 179, 95-107.

Hilal N., Busca G., Hankins N., Mohammad A.W. (2004). The use of ultrafiltration and nanofiltration membranes in the treatment of metal-working fluids. Desalination, 167, 227-238.

Hilal N., Busca G., Waller M.D. (2005). Treatment of metalworking fluids: development of a bioconsortium for the treatment of nanofiltration permeate. Journal of Chemical Technology and Biotechnology, 80, 641-648.

Holbrook R.D., Higgins M.J., Murthy S.N., Fonseca A.D., Fleischer E.J., Daigger G.T., Grizzard T.J., Love N.G., Novak J.T. (2004). Effect of alum addition on the performance of submerged membranes for wastewater treatment. Water Environment Research, 76, 2699-2702.

Hong S.P., Bae T.H., Tak T.M., Hong S., Randall A. (2002). Fouling control in activated sludge submerged hollow fiber membrane bioreactors. Desalination, 143(3), 219-228.

Hu A.Y., Stuckey D.C. (2007). Activated carbon addition to a submerged anaerobic membrane bioreactor: effect on performance, transmembrane pressure, and flux. Journal of Environmental Engineering, 133(1), 73-80.

Huang X., Wu J. (2008). Improvement of membrane filterability of the mixed liquor in a membrane bioreactor by ozonation. Journal of Membrane Science, 318(1-2), 210-216.

Hwang B.K., Lee W.N., Park P.K., Lee C.H., Chang I.S. (2007). Effect of membrane fouling reducer on cake structure and membrane permeability in membrane bioreactor. Journal of Membrane Science, 288(1-2), 149-156.

In-Soung C., Le Clech P., Jefferson B., Judd S. (2002). Membrane Fouling in Membrane Bioreactors for Wastewater Treatment. Journal of Environmental Engineering, 128(11), 1018-1029.

IPPC (2003). Reference documents on Bets Available Techniques for the Textile Industry.

Iritani E., Katagiri N., Sengoku T., Yoo K.M., Kawasaki K., Matsuda A. (2007). Flux decline behaviors in dead-end microfiltration of activated sludge and its supernatant. Journal of Membrane Science, 300, 36-44.

IRSA, Istituto di Ricerca sulle Acque del CNR (1994). Metodi per l'Analisi delle Acque, Po1igrafico e Zecca dello Stato, Rome, Italy.

Itonaga T., Kimura K., Watanabe Y. (2004). Influence of suspension viscosity and colloidal particles on permeability of membrane used in membrane bioreactor (MBR). Water Science and Technology, 50, 301-309.

Iversen V., Bonnet L., Drews A., Lesjean B., Kraume M. (2006). Can we control the fouling with flux enhancing chemicals?, in: Proceedings of EUROMBRA Workshop "Biofouling in membrane systems", 11-12 July, 2006, Trondheim.

Iversen V., Koseoglu H., Yigit N.O., Drews A., Kitis M., Lesjean B., Kraume M. (2009a). Impacts of membrane flux enhancers on activated sludge respiration and nutrient removal in MBRs, Water Research, 43, 822-830.

Iversen V., Villwock J., de la Torre Garcia T., Drews A., Kraume M. (2009b). Impact of flux enhancer for MBR on floc size distribution, dewaterability and shear stability. Desalination and Water Treatment, 6 (1-3), 33-40.

Iversen V., Mehrez R., Horng R.Y., Chen C.H., Meng F., Drews A., Lesjean B., Ernst M., Jekel M., Kraume M. (2009c). Fouling mitigation through flocculants and adsorbents addition in membrane bioreactors: comparing lab and pilot studies. Journal of Membrane Science, 345, 21-30.

Iversen V., Mohaupt J., Drews A., Kraume M., Lesjean B. (2008). Side effects of flux enhancing chemicals in membrane bioreactors (MBRs): study on their biological toxicity and their residual fouling propensity. Water Science and Technology, 57(1), 117-123.

Jang N., Ren X., Choi K., Kim I.S. (2005). Comparison of membrane biofouling in nitrification and denitrification for the membrane bio-reactor (MBR), in: Proceedings of the IWA on Aspire, Singapore.

Jarusutthirak C., Amy G., Croué J.P. (2002). Fouling characteristics of wastewater effluent organic matter (EfOM) isolates on NF and UF membranes. Desalination, 145, 247-255.

Jeison D., van Lier J.B. (2007). Cake formation and consolidation: main factors governing the applicable flux in anaerobic submerged membrane bioreactors (AnSMBR) treating acidified wastewaters. Separation and Purification Technology, 56(1), 71-78.

Ji J., Qiu J., Wong F.S., Li Y. (2008). Enhancement of filterability in MBR achieved by improvement of supernatant and floc characteristics via filter aids addition. Water Research, 42(14), 3611-3622.

Ji L., Zhou J. (2006). Influence of aeration on microbial polymers and membrane fouling in submerged membrane bioreactors. Journal of Membrane Science, 276, 168-177.

Jiang T. (2007). Characterization and Modelling of Soluble Microblial Products in Membrane Bioreactors. PhD thesis, Ghent University, Belgium, pp. 241.

Jiang T., Kennedy M.D., Guinzbourg B.F., Vanrolleghem P.A., Schippers J.C. (2005). Optimising the operation of a mbr pilot plant by quantitative analysis of the membrane fouling mechanism. Water Science and Technology, 51, 19-25.

Jiang T., Myngheer S., De Pauw D.J.W., Spanjers H., Nopens I., Kennedy M.D., Amy G., Vanrolleghem P.A. (2008). Modelling the production and degradation of soluble microbial products (SMP) in membrane bioreactors (MBR). Water Research, 42, 4955-4964.

Jorand F., Zartarian F., Thomas F., Block J.C., Bottero J.Y., Villemin G., Urbain V., Manem, J. (1995). Chemical and structural (2D) linkage between bacteria within activated sludge flocs. Water Research, 29, 1639-1647.

Judd S. (2007). The status of membrane bioreactor technology. Trends in Biotechnology, 26(2), 109-116.

Judd S. (2010). The MBR Book. Principles and Applications of Membrane Bioreactors in Water and Wastewater Treatment. 2nd ed. Elsevier, Oxford.

Judd S. and Jefferson B. (2003). Membranes for Industrial Wastewater Recovery and Re-use. Elsevier, Oxford.

Kang I.J., Lee C.H., Kim K.J. (2003). Characteristics of microfiltration membranes in a membrane coupled sequencing batch reactor system. Water Research, 37(5), 1192-1197.

Kaplan C.W., Kitts C.L. (2003). Bacterial succession in a petroleum land treatment unit. Applied and Environmental Microbiology, 70, 1777-1786.

Kappeler J., Gujer W. (1992). Estimation of kinetic parameters of heterotrophic biomass under aerobic conditions and characterization of wastewater for activated sludge modeling. Water Science and Technology, 25(6), 125-139.

Kayawake E., Narukami Y., Yamagata M. (1991). Anaerobic digestion by a ceramic membrane enclosed reactor. Journal of Fermentation and Bioengineering, 71, 122.

Kim B.R., Anderson S.G., Zemla J.F. (1992a). Aerobic treatment of metal-cutting-fluid wastewater. Water Environment Research, 64, 258–262.

Kim B.R., Devi N.R., Jerome F.Z., Frank L., Harvath P.V. (1994). Biological removal of organic nitrogen and fatty acids from metal-cutting-fluid wastewater. Water Research, 28, 1453–1461.

Kim B.R., Matz M.J., Lipari F. (1989). Treatment of a metalcutting-fluids wastewater using an anaerobic GAC fluidizedbed reactor. Journal - Water Pollution Control Federation, 61, 1430–1439.

Kim B.R., Zemla J.F., Anderson S.G., Stroup D.P., Rai D.N. (1992b). Anaerobic removal of COD in metal-cutting-fluid wastewater. Water Environment Research, 64, 216–222.

Kim I.S., Jang N. (2006). The effect of calcium on the membrane biofouling in the membrane bioreactor (MBR). Water Research, 40, 2756–2764.

Kim J., Yoon T.I. (2010) Direct observations of membrane scale in membrane bioreactor for wastewater treatment application. Water Science and Technology, 61(9), 2267-2272.

Knoblock M.D., Sutton P.M., Mishra P.N., Gupta K., Janson A. (1994). Membrane biological reactor system for treatment of oily wastewaters. Water environment research, 66(2), 133-139.

Koseoglu H., Yigit N.O., Iversen V., Drews A., Kitis M., Lesjean B., Kraume M. (2008). Effects of several different flux enhancing chemicals on filterability and fouling reduction of membrane bioreactor (MBR) mixed liquors. Journal of Membrane Science, 320, 57-64.

Kraume M., Wedi D., Schaller J., Iversen V., Drews A. (2009). Fouling in MBR—what use are lab investigations for full scale operation?. Desalination, 236, 94-103.

Kuhn R., Pollice A., Laera G., Palese L.L., Lippolis R., Papa S. (2007). Standard assays and metaproteomics as new approaches for functional chracterization of membrane bioreactor biomass, in: Membrane Technologies for Wastewater Treatment and Reuse (7), Proceedings of the 2nd IWA Nat. Young Water Professionals Conference, Berlin, June 4–6, 2007, pp. 59–64.

Lapara T.M., Alleman J.E. (1999). Thermophilic aerobic biological wastewater treatment. Water Research, 33, 895-908.

Lapara T.M., Konopka A., Nakatsu C.H., Alleman J.E., (2001). Thermophilic aerobic treatment of a synthetic wastewater in a membrane-coupled bioreactor. Journal of Industrial Microbiology and Biotechnology, 26, 203-209.

Lapara T.M., Nakatsu C.H., Pantea L.M., Alleman J.E. (2002). Stability of the bacterial communities supported by a seven-stage biological process treating pharmaceutical wastewater as revealed by PCR–DGGE. Water Research, 36, 638-646.

Larsen P., Nielsen J.L., Svendsen T.C., Nielsen P.H. (2008). Adhesion characteristics of nitrifying bacteria in activated sludge. Water Research, 42, 2814–2826.

Laspidou C.S., Rittmann B.E. (2002). A Unified Theory for Extracellular Polymeric Substances, Soluble Microbial Products, and Active and Inert Biomass. Water Research, 36, 2711–2720.

Le-Clech P., Chen V., Fane A.G. (2006). Fouling in membrane bioreactors used in wastewater treatment, Journal of Membrane Sciece. 284, 17–53.

Le-Clech P., Fane A., Leslie G., Childress A. (2005a). The operator's perspective. Filtration and Separation, 42, 20-23.

Le-Clech P., Jefferson B., Chang I.S., Judd S.J. (2003a). Critical flux determination by the flux-step method in a submerged membrane bioreactor. Journal of Membrane Science, 227, 81-93.

Le-Clech P., Jefferson B., Judd S.J. (2003b). Impact of aeration, solids concentration and membrane characteristics on the hydraulic performance of a membrane bioreactor. Journal of Membrane Science, 218, 117-129.

Le-Clech P., Jefferson S.J., Judd A. (2005b) Comparison of submerged and sidestream tubular membrane bioreactor configurations. Desalination, 173, 113-122.

Lee J.C., Kim J.S., Kang I.J., Cho M.H., Park P.K., Lee C.H. (2001) Potential and limitations of alum or zeolite addition to improve the performance of a submerged membrane bioreactor. Water Science and Technology, 43, 59-66.

Lee W., Kang S., Shin H. (2003). Sludge characteristics and their contribution to microfiltration in submerged membrane bioreactors. Journal of Membrane Science, 216, 217-227.

Lee W.N., Chang I.S., Hwang B.K., Park P.K., Lee C.H., Huang X. (2007). Changes in biofilm architecture with addition of membrane fouling reducer in a membrane bioreactor. Process Biochemistry, 42(4), 655-661.

Lesjean B., Huisjes E.H. (2008). Survey of the European MBR market: trends and perspectives. Desalination, 231, 71–81.

Lesjean B., Rosenberger S., Laabs C., Jekel M., Gnirss R., Amy G. (2005). Correlation between membrane fouling and soluble/colloidal organic sub- stances in membrane bioreactors for municipal wastewater treatment. Water Science and Technology, 51, 1-8.

Lesjean B., Rosenberger S., Schrotter J.C., Recherche A. (2004). Membrane-aided biological wastewater treatment—an overview of applied systems. Membrane technology, 2004(8), 5-10.

Li H.Q., Jiku F., Schroder H.F. (2000). Assessment of the pollutant elimination efficiency by gas chromatography/mass spectrometry, liquid chromatography, mass spectrometry and tandem mass spectrometry – comparison of conventional and membrane-assisted biological wastewater treatment processes. Journal of Chromatography A, 889(1-2), 155-176.

Li X.Y., Yang S.F. (2007). Influence of loosely bound extracellular polymeric substances (EPS) on the flocculation, sedimentation and dewaterability of activated sludge. Water Research, 41(5), 1022-1030.

Li Y.Z., He Y.L., Liu Y.H., Yang S.C., Zhang G.J. (2005). Comparison of the filtration characteristics between biological powdered activated carbon sludge and activated sludge in submerged membrane bioreactors. Desalination, 174, 305-314.

Liang S., Liu C., Song L. (2007). Soluble microbial products in membrane bioreactor operation: behaviors, characteristics, and fouling potential. Water Research, 41(1), 95-101.

Lim A.L., Bai R. (2003) Membrane fouling and cleaning in microfiltration of activated sludge wastewater. J. Membr. Sci., 216, 279–290.

Little L.W. (1978). Measurement of color in textile dyeing wastewater. Proceeding of thr Symposium Textile Industry Technology. December 5-8, 1978, Williamsburg, VA, pp. 307-310.

Liu Y., Fang H.H.P. (2003). Influences of extracellular polymeric substances (EPS) on flocculation, settling, and dewatering of activated sludge. Critical Reviews in Environmental Science and Technology, 33, 237-273.

Lobos J., Wisniewski C., Heran M., Grasmick A. (2005) Effects of starvation conditions on biomass behaviour for minimization of sludge production in membrane bioreactors. Water Science and Technology, 51, 35-44.

Loh S.T., Beuscher U., Poddar T.K., Porter A.G., Wingard J.M., Husson S.M., Wickramasinghe S.R. (2009). Interplay among membrane properties, protein properties and operating conditions on protein fouling during normal-flow microfiltration. Journal of Membrane Science, 332, 93-103.

Lonon M.K., Abanto M., Findlay R.H. (1999). A pilot study for monitoring changes in the microbiological component of metalworking fluids as a function of time and use in the system. American Industrial Hygiene Association Journal, 60, 480–485.

Lonsdalea H.K. (1982). The growth of membrane technology. Journal of Membrane Science, 10(2-3), 81-181.

Lourenço N.D., Novais J.M., Pinheiro H.M. (2000). Reactive textile dye colour removal in a sequencing batch reactor. Water Science and Technology, 42(5-6), 321-328.

Lowry O.H., Rosebourgh N.J., Farr A.R., Randall R.J. (1951). Protein measurement with the folin phenol reagent. The Journal of Biological Chemistry, 193, 265-275.

Lubbecke S., Vogelpohl A., Dewjanin W. (1995). Wastewater treatment in a biological high-performance system with high biomass concentration. Water Research, 29, 793-802.

Lubello C., Caffaz S., Mangini L., Santianni D., Caretti C. (2007). MBR pilot plant for textile wastewater treatment and reuse. Water Science and Technology, 55(10), 115-24.

Lubello C., Gori R. (2004). Membrane bio-reactor for advanced textile wastewater treatment and reuse. Water Science and Technology, 50(2), 113-9.

Lubello C., Gori R. (2005). Membrane bio-reactor for textile wastewater treatment plant upgrading. Water Science and Technology, 52(4), 91-98.

Lyko S., Al-Halbouni D., Wintgens T., Janot A., Hollender J., Dott W., Melin T. (2007). Polymeric compounds in activated sludge supernatant – characterisation and retention

mechanisms at a full-scale municipal membrane bioreactor. Water Research, 41(17), 3894-3902.

Maki H., Masuda N., Fujiwara Y., Ike M., Fujita M. (1994). Degradation of alkylphenol ethoxylates by Pseumonas sp. Strain TR01. Applied and Environmental Microbiology, 60(7), 2265-2271.

Malpei F., Bonomo L., Rozzi A. (2003). Feasibilility study to upgrade a textile wastewater treatment plant by a hollow fibre membrane bioreactor for effluent reuse. Water Science and Technology, 47(10), 33-39.

Masse A., Sperandio M., Cabassud C. (2006). Comparison of sludge characteristics and performance of a submerged membrane bioreactor and an activated sludge process at high solids retention time. Water Research, 40(12), 2405-2415.

Mattioli D., Malpei F., Bortone G., Rozzi A. (2002). Water minimisation and reuse in the textile industry, in: Lens P., Hulshoff Pol L., Wilderer P., Asano T. (eds.), Water recycling and resource recovery in industry, IWA Publishing, London, pp. 545-584.

McAdam E.J., Judd S.J., Cartmell E., Jefferson B. (2007). Influence of substrate on fouling in anoxic immersed membrane bioreactors. Water Research, 41(17), 3859-3867.

Meng F., Chae S., Drews A., Kraume M., Shin H., Yang F. (2009). Recent advances in membrane bioreactors (MBRs): Membrane fouling and membrane material. Water Research, 43 (6), 1489-1512.

Meng F., Shi B., Yang F., Zhang H. (2007a). Effect of hydraulic retention time on membrane fouling and biomass characteristics in submerged membrane bioreactors. Bioprocess and Biosystems Engineering, 30, 359-367.

Meng F., Shi B., Yang F., Zhang H. (2007b). New insights into membrane fouling in submerged membrane bioreactor based on rheology and hydrodynamics concepts. Journal of Membrane Science, 302(1-2), 87-94.

Meng F., Zhang H., Yang F., Li Y., Xiao J., Zhang X. (2006). Effect of filamentous bacteria on membrane fouling in submerged membrane bioreactor. Journal of Membrane Science, 272, 161-168.

Meraviglia I., Rondi S., Monti S. (2003). Full scale MBR plant for domestic wastewater treatment. (in Italian), in: Proceedings International Conference Application and perspectives of MBRs in wastewater treatment and reuse, 28-29 April, 2003, Cremona, Italy, pp. 1-18.

Min K.N., Ergas S.J., Mermelstein A. (2007). Impact of dissolved oxygen concentration on membrane filtering resistance and soluble organic matter characteristics in membrane

bioreactors. In: Fourth IWA International Membranes Conference, Harrogate, 15-17 May, 2007.

Miyoshi T., Tsuyuhara T., Ogyu R., Kimura K., Watanabe Y. (2009). Seasonal variation in membrane fouling in membrane bioreactors (MBRs) treating municipal wastewater. Water Research, 43, 5109–5118.

Moore J.S., Christensen M., Wilson R.W., Wallace Jr. R.J., Zhang Y., Nash D.R., Shelton B. (2000). Mycobacterial contamination of metalworking fluids: involvement of a possible new taxon of rapidly growing mycobacteria. American Industrial Hygiene Association Journal, 61, 205-213.

Moreau A., Ferreira M.L., van Nieuwenhuijzen A., van der Graaf J. (2009). Overview of MBR activated sludge filterability at European scale, in: Presented at 5th IWA-MTC, Beijing, September 1-3, 2009.

Morgan J.W., Forster C.F., Evison L. (1990). A comparative study of the nature of biopolymers extracted from anaerobic and activated sludges. Water Research, 24, 743-750.

Morgan-Sagastume F., Grant Allen D. (2005). Activated sludge deflocculation under temperature upshifts from 30 to 45°C. Water Research, 39(6), 1061-1074.

Muszynski A., Łebkowska M. (2005). Biodegradation of used metalworking fluids in wastewater treatment. Polish Journal of Environmental Studies, 14 ,73–79.

Muszyński A., Załeska–Radziwiłł M., Łebkowska M., Nowak D. (2007). Biological and Electrochemical Treatment of Used Metalworking Fluids: A Toxicity-Reduction Evaluation. Archives of Environmental Contamination and Toxicology, 52, 483–488.

Nagaoka H., Nemoto H. (2005). Influence of extracellular polymeric sub- stances on nitrogen removal in an intermittently-aerated membrane bioreactor. Water Science and Technology, 51, 151-158.

Nataraj S., Schomäcker R., Kraume M., Mishra I.M., Drews A. (2008). Analyses of polysaccharide fouling mechanisms during crossflow membrane filtration. Journal of Membrane Science, 308, 152-161.

Ng C.A., Sun D., Fane A.G. (2006). Operation of membrane bioreactor with powdered activated carbon addition. Separation Science and Technology, 41, 1447-1466.

Ng H.Y., Hermanowicz S.W. (2005). Membrane bioreactor operation at short solids retention times: performance and biomass characteristics.Water Research, 39(6),981-92.

Ng H.Y., Tan T.W., Ong S.L. (2006). Membrane fouling of submerged membrane bioreactors: impact of mean cell residence time and the contributing factors. Environmental Science and Technology, 40(8), 2706-2713.

Ng, C.A., Sun, D., Zhang, J., Chua, H.C., Bing, W., Tay, S. and Fane, A. (2005) Strategies to improve the sustainable operation of membrane bioreactors, in: Proceedings of International Desalination Association Conference, Singapore.

Ngo H.H., Guo W.S. (2009). Membrane fouling control and enhanced phosphorus removal in an aerated submerged membrane bioreactor using modified green bioflocculant. Bioresource Technology, 100, 4289-4291.

Nolan W.F. (1972). Analysis of water pollution abatement in the textile industry. MSc thesis, Clemson University, Clemson, USA.

Ognier S., Wisnieswski C., Grasmick A. (2001). Biofouling in membrane bioreactors: Phenomenon analysis and modelling, in: Proceedings of MBR 3, Cranfield University, UK.

Ognier S., Wisniewski C., Grasmick A. (2004). Membrane bioreactor fouling in sub-critical filtration conditions: a local critical flux concept. Journal of Membrane Science, 229, 171-177.

Oller I., Malato S., Sánchez-Pérez J.A. (2010) Combination of Advanced Oxidation Processes and biological treatments for wastewater decontamination—A review. Science of the Total Environment, in press.

Owen W.F., Stuckey D.C., Healy J.B., Young L.Y., Mccarty P.L. (1979). Bioassay for Monitoring Biochemical Methane Potential and Anaerobic Toxicity. Water Research, 13, 485-492.

Pang C.M., Hong P., Guo H., Liu W.T. (2005). Biofilm formation characteristics of bacterial isolates retrieved from a reverse osmosis membrane. Environmental Science and Technology, 39(19), 7541-7550.

Park H., Choo K.H., Lee C.H., (1999). Flux enhancement with powdered activated carbon addition in the membrane anaerobic bioreactor. Sep. Sci. Technol. 34, 2781–2792.

Park R.M. (2001). Mortality at an automotive engine foundry and machining complex. Journal of Occupational and Environmental Medicine, 43, 483-493.

Pavlostathis S.G., Giraldo-Gomez E. Kinetics of Anaerobic Treatment: A. Critical Review. Crit. Rev. Environ. Control(1991)

Pearce C.I., Lloyd J.R., Guthrie J.T. (2003). The removal of colour from textile wastewater using whole bacterial cells: a review. Dyes and Pigments, 58(3), 179-196.

Peng R.Y., Cheng C., Greenfield P.F., Wang H.E. (1997). Treatment of winery wastewater in a reactive PU-immobilized anaerobic fluidized bed reactor. Developments in Chemical Engineering and Mineral Processing, 5, 235-250.

Peng R.Y., Lo W.W., Cheng C., Liu C.S., Wu Y.H. (1999). Immobilized fluidized bed bioreactor for continuous lactic acid production, in: Proceedings of the Fourth Conference on Biochemical Engineering, June 27-28, Chiayi, Taiwan, pp. 27-30.

Perez M., Rodriguez-Cano R., Romero L.I., Sales D. (2006). Anaerobic thermophilic digestion of cutting oil wastewater: Effect of co-substrate. Biochemical Engineering Journal, 29, 250–257.

Perez M., Rodriguez-Cano R., Romero L.I., Sales D. (2007). Performance of anaerobic thermophilic fluidized bed in the treatment of cutting-oil wastewater. Bioresource Technology, 98, 3456–3463.

Polak L. (1986). Biological treatability of industrial wastewater and waste machine tool coolants at john dubuque works, in: Proceedings of the 41st Annual Industrial Waste Conference.

Pollice A., Brookes A., Jefferson B., Judd S. (2005). Sub-critical flux fouling in membrane bioreactors – a review of recent literature. Desalination, 174(3), 221-230.

Pollice A., Laera G., Saturno D., Giordano C. (2008). Effects of sludge retention time on the performance of a membrane bioreactor treating municipal sewage. Journal of Membrane Science, 317(1-2), 65-70.

Prieske H., Drews A., Kraume M. (2008). Prediction of the circulation velocity in a membrane bioreactor. Desalination, 231(1-3), 219-226.

Psoch C., Schiewer S. (2005). Long-term study of an intermittent air sparged mbr for synthetic wastewater treatment. Journal of Membrane Science, 260, 56-65.

Rabenstein A., Koch T., Remesch M., Brinksmeier E., Kuever J. (2009). Microbial degradation of water miscible metal working fluids. International Biodeterioration and Biodegradation, 63, 1023–1029.

Ramesh A., Lee D.J., Lai J.Y. (2007). Membrane biofouling by extracellular polymeric substances or soluble mcirobial products from membrane bioreactor sludge. Applied Microbiology and Biotechnology, 74, 699-707.

Ramphao M., Wentzel M.C., Merritt R., Ekama G.A., Young T., Buckley C.A. (2004). Impact of Membrane Solid–Liquid Separation on Design of Biological Nutrient Removal Activated Sludge Systems. Biotechnology and Bioengineering, 89(6).

Remy M., Potier V., Temmink H., Rulkens W. (2010). Why low powdered activated carbon addition reduces membrane fouling in MBRs. Water research, 44, 861-867.

Remy M., van der Marel P., Zwijnenburg A., Rulkens W., Temmink H. (2009). Low dose powdered activated carbon addition at high sludge retention times to reduce fouling in membrane bioreactors. Water research, 43, 345-350.

Richardson J.F. (2002). Chemical Engineering, Volume 2. Elsevier, Oxford

Robinson T., McMullan G., Marchant R., Nigam P. (2001). Remediation of dyes in textile effluent: a critical review on current treatment technologies with a proposed alternative. Bioresource Technology, 77, 247-255.

Rosenberger S., Evenblij H., Poele S.te, Wintgens T., Laabs C. (2005). The importance of liquid phase analyses to understand fouling in membrane assisted activated sludge processes-six case studies of different European research groups. Journal of Membrane Science, 263, 113-126.

Rosenberger S., Kraume M. (2003). Filterability of activated sludge in membrane bioreactors. Desalination, 151(2), 195-200.

Rosenberger S., Laabs C., Lesjean B., Gnirss R., Amy G., Jekel M., Schrotter J.C. (2006). Impact of colloidal and soluble organic material on membrane performance in membrane bioreactors for municipal wastewater treatment. Water Research, 40, 710-720.

Rossmoore H.W. (1981). Antimicrobial agents for water-based metalworking fluids. Journal of Occupational Medicine, 23, 247–254.

Rott U., Minke R. (1999). Overview of wastewater treatment and recycling in the textile processing industry. Water Science and Technology, 40(1), 137-144.

Rozzi A., Ficara E., Rocco A. (2003). Dissolved Oxygen-Stat Titration Respirometry: Principle of Operation and Validation. Journal Of Environmental Engineering, 129(7), 602-609.

Ruth B.F. (1946). Correlating filtration theory with industrial practice. Industrial and Engineering Chemistry, 38(6), 564-571.

Sandin M., Allenmark S., Edebo L. (1990). Selective toxicity of alkanolamines. Antimicrobial Agents and Chemotherapy, 34, 491–493.

Schippers J.C., Verdouw J. (1980). The modified fouling index, a method of determining the fouling characteristics of water. Desalination, 32(1), 137-148.

Schrader, G.A., Zwijnenburg, A. and Wessling, M. (2005) The effect of wwtp effluent zeta-potential on direct nanofiltration performance. J. Membrane Sci., 266, 80–93.

Schreyer H.B., Coughlin R.W. (1999). Effects of stratification in a fluidized bed bioreactor during treatment of metal-working wastewater. Biotechnology and Bioengineering, 63, 129-140.

Shimizu Y., Okuno Y., Uryu K., Ohtsubo S., Watanabe A. (1996). Filtration characteristics of hollow fiber microfiltration membranes used in membrane bioreactor for domestic wastewater treatment.

Shimizu Y., Shimodera K.I., Watanabe A. (1993). Cross flow microfiltration of bacterial cells. Journal of Fermentation and Bioengineering, 76, 493-500.

Snbowden-Swan L.J. (1995). Pollution Prevention in the Textile Industries, in: Freeman H.M. (Ed.), Industrial Pollution Prevention Handbook, McGraw-Hill, Inc., New York.

Sobeck D.C., Higgins M.J. (2002) Examination of three theories for mech- anisms of cation-induced bioflocculation. Water Research, 36, 527-538.

Song K.G., Kim Y., Ahn K.H. (2008). Effect of coagulant addition on membrane fouling and nutrient removal in a submerged membrane bioreactor. Desalination, 221(1-3), 467-474.

Spanjers H., Vanrolleghem P.A., Olsson G., Dold P.L. (1998). Respirometry in control of the activated sludge process: Principles. International Association on Water Quality, London.

Speece R.E. (1996). Anaerobic Biotechnology for Industrial Wastewaters. Archae Press, Nashville.

Stephenson T., Judd S., Jefferson B., Brindle K. (2000). Membrane Bioreactors for Wastewater Treatment. IWA Publishing, London.

Stolz A. (2001). Basic and applied aspects in the microbial degradation of azo dyes. Applied Microbiology and Biotechnology, 56, 69-80.

Stuckey D.C., Hu A. (2003). The submerged anaerobic membrane bioreactor (SAMBR): an intensification of anaerobic wastewater treatment, Presented at the IWA Leading Edge Conference on Drinking Water and Wastewater Treatment Technologies, Noordwijk/Amsterdam, The Netherlands.

Stumm W., Morgan J.J. (1970). Aquatic Chemistry. Wiley-Interscience, New York.

Sun F.Y., Wang X.M., Li X.Y. (2008). Visualisation and characterisation of bioplomer clusters in a submerged membrane bioreactor. Journal of Membrane Science, 325, 691-697.

Sun Y., Wang Y., Huang X. (2007). Relationship between sludge settleability and membrane fouling in a membrane bioreactor. Frontiers of Environmental Science and Engineering in China 1(2), 221-225.

Sutton P.M., Kothair D., Mishra P.N., Hachigian L. (1985). Biological treatment of metalworking fluids: a new application for fluidized bed technology, in: Proceedings of the 58th Annual Water Pollution Control Federation Conference, pp. 19-30.

Sutton P.M., Mishra P.N., Crawford P.M. (1994). Combining biological and physical processes for complete treatment of oily wastewaters. International biodeterioration and biodegradation, 33(1), 3-21.

Svarosky L. (2000). Solid-Liquid Separation, ed. 4. Butterwhort Heinemann, Oxford, UK.

Tam L.S., Tang T.W., Leung W.Y., Chen G.H., Sharma K.R. (2006). A pilot study on performance of a membrane bio-reactor in treating fresh water sewage and saline sewage in Hong Kong. Separation Science and Technology, 41, 1253-1264.

Tan N.C.G. (2001). Integrated and sequential anaerobic/aerobic biodegradation of azo dyes. Ph.D. Thesis. Wageningen University. Wageningen, The Netherlands.

Tardieu, E., Grasmick, A., Geaugey, V. and Manem, J. (1999) Influence of hydro- dynamics on fouling velocity in a recirculated mbr for wastewater treatment. J. Membrane Sci., 156, 131–140.

Tarnacki K., Lyko S., Wintgens T., Melin T., Natau F. (2005). Impact of extra- cellular polymeric substances on the filterability of activated sludge in membrane bioreactors for landfill leachate treatment. Desalination, 179, 181-190.

The Society of Dyers and Colourists (1990). Colorants and Auxiliaries, J. Shore (ed.), vol 2, 1st edn, Manchester, UK.

Tian J.Y., Liang H., Li X., You S.J., Tian S., Li G.B. (2008). Membrane coagulation bioreactor (MCBR) for drinking water treatment. Water Research, 42(14), 3910-3920.

Tidswell E., Russell N., White G. (1996). Ether-bond scission in the biodegradation of alcohol ethoxylate nonionic surfactants by Pseudomonas sp. strain SC25A. Microbiology, 142, 1123-1131.

Van den Broeck R., Van Dierdonck J., Caerts B., Bisson I., Kregersman B., Nijskens P., Dotremont C., Van Impe J.F., Smets I.Y. (2010). The impact of deflocculation–reflocculation on fouling in membrane bioreactors. Separation and Purification Technology, 71, 279-284.

Van der Gast C.J., Knowles C.J., Starkey M., Thompson I.P. (2002). Selection of microbial consortia for treating metal-working fluids. Journal of Industrial Microbiology and Biotechnology, 29, 20-27.

Van der Gast C.J., Knowles C.J., Wright M.A., Thompson I.P. (2001). Identification and characterisation of bacterial populations of an in-use metal-working fluid by phenotypic and genotypic methodology. International Biodeterioration and Biodegradation, 47, 113–123.

Van der Gast C.J., Thompson I.P. (2004). Effects of pH amendment on metal working fluid wastewater biological treatment using a defined bacterial consortium. Biotechnology and Bioengineering, 89, 357-366.

Van der Gast C.J., Whiteley A.S., Lilley A.K., Knowles C.J., Thompson I.P. (2003b). Bacterial community structure and function in a metal-working fluid. Environmental Microbiology, 5, 453-461.

Van der Gast C.J., Whiteley A.S., Starkey M., Knowles C.J., Thompson I.P. (2003a). Bioaugmentation strategies for remediating mixed chemical effluent. Biotechnology Progress, 19, 1156-1161.

Van der Marel P., Zwijnenburg A., Kemperman A., Wessling M., Temmink B.G., van der Meer W. (2009). An improved flux-step method to determine the critical flux and the critical flux for irreversibility in a membrane bioreactor. Journal of Membrane Science, 332, 24–29.

Van der Roest H.F., Lawrence D.P., van Bentem A.G.N. (2002). Membrane Bioreactors for Municipal Wastewater Treatment. IWA publishing, London

Van Kaam R., Anne-Archard D., Gaubert M.A., Albasi C. (2008). Rheological characterization of mixed liquor in a submerged membrane bioreactor: interest for process management. Journal of Membrane Science, 317(1-2), 26-33.

Vandevivere P.C., Bianchi R., Verstraete W. (1998). Treatment and reuse of wastewater from the textile wet-processing industry: Review of emerging technologies. Journal of Chemical Technology and Biotechnology, 72, 289-302.

Vant Oever (2005).MBR focus: is submerged best? Filtration and Separation, 42(5), 24-27.

Vant Oever R.,Borgerink R., Miller P. (2009). OPERATING EXPERIENCE OF 3rd GENERATION MEMBRANE MBR IN EUROPE, in : Procedings of WISA Conference proceeding, Stellenbosch 13 - 15 May 2009.

Wagner J., Rosenwinkel K.H. (2000). Sludge production in membrane bioreactors under different conditions. Water Science and Technology, 4110-4111, 251-258.

Wang S., Guillen G., Hoek E.M.V. (2005). Direct observation of microbial adhesion to membranes. Environmental Science and Technology, 39(17), 6461-6469.

Wang X.M., Li X.Y. (2008). Accumulation of biopolymer clusters in a submerged membrane bioreactor and its effect on membrane fouling. Water Research, 42, 855-862.

Wang Z., Wu Z., Tang S. (2009). Extracellular polymeric substances (EPS) properties and their effects on membrane fouling in a submerged membrane bioreactor. Water Research, 43, 2504-2512.

Wang Z., Wu Z., Yin X., Tian L. (2008). Membrane fouling in a submerged membrane bioreactor (MBR) under sub-critical flux operation: membrane foulant and gel layer characterization. Journal of Membrane Science, 325(1), 238-244.

Wen X., Bu Q., Huang X. (2004). Study on fouling characteristic of an axial hollow fibers cross-flow microfiltration under different flux operations, in: Proceedings of Water Environment – Membrane Technology Conference, Seoul, Korea.

Wicaksana F., Fane A.G., Chen V. (2006). Fibre movement induced by bubbling using submerged hollow fibre membranes. Journal of Membrane Science, 271, 186-195.

Wilén B.M., Jina B., Lanta P. (2003). The influence of key chemical constituents in activated sludge on surface and flocculating properties. Water Research, 37, 2127-2139.

Wisniewski, C. and Grasmick, A. (1998) Floc size distribution in a membrane bioreactor and consequences for membrane fouling. Colloid. Surface. A: Physicochem. Eng. Aspect., 138, 403–411.

Witzig R., Manz W., Rosenberger S., Krüger U., Kraume M., Szewzyk U. (2002). Microbiological aspects of a bioreactor with submerged membranes for aerobic treatment of municipal wastewater. Water Research, 36, 394-402.

Wolborska A., Morawiak A., Dziubinski M. (2006). The Effect of Coagulant PAX-18 on Oxygen Uptake Rate in Activated Sludge. EMChIE, Vienna, Austria.

Wozniak T. (2009). MBR design and operation using MPE-technology (membrane performance enhancer). Desalination, 250, 723-728.

Wu J., Chen F., Huang X., Geng W., Wen X. (2006). Using inorganic coagulants to control membrane fouling in a submerged membrane bioreactor. Desalination, 197(1-3), 124-136.

Wu J., Huang X. (2008). Effect of dosing polymeric ferric sulfate on fouling characteristics, mixed liquor properties and performance in a long-term running membrane bioreactor. Separation and Purification Technology, 63, 45-52.

Wu J., Huang X. (2009). Effect of mixed liquor properties on fouling propensity in membrane bioreactors. Journal of Membrane Science, 342, 88-96.

Wu Z., Wang Z., Huang S., Mai S., Yang C., Wang X., Zhou Z. (2008). Effects of various factors on critical flux in submerged membrane bioreactors for municipal wastewater treatment. Separation and Purification Technology, 62, 56-63.

Xu K., Liu H., Chen J. (2010). Effect of classic methanogenic inhibitors in the quantity and diversity of archaeal community and the reductive homoacetogenic activity during the process of anaerobic sludge digestion. Bioresource Technology, 101, 2600-2607.

Yamamoto K., Hiasa H., Mahmood T., Matsuo T. (1989). Direct Solid-Liquid Separation using Hollow Fiber Membrane in an Activated Sludge aeration Tank. Water Science and Technology 21(4-5), 43-54.

Yamamura H., Kimura K., Watanbe Y. (2007). Mechanism involved in the evolution of physically irreversible fouling in microfiltration and ultrafiltration membranes used for drinking water treatment. Environmental Science and Technology, 41(19), 6789-6794.

Yang W., Cicek N., Ilg J. (2006). State-of-the-art of membrane bioreactors: Worldwide research and commercial applications in North America. Journal of Membrane Science, 270, 201–211.

Yang X.L., Song H.L., Lu J.L., Fu D.F., Cheng B. (2010). Influence of diatomite addition on membrane fouling and performance in a submerged membrane bioreactor. Bioresource Technology, 101, 9178-9184.

Ye Y., Chen V., Fane A.G. (2006). Modeling long term sub-critical filtration of model EPS solutions. Desalination, 191, 318-327.

Ye Y., Le-Clech P., Chen V., Fane, A.G. (2005). Evolution of fouling during crossflow filtration of model EPS solutions. Journal of Membrane Science, 264, 190-199.

Yeom I.T., Nah Y.M., Ahn K.H. (1999). Treatment of household wastewater using an intermittently aerated membrane bioreactor. Desalination, 124, 193-203.

Yoon K.H., Yeon K.M., Lee C.H., Lee S.H., Swaminathan T. (2006). Biofilm structure and extracellular polymeric substances in low and high dissolved oxygen membrane bioreactors. Separation and Purification Technology, 41(7), 1213-1230.

Yoon S.H., Collins J.H. (2006). A novel flux enhancing method for membrane bioreactor (MBR) process using polymer. Desalination, 191(1-3), 52-61.

Yoon S.H., Collins J.H., Dave B., Koppes J. (2007). Use of modified cationic polymers for the reduction of membrane fouling in membrane bioreactor, in: Proceeding of Fourth IWA International Membranes Conference, Harrogate.

Yoon S.H., Collins J.H., Musale D., Sundararajan S., Tsai S.P., Hallsby G.A., Kong J.F., Koppes J., Cachia P. (2005). Effects of flux enhancing polymer on the characteristics of sludge in membrane bioreactor process. Water Science and Technology, 51(6-7), 151-157.

You S.J., Tseng D.H., Deng J.Y. (2008). Using combined membrane processes for textile dyeing wastewater reclamation. Desalination, 234, 426-432.

Yu H.Y., Hu M.X., Xu Z.K., Wang J.L., Wang S.Y. (2005). Surface modification of polypropylene microporous membranes to improve their antifouling property in MBR: NH3 plasma treatment, Separation and Purification Technology, 45, 8-15.

Yun M.A., Yeon K.M., Park J.S., Lee C.H., Chun J.S., Lim D.J. (2006). Characterization of biofilm structure and its effect on membrane permeability in MBR for dye wastewater treatment. Water Research, 40(1), 45-52.

Zhang H.F., Sun B.S., Zhao X.H., Gao Z.H. (2008). Effect of ferric chloride on fouling in membrane bioreactor. Separation and Purification Technology, 63(2), 341-347.

Zhang J., Chua H.C., Zhou J., Fane A.G. (2006). Factors affecting the membrane performance in submerged membrane bioreactors. Journal of Membrane Science, 284(1-2), 54-66.

Zhang Y., Bu D., Liu C.G., Luo X., Gu P. (2004). Study on retarding membrane fouling by ferric salts dosing in membrane bioreactors, in: Proceedings of the IWA Specialty Conference WEMT, June 7-10, 2004, Seoul.